NASA

Orbit Transfer Vehicle Engine Study Phase A, Extension 1

Contract NAS 8-32999
Final Report
Volume II: Study Results
Report No. 32999F-E1
March 1981

Prepared For:
George C. Marshall Space Flight Center
National Aeronautics And Space Administration
Marshall Space Flight Center, Alabama

(NASA-CR-161699) ORBIT TRANSFER VEHICLE ENGINE STUDY, PHASE A, EXTENSION 1: VOLUME 2: STUDY RESULTS Final Report (Aerojet Liquid Rocket Co.) 242 p HC A11/MF A01 CSCL 21H G3/20

N81-21126

Unclas
42067

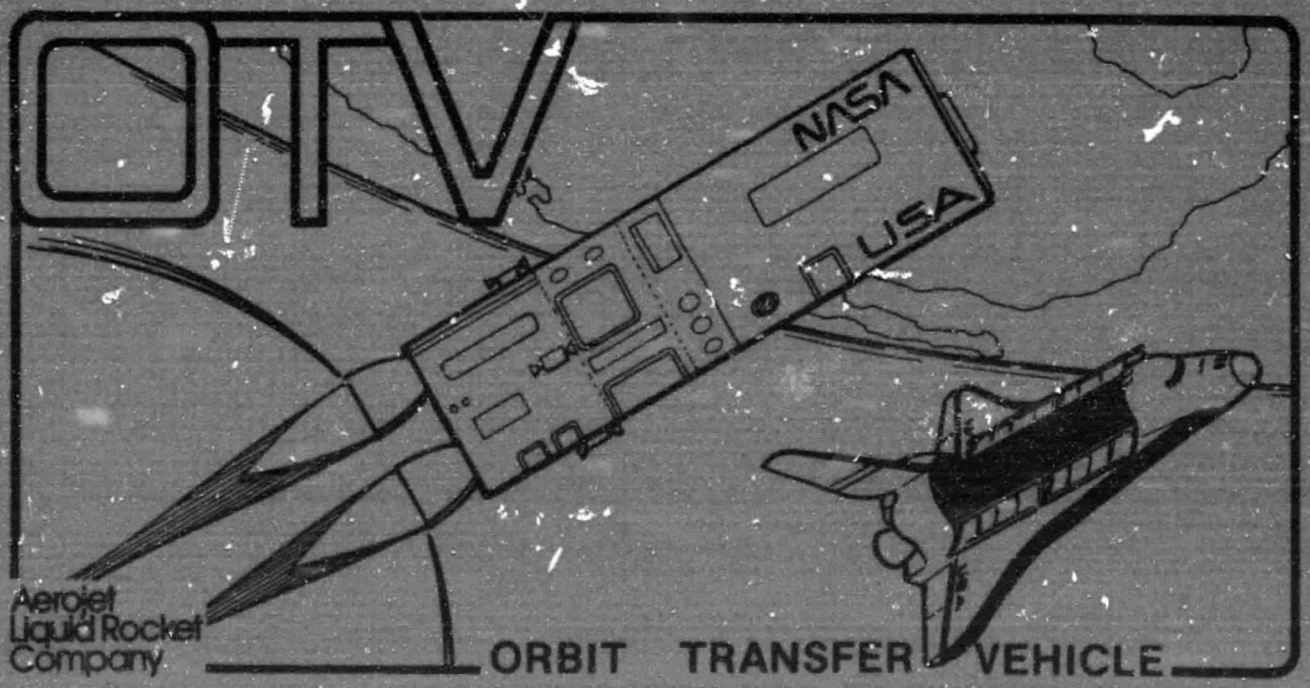

Report 32999 F-E1

15 March 1981

ORBIT TRANSFER VEHICLE ENGINE STUDY
PHASE "A" EXTENSION 1

Contract NAS 8-32999

FINAL REPORT
VOLUME II: STUDY RESULTS

Prepared for

George C. Marshall Space Flight Center
National Aeronautics and Space Administration
Marshall Space Flight Center, Alabama

Prepared by:

J. A. Mellish
Study Manager

Approved by:

L. B. Bassham
Program Manager

Aerojet Liquid Rocket Company
P.O. Box 13222
Sacramento, California 95813

FOREWORD

This final report is submitted for the Orbit Transfer Vehicle (OTV) Engine Phase "A" Study per the requirements of Contract NAS 8-32999, Extension 1 Data Procurement Document No. 559, Data Requirement No. MA-05. This work was performed by the Aerojet Liquid Rocket Company for the NASA-Marshall Space Flight Center, with Mr. Dale H. Blount, NASA/MSFC, as the Contracting Officer Representative (COR). The alternate COR was Mr. James F. Thompson. The ALRC Program Manager was Mr. Larry B. Bassham, and the Study Manager was Mr. Joseph A. Mellish.

The study program consisted of engine system, programmatic, cost, and risk analyses of OTV engine concepts. These evaluations will ultimately lead to the selection and conceptual design of the OTV engine for use by NASA and the OTV vehicle contractor.

The following Aerojet personnel contributed significantly to the study effort and the information contained in this final report:

S. P. Abbott, Turbomachinery Analysis
E. Braun, Crew Safety and Reliability Analysis
K. L. Christensen, Systems Analysis
R. L. Ewen, Thermal Analysis
S. E. Gebben, Crew Safety and Reliability Analysis
J. I. Ito, Performance and Stability Analysis
S. A. Lorenc, Turbomachinery Analysis
A. V. Lundback, Controls System Analysis
J. A. Phipps, Regenerator Analysis
R. L. Sabiers, Turbomachinery Analyais

The final report for this extension is submitted in three volumes:

Volume I - Executive Summary
Volume II - Study Results
Volume III - Study Cost Estimates

TABLE OF CONTENTS

TABLE OF CONTENTS (cont.)

TABLE OF CONTENTS (cont.)

LIST OF TABLES

LIST OF TABLES (cont.)

LIST OF FIGURES

LIST OF FIGURES (cont.)

LIST OF FIGURES (cont.)

LIST OF FIGURES (cont.)

I. INTRODUCTION

A. BACKGROUND

The Space Transportation System (STS) includes an Orbit Transfer Vehicle (OTV) that is carried into low-earth orbit by the Space Shuttle. The primary function of the OTV is to extend the STS operating regime beyond the Shuttle to include orbit plane changes, higher orbits, geosynchronous orbits, and beyond. NASA and the DoD have been studying various types of OTV's in recent years. Data have been accumulated from the analyses of the various concepts, operating modes, and projected missions. The foundation formulated by these studies established the desirability and the benefits of high-performing, versatile OTV operating at low cost.

The OTV's goal is to achieve the same basic characteristics as those of the Space Shuttle, i.e., reusability, operational flexibility, and payload retrieval, along with high reliability and low operating cost. Sufficient data, of enough depth to assure credibility, must be obtained in order to be able to conduct comparative systems analyses for identifying the performance, development, costs, risks, and program requirements for OTV concepts.

A number of different potential vehicle concepts and development appraoches have been under consideration to meet expected mission applications for Orbit Transfer Vehicle (OTV) systems. The OTV systems studies conducted during FY 79/80 examined a variety of propulsive vehicle concepts and evolutionary development steps to accommodate these projected mission needs and included trade studies such as size/staging, potential for use of aero return from high-energy orbits, different engine/propulsion approaches, and others. These systems studies, in conjunction with this OTV engine study, provide comparative data on alternatives and identify concepts/approaches for further study.

I, A, Background (cont.)

For purposes of this OTV engine study (which was initiated prior to the start of the system trade studies), vehicle level assumptions were made on the basis of previous OTV studies. Consequently, these assumptions and guidelines will be superseded by vehicle characteristics and inputs as they are derived from the OTV systems studies.

This program was a continuation of a study of oxygen/hydrogen engines for OTV applications. The subject study extension provides preliminary design data, plans, and cost information which complement the data generated to satisfy the original Statement of Work on Contract NAS 8-32999, dated 6 July 1978 (Ref. 1). These engine data from the original and extension efforts, together with the system studies, will provide the basis to objectively select, define, and design the preferred OTV engine.

B. ORBIT TRANSFER VEHICLE (OTV) CHARACTERISTICS

The vehicle characteristics were defined by the contract Statement of Work (SOW).

The Orbit Transfer Vehicle (OTV) is planned to be a manned, reusable cryogenic upper stage to be used with the Space Transportation System. Initial Operational Capability (IOC) is assumed to be 1987, and the design mission is a four-man, 30-day sortie to geosynchronous orbit.

The required round trip payload to geosynchronous orbit is 13,000 lbm, and the weight of the OTV, with propellants and payload, cannot exceed 97,300 lbm. An Orbiter of 100,000 lbm payload capability is assumed; however, the OTV must be capable of interim operation with the present 65,000 lbm Orbiter. The cargo bay dimensions of the 100,000 lbm Orbiter are assumed to be the same as those of the 65,000 lbm Orbiter, i.e., a cylinder 15 ft in diameter and 60 ft in length. The OTV cannot exceed 34 ft in length. The OTV

is to be earth-based and scheduled to return from geosynchronous orbit for rendezvous with the Orbiter. Both Aeromaneuvering Orbit Transfer Vehicles (AMOTV) and All-Propulsive Orbit Transfer Vehicles (APOTV) are considered. These vehicles are described in NASA Technical Memorandum TMX-73394 (Ref. 2).

C. ENGINE REQUIREMENTS

The requirements for the manned orbit transfer vehicle (MOTV) engine were derived from numerous NASA in-house and contracted studies and are summarized on Table I. The requirements were provided by the contract SOW.

D. ASSUMPTIONS AND GUIDELINES

The following principal assumptions and guidelines were provided by NASA/MSFC in the SOW and were used to conduct this engine study.

1. All engine designs and characteristics will be compatible with the OTV requirements and will be based on 1980 technology.

2. Dimensional allowance will be within Shuttle payload bay specifications, including dynamic envelope limits. (This does not preclude extendible nozzles.)

3. The engine and OTV will be designed to be returned to Earth in the Shuttle and reused; reusability with minimum maintenance/cost for both unmanned and manned missions is a design objective.

4. The OTV engine shall be designed to meet all of the necessary safety and environmental criteria for being carried in the Shuttle payload bay and operating in the vicinity of the manned Shuttle.

TABLE I

OTV ENGINE REQUIREMENTS

Propellants: Hydrogen and Oxygen

Thrust Range: 10-20K lb

Technology Base: 1980 State of the Art

Engine Mixture Ratio: Nominal = 6.0 Range = 6.0 to 7.0

Propellant Inlet Conditions:		H_2	O_2
Boost Pump	NPSH, ft	15	2
	Temp., °R	37.8	162.7

Service Life Between Overhauls: 300 Cycles or 10 Hours

Service-Free Life: 60 Cycles or 2 Hours

Engine Nozzle: Contoured Bell with Extendible/Retractable Section

Maximum Engine Length with Nozzle Retracted: 60 in. (Nominal)

Gimbal Angle: +15°, -6° Pitch

$\pm$6° Yaw

Provide Gaseous Hydrogen & Oxygen Tank Pressurization

Man-Rated with Abort Return Capability

Meet Orbiter Safety and Environmental Criteria

Max P_c Deviations: $\pm$5% of Steady-State Pressure

Adaptable to Extended Low-Thrust Operation (10% of Rated Thrust)

Thrust Chamber Pressure: TBD

Engine Weight: TBD

Engine Specific Impulse: TBD

I, D, Assumptions and Guidelines (cont.)

5. Cost, unless otherwise specified, shall be expressed in FY 1979 dollars.

6. Structural Design Criteria

The following minimum safety and fatigue life factors shall be utilized. It is important to note that these factors are only applicable to designs whose structural integrity has been verified by comprehensive structural testing which demonstrates adherence to the factors specified below. Where structural testing is not feasible, more conservative structural design factors will be supplied by the procuring agency.

a. The structure shall not experience gross (total net section) yielding at 1.1 times the limit load, nor shall failure be experienced at 1.4 times the limit load. For pressure-containing components, failure shall not occur at 1.5 times the limit pressure.

b. Limit load is the maximum predicted external load, pressure, or a combination thereof, expected during the design life.

c. Limit life is maximum expected usefulness of the structure expressed in time and/or cycles of loading.

d. The structure shall be capable of withstanding at least four times the limit life derived from lower boundary fatigue property data.

I, D, Assumptions and Guidelines (cont.)

7. Pressure-containing components shall be pressure-tested at 1.2 times the limit pressure at the design environment, or shall be appropriately adjusted to simulate the design environment, as a quality acceptance criterion for each production component prior to service use. A higher proof-test factor shall be used if fracture mechanics analysis requires it (see 8.b.).

8. Fracture mechanics analysis shall accomplish the following:

   a. Verify that the maximum defect that is possible after final inspection and/or proof testing will not grow to critical size in 4 times the design life of the engine.

   b. Establish the proof-test pressure/oad factor necessary to analytically guarantee 4 times the engine design life.

   c. Establish a list of fracture critical parts. A part is considered fracture critical if unusual (non-routine) processing must be applied to ensure that the requirement described in 8.a. is met.

9. The engine effects on OTV stage performance and weight will be considered in trade studies and systems analyses. A ΔV margin of 3% and an inert weight margin of 10% will be used to determine the OTV performance. The mission velocity requirements are contained in NASA TMX-73394. Payload partials derived from TMX-73394 shall be used to conduct the trade studies.

I, D, Assumptions and Guidelines (cont.)

10. The nominal program mission model contained in NASA TMX-73394 shall be used for both the APOTV and AMOTV to perform the engine program cost analysis.

II. SUMMARY

A. STUDY OBJECTIVES AND SCOPE

The major objectives of this Phase "A" engine study extension were to (1) optimize the advanced expander cycle engine for OTV applications; (2) investigate the feasibility of providing low-thrust capability within the same expander cycle engine; (3) provide additional safety, reliability, development risk, cost, and planning data on OTV engine candidates; and (4) provide design and programmatic parametric data on the OTV engines for use by NASA and OTV system contractors. The original and engine study extensions, in conjunction with the system studies, provide comparative data on engine design alternatives and identify engine requirements, concepts, and approaches recommended for further study on a subsequent conceptual design phase.

Specific study objectives were as follows:

- Perform analytical studies to optimize the advanced expander cycle engine thrust chamber geometry and cooling, engine cycle, and controls.

- Investigate the feasibility and design impact of kitting to provide extended low-thrust operating capability in the advanced expander cycle and identify technology requirements.

- Perform in-depth analyses to provide comparative data on development risk, crew safety, and mission reliability for both advanced expander cycle and staged-combustion cycle OTV engine candidates.

- Prepare a work breakdown structure (WBS), planning (schedules), and detailed cost estimate for a 20,000 lbF staged-combustion cycle engine for comparison with the data generated under Contract NAS 8-32999 for the advanced expander cycle engine.

II, A, Study Objectives and Scope (cont.)

- Support the OTV systems studies contractors in the application of OTV engine parametric data and provide updated engine design information.

- Prepare a final report at the completion of the study which documents the technical details and programmatic assessments that resulted from it.

To accomplish the program objectives, a study program composed of five (5) major tasks and a reporting task was conducted. The technical study tasks were:

Task I: Advanced Expander Cycle Engine Optimization
Task II: Alternate Low-Thrust Capability
Task III: Safety, Reliability, and Development Risk Comparison
Task IV: Cost and Planning Comparison
Task V: Vehicle Systems Studies Support

The final report is submitted in three volumes:

Volume I: Executive Summary
Volume II: Study Results
Volume III: Study Cost Estimates

This volume is structured by the study tasks and provides the study supporting data, assumptions, rationale, conclusions, and recommendations. The cost estimate associated with Task IV is reported separately in Volume III (Ref. 3).

B. RESULTS AND CONCLUSIONS

Because of the advantage of the Advanced Expander Cycle Engine brought out in the initial studies (Ref. 1), further design optimization and comparative analyses were undertaken in this Phase A, Extension 1 effort. The major results and conclusions derived from this study effort are summarized herein. The primary areas covered are (1) thrust chamber geometry optimization, (2) expander cycle optimization, (3) alternate low-thrust capability, (4) safety and reliability, (5) development risk comparison, and (6) cost comparisons. All of the results obtained in this study and its predecessor were used to baseline the initial design concept for the OTV Advanced Expander Cycle Engine Point Design Study (Reference 4).

1. Thrust Chamber Geometry Optimization

Heat transfer, cycle, and performance/weight tradeoff analyses were conducted to determine the effect of combustion chamber length and contraction ratio upon the expander cycle power balance, engine performance, and engine weight. Chamber contraction ratio and length (L') were varied in order that the tradeoffs among heat load, required pressure drop, and nozzle area ratio (restricted by stowed length) could be made.

Longer chambers lower the energy release loss, increase the hydrogen outlet temperature, and increase the coolant jacket pressure drop. In some cases, the increased turbine inlet temperature more than compensates for the increased pressure loss and results in higher thrust chamber pressure. For an engine with a fixed envelope (length), chamber pressure increases result in higher area ratios and, hence, higher performance (I_s). Conversely, longer chambers reduce the length of the nozzle that can be fit in the fixed length constraint, thereby reducing the area ratio and performance. Longer chambers also result in heavier engine weights.

II, B, Results and Conclusions (cont.)

The chamber contraction ratio produces effects similar to those of chamber length. High chamber contraction ratios reduce the coolant jacket pressure drop and coolant outlet temperature (turbine inlet). Chamber contraction ratio increases also result in heavier chambers.

Heat transfer analyses established the differences in chamber coolant jacket pressure drop and coolant outlet temperature due to variations in combustion chamber length and contraction ratio. These results were subsequently used in cycle power balance analyses to establish the attainable chamber pressure as a function of chamber length and contraction ratio. Delivered performance and engine weight were then calculated at these chamber pressures. Weight and specific impulse tradeoffs were made by using the payload partials derived from NASA TMX-73394 (Reference 2).

The results are summarized in Figure 1 at a thrust level of 15,000 lb. On the basis of these results, a chamber length of 18 in. and a contraction ratio of 3.66 were selected as the baseline values. These results were not affected by the engine thrust level.

2. Expander Cycle Optimization

The expander cycle arrangement and various methods for increasing the turbine drive power were also investigated. The cycle variations included in the evaluations were (1) parallel turbine drive, (2) series turbine drive, (3) turbine exhaust gas heat regeneration, and (4) turbine exhaust gas reheat. Simplified schematics for these cycles are shown in Figure 2.

The primary issue in the series versus parallel turbines comparisons is whether the higher flowrate, higher efficiency turbines can compensate for the turbine pressure drops while operated in series. The oxidizer pump

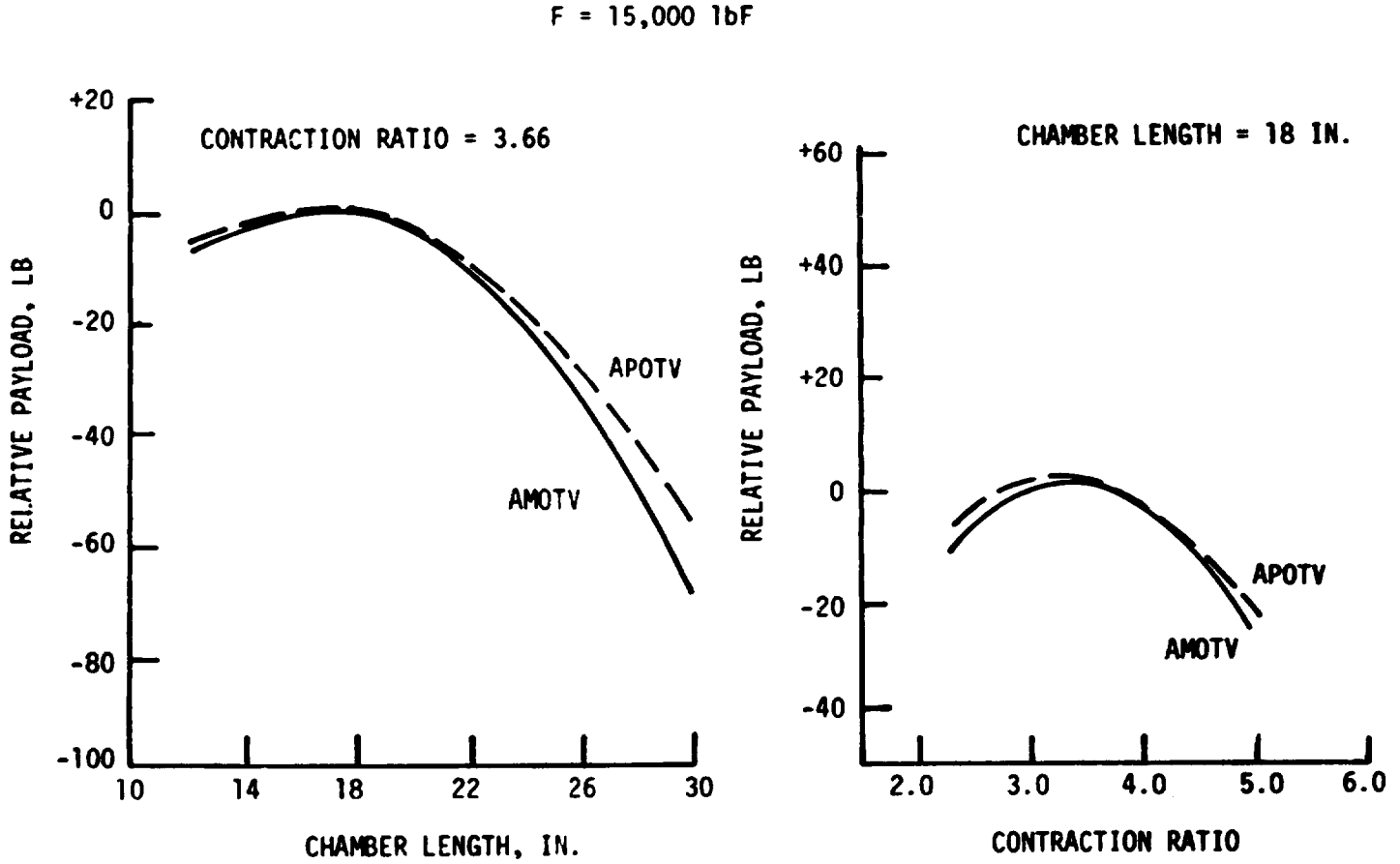

Figure 1. Geometry Optimization on Payload

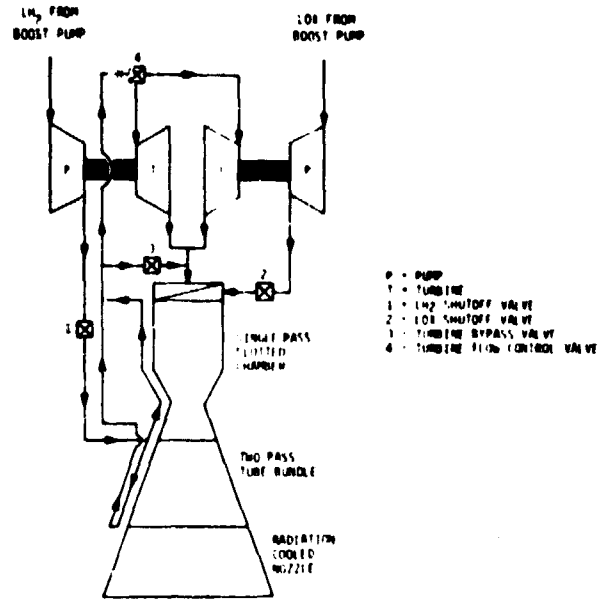

Parallel Turbines Advanced Expander Cycle Flow Schematic

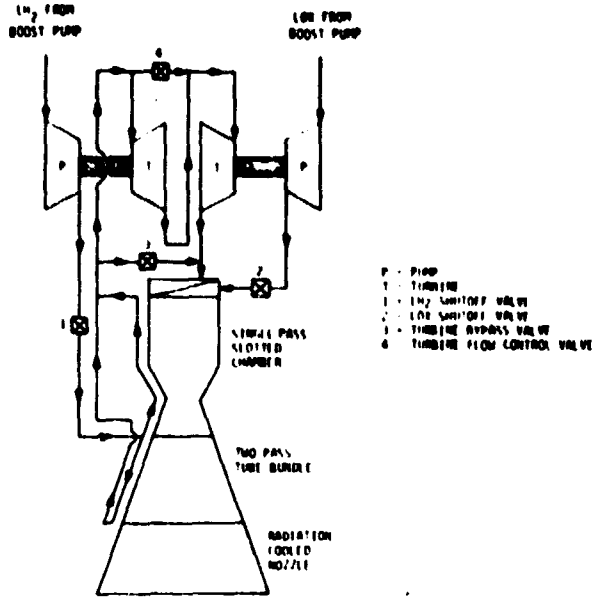

Series Turbines Advanced Expander Cycle Flow Schematic

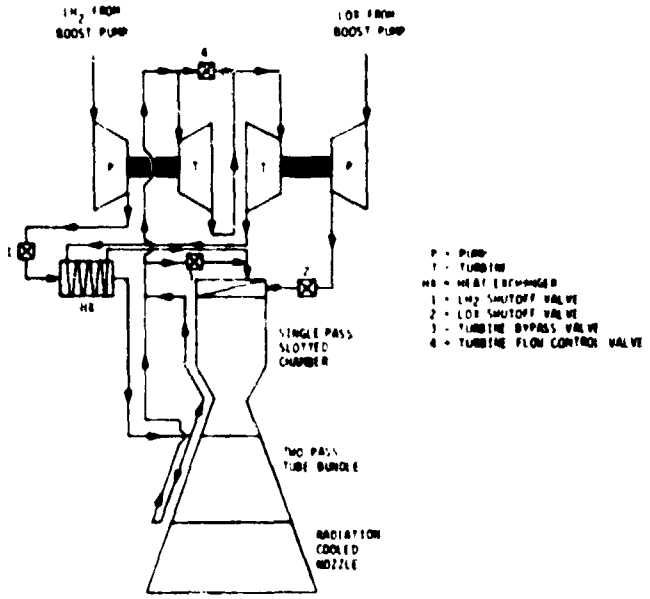

Turbine Exhaust Heat Regeneration, Series Turbines, Advanced Expander Cycle Flow Schematic

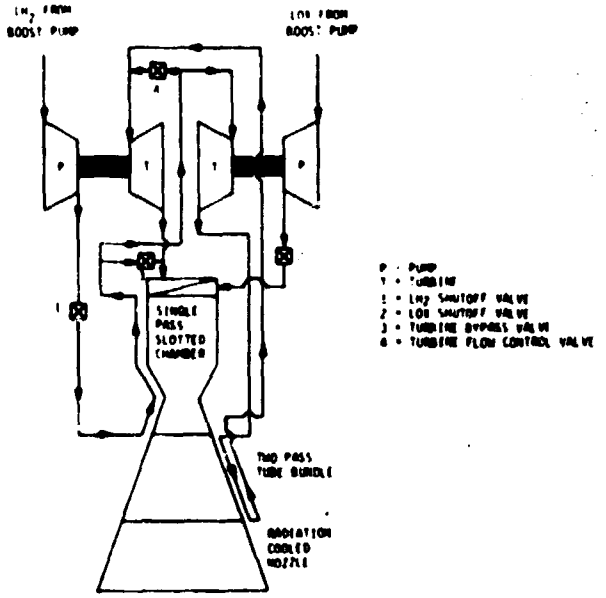

Turbine Exhaust Gas Reheat, Series Turbines, Advanced Expander Cycle Flow Schematic

Figure 2. Engine Cycle Optimization, Cycles Considered

II, B, Results and Conclusions (cont.)

has a low horsepower requirement and, hence, its turbine takes a very low flow, with a corresponding low efficiency in the parallel turbine case.

The regenerator concept employs a heat exchanger to transfer energy from the turbine exhaust gas to the liquid hydrogen discharging from the pump prior to entering the combustion chamber coolant jacket. From the regenerator, the turbine exhaust gas enters the injector. The heated hydrogen enters the cooling passageways of the thrust chamber jacket and nozzle and then drives the turbines. Utilizing a turbine exhaust gas regenerator in the expander cycle results in an increased heat flow to the hydrogen and, thus, a higher turbine inlet temperature. This can result in more turbine horsepower output, higher chamber pressure, or in more turbine bypass and/or cycle margin if desired. The full benefit of the increased heat flow is offset partly by a simultaneous increase in system pressure losses. A parametric study was conducted to optimize the engine performance and identify regenerator operating conditions.

In the turbine exhaust gas reheat cycle, the hydrogen flow is first used to cool the combustion chamber and then drives the low horsepower oxidizer turbopump. The low horsepower pump is driven first to take only a small pressure and temperature drop across the turbine. The hydrogen flow is then used to cool the fixed portion of the nozzle, regaining some temperature, before driving the high horsepower hydrogen pump.

The results of the cycle evaluations and performance/weight trade analyses are summarized in Table II. The table shows that the largest benefit is obtained with a series turbine arrangement rather than with parallel turbines. Chamber pressure gains are modest. Performance improvements are small because the rate of change in specific impulse with nozzle area ratio in the range being analyzed is small. The small performance improvement does not make up for the additional regenerator weight. The weight shown is for an aluminum regenerator.

TABLE II

EXPANDER CYCLE OPTIMIZATION SUMMARY

Thrust = 15,000 lb
Engine Length = 120 in. (Nozzle Extended)

Cycle	Chamber Pressure, psia	Nozzle Area Ratio	Engine Specific Impulse, sec	Engine Weight, lb	AMOTV Relative Payload, lb
Parallel Turbines	1200	473	477.2	502	0
Series Turbines	1345	530	478.1	514	+53
Turbine Exhaust Heat Regen. & Series Turbines	1375	542	478.3	535	+44
Turbine Exhaust Reheat & Series Turbine	1365	538	478.2	520	+53

NOTE: $\Delta PL/\Delta I_s$ = 73 lb/sec $\Delta PL/\Delta W_E$ = -1.1 lb/lb

II, B, Results and Conclusions (cont.)

The cycle comparisons were made at 10, 15, and 20K lbF, but the thrust level did not alter the basic conclusions.

Based upon the results shown, a series turbine cycle was baselined. Because performance improvements were so small, it was decided to baseline the chamber pressure at 1200 psia and, hence, apply the series turbine performance improvement to the engine power balance margin. This results in only a slightly conservative state-of-the-art design point. In addition, the regenerator cycle was judged to provide a good backup if component performance and pressure drops are worse than design analyses predict.

3. Alternate Low-Thrust Capability

Operation of a 15K lbF expander cycle engine at low-thrust in a range of 1K to 2K lbF was also analytically investigated. Operation at 10% of rated thrust was feasible by means of part replacement and addition (i.e., by "kitting" the engine). The recommended TCA "kits" consist of smaller diameter, oxidizer coaxial injection elements and an orifice in the hydrogen line downstream of the thrust chamber coolant jacket exit. The new oxidizer injection elements are required to avoid chugging instability, and the orifice is required to maintain the coolant jacket exit pressure well above the critical pressure of hydrogen to avoid the problems associated with two-phase coolant flow. Because the turbine inlet temperature increases as the thrust level is decreased, the expander cycle power balance margin is significantly increased at low-thrust. This makes orificing the coolant jacket exit feasible.

Oxidizer pump stability could be a problem at a thrust level of less than 2K lbF. However, a recirculation flow line and valve could alleviate the problem and have been recommended as the state-of-the-art "kit."

The alternate low-thrust conclusions are summarized in Table III.

TABLE III

ALTERNATE LOW-THRUST CAPABILITY CONCLUSIONS

- "Kit" injector by changing oxidizer injection elements
- Engine service life and reliability is not reduced
- Marginal coolant flow stability at 10%
- Marginal pump stability at thrust levels $\leq$10%; ox. pump recirculation flow recommended
- Modification to controls not required
- Large power balance margin at low thrust
- Effect upon engine weight is negligible
- DDT&E cost impact $\sim$\$15M (injector mod. only)
- Experimental verification required

II, B, Results and Conclusions (cont.)

4. Safety and Reliability

Design impacts resulting from the man-rating, safety, and reliability requirements that were previously identified (Ref. 1) are as follows:

- Engine should be designed for a multi-engine installation (preferably twin engines)
- Series-redundant main propellant valves are required
- Redundant spark igniter is required
- Dual coils should be used on all valves identified by FMEA as single point failures

A multiple-engine installation is necessary to meet the crew safety requirements. The series-redundant main propellant valves are required to assure that the engine will shut down. They also inhibit leakage of propellant through the engine into the Orbiter's payload bay. Redundant spark ignition is required to assure that the engine will start on all burns. Dual coils are required to assure that the actuator will function and provide sufficient force to open critical valves.

The conclusions derived from the updated analyses performed in these extension efforts are summarized in Table IV.

5. Development Risk Comparison

The objective of this subtask was to develop a comparison between the engine concepts detailed in the initial efforts on Contracts NAS 8-32996 (Ref. 5) and NAS 8-32999 (Ref. 1) for engine development risk.

TABLE IV

SAFETY AND RELIABILITY ANALYSIS CONCLUSIONS

- Quantifying crew risk demands judgment.
  - Comparison with other hazardous careers indicates that 2.5×10^{-4} is a realistic goal.
- A single engine does not meet crew risk requirements.
- Twin 10K lbF engines are a good compromise in terms of crew risk, mission reliability, weight, payload, and cost considerations.
- Three 10K lbF engines are most attractive for minimum mission failure rate and crew risk when complete engine-out is assumed as acceptable.
- Compared to a staged-combustion cycle engine, the expander cycle has a lower failure rate and less crew risk.
- Twin 10K lbF expander cycle engines are the best option for minimum crew risk and maximum mission reliability.
- Maximum reliability and minimum crew risk are best achieved when introduced early in the engine design process.

II, B, Results and Conclusions (cont.)

The development risk comparison is expressed in terms of the probability of achieving the schedules shown in the referenced studies and of attaining slipped and advanced versions of this schedule. In addition, schedule cost impacts are also established by using the costs reported in Reference 6. The approach to the study was to evaluate potential problems that might occur during the engine development program and to assess the impact of the occurrence of these problems upon both the DDT&E schedule and cost. The engine concepts recommended from Contracts NAS 8-32996 and NAS 8-32999 are the staged combustion and expander cycles, respectively.

The primary components which create risk factors for each of the engine cycles shown below are as follows:

Staged-Combustion Cycle	Expander Cycle
° Preburner	° Combustion Chamber/Injector
° Combustion Chamber/Injector	° Turbomachinery
° Turbomachinery	

The development schedule and cost risk assessment is summarized in Table V. The cost overrun estimates for the nominal and long schedules were determined by maintaining the short schedule manloading over the extended program durations. There is no cost risk associated with the long program because it has been planned to handle all foreseeable problems.

The data in Table V show that both schedule and cost risk are greater with a staged-combustion cycle engine. This is primarily due to the additional combustion device (preburner) and increased system interactions. Using a nominal program as a baseline, the schedule risk with a staged-combustion cycle engine is one year greater and the cost risk is almost 3 times greater than with an expander cycle engine.

TABLE V

DEVELOPMENT RISK ASSESSMENT (10K lbF ENGINES)

Engine Cycle	Planned Schedule	Planned DDT&E Duration, Years	Schedule Risk, Years	Potential DDT&E Duration, Years	Potential DDT&E Cost Overrun Estimates, Million $
Expander	Short(1)	4.5	1.0 to 2.5	5.5 to 7.0	41 (probable) to 107 (Max)
	Nominal(2)	5.5	1.5	7.0	66 (probable)
	Long(3)	7.0	---	7.0	---
Staged Combustion	Short(1)	4.75	1.0 to 3.5	5.75 to 8.25	101 (probable) to 295 (Max)
	Nominal(2)	5.75	2.50	8.25	194 (probable)
	Long(3)	8.25	---	8.25	---

(1) Assumes 100% success-oriented program.
(2) Program planned to handle an average number of development problems.
(3) Program planned to handle all potential development problems.

6. Cost Comparisons

Study cost estimates were prepared for both the expander cycle engine (Ref. 6) and the staged-combustion cycle engine (Ref. 3). Compared to an expander cycle engine, the staged-combustion cycle engine is more costly in all program phases, as shown below.

Program Phase	Staged-Combustion Cycle Cost Increase, Million, $
DDT&E	110
Production	30
Operations (10 years)	5

Costs were compared at the 20K lb thrust level because that was the design thrust recommended by Ref. 5.

The cost differences between the engine cycles can be explained primarily by the following:

- Elimination of a preburner lowers expander cycle DDT&E costs
- Fewer components lower expander cycle production costs
- Lower follow-on spares costs lower expander cycle operations cost

The expander cycle engine is the lower-risk and lower-cost OTV engine option.

II, B, Results and Conclusions (cont.)

7. Baseline Phase A Engine

The results of the Phase A studies have led to the selection of a series turbine drive advanced expander cycle (AEC) engine. The baseline engine cycle schematic and engine characteristics, established to initiate the Point Design studies under Contract NAS 8-33574, are shown on Figure 3. A nominal thrust of 15K lb was selected by NASA/MSFC.

The O_2/H_2 expander cycle engine uses a series turbine drive cycle (Figure 3). The engine uses hydraulically driven boost pumps, with the flow tapped off the main pump stages. Fuel flows from the pump discharge to the thrust chamber where 85% of the hydrogen flow is used to cool the slotted copper chamber in a single pass from an area ratio of 10.6:1 to the injector head-end. Fifteen (15) percent of the hydrogen is used to cool the tube bundle nozzle in two passes from an area ratio of 10.6:1 to the end of the fixed nozzle (ϵ = 172:1). The coolant flows are merged, and 6% of the total engine hydrogen flow is used to bypass both turbines to provide cycle power balance margin and thrust control. The remaining hydrogen flow first drives the fuel pump turbine and then the oxidizer pump turbine. After driving the oxidizer pump turbine, a small amount of heated hydrogen is tapped off for hydrogen tank pressurization. The remaining hydrogen flow is then injected into the combustion chamber.

At rated thrust operation, oxidizer flows from the main pump discharge directly to the thrust chamber and is injected in a liquid state. A small amount of oxidizer is tapped off and heated by the hydrogen turbine bypass flowrate in a heat exchanger to provide LOX tank pressuriation.

A lightweight, state-of-theart Columbium nozzle extension was selected as the baseline on the basis of ALRC experience gained on the Transtage, Apollo, SPS, and OMS engine programs.

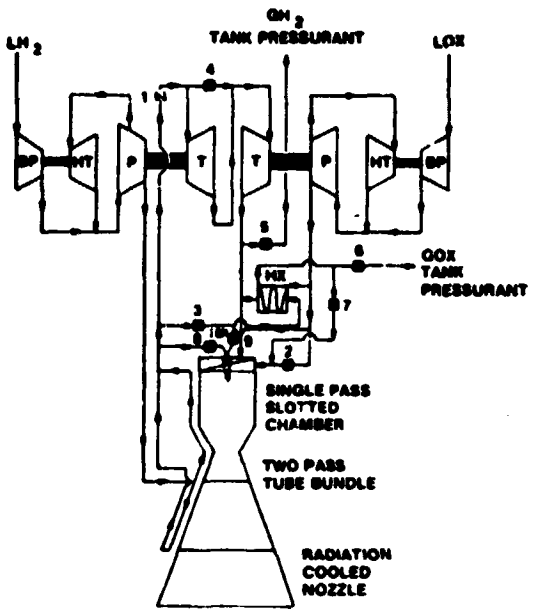

BP	BOOST PUMP
HT	HYDRAULIC TURBINE
P	PUMP
T	TURBINE
1	LH 2 SHUTOFF VALVE
2	LOX SHUTOFF VALVE
3	TURBINE BYPASS VALVE
4	TURBINE FLOW CONTROL VALVE
5	GH 2 PRESSURIZATION FLOW VALVE
6	GOX PRESSURIZATION FLOW VALVE
7	GOX START BYPASS VALVE
8	IGNITER FUEL VALVE
9	IGNITER OX VALVE
HX	HEAT EXCHANGER
IGN	IGNITION SYSTEM

RATED VACUUM THRUST, LB	15000
NOMINAL MIXTURE RATIO	6.0
CHAMBER PRESSURE	1250
NOZZLE AREA RATIO	473
DELIVERED SPECIFIC IMPULSE, SEC	477.2
ENGINE DRY WEIGHT, LB	562
ENGINE LENGTH, IN.	
NOZZLE EXTENSION RETRACTED	69
NOZZLE EXTENDED	120
NOZZLE EXIT DIAMETER, IN.	66.7
ENGINE FLOW RATES, LB/SEC	
HYDROGEN	4.49
OXYGEN	26.94

Figure 3. Baseline Phase A Advanced Expander Cycle Engine Schematic

II, B, Results and Conclusions (cont.)

The engine is also capable of operating in a tank-head idle mode and is adaptable to extended low-thrust operation at a thrust level of 1.5K lb.

III. TASK I: ADVANCED EXPANDER CYCLE ENGINE OPTIMIZATION

The objective of this task was to optimize the performance of expander cycle engines at vacuum thrust levels of 10K, 15K, and 20K lb. This optimization was conducted for a maximum engine length with an extendible nozzle in the retracted position of 60 in. and an engine mixture ratio of 6.0:1. The information generated in this task formed the basis for an expander cycle engine point design study.

The optimization reported upon herein consists of thrust chamber geometry, cycle and controls analyses. In addition, the sensitivity of a recommended baseline expander cycle to component performance variations was determined and the chilldown/start propellant consumptions were estimated.

A. THRUST CHAMBER GEOMETRY OPTIMIZATION

This subtask consisted of heat transfer, cycle, and performance/weight tradeoff analyses to determine the effect the combustion chamber length and contraction ratio upon the cycle power balance, engine performance, and engine weight.

Performance analyses have shown (Ref. 1) that a minimum chamber length of about 12 in. is required to meet a Phase "A" ERE goal of 99.5%. Longer chambers lower the energy release loss, increase the hydrogen outlet temperature, and increase the coolant jacket pressure drop. In some cases, the increased turbine inlet temperature more than compensates for the increased pressure loss and results in higher thrust chamber pressure. For an engine with a fixed envelope (length), chamber pressure increases result in higher area ratios and, hence, higher performance (I_s). Conversely, longer chambers reduce the length of the nozzle that can be fit in the fixed length constraint, thereby reducing the area ratio and performance. Longer chambers also result in heavier engine weights.

III, A, Thrust Chamber Geometry Optimization (cont.)

The chamber contraction ratio has effects similar to those of chamber length. High chamber contraction ratios reduce the coolant jacket pressure drop and coolant outlet temperature (turbine inlet). Chamber contraction ratio increases also result in heavier chambers.

Heat transfer analyses were undertaken to establish the differences in chamber coolant jacket pressure drop and coolant outlet temperature due to variations in combustion chamber length and contraction ratio. Baseline values selected during the initial study efforts (Ref. 1) were a chamber length of 18 in. and a contraction ratio of 3.66. These selections were based upon the results of analyses performed in other past contractual efforts (Refs. 7, 8, and 9).

Chamber contraction ratio length (L') were varied in order that the tradeoffs among heat load, required pressure drop, and nozzle area ratio (restricted by stowed length) could be used in system optimization studies. These studies were conducted at each thrust level for a range of chamber pressures as shown below:

Thrust, lbF,	Chamber Pressure, psia
10K	1300 ± 200
15K	1200 ± 200
20K	1100 ± 200

The nominal chamber pressure values were selected during the initial Phase "A" (Ref. 1) efforts.

III, A, Thrust Chamber Geometry Optimization (cont.)

For each thrust and chamber pressure combination, chamber designs were generated as a function of L' (~12 to 30 in.) for contraction ratios of 2.32, 2.99, 3.66, and 5.0.

Design criteria and procedures used herein were identical to those used in the conduct of Task III of the original contract (Ref. 1). The channel widths in the cylindrical section were optimized for minimum pressure drop for each design (within a wall strength criterion which defines the maximum allowable channel width). This constraint was encountered in all designs with a contraction ratio of 5.0 and at the 15K and 20K thrust levels for a contraction ratio of 3.66. Channel depths are defined by the wall temperature limits associated with a cycle life of 300 cycles, provided that the channel aspect ratio (depth/width) does not exceed 5:1. All chambers are one-pass designs, with 85% of the total hydrogen flowing from an area ratio of 8:1 to the injector. This value was changed to 10.6:1 during the point design study. The fixed portion of the nozzle, from an area ratio of 8:1 to the extendible nozzle attachment point, is regeneratively cooled with the remaining 15% of the hydrogen flow. This fixed nozzle portion is a two-pass tube bundle design. The nozzle extention is a radiation-cooled design.

Figures 4 through 7 present the chamber pressure drop results for the four contraction ratios considered in this study at the nominal thrust chamber pressures. Pressure drop is generally reduced with increasing thrust and contraction ratio. The exception occurs at a contraction ratio of 5.0 (see Figure 7). This figure shows that the pressure drops for 20K lb thrust are slightly higher than those for 15K lb thrust. This occurs because the chamber channel designs at 20K lb thrust became aspect ratio (channel depth/width) limited at almost all axial locations. In all cases, the tube bundle nozzle pressure drops are very small (6 to 12 psi) and, hence, the chamber pressure drop governs the engine pressure schedule.

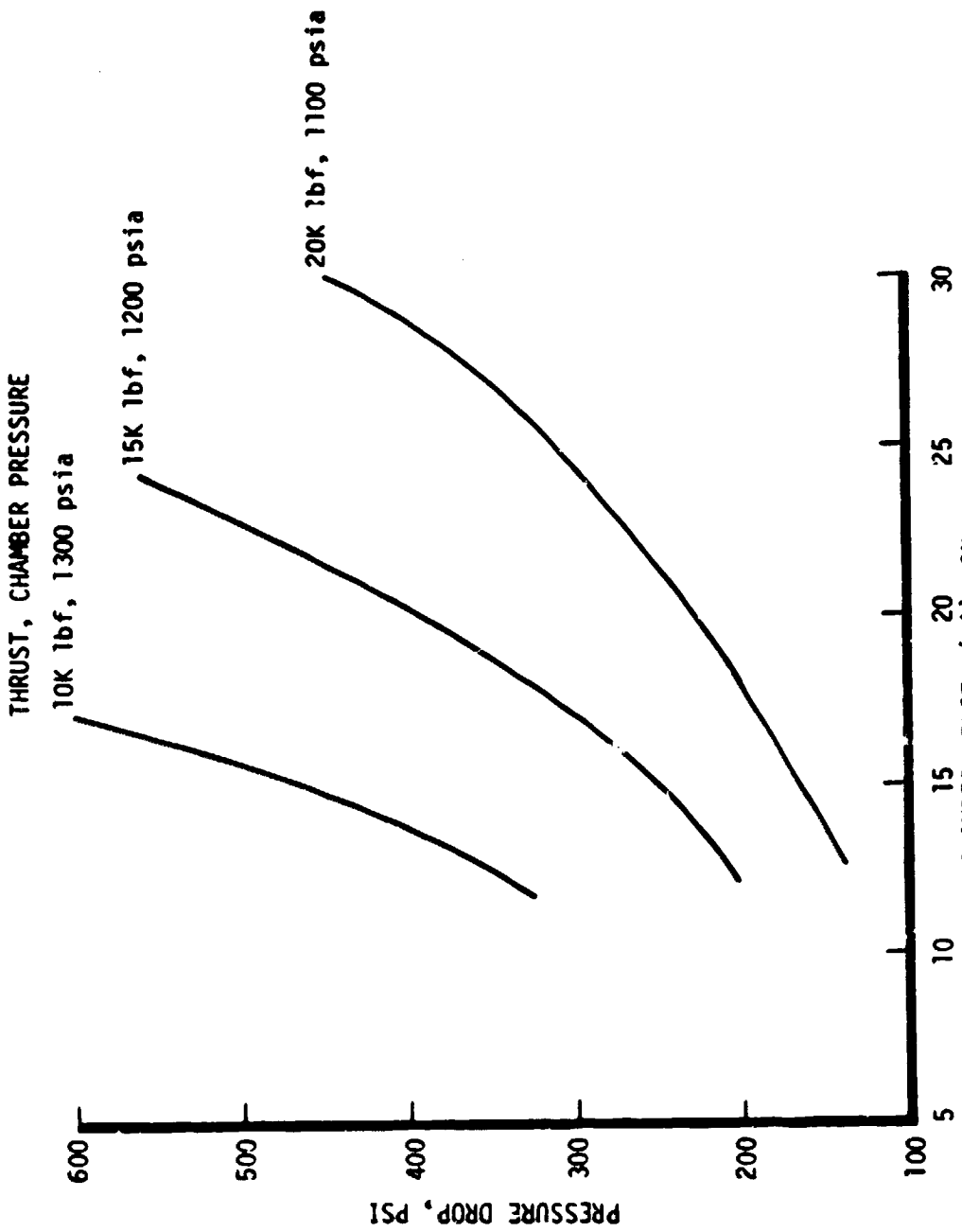

Figure 4. Chamber Pressure Drop Requirements, Contraction Ratio = 2.32

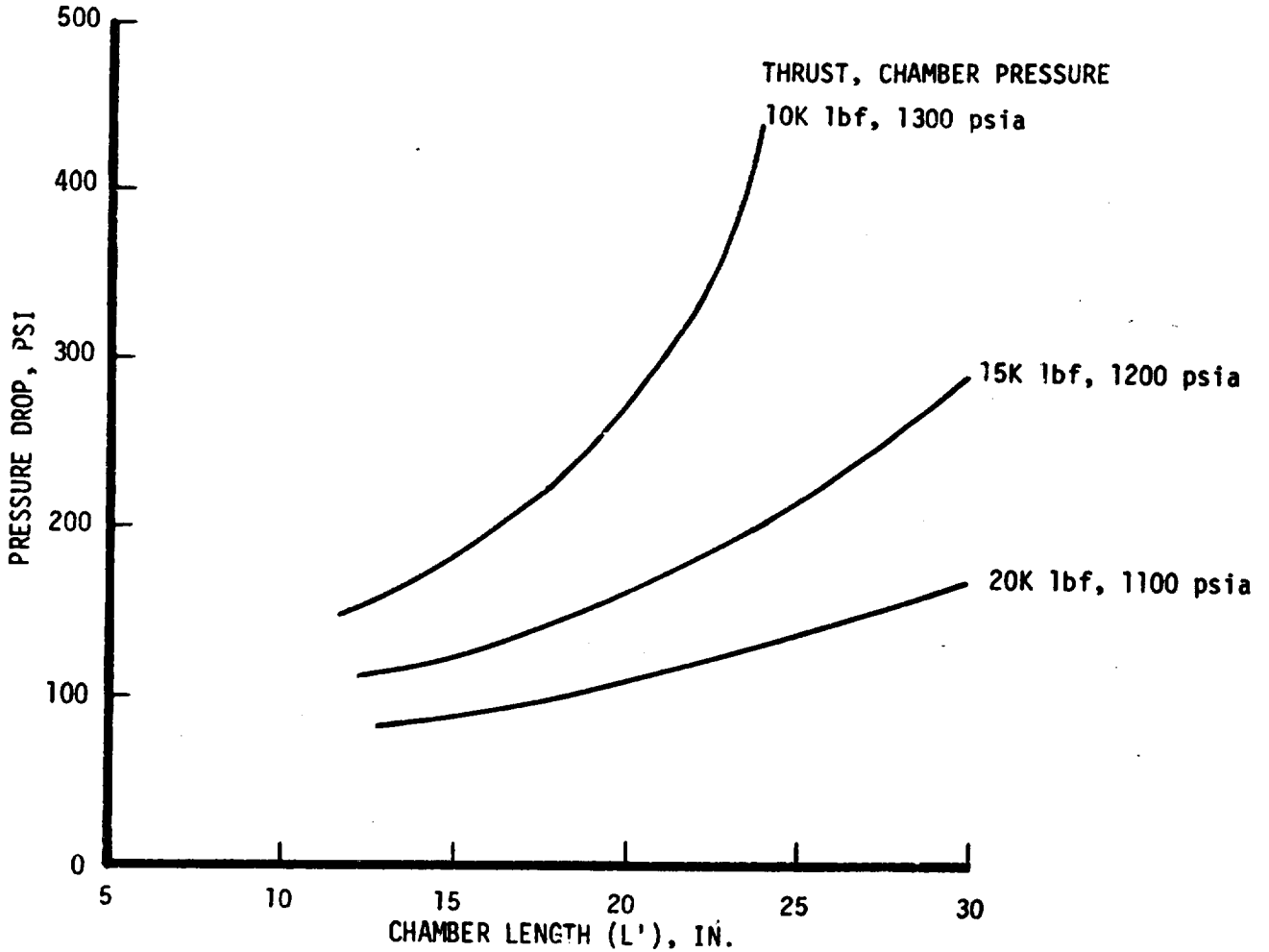

Figure 5. Chamber Pressure Drop Requirements, Contraction Ratio = 2.99

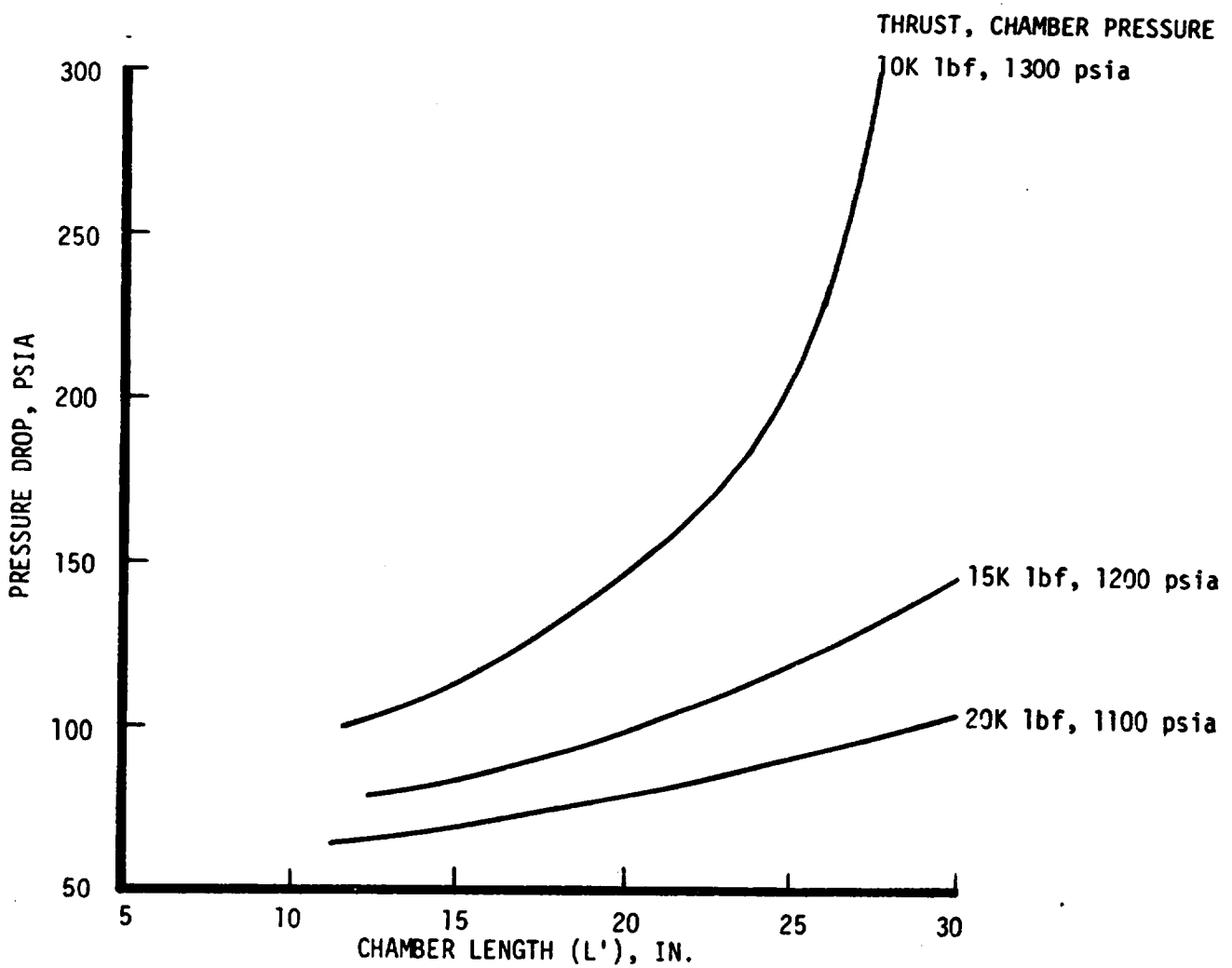

Figure 6. Chamber Pressure Drop Requirements, Contraction Ratio = 3.66

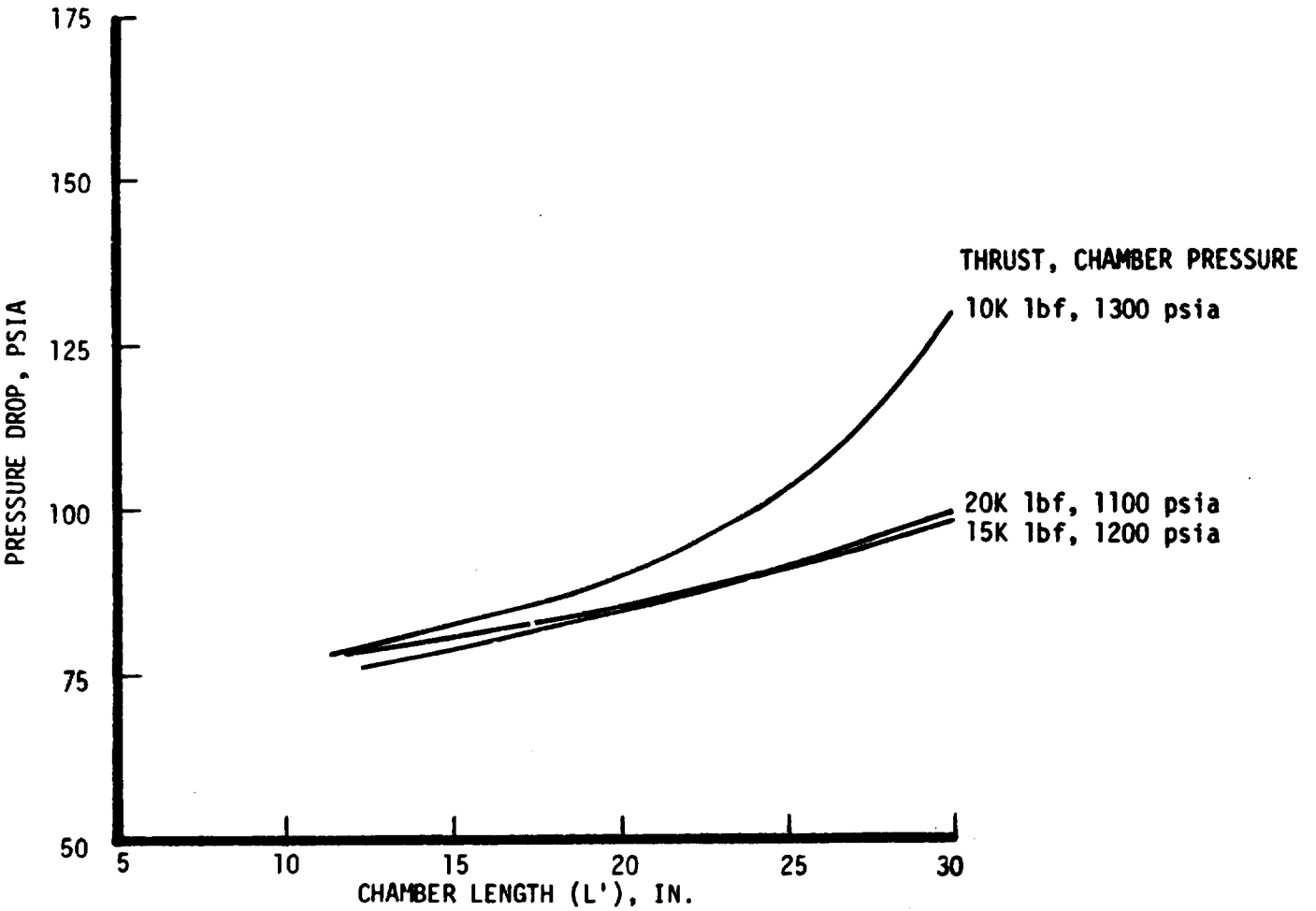

Figure 7. Chamber Pressure Drop Requirements, Contraction Ratio = 5.00

III, A, Thrust Chamber Geometry Optimization (cont.)

The total turbine flowrate is the sum of the chamber and nozzle coolant flows. The turbine inlet temperature was determined by establishing the coolant bulk temperature rises in both the chamber and nozzle coolant jacket. Eighty-five percent of the hydrogen flow is used to cool the chamber, and the remaining 15% is used to cool the fixed nozzle. The total nozzle heat load varies with L' because the cooled area ratio changes. The calculated turbine inlet temperatures for the four contraction ratios considered and at the respective baseline chamber pressure values are presented in Figures 8, 9, 10, and 11. The data show that the turbine inlet temperature increases with reduced thrust and contraction ratio.

Engine cycle power balance analysis was performed on the basis of the heat transfer analyses results to establish the attainable chamber pressure as a function of chamber length and contraction ratio, holding pump discharge pressure constant at the nominal values for each thrust level. Delivered performance and engine weight was then calculated at these chamber pressures. Weight and specific impulse tradeoffs were made by using the payload partials derived from NASA TMX-73394 (Ref.2). These partials are:

	AMOTV	APOTV
$\Delta W_{PL}/\Delta I_S$, lb/sec	+73	+60
$\Delta W_{PL}/\Delta W_{ENG}$, lb/sec	-1.1	-1.1

The baseline engine cycle used in this portion of the study was a parallel turbine drive cycle which is shown by the simplified cycle schematic of Figure 12.

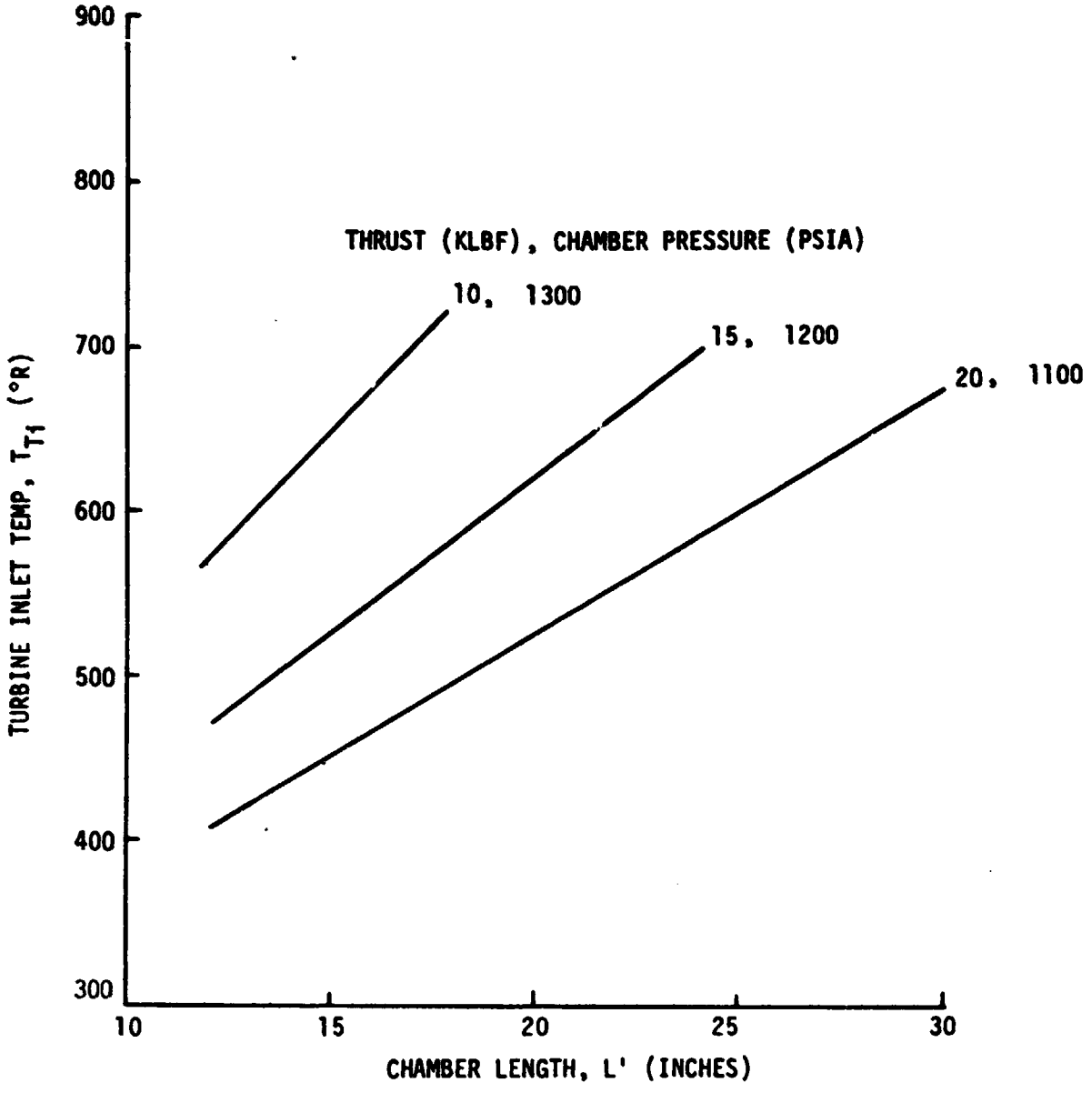

Figure 8. Turbine Inlet Temperature vs Chamber Length (Contraction Ratio = 2.32)

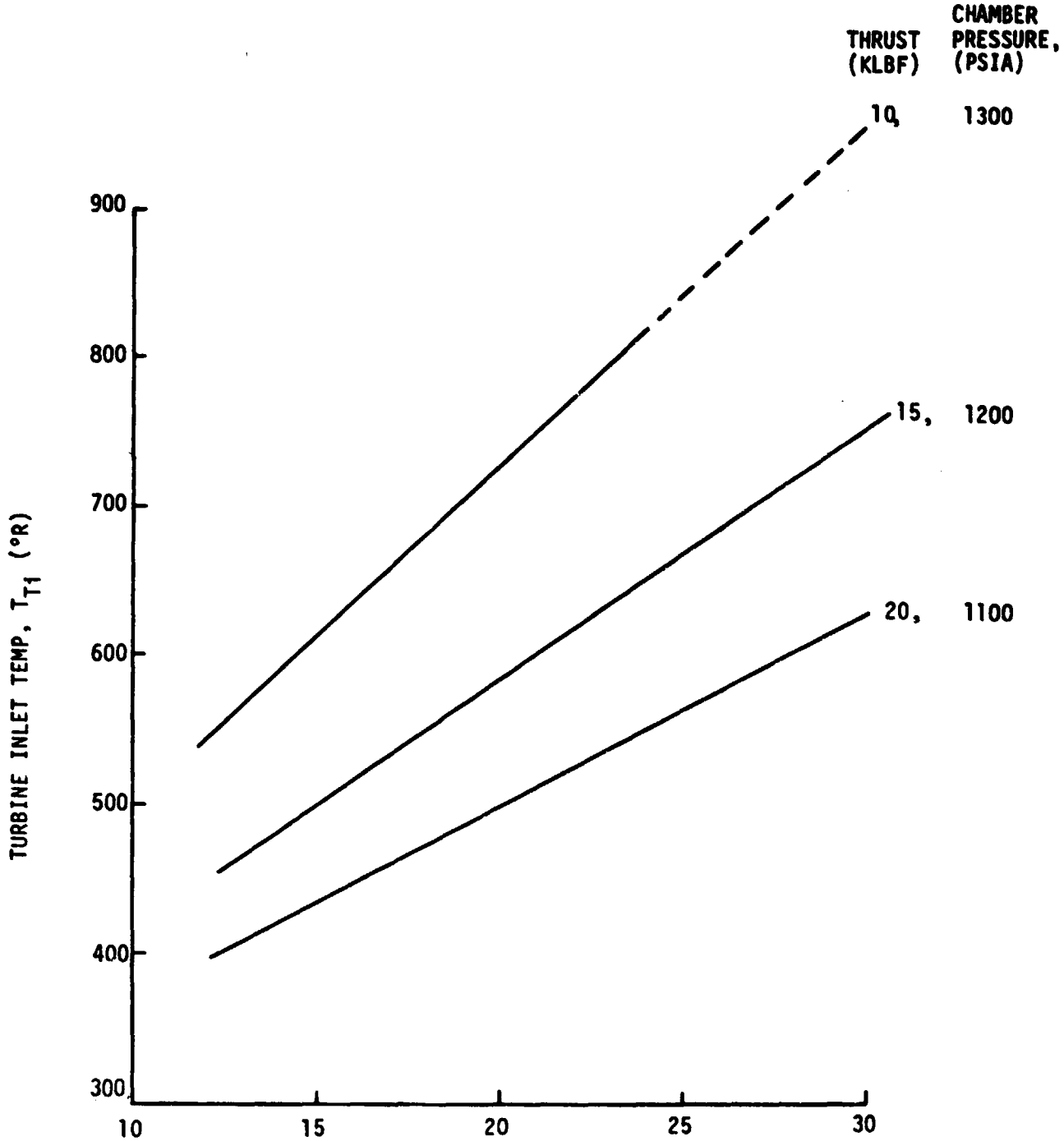

Figure 9. Turbine Inlet Temperature vs Chamber Length (Contraction Ratio = 2.99)

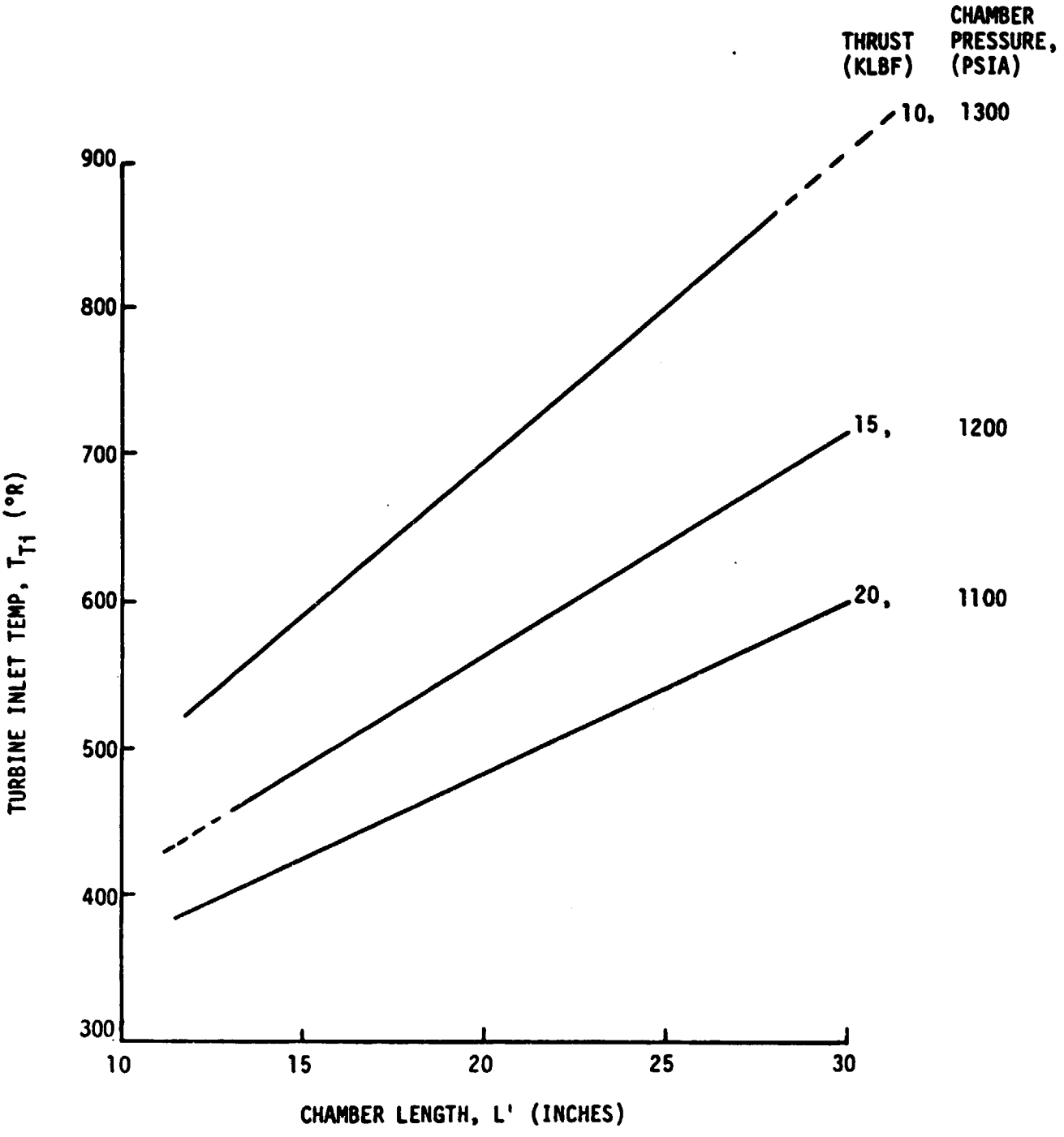

Figure 10. Turbine Inlet Temperature vs Chamber Length (Contraction Ratio = 3.66)

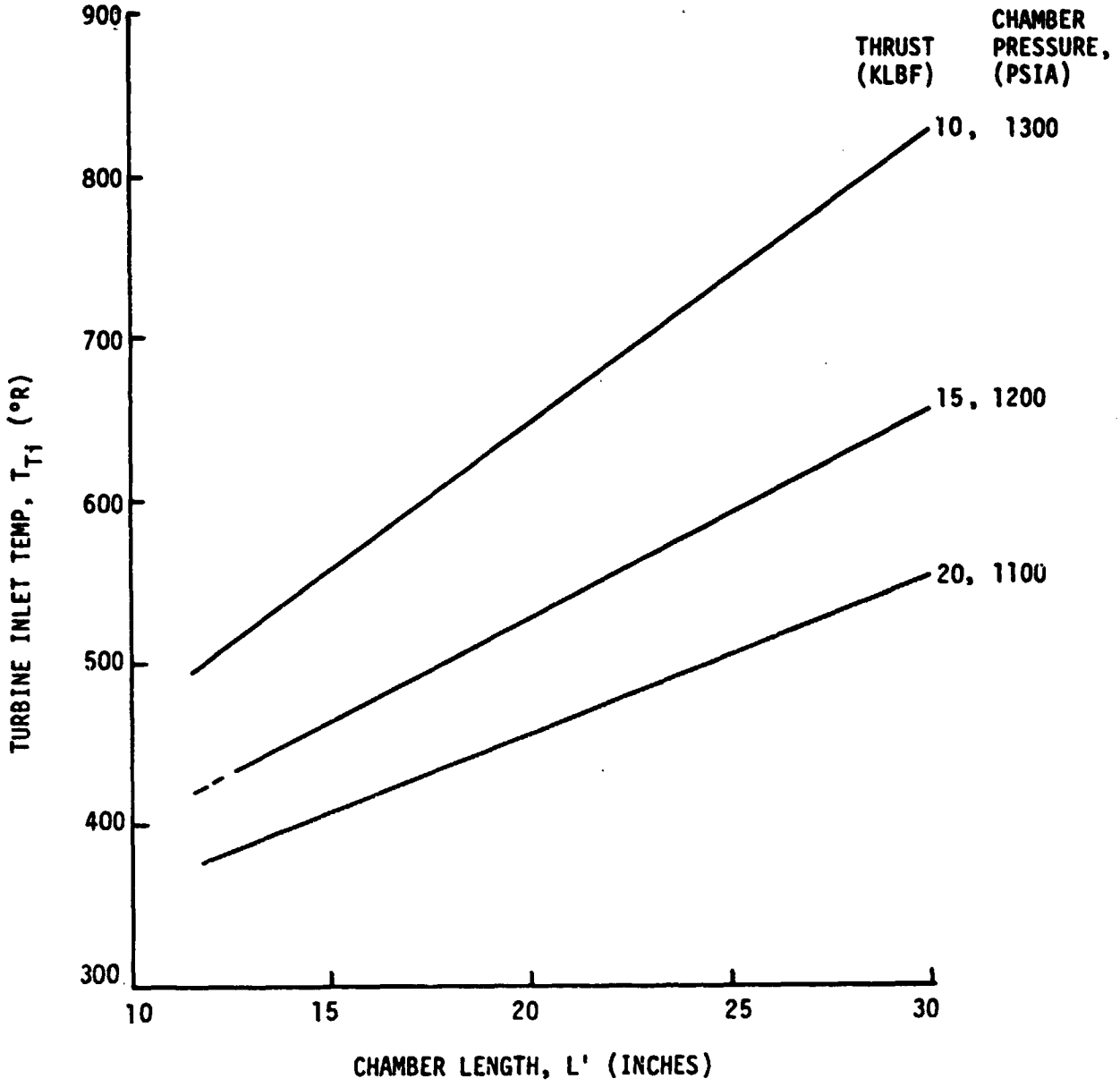

Figure 11. Turbine Inlet Temperature vs Chamber Length (Contraction Ratio = 5.00)

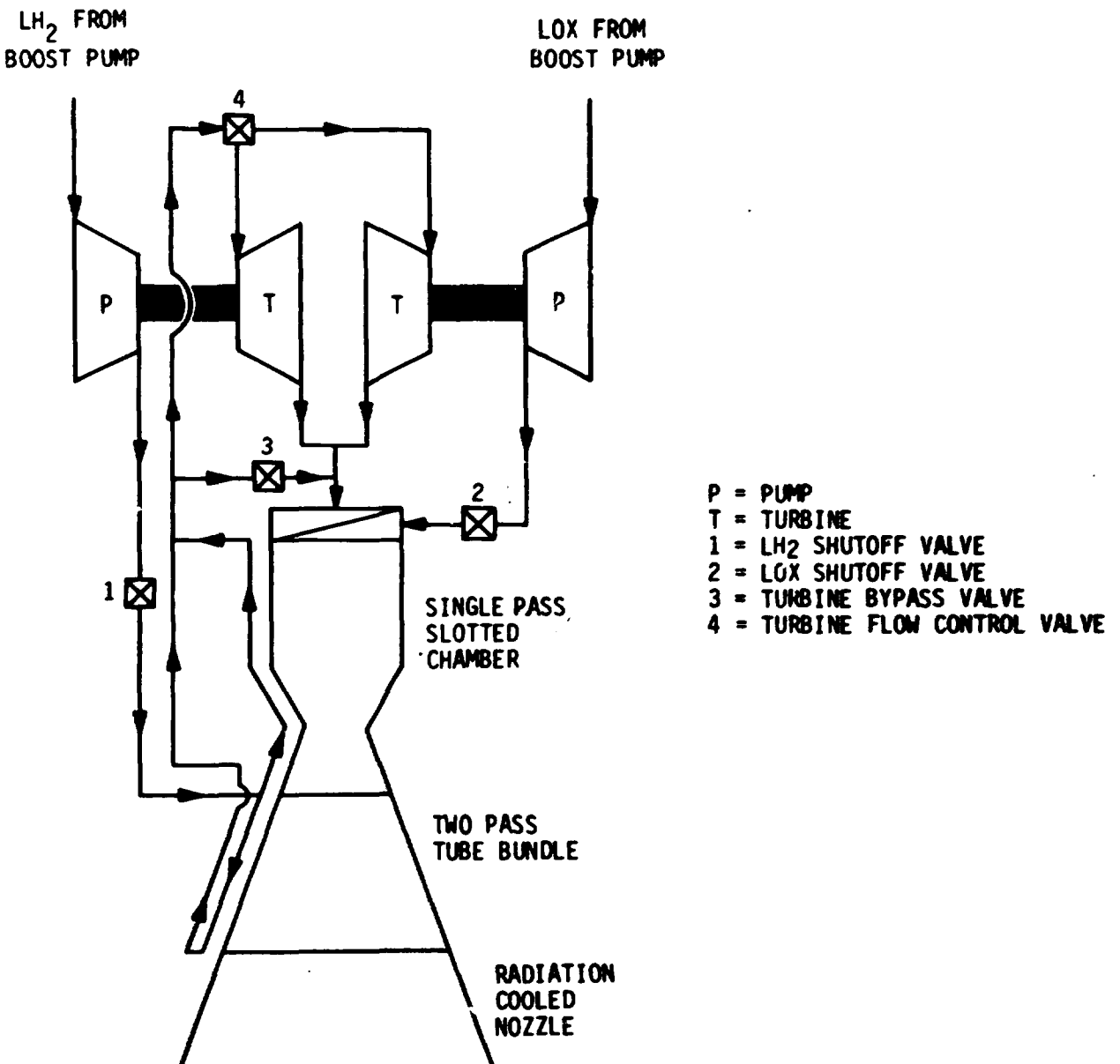

Figure 12. Parallel Turbine Advanced Expander Cycle Flow Schematic

The results of the power balance and tradeoff analyses are displayed on Figures 13 through 21. The figures show that the baseline chamber length of 18 in. and a contraction ratio of 3.66 are either optimum or very nearly so at all thrust levels. Therefore, these values were used throughout the remaining study efforts.

B. CYCLE OPTIMIZATION

The baseline expander engine cycle selected in the prior Phase "A" study efforts was the parallel turbine drive concept previously shown on Figure 12. Cycle variations were analyzed in this subtask to optimize the engine. Concepts considered were (1) series turbines drive, (2) turbine exhaust heat regeneration, and (3) turbine exhaust reheat. A description of each of these cycles, accompanied by a comparative analysis for each, is presented in the following paragraphs. Cycle power balance analyses were conducted for nominal chamber pressure values of 1300, 1200, and 1100 psia at thrust levels of 10K, 15K, and 20K lb, respectively, as well as for fixed pump discharge pressures in order to obtain higher chamber pressure levels.

1. Series vs Parallel Turbines

The primary issue in these comparisons in whether the higher flowrate, higher efficiency turbines can compensate for the turbine pressure drops when operated in series. A simplified flow schematic of the series turbine arrangement is shown on Figure 22.

To support the cycle power balance analyses, a turbomachinery analysis was conducted to obtain component efficiency data that are representative of the two turbine drive cycles. The efficiencies of the pump and turbines were evaluated as a function of thrust level for both the parallel

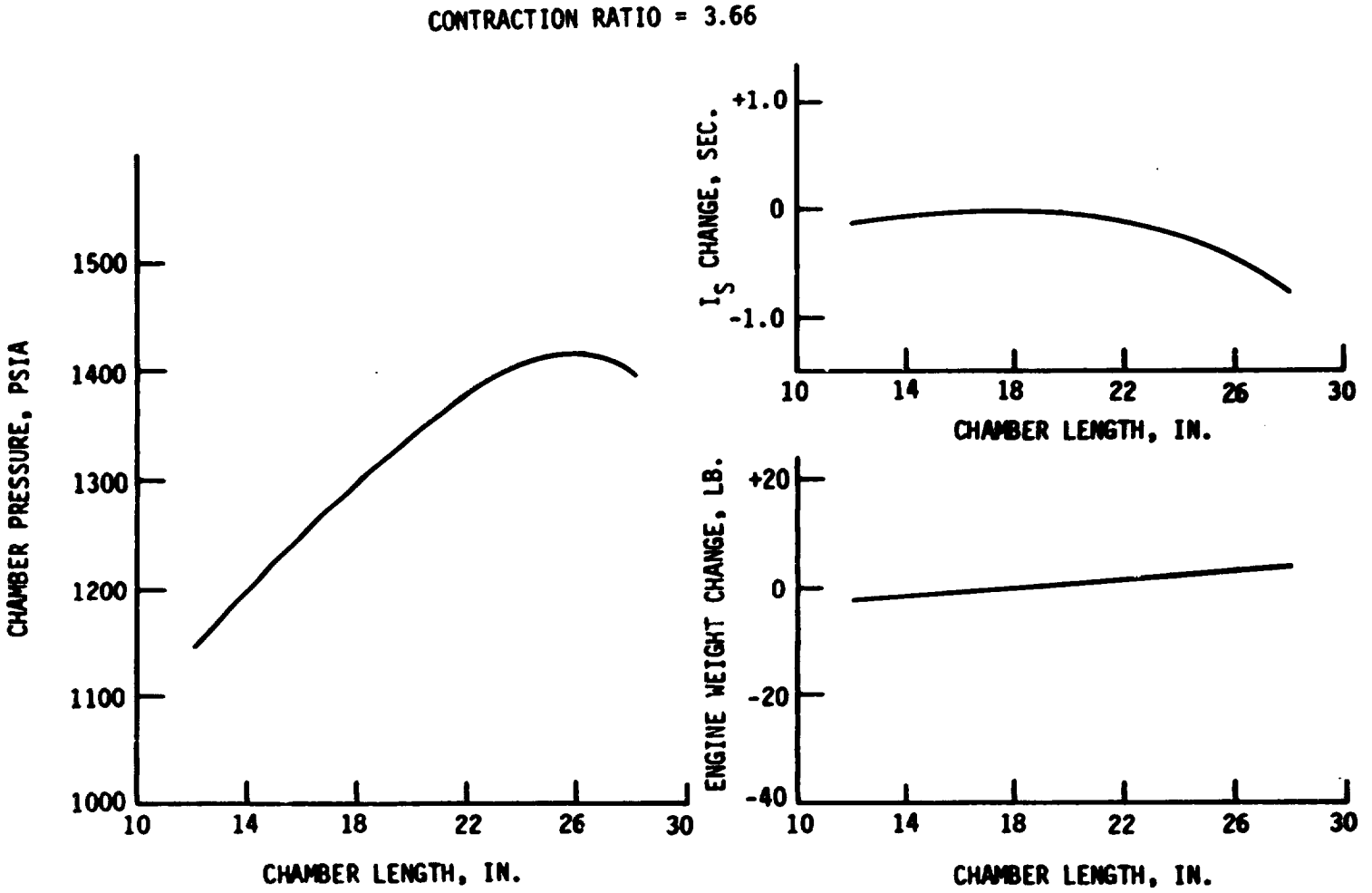

Figure 13. Chamber Length Effects at F = 10,000 lb

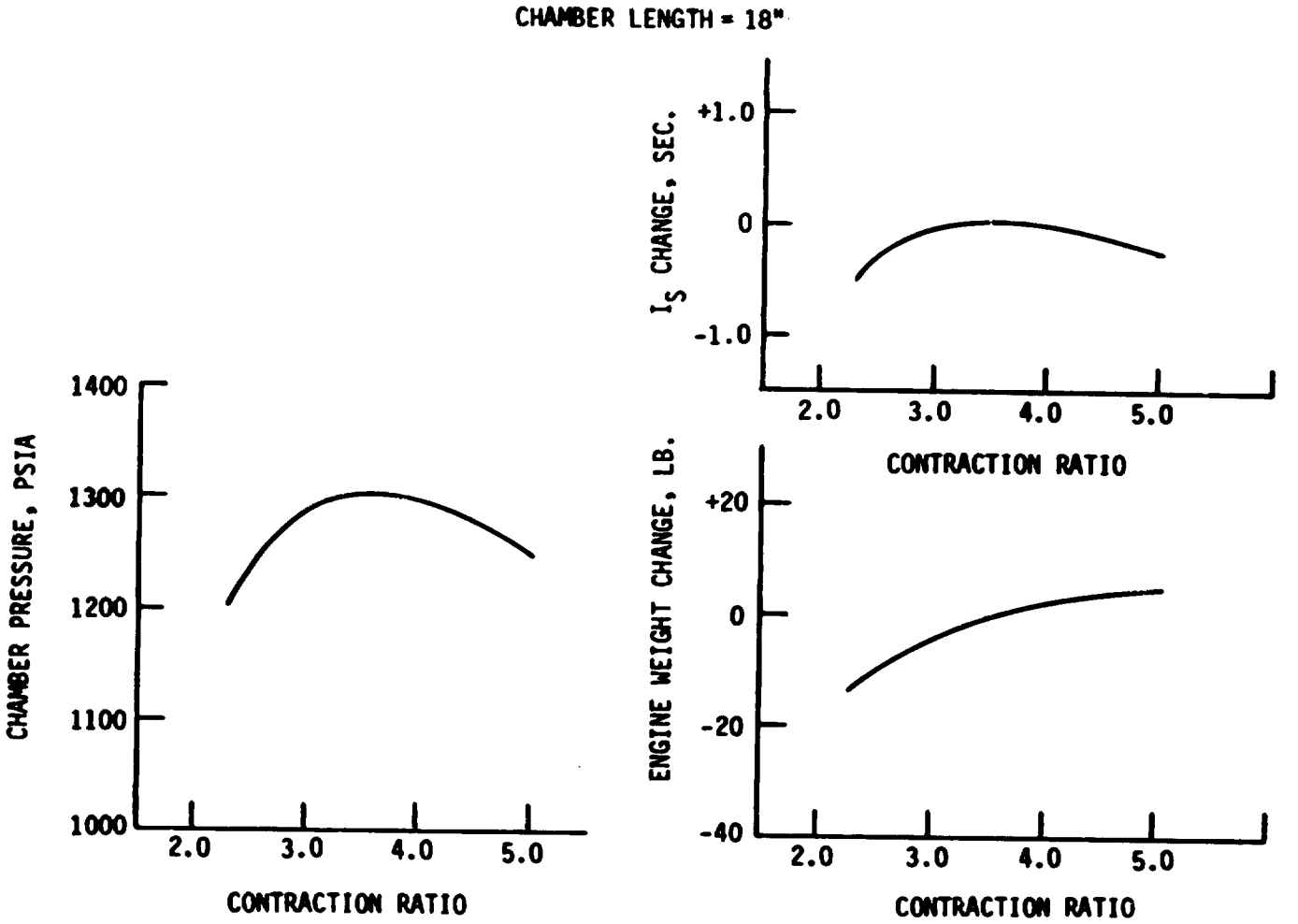

Figure 14. Contraction Ratio Effects at F = 10,000 lb

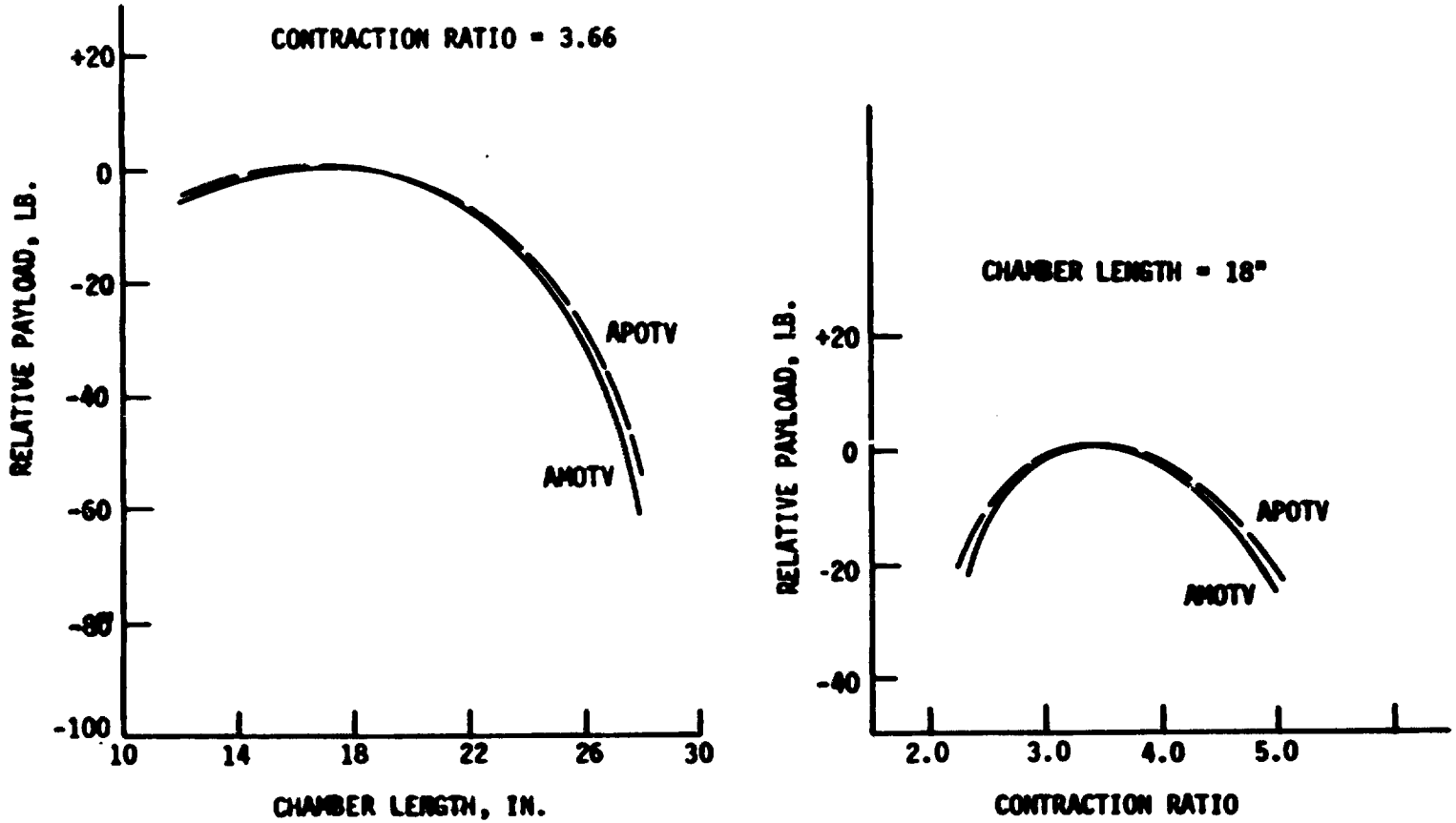

Figure 15. Chamber Length and Contraction Ratio Optimization at F = 10,000 lb

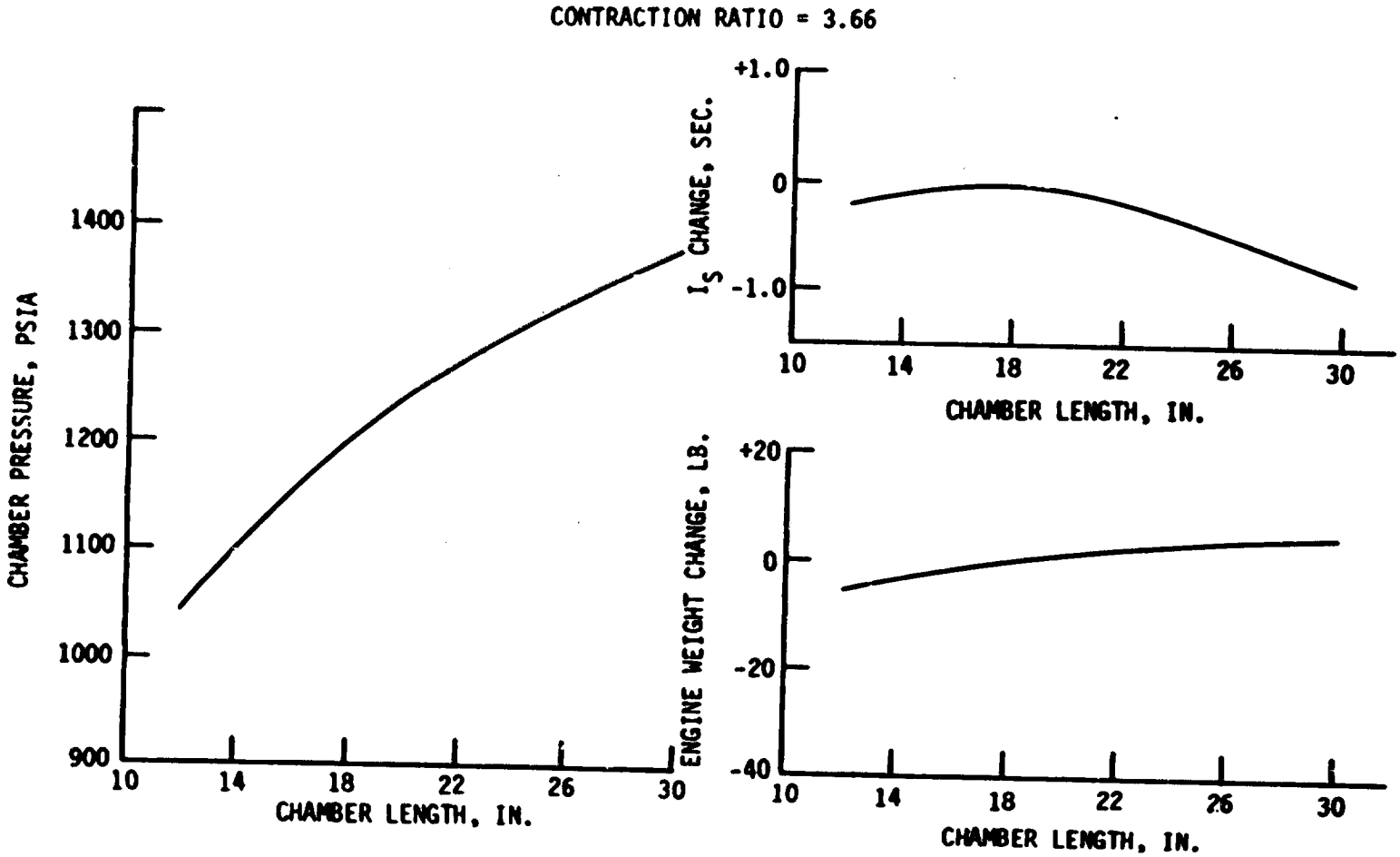

Figure 16. Chamber Length Effects at F = 15,000 lb

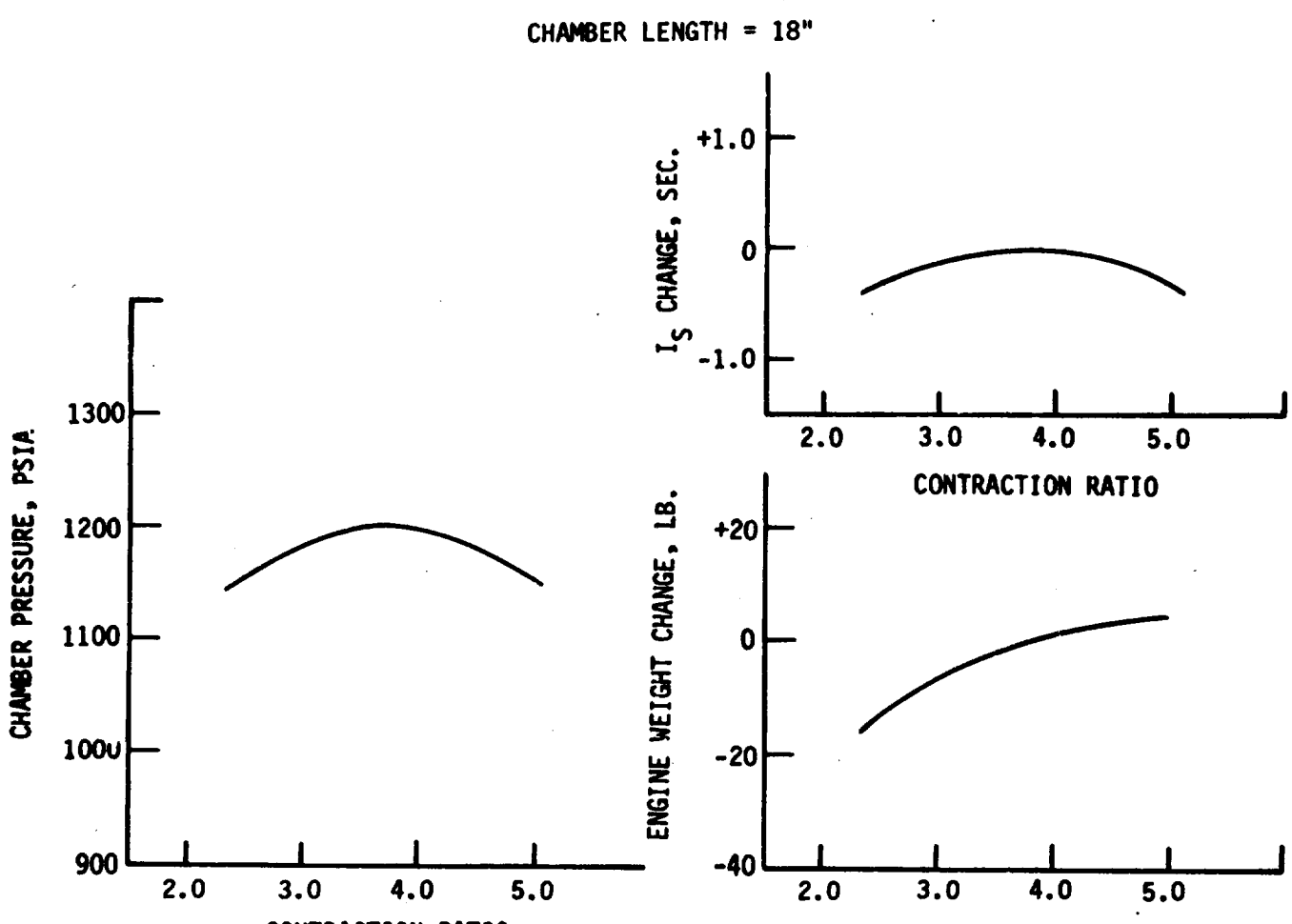

Figure 17. Contraction Ratio Effects at F = 15,000 lb

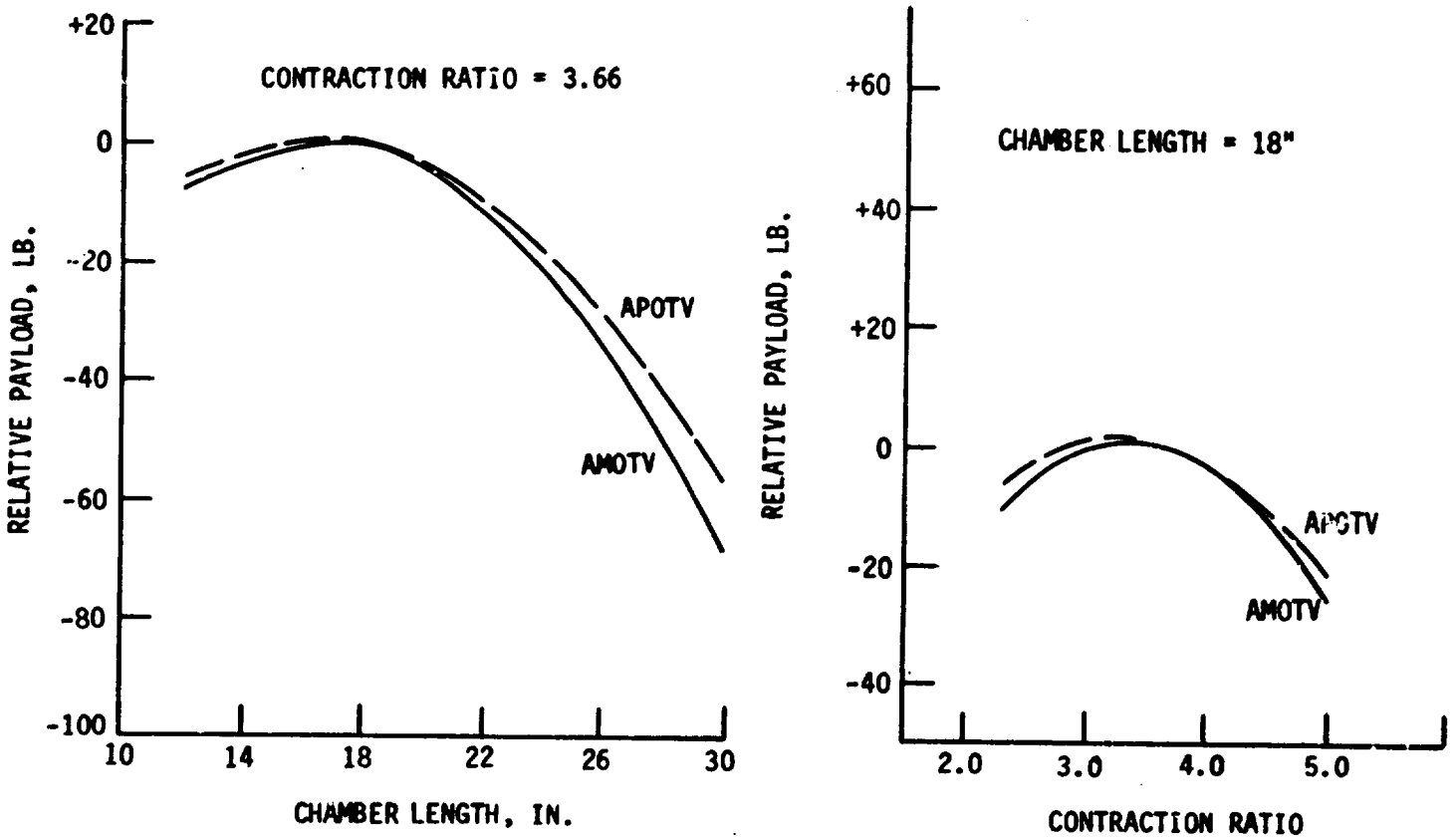

Figure 18. Chamber Length and Contraction Ratio Optimization at F = 15,000 lb

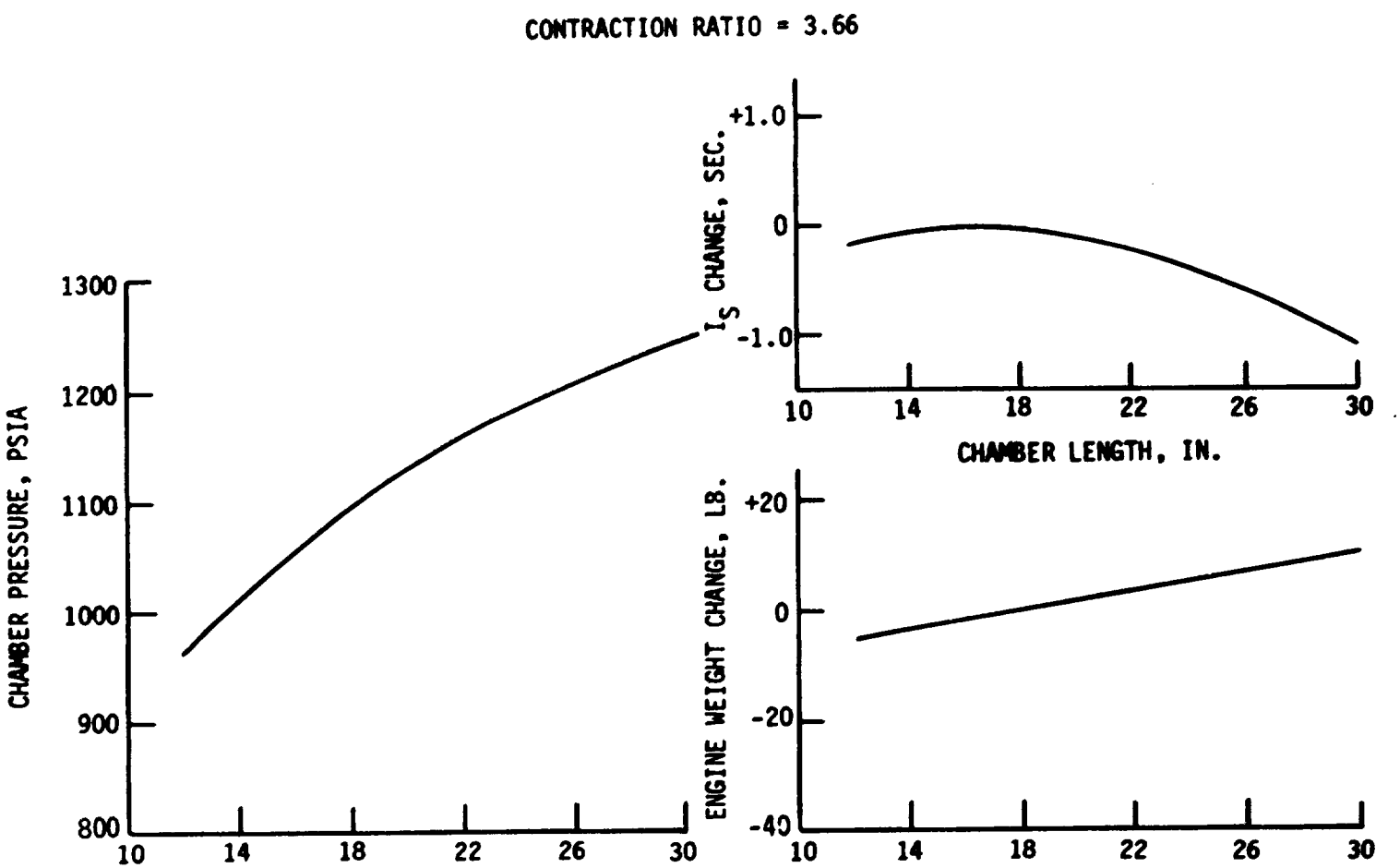

Figure 19. Chamber Length Effects at F = 20,000 lb

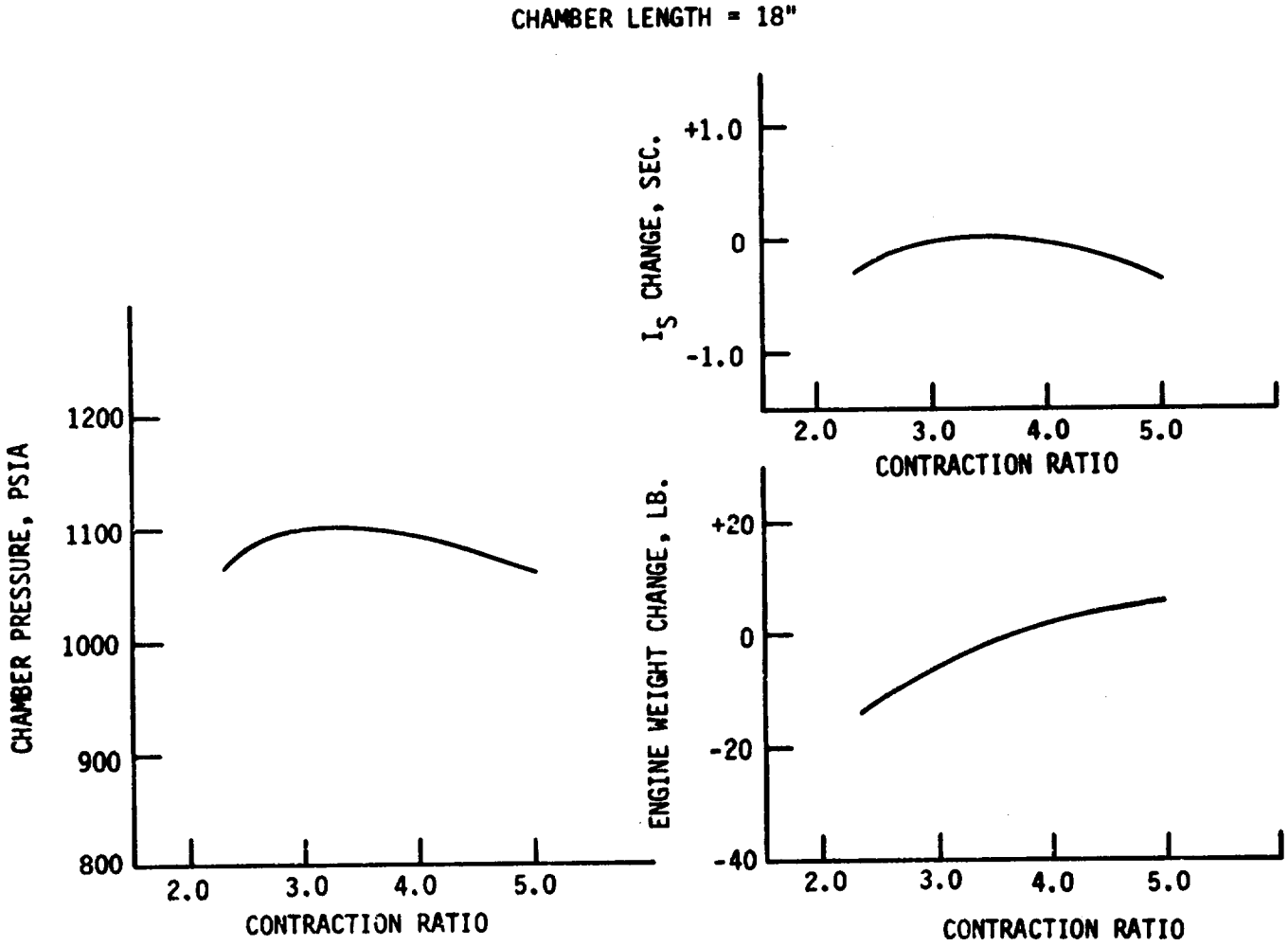

Figure 20. Contraction Ratio Effects at F = 20,000 lb

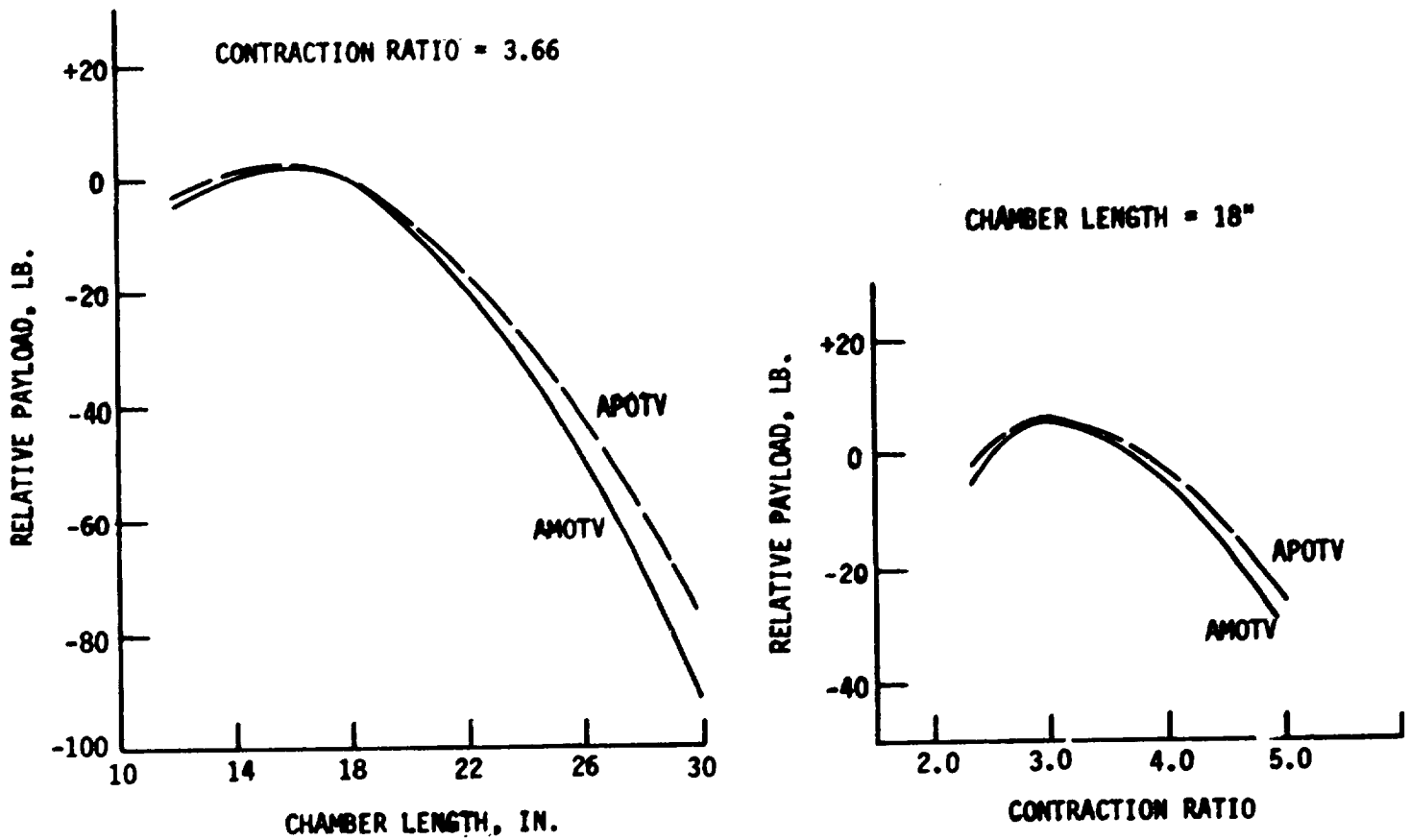

Figure 21. Chamber Length and Contraction Ratio Optimization at F = 20,000 lb

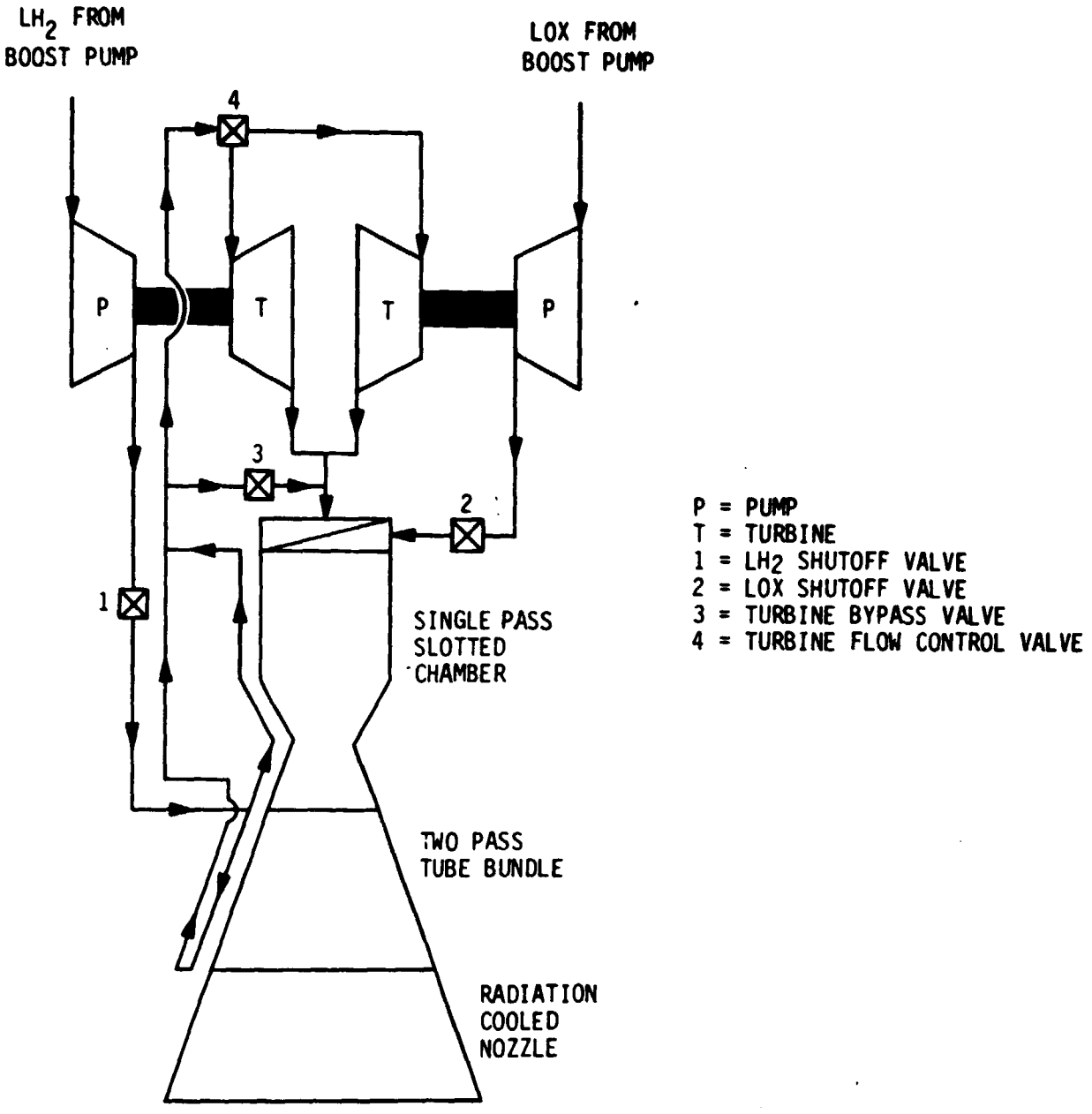

Figure 22. Series Turbine Advanced Expander Cycle Flow Schematic

and series turbine drive cycle cases. The results of this turbomachinery analysis are shown in Figure 23. Cycle power balance analyses were then conducted on the basis of these efficiency data. The cycle power balances were initially conducted for chamber pressures of 1300, 1200, and 1100 psia at thrust levels of 10K, 15K, and 20K lb, respectively. Cycles were first compared on the basis of fuel pump discharge pressure requirements. Since the fuel circuit governs the engine power balance, the fuel pump discharge pressure level indicates the ease in which the power balance can be obtained. Lower discharge pressures also mean lower engine weight, although weight effects are not significant enough to form the basis for a decision.

The parallel turbine power balance results are shown on Tables VI, VII and VIII. The series turbine results are displayed in Tables IX, X, and XI. These tables show the engine system pressure schedule and the parameters necessary to determine a cycle power balance. Althouth the boost pumps were not evaluated in this analysis, the main oxidizer and fuel pump horsepower were increased by 5% and 3%, repsectively, to account for the additional flowrate required to drive hydraulic boost pump turbines. These horsepower penalties were calculated for the main pump inlet pressure conditions shown on the tables. All pressures shown in the power balance tables are total pressures. The turbine pressure ratio is the ratio of the turbine inlet total pressure to the turbine exit static pressure. The outlet pressure is then converted to a total pressure.

The tables show that the series turbine arrangement has much lower fuel pump discharge pressure requirements. As compared to the parallel turbine arrangement, this discharge pressure is reduced by 850, 700, and 540 psia at thrust levels of 10K, 15K, and 20K lb, respectively. These reductions in fuel pump discharge pressure requirements certainly appear to be significant enough to warrant baselining a series rather than

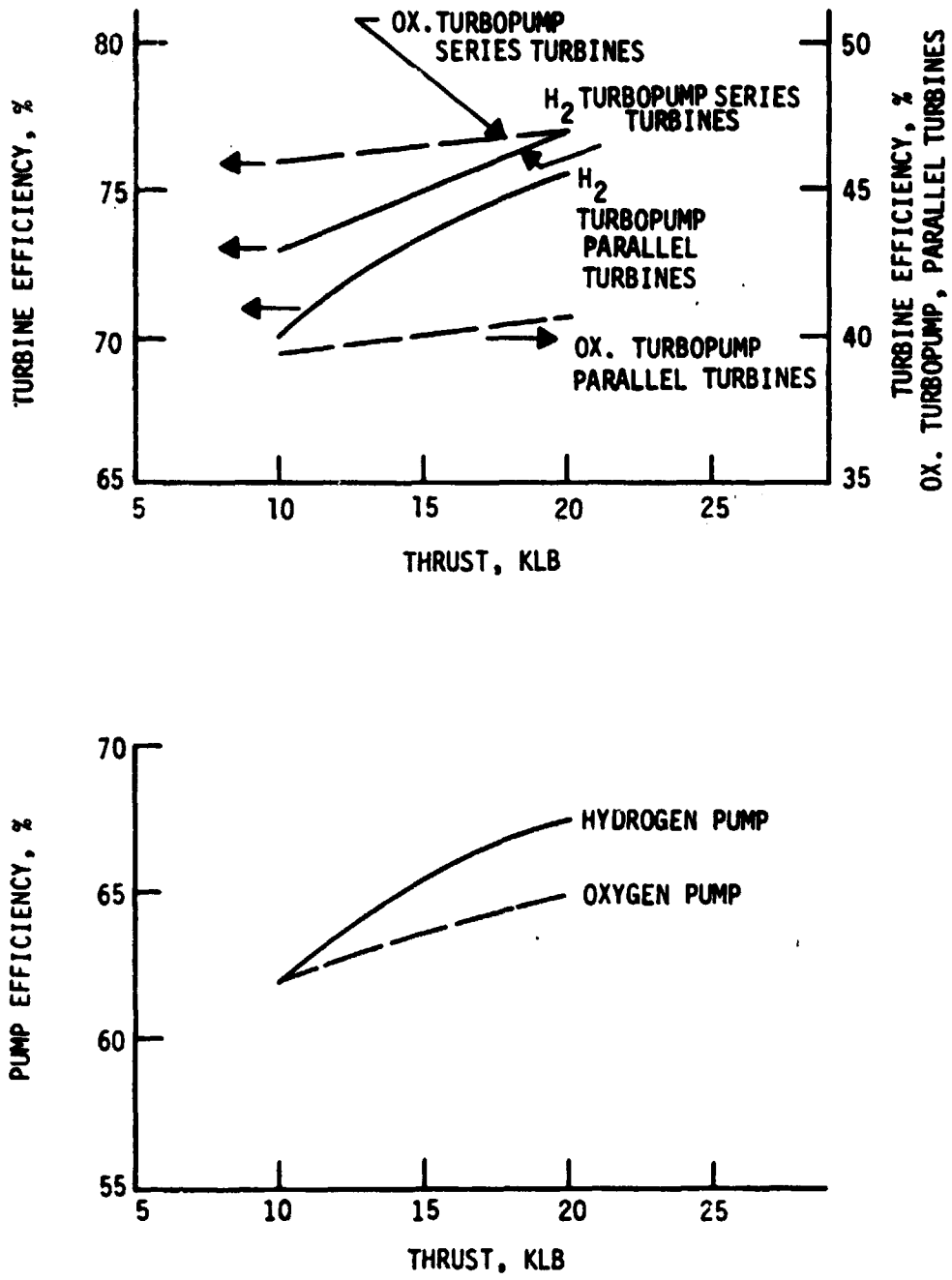

Figure 23. Turbomachinery Efficiency Parametric Data

TABLE VI

PARALLEL TURBINES POWER BALANCE (F - 10K LB)

POWER BALANCE:
EXPANDER CYCLE
PARALLEL TURBINES
NO REHEAT
BOOST PUMPS

PRESSURE SCHEDULE (PSIA)

	FUEL CIRCUIT	LOX CIRCUIT
1.PUMP INLET	51.00	46.60
2.PUMP PRESSURE RISE	3494.48	1561.43
3.PUMP DISCHARGE	3545.48	1608.03
4.LINE PRESSURE DROP	10.00	25.00
5.VALVE INLET	3535.48	1583.03
6.VALVE PRESSURE DROP	35.35	15.83
7.VALVE OUTLET	3500.13	1567.20
8.LINE PRESSURE DROP	30.00	--
9.COOLANT JACKET INLET	3470.13	--
10.COOLANT JACKET PRESSURE DROP	131.00	--
11.COOLANT JACKET OUTLET	3339.13	--
12.LINE PRESSURE DROP	20.00	--
12A.SPLITTER VALVE INLET	3319.13	--
12B.SPLITTER VALVE PRESSURE DROP	33.19	--
12C.SPLITTER VALVE EXIT	3285.94	--
12D.LINE PRESSURE DROP	10.00	--
13.TURBINE INLET	3275.94	--
14.TURBINE PRESSURE RATIO(PIN/POUT)	2.284	--
15.TURBINE OUTLET	1470.87	--
16.LINE PRESSURE DROP	36.77	15.00
17.TCA INJECTOR INLET	1434.10	1552.20
18.TCA INJECTOR PRESSURE DROP	114.73	232.83
19.TCA INJECTOR FACE	1319.37	1319.37
20.TCA PRESSURE DROP	19.37	19.37
21.CHAMBER PRESSURE	1300.00	1300.00

FLOWRATES (LBM/SEC)
TEMP DROP (DEGREES R)
CP(BTU/LB-R)
(FC=FUEL CIRCUIT)
(OC=OX CIRCUIT)
(T-S=TOTAL TO STATIC TEMP)
(T=TOTAL TEMP)

1.FC TURBINE FLOW	2.15
2.OC TURBINE FLOW	.65
3.TURB INLET TEMP(T)	653.00
4.FC TURB T DROP(T-S)	136.20
5.OC TURB T DROP(T-S)	136.20
6.FC TURB EXIT T(T)	557.66
7.OC TURB EXIT T(T)	599.34
8.DRIVE GAS GAMMA	1.395
9.DRIVE GAS CP	3.530

HORSEPOWERS
AND EFFICIENCIES

(FC=FUEL CIRCUIT)
(OC=OX CIRCUIT)
(T-S=TOTAL TO STATIC TEMP)
(T=TOTAL TEMP)

1.FC TURB HORSEPOW	1023.02
2.OC TURB HORSEPOW	173.50
3.FUEL PUMP SHP	1023.02
4.OX PUMP SHP	173.50
5.FC TURB EFF	.700
6.OC TURB EFF	.394
7.FUEL PUMP EFF	.620
8.OX PUMP EFF	.620
9.TOTAL FUEL FLOW	2.97
10.TOTAL OX FLOW	17.85
11.TURB BYPASS FLOW	.18

TABLE VII

PARALLEL TURBINES POWER BALANCE (F = 15K LB)

POWER BALANCE:
EXPANDER CYCLE
PARALLEL TURBINES
NO REHEAT
BOOST PUMPS

PRESSURE SCHEDULE (PSIA)

	FUEL CIRCUIT	LOX CIRCUIT
1.PUMP INLET	51.00	46.60
2.PUMP PRESSURE RISE	3123.13	1440.83
3.PUMP DISCHARGE	3174.13	1487.43
4.LINE PRESSURE DROP	10.00	25.00
5.VALVE INLET	3164.13	1462.43
6.VALVE PRESSURE DROP	31.66	14.62
7.VALVE OUTLET	3132.48	1447.80
8.LINE PRESSURE DROP	30.00	--
9.COOLANT JACKET INLET	3102.48	--
10.COOLANT JACKET PRESSURE DROP	92.00	--
11.COOLANT JACKET OUTLET	3010.48	--
12.LINE PRESSURE DROP	20.00	--
12A.SPLITTER VALVE INLET	2990.48	--
12B.SPLITTER VALVE PRESSURE DROP	29.90	--
12C.SPLITTER VALVE EXIT	2960.58	--
12D.LINE PRESSURE DROP	10.00	--
13.TURBINE INLET	2950.58	--
14.TURBINE PRESSURE RATIO(PIN/POUT)	2.229	--
15.TURBINE OUTLET	1357.73	--
16.LINE PRESSURE DROP	33.96	15.00
17.TCA INJECTOR INLET	1323.78	1432.80
18.TCA INJECTOR PRESSURE DROP	105.90	214.92
19.TCA INJECTOR FACE	1217.88	1217.88
20.TCA PRESSURE DROP	17.88	17.88
21.CHAMBER PRESSURE	1200.00	1200.00

FLOWRATES (LBM/SEC)
TEMP DROP (DEGREES R)
CP(BTU/LB-R)
(FC=FUEL CIRCUIT)
(OC=OX CIRCUIT)
(T-S=TOTAL TO STATIC TEMP)
(T=TOTAL TEMP)

1.FC TURBINE FLOW	3.17
2.OC TURBINE FLOW	1.05
3.TURB INLET TEMP(T)	535.00
4.FC TURB T DROP(T-S)	108.63
5.OC TURB T DROP(T-S)	108.63
6.FC TURB EXIT T(T)	455.27
7.OC TURB EXIT T(T)	491.55
8.DRIVE GAS GAMMA	1.395
9.DRIVE GAS CP	3.652

HORSEPOWERS
AND EFFICIENCIES

(FC=FUEL CIRCUIT)
(OC=OX CIRCUIT)
(T-S=TOTAL TO STATIC TEMP)
(T=TOTAL TEMP)

1.FC TURB HORSEPOW	1306.34
2.OC TURB HORSEPOW	235.57
3.FUEL PUMP SHP	1306.34
4.OX PUMP SHP	235.57
5.FC TURB EFF	.734
6.OC TURB EFF	.800
7.FUEL PUMP EFF	.655
8.OX PUMP EFF	.636
9.TOTAL FUEL FLOW	4.89
10.TOTAL OX FLOW	26.94
11.TURB BYPASS FLOW	.27

TABLE VIII

PARALLEL TURBINES POWER BALANCE (F = 20K LB)

POWER BALANCE
EXPANDER CYCLE:
SERIES TURBINES
NO REHEAT
BOOST PUMPS

PRESSURE SCHEDULE (PSIA)

	FUEL CIRCUIT	LOX CIRCUIT
1.PUMP INLET	51.00	46.00
2.PUMP PRESSURE RISE	2173.98	1320.22
3.PUMP DISCHARGE	2224.98	1366.02
4.LINE PRESSURE DROP	10.00	25.00
5.VALVE INLET	2214.98	1341.02
6.VALVE PRESSURE DROP	22.15	13.42
7.VALVE OUTLET	2192.81	1328.40
8.LINE PRESSURE DROP	30.00	15.00
9.COOLANT JACKET INLET	2162.81	--
10.COOLANT JACKET PRESSURE DROP	76.00	--
11.COOLANT JACKET OUTLET	2086.81	--
12.LINE PRESSURE DROP	30.00	--
13.FUEL CIRCUIT TURBINE INLET	2056.81	--
14.FUEL CIRCUIT TURBINE PRESSURE RAT.	1.518	--
15.FUEL CIRCUIT TURBINE EXIT	1393.77	--
15A.BETWEEN TURBINES PRESSURE DROP	44.84	--
15B.OX CIRCUIT TURBINE INLET	1348.92	--
15C.OX CIRCUIT TURBINE PRESSURE RAT.	1.109	--
15D.OX CIRCUIT TURBINE EXIT	1247.64	--
16.LINE PRESSURE DROP	31.14	--
17.TCA INJECTOR INLET	1216.50	1313.46
18.TCA INJECTOR PRESSURE DROP	100.11	197.01
19.TCA INJECTOR FACE	1116.39	1116.39
20.TCA PRESSURE DROP	16.39	16.39
21.CHAMBER PRESSURE	1100.00	1100.00

	FLOWRATES (LBM/SEC) TEMP DROP (DEGREES R) CP(BTU/LBM-R) (FC=FUEL CIRCUIT) (OC=OX CIRCUIT) (T-S=TOTAL TO STATIC TEMP) (T=TOTAL TEMP)
1.FC TURBINE FLOW	5.66
2.OC TURBINE FLOW	5.66
3.FC TURB T DROP(T-S)	90.89
4.OC TURB T DROP(T-S)	12.18
5.FC TURB INLET T(T)	463.00
6.FC TURB EXIT T(T)	423.81
7.OC TURB IN T(T)	423.81
8.OC TURB EXIT T(T)	414.64
9.DRIVE GAS CP	3.771
10.DRIVE GAS GAMMA	1.391
11.BYPASS FLOW	.36

	HORSEPOWERS AND EFFICIENCIES (FC=FUEL CIRCUIT) (OC=OX CIRCUIT) (T-S=TOTAL TO STATIC TEMP) (T=TOTAL TEMP)
1.FC TURB HORSEPOW	1183.95
2.OC TURB HORSEPOW	283.30
3.FL PUMP BHP	1183.95
4.OX PUMP BHP	283.30
5.FC TURB EFF	.770
6.OC TURBINE EFF	.770
7.FUEL PUMP EFF	.675
8.OX PUMP EFF	.650
9.OX FLOW	36.15
10.TOTAL FUEL FLO	6.03

TABLE IX

SERIES TURBINES POWER BALANCE (F = 10K LB)

POWER BALANCE
EXPANDER CYCLE:
SERIES TURBINES
NO REHEAT
BOOST PUMPS

PRESSURE SCHEDULE (PSIA)

	FUEL CIRCUIT	LOX CIRCUIT
1.PUMP INLET	51.00	46.00
2.PUMP PRESSURE RISE	2044.05	1561.43
3.PUMP DISCHARGE	2095.05	1608.03
4.LINE PRESSURE DROP	10.00	25.00
5.VALVE INLET	2085.05	1583.03
6.VALVE PRESSURE DROP	26.85	15.83
7.VALVE OUTLET	2058.59	1567.20
8.LINE PRESSURE DROP	30.00	15.00
9.COOLANT JACKET INLET	2028.59	--
10.COOLANT JACKET PRESSURE DROP	131.00	--
11.COOLANT JACKET OUTLET	2497.59	--
12.LINE PRESSURE DROP	30.00	--
13.FUEL CIRCUIT TURBINE INLET	2467.59	--
14.FUEL CIRCUIT TURBINE PRESSURE RAT.	1.548	--
15.FUEL CIRCUIT TURBINE EXIT	1635.41	--
15A.BETWEEN TURBINES PRESSURE DROP	50.00	--
15B.OX CIRCUIT TURBINE INLET	1584.52	--
15C.OX CIRCUIT TURBINE PRESSURE RAT.	1.103	--
15D.OX CIRCUIT TURBINE EXIT	1474.07	--
16.LINE PRESSURE DROP	36.79	--
17.TCA INJECTOR INLET	1437.27	1552.24
18.TCA INJECTOR PRESSURE DROP	117.96	232.83
19.TCA INJECTOR FACE	1319.37	1319.37
20.TCA PRESSURE DROP	19.37	19.37
21.CHAMBER PRESSURE	1300.00	1300.00

FLOW-RATES (LBM/SEC)
TEMP DROP (DEGREES R)
CP(BTU/LBM-R)
(FC=FUEL CIRCUIT)
(OC=OX CIRCUIT)
(T-S=TOTAL TO STATIC TEMP)
(T=TOTAL TEMP)

1.FC TURBINE FLOW	2.80
2.OC TURBINE FLOW	2.20
3.FC TURB T DROP(T-S)	75.95
4.OC TURB T DROP(T-S)	10.35
5.FC TURB INLET T(T)	653.00
6.FC TURB EXIT T(T)	597.50
7.FC TURB IN T(T)	597.50
8.OC TURB EXIT T(T)	585.13
9.DRIVE GAS CP	3.538
10.DRIVE GAS GAMMA	1.395
11.BYPASS FLOW	.18

HORSEPOWERS
AND EFFICIENCIES

(FC=FUEL CIRCUIT)
(OC=OX CIRCUIT)
(T-S=TOTAL TO STATIC TEMP)
(T=TOTAL TEMP)

1.FC TURB HORSEPOW	778.17
2.OC TURB HORSEPOW	173.50
3.FL PUMP SHP	778.17
4.OX PUMP SHP	173.50
5.FC TURB EFF	.730
6.OC TURBINE EFF	.760
7.FUEL PUMP EFF	.620
8.OX PUMP EFF	.620
9.OX FLOW	17.05
10.TOTAL FUEL FLO	2.97

TABLE X

SERIES TURBINES POWER BALANCE (F = 15K LB)

POWER BALANCE
EXPANDER CYCLE:
SERIES TURBINES
NO REHEAT
BOOST PUMPS

	PRESSURE SCHEDULE (PSIA) FUEL CIRCUIT	LOX CIRCUIT
1.PUMP INLET	51.00	46.00
2.PUMP PRESSURE RISE	2422.32	1400.03
3.PUMP DISCHARGE	2473.32	1407.03
4.LINE PRESSURE DROP	10.00	25.00
5.VALVE INLET	2463.32	1382.03
6.VALVE PRESSURE DROP	24.63	14.82
7.VALVE OUTLET	2438.69	1447.86
8.LINE PRESSURE DROP	30.00	15.00
9.COOLANT JACKET INLET	2408.69	--
10.COOLANT JACKET PRESSURE DROP	92.09	--
11.COOLANT JACKET OUTLET	2316.69	--
12.LINE PRESSURE DROP	30.03	--
13.FUEL CIRCUIT TURBINE INLET	2286.69	--
14.FUEL CIRCUIT TURBINE PRESSURE RAT.	1.508	--
15.FUEL CIRCUIT TURBINE EXIT	1518.59	--
15A.BETWEEN TURBINES PRESSURE DROP	47.96	--
15B.OX CIRCUIT TURBINE INLET	1470.58	--
15C.OX CIRCUIT TURBINE PRESSURE RAT.	1.169	--
15D.OX CIRCUIT TURBINE EXIT	1300.00	--
16.LINE PRESSURE DROP	33.96	--
17.TCA INJECTOR INLET	1326.00	1432.00
18.TCA INJECTOR PRESSURE DROP	108.06	214.92
19.TCA INJECTOR FACE	1217.00	1217.00
20.TCA PRESSURE DROP	17.00	17.00
21.CHAMBER PRESSURE	1200.00	1200.00

	FLOWRATES (LBM/SEC) TEMP RISE (DEGREES R) CP(BTU/LBM-R) (FC=FUEL CIRCUIT) (OC=OX CIRCUIT) (T-S=TOTAL TO STATIC TEMP) (T=TOTAL TEMP)	HORSEPOWERS AND EFFICIENCIES (FC=FUEL CIRCUIT) (OC=OX CIRCUIT) (T-S=TOTAL TO STATIC TEMP) (T=TOTAL TEMP)
1.FC TURBINE FLOW	4.22	1.FC TURB HORSEPOW 1013.21
2.OC TURBINE FLOW	4.22	2.OC TURB HORSEPOW 239.57
3.FC TURB T DROP(T-S)	61.96	3.FL PUMP SHP 1013.21
4.OC TURB T DROP(T-S)	14.12	4.OX PUMP SHP 239.57
5.FC TURB INLET T(T)	535.00	5.FC TURB EFF .750
6.FC TURB EXIT T(T)	488.53	6.OC TURBINE EFF .705
7.OC TURB IN T(T)	488.53	7.FUEL PUMP EFF .655
8.OC TURB EXIT T(T)	477.73	8.OX PUMP EFF .636
9.DRIVE GAS CP	3.652	9.OX FLOW 20.94
10.DRIVE GAS GAMMA	1.395	10.TOTAL FUEL FLO 8.09
11.BYPASS FLOW	.27	

TABLE XI

SERIES TURBINES POWER BALANCE (F = 20K LB)

POWER BALANCE:
EXPANDER CYCLE
PARALLEL TURBINES
NO REHEAT
BOOST PUMPS

PRESSURE SCHEDULE (PSIA)

	FUEL CIRCUIT	LOX CIRCUIT
1.PUMP INLET	51.06	46.00
2.PUMP PRESSURE RISE	2713.26	1320.22
3.PUMP DISCHARGE	2764.26	1366.02
4.LINE PRESSURE DROP	10.00	25.00
5.VALVE INLET	2754.26	1341.02
6.VALVE PRESSURE DROP	27.54	13.42
7.VALVE OUTLET	2726.66	1328.00
8.LINE PRESSURE DROP	30.00	--
9.COOLANT JACKET INLET	2696.66	--
10.COOLANT JACKET PRESSURE DROP	76.00	--
11.COOLANT JACKET OUTLET	2620.66	--
12.LINE PRESSURE DROP	20.00	--
12A.SPLITTER VALVE INLET	2600.66	--
12B.SPLITTER VALVE PRESSURE DROP	26.01	--
12C.SPLITTER VALVE EXIT	2574.65	--
12D.LINE PRESSURE DROP	10.00	--
13.TURBINE INLET	2564.65	--
14.TURBINE PRESSURE RATIO(PIN/POUT)	2.115	--
15.TURBINE OUTLET	1244.50	--
16.LINE PRESSURE DROP	31.11	15.00
17.TCA INJECTOR INLET	1213.47	1313.40
18.TCA INJECTOR PRESSURE DROP	97.00	197.01
19.TCA INJECTOR FACE	1116.39	1116.39
20.TCA PRESSURE DROP	16.39	16.39
21.CHAMBER PRESSURE	1100.00	1100.00

	FLOWRATES (LBM/SEC) TEMP DROP (DEGREES R) CP(BTU/LB-R) (FC=FUEL CIRCUIT) (OC=LOX CIRCUIT) (T-S=TOTAL TO STATIC TEMP) (T=TOTAL TEMP)	NCRSEPOWERS AND EFFICIENCIES (FC=FUEL CIRCUIT) (OC=LOX CIRCUIT) (T-S=TOTAL TO STATIC TEMP) (T=TOTAL TEMP)
1.FC TURBINE FLOW	0.17	1.FC TURB NCRSEPOW = 1477.62
2.OC TURBINE FLOW	1.49	2.OC TURB NCRSEPOW = 203.39
3.TURB INLET TEMP(T)	693.80	3.FUEL PUMP SHP 1477.62
4.FC TURB T DROP(T-S)	87.79	4.OX PUMP SHP 203.39
5.OC TURB T DROP(T-S)	47.79	5.FC TURB EFF .756
6.FC TURB EXIT T(T)	306.63	6.OC TURB EFF .486
7.OC TURB EXIT T(T)	227.30	7.FUEL PUMP EFF .675
8.DRIVE GAS GAMMA	1.391	8.OX PUMP EFF .650
9.DRIVE GAS CP	3.771	9.TOTAL FUEL FLOW 6.03
		10.TOTAL OX FLOW 36.15
		11.TURB BYPASS FLOW .36

III, B, Cycle Optimization (cont.)

a parallel turbine arrangement. All power balances were conducted using a 6% turbine bypass flowrate. With the series turbine arrangement, this flowrate could be increased somewhat at the expense of fuel pump discharge pressure to provide more cycle margin and reduce the development risk.

The series turbine arrangement could also achieve a higher operating chamber pressure and, hence, higher area ratio and performance within the fixed envelope constraint. With the fuel pump discharge pressures held constant at the values obtained for the parallel turbine arrangement, the following results were achieved:

Thrust, K lb	Cycle	Fuel Pump Discharge Pressure, psia	Chamber Pressure, psia	Engine Specific Impulse, sec.	Nozzle Area Ratio
10	Parallel Turbines	3545	1300	480.2	792
15	↓	3174	1200	477.2	473
20	↓	2764	1100	474.2	322
10	Series Turbines	3545	1480	481.2	900
15	↓	3174	1345	478.1	530
20	↓	2764	1225	475.1	360

The data show that the performance gains are small (about 1 sec) because the rate of change in specific impulse with area ratio decreases as area ratio increases. This can be seen from Figure 24. As discussed in Section III,D, of this report, the effect of the operating chamber pressure on engine weight is negligible over a small range.

Based upon this analysis, it would appear more desirable to accept a lower chamber pressure with a small decrease in specific impulse

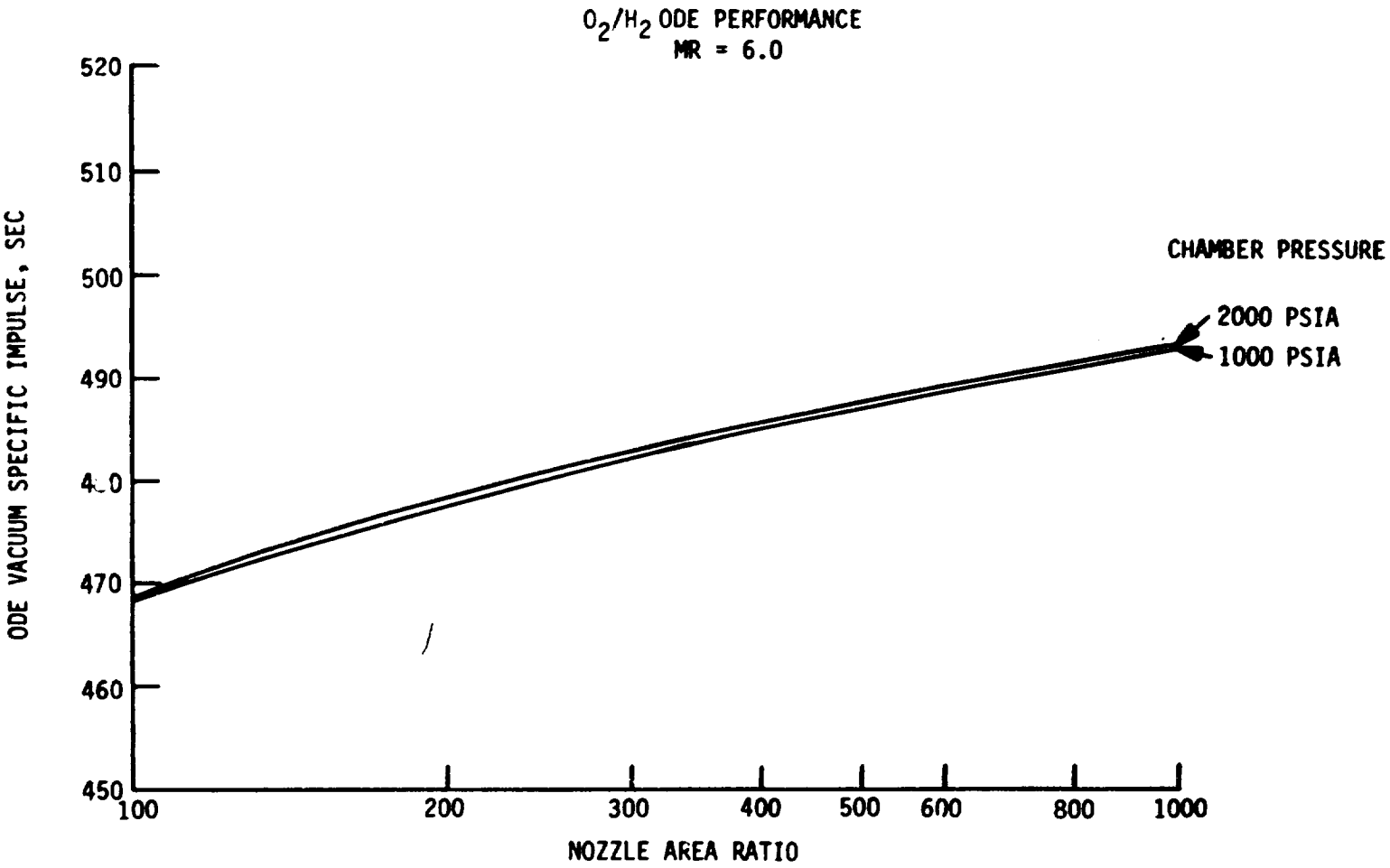

Figure 24. O_2/H_2 ODE Performance, MR = 6.0

($\leq$ 1 sec). This would increase the cycle power balance margin and provide a contingency that may be required during the engine development program.

2. Turbine Exhaust Heat Regeneration Cycle Analysis

The objective of this portion of the study was to evaluate the use of a turbine exhaust gas regenerator in the expander cycle engine and to identify optimized operating conditions. Regenerator performance for 10K, 15K, and 20K lb thrust was evaluated, placing particular emphasis on the series turbine engine configuration which was selected on the basis of the results presented in Paragraph III,B,1.

The regenerator concept employs a heat exchanger to transfer energy from the turbine exhaust gas to the liquid hydrogen discharging from the pump prior to entering the combustion chamber coolant jacket. From the regenerator, the turbine exhaust gas enters the injector. The heated hydrogen enters the cooling passageways of the thrust chamber jacket and nozzle and then drives the turbines. A simplified engine cycle schematic is shown in Figure 25.

Utilizing a turbine exhaust gas regenerator in the expander cycle results in an increased heat flow to the hydrogen and, thus, a higher turbine inlet temperature. This can result in more turbine horsepower output, higher chamber pressure, or in more turbine bypass and/or cycle margin if desired. The full benefit of the increased heat flow is offset partly by a simultaneous increase in system pressure losses. A parametric study was conducted to optimize the engine performance and identify regenerator operating conditions. Pertinent details are included in the following discussion.

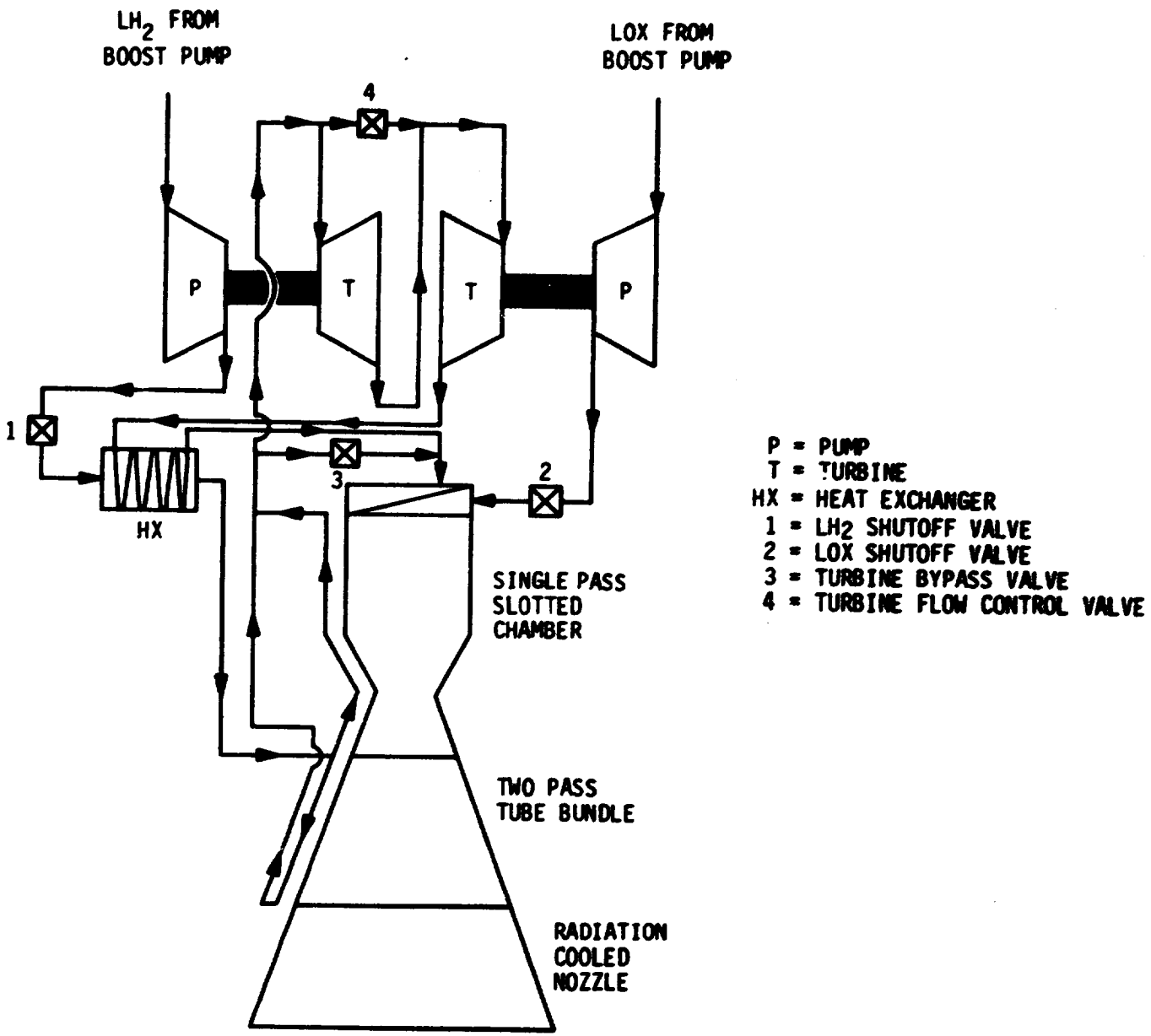

Figure 25. Turbine Exhaust Heat Regeneration/Series Turbines - Advanced Expander Cycle Flow Schematic

III, B, Cycle Optimization (cont.)

a. Regenerative Chamber

The use of the regenerator results in an increased hydrogen coolant inlet temperature to the regenerative chamber liner. The effect of this is an increase in the pressure losses through the chamber liner for the same chamber heat flow. Figure 26 depicts the relationships for 10K, 15K, and 20K thrust levels. The regenerator outlet temperature (for the hydrogen coolant) and the jacket coolant inlet temperature are assumed to be the same in this analysis.

b. Engine Cycle Power Balance

Utilizing the total heat flow to the coolant to determine turbine inlet temperature and the aforementioned jacket pressure loss relationships, engine cycle power balances were predicted for various regenerator performance levels.

The series turbine engine performance and power balance model was used for each thrust level for each of the baseline configurations. The baseline parameters at each thrust level are presented in the table below.

	PARAMETER	THRUST, lb 10,000	15,000	20,000
Chamber Pressure	Pc, psia	1300	1200	1100
Fuel Flowrate	$\dot{w}_{fuel}$, lb/sec	3.0	4.5	6.0
Engine Mixture Ratio	MR	6.0	6.0	6.0
Chamber Length	L', in.	18	18	18
Chamber Contraction Ratio	C_R	3.66	3.66	3.66
Ox Pump Efficiency	η_{po}	.620	.636	.650

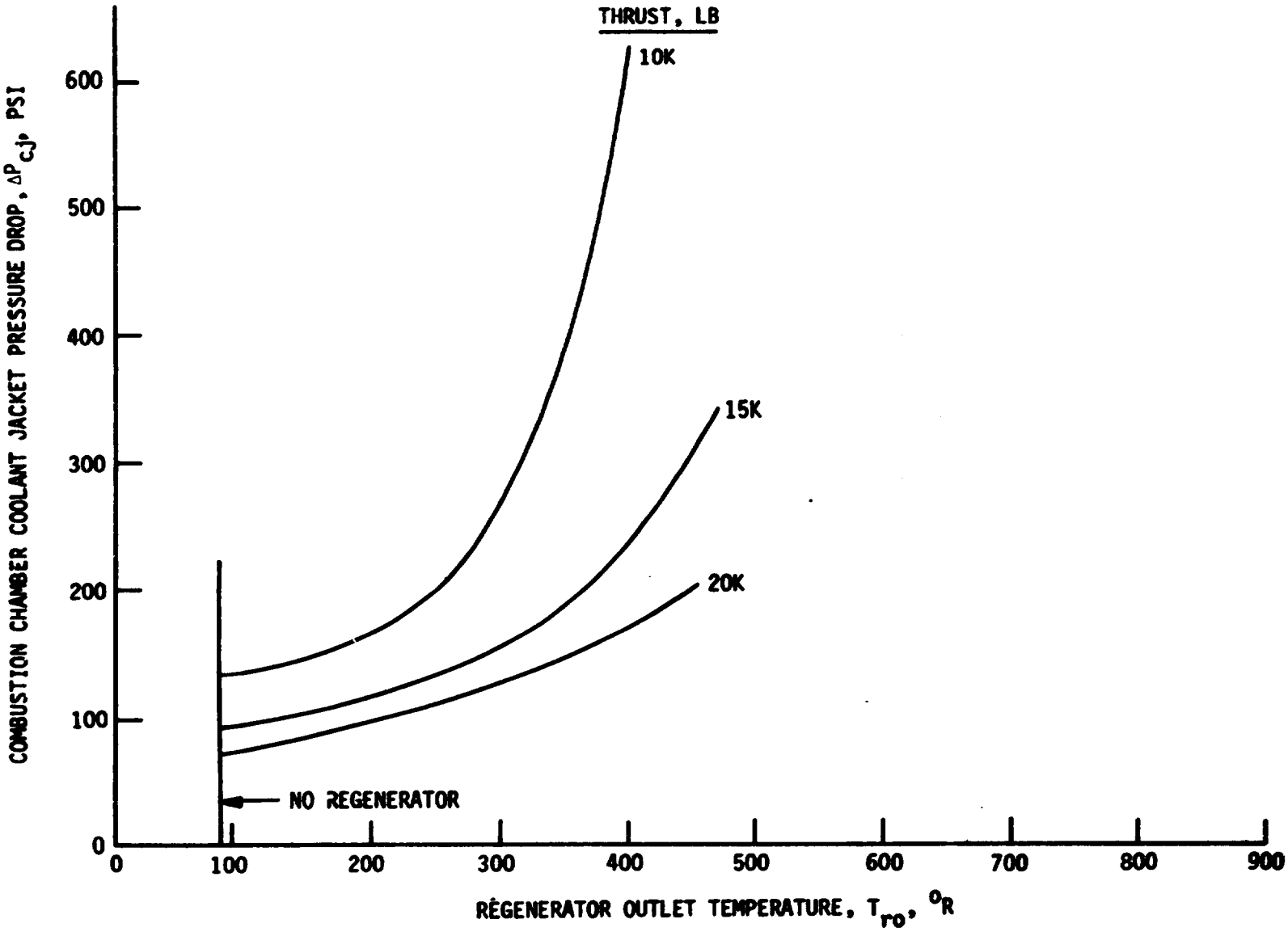

Figure 26. Effect of Increased Jacket Inlet Temperature on Jacket Pressure Losses

III, B, Cycle Optimization (cont.)

PARAMETER		THRUST, lb 10,000	15,000	20,000
Fuel Pump Efficiency	η_{pf}	.620	.655	.675
Ox Turbine Efficiency	η_{to}	.760	.765	.770
Fuel Turbine Efficiency	η_{tf}	.730	.750	.770

Pressure losses through the regenerator (both the cold circuit and hot-gas circuit) were varied from 50 psia to 200 psia to determine their effect and sensitivity.

Because the previous analysis showed only minor performance variations with chamber pressure, the approach in this subtask was to hold chamber pressure constant. However, the chamber pressure and performance potential were also addressed.

The major engine operating parameters of interest for the constant chamber pressure cases are the fuel (hydrogen) pump discharge pressure and the turbine pressure ratio. These parameters are used to assess the cycle's sensitivity to variations in component performance. For a given thrust and flowrate, a minimum discharge pressure and pressure ratio are desirable. For ease of comparison, an overall pressure ratio, across both fuel and oxidizer turbines, was used in the series turbine analysis.

Figure 27 graphically presents the results of the engine power balance data. From this figure, the optimum regenerator outlet temperatures were selected as follows:

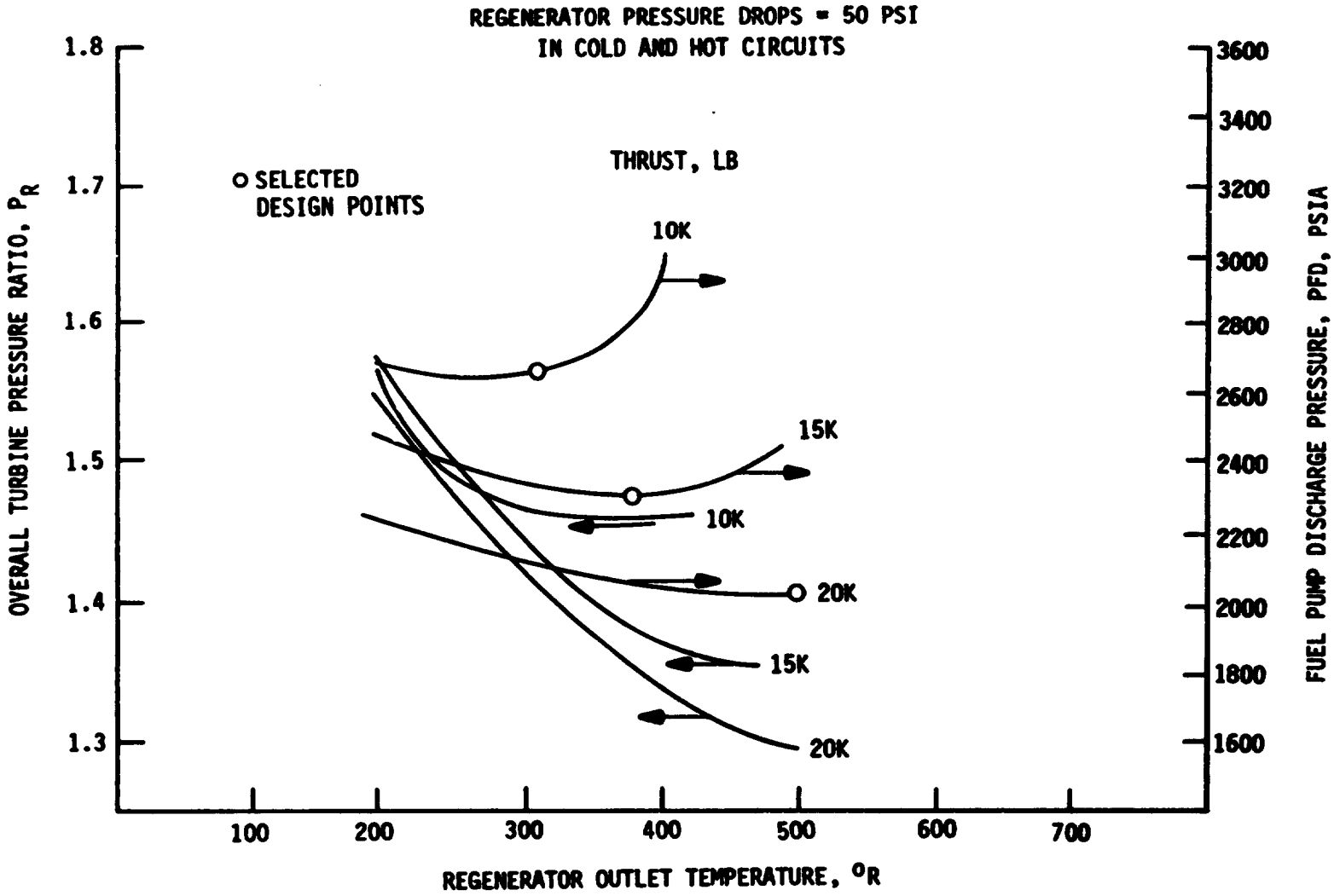

Figure 27. Regeneration Outlet Temperature Optimization

III, B, Cycle Optimization (cont.)

THRUST, lb	REGENERATOR OUTLET TEMPERATURE °R
10,000	310
15,000	380
20,000	500

As already discussed, the regenerator pressure losses were varied to determine the effect on the engine power balance. From the results shown in Figure 28, it can be concluded that 1) the fuel pump discharge pressure and turbine pressure ratio are obviously reduced if the regenerator pressure losses are decreased, and 2) the selection of the optimized regenerator outlet temperature is not significantly affected by the level of regenerator pressure losses.

c. Regenerator Characteristics

Previous in-house IR&D studies determined that a platelet type heat exchanger would be capable of providing the large amount of heat transfer surface area with a minimum packaging size. Many small passageways would be used to pass the fluids.

The inlet conditions and the selected cold circuit outlet temperature determined the gas outlet temperature. The turbine exhaust gas temperature at the regenerator inlet was estimated from preliminary engine cycle power balances. The regenerator inlet and outlet temperatures are shown below.

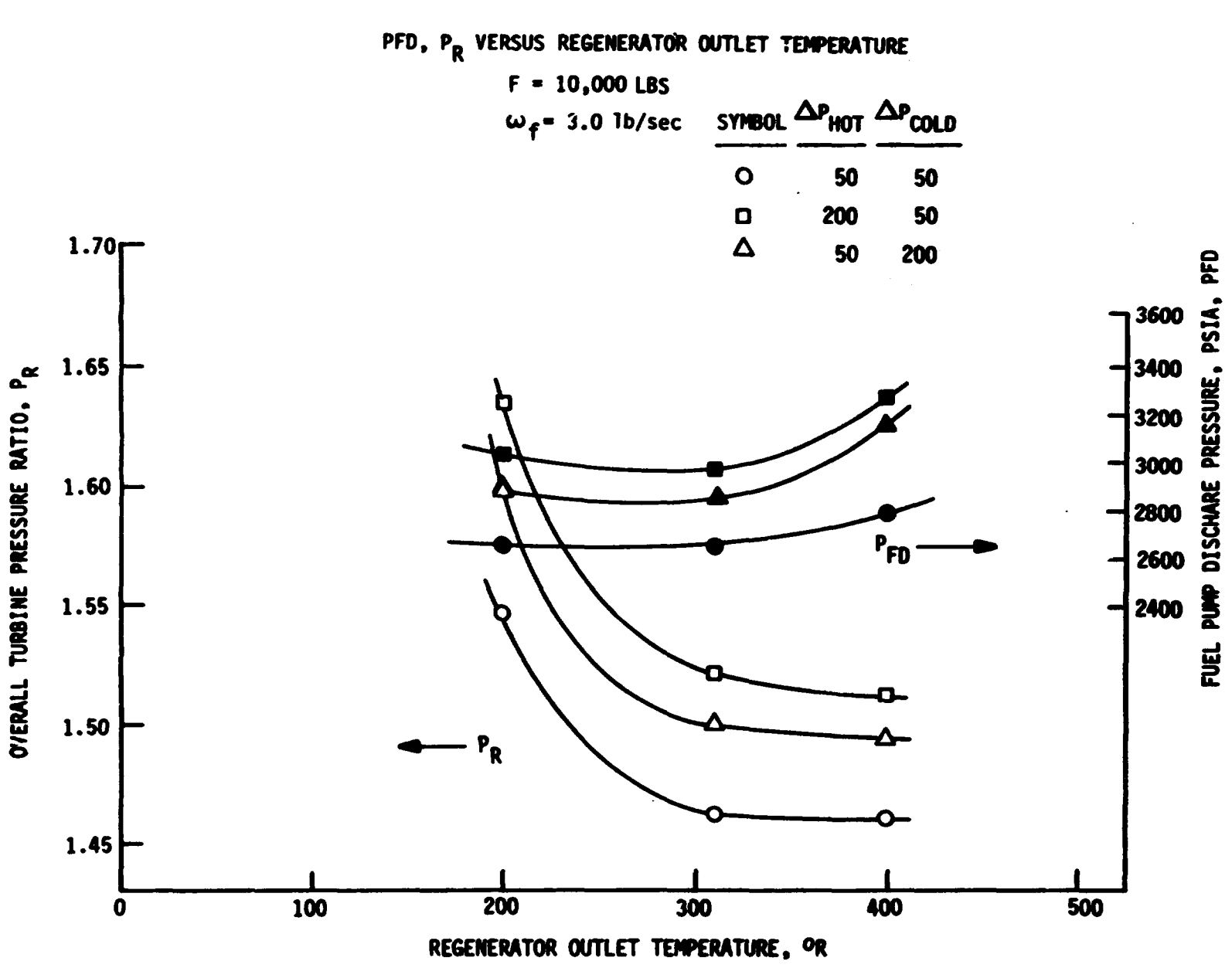

Figure 28. Effect of Regenerator Pressure Losses on Engine Power Balance

III, B, Cycle Optimization (cont.)

	TEMPERATURE, °R			
THRUST	COLD IN	COLD OUT	HOT IN	HOT OUT
10K	90	310	750	510
15K	90	380	780	490
20K	90	500	860	425

The cold circuit inlet and hot-gas inlet pressures utilized for estimating fluid properties for all thrust levels, were 3000 psi and 1500 psi, respectively. A deviation from these values does not significantly affect the results of these preliminary studies.

A steady-state heat transfer model, developed during an ALRC IR&D study, was used to estimate the size, weight, and pressure drop relationships for a counterflow heat exchanger core. The independent variable in determining these relationships is the number of channels or, since the channel geometry is fixed, the frontal area.

The regenerator pressure losses were assumed to be twice those predicted for the core frictional and inlet/outlet pressure losses. The weight of the 10K lbF regenerator was estimated to be twice that of the core. Scaled weights for the 15K lbF and 20K lbF regenerators, based on the number of channels, were estimated to be 1.5 and 1.3 times the core weight, respectively. Figures 29, 30, and 31 present the results of the heat exchanger modeling. The data is shown for stainless steel regenerators although weight estimates for aluminum regenerators were also made.

From the appropriate curves, regenerator design points (weight, pressure losses) were selected and are shown below. The considerations

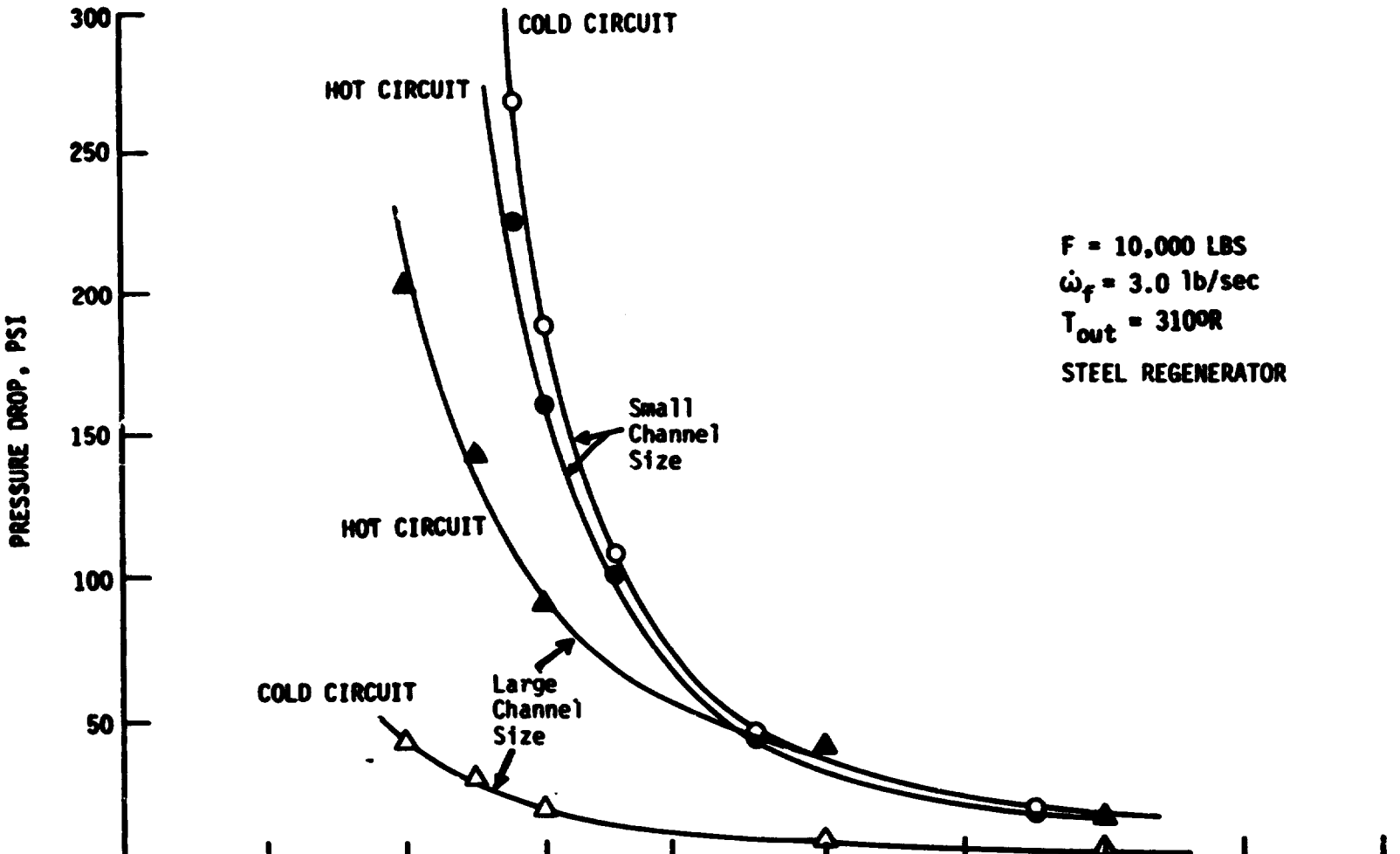

Figure 29. 10K Regenerator Weight-Pressure Loss Relationships

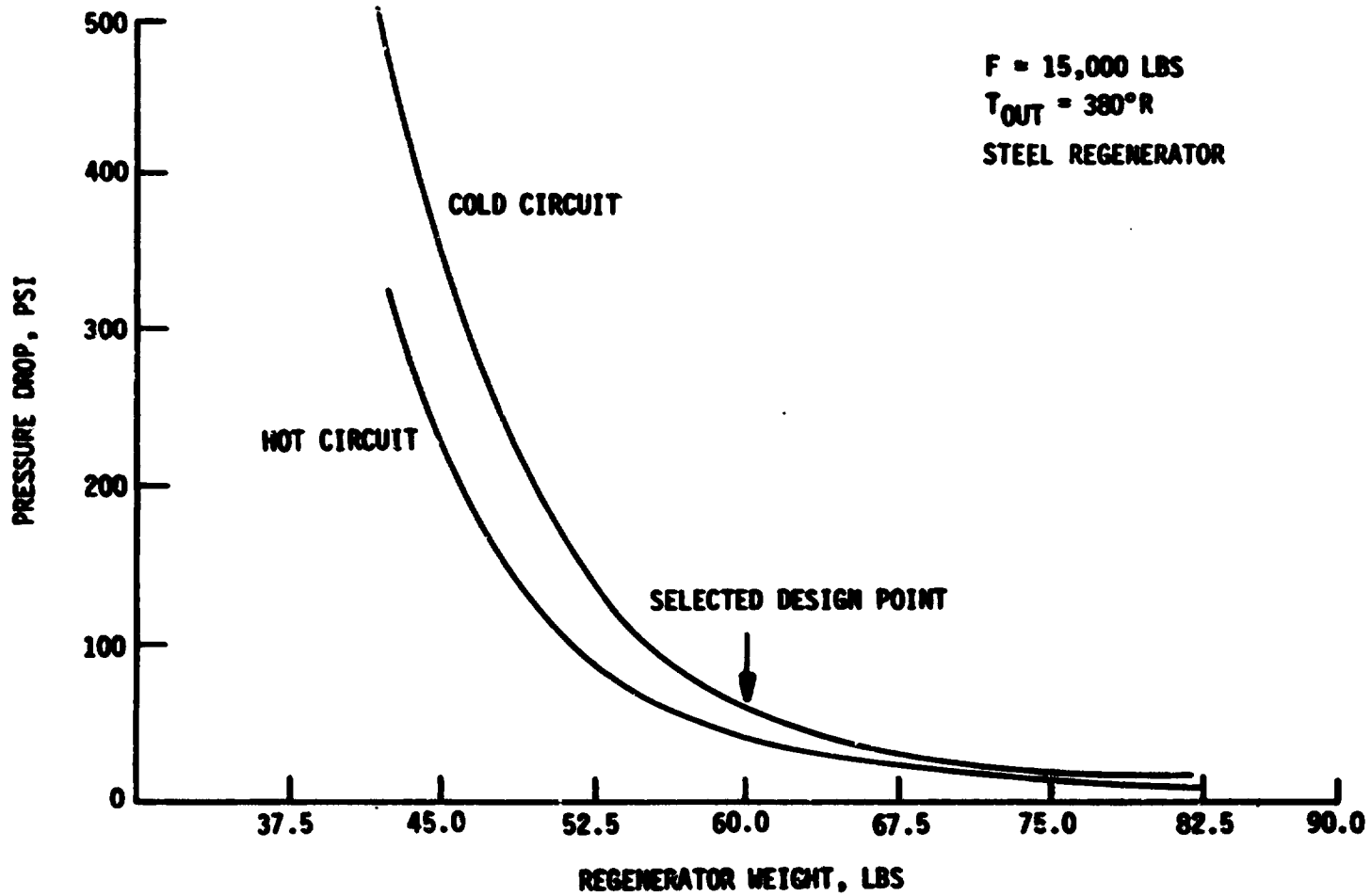

Figure 30. 15K Regenerator Weight-Pressure Loss Relationships

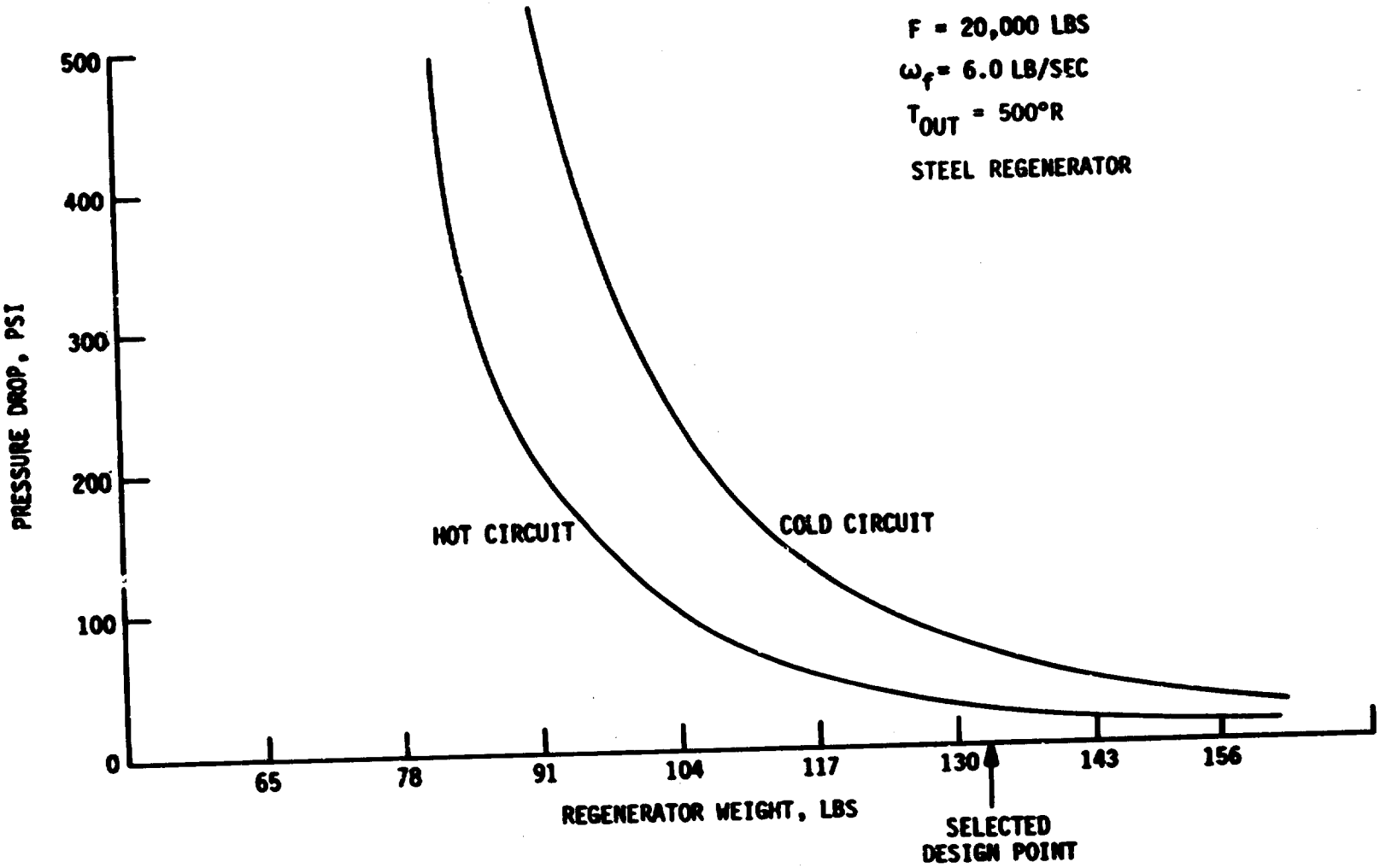

Figure 31. 20K Regenerator Weight-Pressure Loss Relationships

in selecting these points were minimum weight in a region of lesser sensitivity of pressure drop to weight fluctuations (as a result of operation or design changes).

	THRUST, lb		
	10,000	15,000	20,000
Temp, hot in (°R)	750	780	860
Temp, hot out (°R)	510	490	425
Temp, cold in (°R)	90	90	90
Temp, cold out (°R)	310	380	500
ΔP (cold circuit) (psi)	35	60	60
ΔP (hot circuit) (psi)	35	40	25
Weight (lb), Steel	36	60	133
Aluminum	12	21	46

The drastic increase in weight for the 20K lbF from the 15K lbF regenerator results from the high heat flow required to increase the large fuel flow (6.0 lb/sec.) to the high temperature (500°R). The 500°R point was selected disregarding weight. Reducing the temperature output level will reduce the weight, with a small increase in fuel pump discharge pressure and also an increase in turbine pressure ratio. The minimum regenerator weight that can be obtained is about 95 lb, although the pressure drop becomes excessive at that point.

d. Cycle Comparisons

Engine power balance calculations at or very near the optimum selected conditions for the series turbine/turbine exhaust heat regeneration cycles are shown in Tables XII, XIII, and XIV. These results are compared to the series turbine (without a regenerator) cycles below for

TABLE XII

TURBINE EXHAUST HEAT REGENERATION, SERIES TURBINES, POWER BALANCE (F = 10K lb)

POWER BALANCE
EXPANDER CYCLE:
SERIES TURBINES
TURBINE EXHAUST HEAT REGENERATION
BOOST PUMPS

PRESSURE SCHEDULE (PSIA)

	FUEL CIRCUIT	LOX CIRCUIT
1.PUMP INLET	51.00	40.00
2.PUMP PRESSURE RISE	2594.07	1541.43
3.PUMP DISCHARGE	2645.07	1581.43
4.LINE PRESSURE DROP	10.00	25.00
5.VALVE INLET	2635.07	1583.43
6.VALVE PRESSURE DROP	20.35	15.83
7.VALVE OUTLET	2608.72	1567.20
8.LINE PRESSURE DROP	10.00	15.00
8A.HEAT EXCHANGER INLET	2598.72	--
8B.HEAT EXCHANGER PRESSURE DROP	50.00	--
8C.HEAT EXCHANGER DISCHARGE	2548.72	--
8D.LINE PRESSURE DROP	30.00	--
9.COOLANT JACKET INLET	2518.72	--
10.COOLANT JACKET PRESSURE DROP	285.00	--
11.COOLANT JACKET OUTLET	2233.72	--
12.LINE PRESSURE DROP	30.00	--
13.FUEL CIRCUIT TURBINE INLET	2203.72	--
14.FUEL CIRCUIT TURBINE PRESSURE RAT.	1.359	--
15.FUEL CIRCUIT TURBINE EXIT	1000.98	--
15A.BETWEEN TURBINES PRESSURE DROP	51.67	--
15B.LOX CIRCUIT TURBINE INLET	1015.31	--
15C.LOX CIRCUIT TURBINE PRESSURE RAT.	1.977	--
15D.LOX CIRCUIT TURBINE EXIT	1540.18	--
16.LINE PRESSURE DROP	36.65	--
16A.HEAT EXCHANGER INLET	1507.51	--
16B.HEAT EXCHANGER PRESSURE DROP	50.00	--
16C.HEAT EXCHANGER DISCHARGE	1457.51	--
16D.LINE PRESSURE DROP	19.33	--
17.TCA INJECTOR INLET	1438.18	1552.20
18.TCA INJECTOR PRESSURE DROP	118.81	232.83
19.TCA INJECTOR FACE	1319.37	1319.37
20.TCA PRESSURE DROP	19.37	19.37
21.CHAMBER PRESSURE	1300.00	1300.00

FLOWRATES (LBM/SEC)
TEMP DROP (DEGREES R)
CP(BTU/LBM-R)
(FC=FUEL CIRCUIT)
(OC=OX CIRCUIT)
(T-S=TOTAL TO STATIC TEMP)
(T=TOTAL TEMP)

1.FC TURBINE FLOW	2.80
2.OC TURBINE FLOW	2.80
3.FC TURB T DROP(T-S)	78.50
4.OC TURB T DROP(T-S)	16.35
5.FC TURB INLET T(T	902.00
6.FC TURB EXIT T(T)	847.61
7.OC TURB INLET T(T)	847.61
8.OC TURB EXIT T(T)	835.19
9.DRIVE GAS CP	3.510
10.DRIVE GAS GAMMA	1.395

HORSEPOWERS
AND EFFICIENCIES

(FC=FUEL CIRCUIT)
(OC=OX CIRCUIT)
(T-S=TOTAL TO STATIC TEMP)
(T=TOTAL TEMP)

1.FC TURB HORSEPOW	750.46
2.OC TURB HORSEPOW	173.50
3.FC PUMP SHP	750.02
4.OX PUMP SHP	173.50
5.FC TURBINE EFF	.738
6.OC TURBINE EFF	.760
7.FUEL PUMP EFF	.620
8.OX PUMP EFF	.620
9.OX FLOW	17.85
10.TOTAL FUEL FLO	2.97
11.TURBINE BYPASS FLOW	.18

TABLE XIII

TURBINE EXHAUST HEAT REGENERATION, SERIES TURBINES, POWER BALANCE (F = 15K lb)

POWER BALANCE
EXPANDER CYCLE1
SERIES TURBINES
TURBINE EXHAUST HEAT REGENERATION
BOOST PUMPS

PRESSURE SCHEDULE (PSIA)

	FUEL CIRCUIT	LOX CIRCUIT
1.PUMP INLET	51.00	46.00
2.PUMP PRESSURE RISE	2279.59	1440.83
3.PUMP DISCHARGE	2330.59	1487.43
4.LINE PRESSURE DROP	10.00	25.00
5.VALVE INLET	2320.59	1462.43
6.VALVE PRESSURE DROP	23.21	14.62
7.VALVE OUTLET	2297.38	1447.80
8.LINE PRESSURE DROP	10.00	15.00
8A.HEAT EXCHANGER INLET	2287.38	--
8B.HEAT EXCHANGER PRESSURE DROP	50.00	--
8C.HEAT EXCHANGER DISCHARGE	2237.38	--
8D.LINE PRESSURE DROP	30.00	--
9.COOLANT JACKET INLET	2207.38	--
10.COOLANT JACKET PRESSURE DROP	158.00	--
11.COOLANT JACKET OUTLET	2049.38	--
12.LINE PRESSURE DROP	30.00	--
13.FUEL CIRCUIT TURBINE INLET	2019.38	--
14.FUEL CIRCUIT TURBINE PRESSURE RAT.	1.317	--
15.FUEL CIRCUIT TURBINE EXIT	1569.09	--
15A.BETWEEN TURBINES PRESSURE DROP	68.73	--
15B.GG CIRCUIT TURBINE INLET	1500.35	--
15C.OX CIRCUIT TURBINE PRESSURE RAT.	1.075	--
15D.OX CIRCUIT TURBINE EXIT	1431.60	--
16.LINE PRESSURE DROP	35.79	--
16A.HEAT EXCHANGER INLET	1395.81	--
16B.HEAT EXCHANGER PRESSURE DROP	50.00	--
16C.HEAT EXCHANGER DISCHARGE	1345.81	--
16D.LINE PRESSURE DROP	17.84	--
17.TCA INJECTOR INLET	1327.91	1432.60
18.TCA INJECTOR PRESSURE DROP	110.03	214.92
19.TCA INJECTOR FACE	1217.88	1217.88
20.TCA PRESSURE DROP	17.88	17.88
21.CHAMBER PRESSURE	1200.00	1200.00

FLOWRATES (LBM/SEC)
TEMP DROP (DEGREES R)
CP(BTU/LBM-R)
(FC=FUEL CIRCUIT)
(OC=OX CIRCUIT)
(T-S=TOTAL TO STATIC TEMP)
(T=TOTAL TEMP)

1.FC TURBINE FLOW	4.22
2.OC TURBINE FLOW	4.22
3.FC TURB T DROP(T-S)	60.32
4.OC TURB T DROP(T-S)	14.61
5.FC TURB INLET T(T	764.00
6.FC TURB EXIT T(T)	718.70
7.OC TURB INLET T(T)	718.70
8.OC TURB EXIT T(T)	707.56
9.DRIVE GAS CP	3.530
10.DRIVE GAS GAMMA	1.395

HORSEPOWERS
AND EFFICIENCIES

(FC=FUEL CIRCUIT)
(OC=OX CIRCUIT)
(T-S=TOTAL TO STATIC TEMP)
(T=TOTAL TEMP)

1.FC TURB HORSEPOW	993.50
2.OC TURB HORSEPOW	235.57
3.FC PUMP BHP	993.50
4.OX PUMP BHP	235.57
5.FC TURBINE EFF	.750
6.OC TURBINE EFF	.705
7.FUEL PUMP EFF	.695
8.OX PUMP EFF	.630
9.OX FLOW	20.94
10.TOTAL FUEL FLO	4.49
11.TURBINE BYPASS FLOW	.27

TABLE XIV

TURBINE EXHAUST HEAT REGENERATION, SERIES TURBINES, POWER BALANCE (F = 20K lb)

POWER BALANCE
EXPANDER CYCLE:
SERIES TURBINES
TURBINE EXHAUST HEAT REGENERATION
BOOST PUMPS

PRESSURE SCHEDULE (PSIA)

	FUEL CIRCUIT	LOX CIRCUIT
1.PUMP INLET	51.00	46.00
2.PUMP PRESSURE RISE	1985.00	1320.22
3.PUMP DISCHARGE	2036.00	1366.02
4.LINE PRESSURE DROP	10.00	25.00
5.VALVE INLET	2026.00	1341.02
6.VALVE PRESSURE DROP	20.26	13.02
7.VALVE OUTLET	2005.78	1328.40
8.LINE PRESSURE DROP	10.00	15.00
8A.HEAT EXCHANGER INLET	1995.78	--
8B.HEAT EXCHANGER PRESSURE DROP	50.00	--
8C.HEAT EXCHANGER DISCHARGE	1945.78	--
8D.LINE PRESSURE DROP	30.00	--
9.COOLANT JACKET INLET	1915.78	--
10.COOLANT JACKET PRESSURE DROP	200.00	--
11.COOLANT JACKET OUTLET	1715.78	--
12.LINE PRESSURE DROP	30.00	--
13.FUEL CIRCUIT TURBINE INLET	1685.78	--
14.FUEL CIRCUIT TURBINE PRESSURE RAT.	1.233	--
15.FUEL CIRCUIT TURBINE EXIT	1402.58	--
15A.BETWEEN TURBINES PRESSURE DROP	45.08	--
15B.OX CIRCUIT TURBINE INLET	1357.51	--
15C.OX CIRCUIT TURBINE PRESSURE RAT.	1.058	--
15D.OX CIRCUIT TURBINE EXIT	1316.59	--
16.LINE PRESSURE DROP	32.91	--
16A.HEAT EXCHANGER INLET	1283.67	--
16B.HEAT EXCHANGER PRESSURE DROP	50.00	--
16C.HEAT EXCHANGER DISCHARGE	1233.67	--
16D.LINE PRESSURE DROP	16.46	--
17.TCA INJECTOR INLET	1217.22	1313.40
18.TCA INJECTOR PRESSURE DROP	100.83	197.01
19.TCA INJECTOR FACE	1116.39	1116.39
20.TCA PRESSURE DROP	16.39	16.39
21.CHAMBER PRESSURE	1100.00	1100.00

FLOWRATES (LBM/SEC)
TEMP DROP (DEGREES R)
CP(BTU/LBM-R)
(FC=FUEL CIRCUIT)
(OC=OX CIRCUIT)
(T-S=TOTAL TO STATIC TEMP)
(T=TOTAL TEMP)

1.FC TURBINE FLOW	5.66
2.OC TURBINE FLOW	5.66
3.FC TURB T DROP(T-S)	49.64
4.OC TURB T DROP(T-S)	13.01
5.FC TURB INLET T(T	863.00
6.FC TURB EXIT T(T)	824.77
7.OC TURB INLET T(T)	824.77
8.OC TURB EXIT T(T)	814.75
9.DRIVE GAS CP	3.530
10.DRIVE GAS GAMMA	1.395

HORSEPOWERS
AND EFFICIENCIES

(FC=FUEL CIRCUIT)
(OC=OX CIRCUIT)
(T-S=TOTAL TO STATIC TEMP)
(T=TOTAL TEMP)

1.FC TURB HORSEPOW	1081.06
2.OC TURB HORSEPOW	283.39
3.FC PUMP SHP	1081.06
4.OX PUMP SHP	283.39
5.FC TURBINE EFF	.770
6.OC TURBINE EFF	.770
7.FUEL PUMP EFF	.675
8.OX PUMP EFF	.650
9.OX FLOW	34.15
10.TOTAL FUEL FLO	6.03
11.TURBINE BYPASS FLOW	.36

III, B, Cycle Optimization (cont.)

fixed chamber pressures at each thrust level which results in equal performance engines.

Thrust, lb	Chamber Pressure psia	Series Turbine Cycle	Turbine Exhaust Heat Regeneration, Series Turbines Cycle
10,000	1300	2695	2645
15,000	1200	2473	2331
20,000	1100	2225	2036

The above comparisons show that the regenerator pays off more as the thrust is increased. This occurs because the baseline higher thrust cases have lower turbine inlet temperatures and more thermal enhancement is possible. The comparison also shows that, for these cases, the gains with a regenerator are modest. Therefore, the value of adding an engine component and increasing the system complexity and weight is questionable. The addition of a regenerator is probably best held as a design backup, if needed.

Comparisons were also made on the basis of system performance. For this analysis, the fuel pump discharge pressures at each thrust level were fixed at the series turbine values. Engine performance and weight trades were then performed. The results of this analysis are presented on Table XV. The table shows that the turbine exhaust heat regeneration concept does not pay off on a payload basis. Performance increases are not large enough to compensate for the weight increases.

Because a parallel turbine drive cycle has been shown to be more sensitive than the series turbine cycle, an analysis was conducted to show the effect of a regenerator on this cycle. Figure 32 is a

TABLE XV

SERIES TURBINES-TURBINES EXHAUST HEAT REGENERATION
PERFORMANCE/WEIGHT TRADES

THRUST klb	CYCLE	FUEL PUMP DISCHARGE PRESSURE, psia	CHAMBER PRESSURE, psia	NOZZLE AREA RATIO	ENGINE SPECIFIC IMPULSE, sec	ENGINE[1] WEIGHT CHANGE, lb	CHANGE IN AMOTV PAYLOAD, lb
10	Series Turbines	2695	1300	792	480.2	0	----
10	Turbine Exhaust Heat Regeneration	2695	1311	800	480.3	36/12	-32/-6
15	Series Turbines	2473	1200	473	477.2	0	----
15	Turbine Exhaust Heat Regeneration	2473	1230	485	477.4	60/21	-54/-9
20	Series Turbines	2225	1100	322	474.2	0	----
20	Turbine Exhaust Heat Regeneration	2225	1145	335	474.6	133/46	-117/-21

(1) Series Turbines Used as the Base in all Cases; First Number for Steel Regenerator and Second for Aluminum

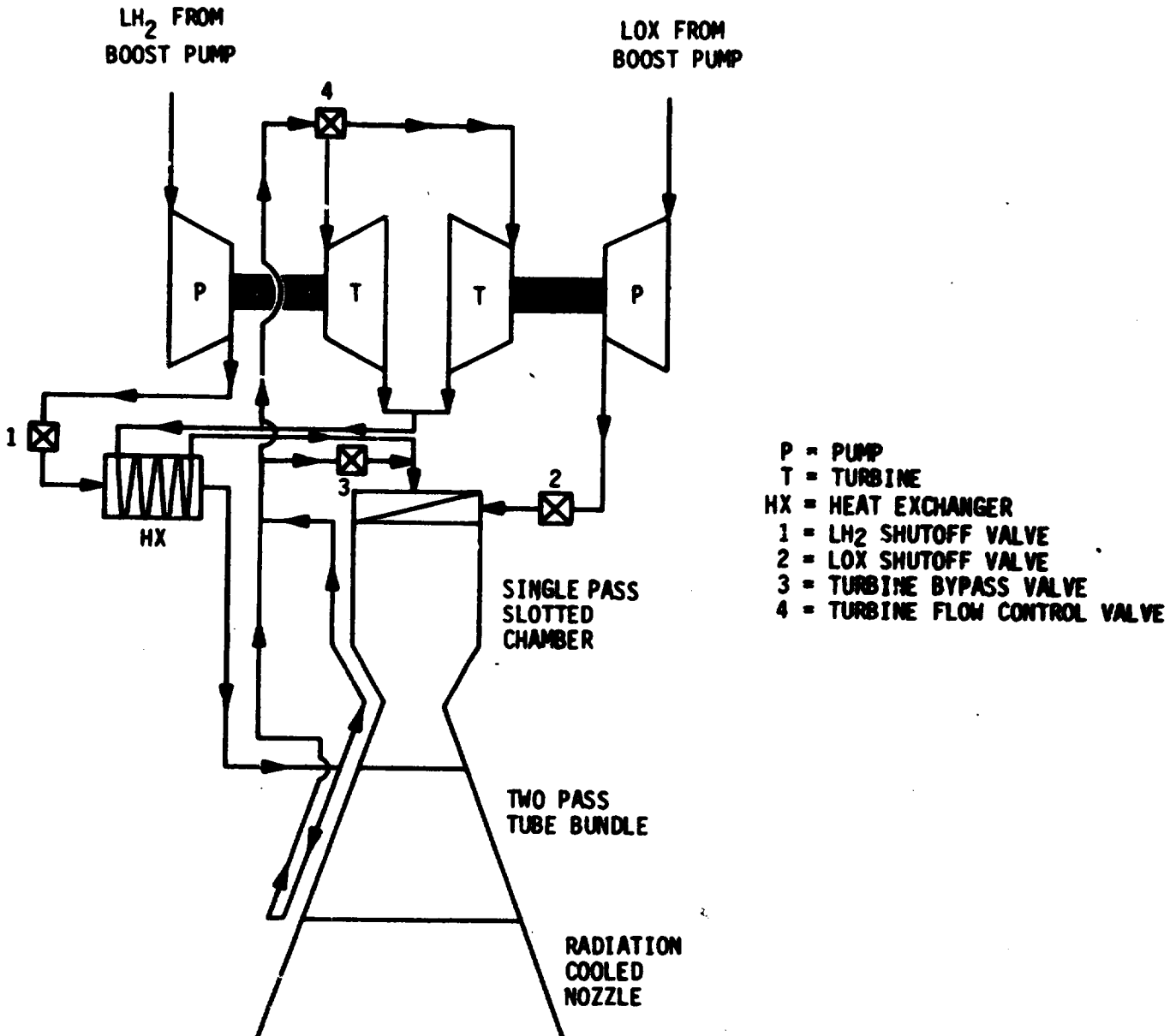

Figure 32. Turbine Exhaust Heat Regeneration / Parallel Turbines-
Advanced Expander Cycle Flow Schematic

III, B, Cycle Optimization (cont.)

simplified schematic of the parallel turbine/turbine exhaust heat regenerator cycle. A power balance at 10K lb thrust is shown on Table XVI for 1300 psia chamber pressure. The fuel pump discharge pressure is 2936 psia, compared to 3545 psia without a regenerator. This is a 609 psia reduction in the discharge pressure requirements. This converts to a 130 psia gain in thrust chamber pressure if the fuel pump discharge pressure is held constant. This chamber pressure gain would represent a 0.7 sec gain in specific impulse. The AMOTV performance/weight trade follows:

$$\Delta W_{PL} = \frac{\Delta W_{PL}}{\Delta I_s} \times \Delta I_s = +73 \frac{lb}{sec} \times .7 \text{ sec} = +51.1 \text{ lb}$$

$$\Delta W_{PL} = \frac{\Delta W_{PL}}{\Delta W_{eng}} \times \Delta W_{eng} = -1.1 \frac{lb}{lb} \times 36 \text{ lb} = -39.6 \text{ lb}$$

$$\text{TOTAL} \quad \Delta W_{PL} = +11.5 \text{ lb}$$

For this case, the addition of a regenerator shows a small gain. However, for the same case (i.e., P_{FD} = 3545, F = 10K lb), the series turbine arrangement, without a regenerator, has a 1 sec performance gain or a relative payload of +73 lb. This is a net payload advantage of 61.5 lb when compared to the above example.

3. Turbine Exhaust Gas Reheat Cycle Analysis

A simplified schematic of the turbine exhaust gas reheat cycle is shown in Figure 33. In this cycle, the hydrogen flow is first used to cool the combustion chamber and then drives the low horsepower oxidizer turbopump. The low horsepower pump is driven first to take only small pressure and temperature drops across the turbine. The hydrogen flow is then used

TABLE XVI

TURBINE EXHAUST HEAT REGENERATION, PARALLEL TURBINES, POWER BALANCE (F = 10K lb)

POWER BALANCE:
EXPANDER CYCLE
PARALLEL TURBINES
TURBINE EXHAUST REGENERATION
BOOST PUMPS

PRESSURE SCHEDULE (PSIA)

	FUEL CIRCUIT	LOX CIRCUIT
1.PUMP INLET	51.00	46.00
2.PUMP PRESSURE RISE	2885.13	1561.43
3.PUMP DISCHARGE	2936.13	1608.03
4.LINE PRESSURE DROP	10.00	25.00
5.VALVE INLET	2926.13	1583.03
6.VALVE PRESSURE DROP	29.26	15.83
7.VALVE OUTLET	2896.87	1567.20
8.LINE PRESSURE DROP	10.00	15.00
8A.HEAT EXCHANGER INLET	2886.87	--
8B.HEAT EXCHANGER PRESSURE DROP	50.00	--
8C.HEAT EXCHANGER EXIT	2836.87	--
8D.LINE PRESSURE DROP	30.00	--
9.COOLANT JACKET INLET	2806.87	--
10.COOLANT JACKET PRESSURE DROP	285.00	--
11.COOLANT JACKET OUTLET	2521.87	--
12.LINE PRESSURE DROP	20.00	--
12A.SPLITTER VALVE INLET	2501.87	--
12B.SPLITTER VALVE PRESSURE DROP	25.02	--
12C.SPLITTER VALVE EXIT	2476.85	--
12D.LINE PRESSURE DROP	10.00	--
13.TURBINE INLET	2466.85	--
14.TURBINE PRESSURE RATIO(PIN/POUT)	1.62	--
15.TURBINE OUTLET	1562.21	--
16.LINE PRESSURE DROP	39.06	--
16A.HEAT EXCHANGER INLET	1523.15	--
16B.HEAT EXCHANGER(TURBINE EXHAUST)	50.00	--
16C.HEAT EXCHANGER EXIT	1473.15	--
16D.LINE PRESSURE DROP	39.06	--
17.TCA INJECTOR INLET	1434.10	1552.20
18.TCA INJECTOR PRESSURE DROP	114.73	232.83
19.TCA INJECTOR FACE	1319.37	1319.37
20.TCA PRESSURE DROP	19.37	19.37
21.CHAMBER PRESSURE	1300.00	1300.00

FLOWRATES (LBM/SEC)
TEMP DROP (DEGREES R)
CP(BTU/LBM-R)
(FC=FUEL CIRCUIT)
(OC=OX CIRCUIT)
(T-S=TOTAL TO STATIC TEMP)
(T=TOTAL TEMP)

1.FC TURBINE FLOW	2.05
2.OC TURBINE FLOW	.78
3.FC TURB T DROP(T-S)	114.34
4.OC TURB T DROP(T-S)	114.34
5.TURB INLET T(T)	895.00
6.FC TURB EXIT T(T)	814.96
7.OC TURB EXIT T(T)	849.95
8.DRIVE GAS GAMMA	1.395
9.DRIVE GAS CP	3.530

HORSEPOWERS
AND EFFICIENCIES

(FC=FUEL CIRCUIT)
(OC=OX CIRCUIT)
(T-S=TOTAL TO STATIC TEMP)
(T=TOTAL TEMP)

1.FC TURB HORSEPOW	818.02
2.OC TURB HORSEPOW	175.35
3.FL PUMP SHP	818.02
4.OX PUMP SHP	175.35
5.FC TURBINE EFF	.700
6.OC TURB EFF	.394
7.FUEL PUMP EFF	.647
8.OX PUMP EFF	.620
9.TOTAL OX FLO	18.04
10.TOTAL FL FLO	3.01
11.TURB BYPASS FLOW	.18

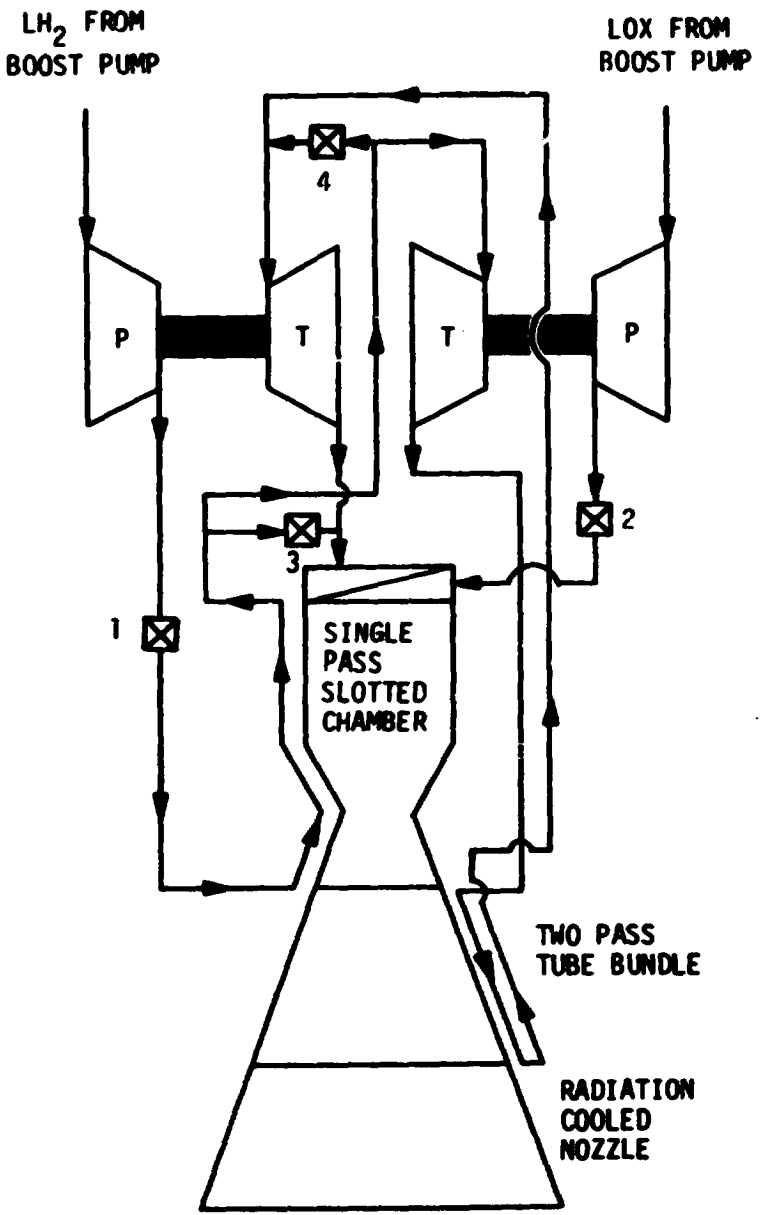

P = PUMP
T = TURBINE
1 = LH_2 SHUTOFF VALVE
2 = LOX SHUTOFF VALVE
3 = TURBINE BYPASS VALVE
4 = TURBINE FLOW CONTROL VALVE

Figure 33. Turbine Exhaust Gas Reheat/Series Turbines - Advanced Expander Cycle Flow Schematic

III, B, Cycle Optimization (cont.)

to cool the fixed portion of the nozzle before driving the high horsepower hydrogen pump. Six percent of the hydrogen flow again bypasses the turbines, which means that the fixed nozzle is cooled with 94 percent of the hydrogen flow.

Using the selected baseline chamber geometry, thermal analyses were conducted to support this investigation. The chamber designs, previously discussed, were cooled with 85% of the hydrogen flow. In this case, it is possible to cool with 100% of the hydrogen flow. This results in a small pressure drop increase, as shown in Table XVII.

Two-pass A-286 tube bundles were designed to cool the nozzle from an area ratio of 8:1 to the end of the fixed nozzle section. All designs are based on round tubes with a lineraly tapered wall thickness. Wall thicknesses at each end were selected to meet wall strength criteria; nowever, the forward end wall thickness was not allowed to be less than 0.007 inch. For each thrust level, the number of tubes was varied in order to define a design with wall temperatures consistent with the cycle life criteria. The resultant number of tubes, pressure drop, and hydrogen outlet temperature are shown in Table XVII. Temperature rises obtained in the nozzle are significant, whereas the pressure drops are small. The nozzle coolant inlet temperatures and pressures were calculated from preliminary cycle power balances and used as input to the thermal analyses.

The results of the power balance analyses are displayed on Tables XVIII, XIX, and XX at thrust levels of 10K, 15K, and 20K lb, respectively. The cycle does have increased warm gas plumbing, and these pressure drops have been accounted for as noted by the line drops in the pressure schedules. Turbomachinery efficiencies are the same as used in

TABLE XVII

TURBINE EXHAUST REHEAT CYCLE COOLING EVALUATION

THRUST KlbF	INLET PRESSURE, psia	INLET TEMPERATURE, °R	CHAMBER ΔP, psia (1)	CHAMBER ΔP, psia (2)	COOLED AREA RATIO	NUMBER OF TUBES	TUBE ΔP, psi	OUTLET TEMPERATURE, °R
10	2210	602	136	131	297	56	6.2	731
15	2040	484	95	92	186	58	4.8	590
20	1850	421	82	76	118	60	4.1	510

(1) Chamber cooled with 100% of the total hydrogen flow
(2) Chamber cooled with 85% of the total hydrogen flow

TABLE XVIII

TURBINE EXHAUST GAS REHEAT, SERIES TURBINES, POWER BALANCE (F = 10K lb)

POWER BALANCE
EXPANDER CYCLE)
SERIES TURBINES(1ST=OX CIRCUIT;2ND=FUEL CIRCUIT)
SEPARATE CHAMBER AND NOZZLE COOLANT JACKETS
BOOST PUMPS

PRESSURE SCHEDULE (PSIA)

	FUEL CIRCUIT	LOX CIRCUIT
1.PUMP INLET	51.00	46.00
2.PUMP PRESSURE RISE	2498.24	1561.43
3.PUMP DISCHARGE	2549.24	1608.03
4.LINE PRESSURE DROP	16.00	25.00
5.VALVE INLET	2533.24	1583.03
6.VALVE PRESSURE DROP	25.39	15.83
7.VALVE OUTLET	2513.85	1567.20
8.LINE PRESSURE DROP	30.00	15.00
9.CHAMBER COOLANT JACKET INLET	2483.85	--
10.CHAMBER COOLANT JACKET P DROP	131.00	--
11.CHAMBER COOLANT JACKET OUTLET	2352.85	--
12.LINE PRESSURE DROP	30.00	--
13.OX CIRCUIT TURBINE INLET	2322.85	--
14.OX CIRCUIT TURBINE PRESSURE RATIO	1.100	--
15.OX CIRCUIT TURBINE EXIT	2166.31	--
15A.LINE PRESSURE DROP	64.16	--
15B.NOZZLE COOLANT JACKET INLET	2102.15	--
15C.NOZZLE COOLANT JACKET P DROP	6.00	--
15D.NOZZLE COOLANT JACKET EXIT	2096.15	--
15E.LINE PRESSURE DROP	21.39	--
15F.FUEL CIRCUIT TURBINE INLET	2074.77	--
15G.FUEL CIRCUIT TURBINE PRESSURE RAT	1.441	--
15H.FUEL CIRCUIT TURBINE EXIT	1477.14	--
16.LINE PRESSURE DROP	37.87	--
17.TCA INJECTOR INLET	1439.26	1552.20
18.TCA INJECTOR PRESSURE DROP	119.89	232.83
19.TCA INJECTOR FACE	1319.37	1319.37
20.TCA PRESSURE DROP	19.37	19.37
21.CHAMBER PRESSURE	1300.00	1300.00

FLOWRATES (LBM/SEC)
TEMP DROP (DEGREES R)
CP(BTU/LBM-R)
(FC=FUEL CIRCUIT)
(OC=OX CIRCUIT)
(T-S=TOTAL TO STATIC TEMP)
(T=TOTAL TEMP)

1.FC TURBINE FLOW	2.88
2.OC TURBINE FLOW	2.88
3.FC TURB T DROP(T-S)	71.75
4.OC TURB T DROP(T-S)	16.31
5.FC TURB IN T(T)	730.60
6.FC TURB EXIT T(T)	670.23
7.OC TURB IN T(T)	618.00
8.OC TURB EXIT T(T)	601.60
9.DRIVE GAS (FROM CHMBR)CP	3.538
10.DRIVE GAS GAMMA	1.395
11.DRIVE GAS(FROM NOZ)CP	3.538
12.DRIVE GAS(FROM NOZ)GAMMA	1.395
13.TURBINE BYPASS FLOW	.18

HORSEPOWERS
AND EFFICIENCIES

(FC=FUEL CIRCUIT)
(OC=OX CIRCUIT)
(T-S=TOTAL TO STATIC TEMP)
(T=TOTAL TEMP)

1.FC TURB HORSEPOW	731.37
2.OC TURB HORSEPOW	173.50
3.FL PUMP BHP	731.37
4.OX PUMP BHP	173.50
5.FC TURBINE EFF	.730
6.OC TURB EFF	.760
7.FUEL PUMP EFF	.620
8.OX PUMP EFF	.620
9.OX FLO	17.05
10.TOTAL FUEL FLO	2.97

SINPUT

TABLE XIX

TURBINE EXHAUST GAS REHEAT, SERIES TURBINES, POWER BALANCE (F = 15K lb)

POWER BALANCE
EXPANDER CYCLE
SERIES TURBINES(1ST=OX CIRCUIT;2ND=FUEL CIRCUIT)
SEPARATE CHAMBER AND NOZZLE COOLANT JACKETS
BOOST PUMPS

PRESSURE SCHEDULE (PSIA)

	FUEL CIRCUIT	LOX CIRCUIT
1,PUMP INLET	51.00	86.60
2,PUMP PRESSURE RISE	2332.37	1440.83
3,PUMP DISCHARGE	2383.37	1487.43
4,LINE PRESSURE DROP	10.00	25.00
5,VALVE INLET	2373.37	1462.43
6,VALVE PRESSURE DROP	23.73	14.62
7,VALVE OUTLET	2349.64	1447.80
8,LINE PRESSURE DROP	30.00	15.00
9,CHAMBER COOLANT JACKET INLET	2319.64	--
10,CHAMBER COOLANT JACKET P DROP	92.00	--
11,CHAMBER COOLANT JACKET OUTLET	2227.64	--
12,LINE PRESSURE DROP	30.00	--
13,OX CIRCUIT TURBINE INLET	2197.64	--
14,OX CIRCUIT TURBINE PRESSURE RATIO	1.106	--
15,OX CIRCUIT TURBINE EXIT	2038.40	--
15A,LINE PRESSURE DROP	60.96	--
15B,NOZZLE COOLANT JACKET INLET	1977.44	--
15C,NOZZLE COOLANT JACKET P DROP	5.00	--
15D,NOZZLE COOLANT JACKET EXIT	1972.44	--
15E,LINE PRESSURE DROP	20.32	--
15F,FUEL CIRCUIT TURBINE INLET	1952.12	--
15G,FUEL CIRCUIT TURBINE PRESSURE RAT	1.470	--
15H,FUEL CIRCUIT TURBINE EXIT	1362.03	--
16,LINE PRESSURE DROP	34.92	--
17,TCA INJECTOR INLET	1327.10	1432.80
18,TCA INJECTOR PRESSURE DROP	109.22	214.92
19,TCA INJECTOR FACE	1217.88	1217.88
20,TCA PRESSURE DROP	17.88	17.88
21,CHAMBER PRESSURE	1200.00	1200.00

FLOWRATES (LBM/SEC)
TEMP DROP (DEGREES R)
CP(BTU/LBM-R)
(FC=FUEL CIRCUIT)
(OC=OX CIRCUIT)
(T-S=TOTAL TO STATIC TEMP)
(T=TOTAL TEMP)

1,FC TURBINE FLOW	4.22
2,OC TURBINE FLOW	4.22
3,FC TURB T DROP(T-S)	61.02
4,OC TURB T DROP(T-S)	13.88
5,FC TURB IN T(T)	590.38
6,FC TURB EXIT T(T)	544.62
7,OC TURB IN T(T)	495.00
8,OC TURB EXIT T(T)	488.38
9,DRIVE GAS (FROM CHMBR)CP	3.716
10,DRIVE GAS GAMMA	1.394
11,DRIVE GAS(FROM NOZ)CP	3.570
12,DRIVE GAS(FROM NOZ)GAMMA	1.395
13,TURBINE BYPASS FLOW	.27

HORSEPOWERS
AND EFFICIENCIES

(FC=FUEL CIRCUIT)
(OC=OX CIRCUIT)
(T-S=TOTAL TO STATIC TEMP)
(T=TOTAL TEMP)

1,FC TURB HORSEPOW	975.58
2,OC TURB HORSEPOW	235.57
3,FL PUMP SHP	975.58
4,OX PUMP SHP	235.57
5,FC TURBINE EFF	.750
6,OC TURB EFF	.765
7,FUEL PUMP EFF	.655
8,OX PUMP EFF	.636
9,OX FLO	20.94
10,TOTAL FUEL FLO	4.49

$INPUT

TABLE XX

TURBINE EXHAUST GAS REHEAT, SERIES TURBINES, POWER BALANCE (F = 20K lb)

POWER BALANCE
EXPANDER CYCLE
SERIES TURBINES(1ST=OX CIRCUIT;2ND=FUEL CIRCUIT)
SEPARATE CHAMBER AND NOZZLE COOLANT JACKETS
BOOST PUMPS

PRESSURE SCHEDULE (PSIA)

	FUEL CIRCUIT	LOX CIRCUIT
1.PUMP INLET	51.00	46.60
2.PUMP PRESSURE RISE	2093.50	1320.22
3.PUMP DISCHARGE	2144.50	1366.82
4.LINE PRESSURE DROP	10.00	25.00
5.VALVE INLET	2134.50	1341.82
6.VALVE PRESSURE DROP	21.34	13.42
7.VALVE OUTLET	2113.15	1328.40
8.LINE PRESSURE DROP	30.00	15.00
9.CHAMBER COOLANT JACKET INLET	2083.15	--
10.CHAMBER COOLANT JACKET P DROP	76.00	--
11.CHAMBER COOLANT JACKET OUTLET	2007.15	--
12.LINE PRESSURE DROP	30.00	--
13.OX CIRCUIT TURBINE INLET	1977.15	--
14.OX CIRCUIT TURBINE PRESSURE RATIO	1.107	--
15.OX CIRCUIT TURBINE EXIT	1832.28	--
15A.LINE PRESSURE DROP	55.81	--
15B.NOZZLE COOLANT JACKET INLET	1776.48	--
15C.NOZZLE COOLANT JACKET P DROP	4.00	--
15D.NOZZLE COOLANT JACKET EXIT	1772.48	--
15E.LINE PRESSURE DROP	18.60	--
15F.FUEL CIRCUIT TURBINE INLET	1753.87	--
15G.FUEL CIRCUIT TURBINE PRESSURE RAT	1.461	--
15H.FUEL CIRCUIT TURBINE EXIT	1248.68	--
16.LINE PRESSURE DROP	32.02	--
17.TCA INJECTOR INLET	1216.66	1313.40
18.TCA INJECTOR PRESSURE DROP	100.27	197.01
19.TCA INJECTOR FACE	1116.39	1116.39
20.TCA PRESSURE DROP	16.39	16.39
21.CHAMBER PRESSURE	1100.00	1100.00

FLOWRATES (LBM/SEC)
TEMP DROP (DEGREES K)
CP(BTU/LBM-R)
(FC=FUEL CIRCUIT)
(OC=OX CIRCUIT)
(T-S=TOTAL TO STATIC TEMP)
(T=TOTAL TEMP)

1.FC TURBINE FLOW	5.66
2.OC TURBINE FLOW	5.66
3.FC TURB T DROP(T-S)	50.06
4.OC TURB T DROP(T-S)	11.99
5.FC TURB IN T(T)	909.77
6.FC TURB EXIT T(T)	871.22
7.OC TURB IN T(T)	430.00
8.OC TURB EXIT T(T)	420.77
9.DRIVE GAS (FROM CHMBR)CP	3.832
10.DRIVE GAS GAMMA	1.367
11.DRIVE GAS(FROM NOZ)CP	3.692
12.DRIVE GAS(FROM NOZ)GAMMA	1.395
13.TURBINE BYPASS FLOW	.36

HORSEPOWERS
AND EFFICIENCIES

(FC=FUEL CIRCUIT)
(OC=OX CIRCUIT)
(T-S=TOTAL TO STATIC TEMP)
(T=TOTAL TEMP)

1.FC TURB HORSEPOW	1140.13
2.OC TURB HORSEPOW	283.39
3.FL PUMP BHP	1140.13
4.OX PUMP BHP	283.39
5.FC TURBINE EFF	.770
6.OC TURB EFF	.770
7.FUEL PUMP EFF	.675
8.OX PUMP EFF	.650
9.OX FLO	30.15
10.TOTAL FUEL FLO	6.03

C-2

the series turbine cycle evaluations. The tables show that this cycle has slightly reduced fuel pump discharge pressure requirements when compared to the series turbine arrangement at fixed chamber pressures. These discharge pressures are as follows:

	Fuel Pump Discharge Pressure, psia	
Thrust, lb	Series Turbine Cycle	Turbine Exhaust Gas Reheat Cycle
10K	2695	2549
15K	2473	2383
20K	2225	2145

Performing the optimization for a given set of discharge pressures results in the following comparisons:

Thrust lb	Cycle	FUEL PUMP DISCHARGE PRESSURE, psia	CHAMBER PRESSURE, psia	ENGINE SPECIFIC IMPULSE, sec
10	Series Turbines	2695	1300	480.2
15		2473	1200	477.2
20		2225	1100	474.2
10	Turbine Exhaust Gas Reheat	2695	1330	480.4
15		2473	1220	477.4
20		2225	1120	474.4

III, B, Cycle Optimization (cont.)

The small reductions in discharge pressure requirements or the 3.2 sec increase in performance are not considered significant enough to offset the additional cycle complexity and component interactions to where it would warrant a selection of this cycle over a series turbine drive cycle.

4. Cycle Analysis Summary

The results of all power balance and performance/weight trade analyses are summarized in Tables XXI and XXII.

Table XXI shows that the largest benefit is obtained with a series turbine arrangement rather than with parallel turbines. Further reductions in fuel pump discharge pressure requirements and turbine pressure ratios which reduce cycle sensitivity can be obtained through turbine exhaust heat regeneration or turbine exhaust reheat schemes.

Table XXII compares the performance of the new cycles to the original parallel turbine cycle baseline. Relative payloads are all computed using the parallel turbine cycle as a baseline for each thrust level. No attempt is made to compare the relative payload capability of the various thrust levels. This table shows that while the turbine exhaust reheat cycle has the highest performance potential, the series turbine cycle arrangement offers about the same capability.

C. CONTROLS ANALYSIS

The objectives of this controls study were to provide a preliminary definition of the controls required to operate the series turbine advanced expander cycle engine to determine the operational sequence and to establish

TABLE XXI

CYCLE OPTIMIZATION POWER BALANCE DATA SUMMARY
(FIXED CHAMBER PRESSURES)

THRUST, lb	CHAMBER PRESSURE, psia	CYCLE	FUEL PUMP DISCHARGE PRESSURE, psia	TURBINE PRESSURE RATIO	
				FUEL	OX.
10,000	1300	Parallel Turbines	3545	2.284	2.284
15,000	1200	↓	3174	2.229	2.229
20,000	1100		2764	2.113	2.113
10,000	1300	Series Turbines	2695	1.548	1.103
15,000	1200	↓	2473	1.544	1.109
20,000	1100		2225	1.514	1.109
10,000	1300	Turbine Exhaust Heat	2645	1.356	1.071
15,000	1200	Regeneration With	2331	1.337	1.075
20,000	1100	Series Turbines	2036	1.233	1.058
10,000	1300	Turbine Exhaust Heat Regeneration With Parallel Turbines	2936	1.620	1.620
10,000	1300	Turbine Exhaust	2549	1.441	1.100
15,000	1200	Reheat With Series	2383	1.470	1.106
20,000	1100	Turbines	2145	1.440	1.107

TABLE XXII

CYCLE PERFORMANCE OPTIMIZATION DATA SUMMARY (FIXED FUEL PUMP DISCHARGE PRESSURES)

THRUST, lb	CYCLE	FUEL PUMP DISCHARGE PRESSURE, psia	CHAMBER PRESSURE, psia	ENGINE SPECIFIC IMPULSE, sec	ENGINE WEIGHT, lb	AMGTV RELATIVE PAYLOAD, lb
10,000	Parallel Turbines	3545	1300	480.2	447	0
15,000	↓	3174	1200	477.2	502	0
20,000		2764	1100	474.2	554	0
10,000	Series Turbines	3545	1480	481.2	455	+64
15,000	↓	3174	1345	478.1	514	+53
20,000		2764	1225	475.1	567	+51
10,000	Turbine Exhaust Heat	3545	1490	481.2	492/467(1)	+24/+51(1)
15,000	Regeneration With	3174	1375	478.3	581/535	-7/+44
20,000	Series Turbines	2764	1270	475.4	710/606	-84/+30
10,000	Turbine Exhaust Heat Regeneration With Parallel Turbines	3545	1430	480.9	488/464	+6/+32
10,000	Turbine Exhaust	3545	1510	481.3	457	+69
15,000	Reheat With Series	3174	1365	478.2	520	+53
20,000	Turbines	2764	1245	475.3	572	+61

(1) Stainless Steel Regenerator/Aluminum Regenerator

preliminary sizes and weights for these controls.

One of the primary goals was to minimize system complexity, in terms of reducing the number of active controls, while providing a safe and reliable operating system. As a result, two basic systems were defined and evaluated on a qualitative basis. The first system is identified as an active (closed-loop) system and contains two closed-loop control valves along with other valves which have on-off functions. A schematic of this system is shown in Figure 34. The other system is identified as a passive (open-loop) system and consists primarily of on-off valves, with two of the valves identified as three position on-off valves. This system is shown in Figure 35.

The passive system provides reduced complexity and, hence, is inherently more reliable on a statistical basis. However, use of this system results in larger variations in mixture ratio and thrust. A transient and steady-state analysis is required to determine the magnitude of these variations, which can then be compared to the requirements for safe engine operation. This is beyond the scope of the current study. However, engine cycle sensitivity analyses (Section III,D.) have shown a worse case chamber pressure variation of 12.1%, based on major components operating at worse case conditions. Therefore, due to engine system uncertainties at this phase of design evolution, initial control system design efforts are recommended to be based on an active (closed-loop) control system. It should be noted that the valve configuration and actuation options presented in this preliminary study are typical candidates and were selected without the benefit of a detailed design tradeoff study. Additional studies are also necessary to cover the required instrumentation, engine harness, and controller along with the engine purge, bleed, vent, and drain procedures. A summary of the preliminary component candidates is presented in Table XXIII.

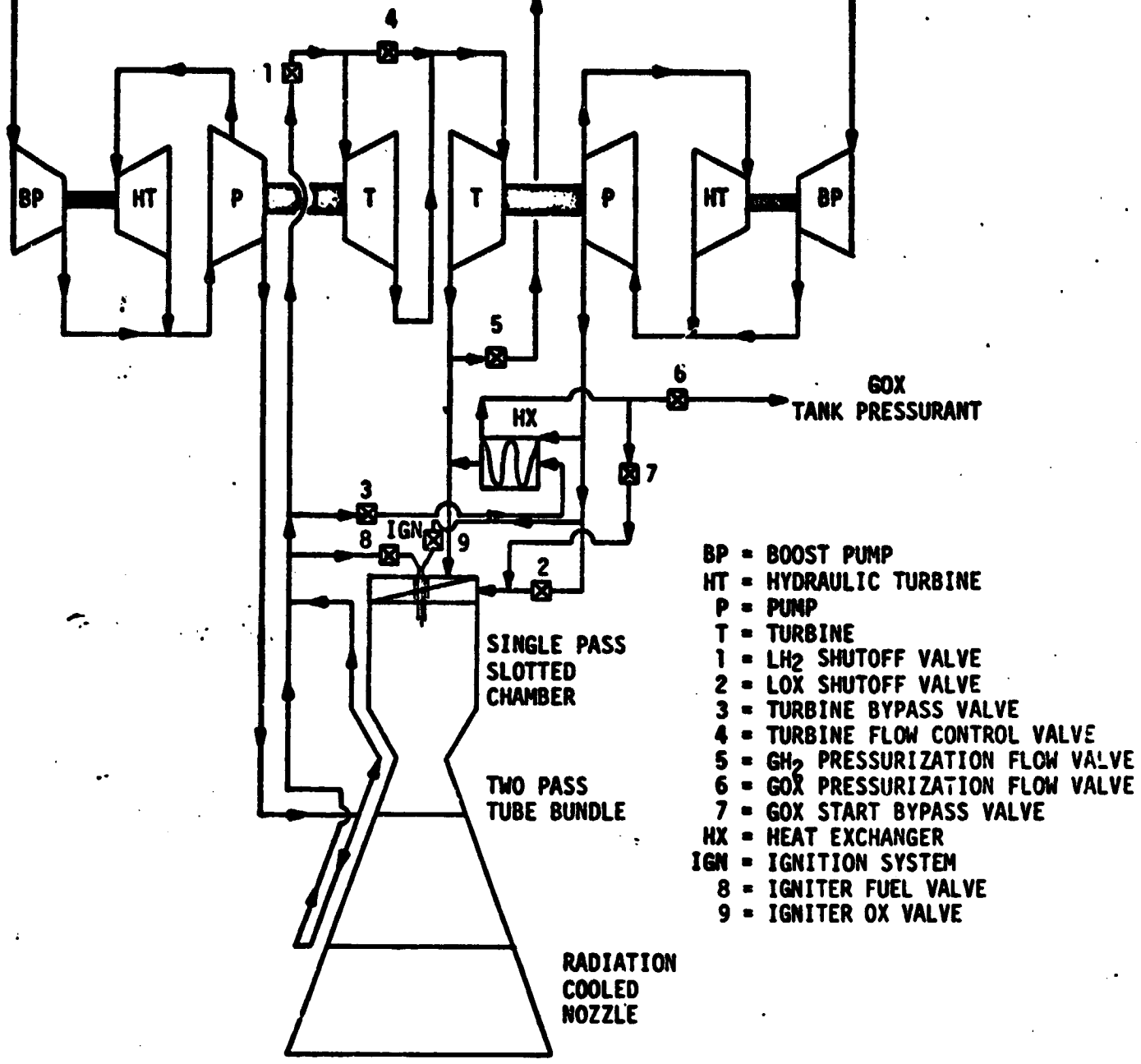

Figure 34. Series Turbine Advanced Expander Cycle Flow Schematic, Active Control System

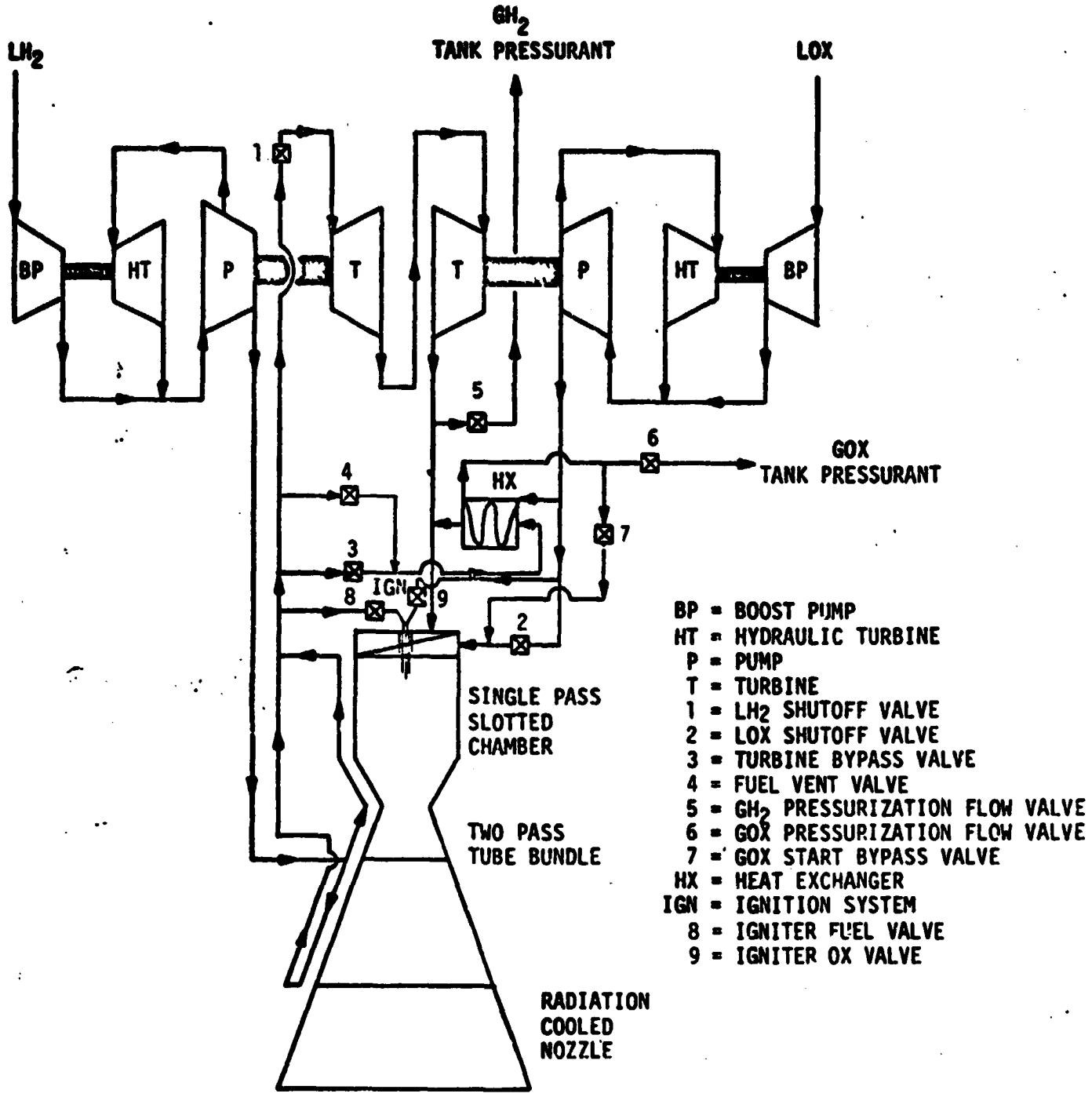

Figure 35. Series Turbine Advanced Expander Cycle Flow Schematic, Passive Control System

TABLE XXIII

PRELIMINARY CONTROLS COMPONENT DEFINITION

COMPONENT	TYPE SYSTEM ACTIVE	TYPE SYSTEM PASSIVE	OPER. PRESS. (PSIA)	LINE SIZE (IN)	ACTUATION METHOD SYSTEM ACTIVE	ACTUATION METHOD SYSTEM PASSIVE	ESTIMATED WT. (LBS) SYSTEM ACTIVE	ESTIMATED WT. (LBS) SYSTEM PASSIVE
LH_2 SHUTOFF VALVE	BALL	BALL	~ 2140	1.5	PENUMATIC (GH_e)	PNEUMATIC (GH_e)	14.0	14.0
LO_2 SHUTOFF VALVE	BALL	BALL	~ 1437	1.5	PNEUMATIC (GOX)	PNEUMATIC (GOX)	14.0	16.0
TURBINE BYPASS VALVE	VISOR	POPPET	~ 2140	1.5	ELECTRIC MOTOR	PNEUMATIC (GH_2)	18.0	16.0
TURBINE FLOW CONTROL	BUTTERFLY		~ 2100	1.5	ELECTRIC MOTOR		17.0	
FUEL VENT VALVE		POPPET	~ 2140	1.5		PENUMATIC (GH_e)		12.0
TANK PRESSURIZATION VLVS (2 EA (GOX/GH_2)	POPPET	POPPET	1400/1300	.75	PNEUMATIC (GOX/GH_2)	PNEUMATIC (GOX/GH_2)	8	6
GO_2 START BYPASS VALVE	POPPET	POPPET	~ 1400	1.25	PNEUMATIC (GOX)	PNEUMATIC (GOX)	6.5	6.5
IGNITER VLVS- 2 EA (GOX/GH_2)	POPPET	POPPET	1437/2140	.25	ELECTRIC SOLENOID	ELECTRIC SOLENOID	2.4	2.4
							79.9	72.9
							(TOTAL)	

III, C, Controls Analysis (cont.)

1. Controls Definition

a. Active System Components

(1) Fuel Shutoff Valve

The primary functions of the fuel shutoff valve (Valve #1 in Figure 34) are to terminate fuel flow at engine shutdown and to prevent flow through the turbines during the tank-head idle mode. To provide these functions, the valve is a normally closed on-off valve. To provide high shutoff and leakage reliability, the valve is series-redundant and is fail-safe to the closed position in the event of electrical power loss. The preliminary selected configuration is a ball valve incorporating a shutoff seal that is only in contact with the ball in the closed position. This provides high cycle life with low leakage while minimizing flow resistance in the fully open position. The valve can be actuated using either a pneumatic (GH_e) or electric motor drive actuator because engine system pressures will be low when this valve is required to open.

Consideration was given to locating this valve downstream of the turbines to minimize the shutdown transient. However, it is estimated that the back pressure generated by valve ΔP would adversely affect the pressure ratio across the pump turbines. Consideration was also given to incorporating the tank-head idle mode shutoff function in the turbine flow control valve (Valve #4). However, this would require a larger, heavier 3-way valve which would also have to be located upstream of the fuel turbine inlet, as shown in Figure 34. The exact location of this valve should be determined after the transient analysis and design studies have been accomplished. During these studies, consideration must also be given to the redundancy requirements.

III, C Controls Analysis (cont.)

(2) Oxidizer Shutoff Valve

The main purpose of the oxidizer shutoff valve (Valve #2) is to terminate oxidizer flow at engine shutdown. The valve is located as close to the injector as possible to minimize the residual oxidizer in the system downstream of the valve at engine shutdown. This valve is a normally closed on-off valve and will be fail-safe to the closed position in the event of electrical power loss. To provide high reliability in the shutoff mode, the valve is series-redundant. In this location, it is important to have low shutoff leakage combined with high cycle life and low flow resistance. These requirements can be satisfied by use of a ball valve with a shutoff seal that only contacts the ball in the closed position. Because the oxidizer shutoff valve is required to open during the transient from tank-head idle to pumped idle, rising oxidizer pump discharge pressure could be utilized to actuate this valve to the open position.

(3) Turbine Bypass Valve

The functions of this valve (Valve #3) are to control the total flow of GH_2 to the injector during tank-head idle and to control bypass flow around the pump turbines during pumped idle and at full-thrust operation. The valve is fully open at tank-head idle and almost closed at full thrust. This valve can also be utilized to limit overshoot during the transient from pumped idle to full thrust. The valve is closed for engine shutdown and then opened following shutdown after the prevalves have been closed to prevent excessive pressure buildup in the engine fuel circuit.

A preferred candidate for this application is a visor valve that has a contoured flow area machined into the visor to

provide the required area vs position characteristics. Actuation of this valve can be provided by electric motor drive. A valve of this type was designed and fabricated by Aerojet for use on the NERVA Nuclear Rocket Engine Program. Valve control is a closed loop system which will sense and control thrust chamber pressure. In the event of vehicle electrical power loss, a pneumatic override can be provided to make the valve fail-safe to the open position. The valve location is shown in Figure 34.

(4) Turbine Flow Control Valve

The turbine flow control valve (Valve #4) provides proportional GH_2 flow control to the fuel and oxidizer pump turbines to maintain the required engine mixture ratio. This function can be provided by a simple butterfly valve driven by an electric motor actuator. The control system would be closed-loop and would sense fuel and oxidizer injector pressure to control mixture ratio. The valve is located in the turbine drive circuit, as shown in Figure 34.

(5) Fuel and Oxidizer Tank Pressurization Valves

The functions of the tank pressurization valves (Valves #5 and #6) are to control the flow of the fuel and oxidizer from the engine for the purpose of pressurizing the fuel and oxidizer tanks. The valves are normally closed modulating valves, made fail-safe to the closed position. Poppet valves can be used to provide low leakage and high cycle life. The valves are closed during tank-head idle and while the engine is not operating to prevent pressurant gas backflow into the engine system. The valves are open and modulating during pumped idle and full-thrust operation to control tank pressurization. Valve actuation can be provided by engine propellant pressure rise during the transition from tank-head idle to pumped idle. Propellant tank pressures are sensed to control valve

modulation. The fuel valve is located downstream of the pump turbines, and the oxidizer valve is located downstream of the GO_2 heat exchanger, as shown in Figure 34.

(6) GO_2 Start Bypass Valve

The main function of the GO_2 start bypass valve (Valve #7) is to control the flow of gaseous oxygen from the heat exchanger to the injector during tank-head idle. The valve is also required to remain closed at engine shutdown to prevent bypassing oxidizer flow around the LO_2 shutoff valve. This function can be performed by using either a poppet or sleeve valve. The valve is open during the tank-head idle mode and closed by the rising oxidizer pressure during the transition to the pumped idle position. At engine shutdown, the valve remains closed until the LO_2 prevalve is closed. Following LO_2 prevalve closure, the GO_2 start bypass valve will open. Therefore, the valve will be an on-off, normally open, latching-type valve and will be fail-safe to the open position. A solenoid-operated latch will hold the valve closed during engine shutdown. When the LO_2 pre-valve is closed, or if vehicle electrical power is lost, the latch will desengage and the valve will open to prevent the buildup of excessive pressure in the oxidizer circuit. The valve is located between the GO_2 heat exchanger and the injector, as shown in Figure 34.

(7) Igniter Valves

The functions of the fuel and oxidizer igniter valves (Valves #8 and #9) are to initiate propellant flow to the ignition system at the beginning of the tank-head idle mode and to terminate propellant flow at engine shutdown. The valves are normally closed, solenoid-operated on-off valves which will fail closed in the event of electrical

power loss. The solenoids will have a dual coil and connector configuration to provide high opening reliability. The valves are located in the igniter circuit adjacent to the injector, as shown in Figure 34.

b. Passive System Components

(1) LH_2 Shutoff Valve, GO_2 Start Bypass Valve and Igniter Valves

These valves are identical to those previously described for use in the active system.

(2) Oxidizer Shutoff Valve

The primary functions of the oxidizer shutoff valve (Valve #2 on Figure 35) are to control mixture ratio in the pumped idle and full-thrust modes of operation and to terminate oxidizer flow at engine shutdown. The valve is located close to the injector to minimize residual oxidizer in the system downstream of the valve at engine shutdown. To provide high reliability in the shutoff mode, a series-redundant ball valve configuration is used. To maintain low leakage and high cycle life, the shutoff seal will only contact the ball when the valve is in the closed position. This type of valve can be designed using a two-stage, externally adjustable actuator. The valve is classified as a three-position, on-off valve and is fail-safe to the closed position in the event of electrical power loss. This normally closed valve is actuated to the pumped idle position by one actuator stage and then to the full-thrust position by the other stage via oxidizer pump discharge pressure. Each actuator stage requires an external mechanical adjustment to adjust the valve flow area. The valve can be adjusted initially during component flow tests, and then trimmed during engine

acceptance tests, to produce the engine steady-state mixture ratios required for the specified missions. The valve is located as shown in Figure 35.

(3) Turbine Bypass Valve

The function of this valve (Valve #3) is to control bypass flow around the pump turbines during the pumped-idle and full-thrust modes. The valve remains closed during the tank-head idle mode. This valve can be a coaxial-type valve, with a balanced poppet or sleeve closure element actuated by a two-stage, externally adjustable actuator. The valve is a normally closed, three-position, on-off valve similar in design to the LO_2 shutoff valve. The first actuator stage can utilize rising pump discharge pressure to fully open the valve to the pumped-idle position. The second actuator stage would partially close the valve to the full-thrust position. External actuator mechanical adjustments can be provided to trim engine thrust levels in the pumped-idle and full-thrust modes. The valve is closed following engine shutdown and will be fail-safe to the closed position in the event of electrical power loss. The location of this valve is shown on Figure 35.

(4) Fuel Vent Valve

The fuel vent valve (Valve #4) is provided to control the total flow of hydrogen to the thrust chamber during tank-head idle. Following engine shutdown, the valve is opened to prevent excessive pressure buildup in the engine fuel circuit. The valve can also be used to control pump acceleration and thrust overshoot during engine transient operation. The valve can be a normally open, on-off valve and will be fail-safe to the open position in the event of vehicle power loss. This valve can be a balanced poppet of sleeve valve that is operated by a pneumatic (GH_e)

actuator. The valve is located as shown in Figure 35.

(5) Fuel and Oxidizer Tank Pressurization Valves

The functions of the tank pressurization valves (Valves #5 and #6) are to control the flow of fuel and oxidizer from the engine for the purpose of pressurizing the fuel and oxidizer tanks. For a passive system, the valves are normally closed on-off valves, fail-safe to the closed position. Tank pressurization analyses are required to determine if an on-off valve, orificed to control pressurization flow, is adequate to maintain tank feed pressure limits during engine operation. Poppet valves can be used to provide low leakage and high cycle life. The valves are closed during tank head idle and, when the engine is not operating, to prevent pressurant gas backflow into the engine system. The valves are open during pumped idle and full thrust operation. Valve actuation can be provided by engine propellant pressure rise during the transition from tank head idle to pumped idle. The fuel valve can be located downstream of the pump turbines and the oxidizer valve can be located downstream of the GO_2 heat exchanger as shown on Figure 35.

2. System Operation

The engine system will be designed for stable and reliable operation in the three different operating modes and during the transition from one operating mode to another. The following discussion describes operation of both the active and passive systems and lists concerns that should be evaluated during the engine transient analysis connected with engine design activities.

III, C, Controls Analysis (cont.)

a. Active System

(1) Tank Head Idle Mode

During tank-head idle, propellants at tank vapor pressure are circulated through the engine to condition the system and provide low thrust propulsive burning of the chilldown propellants. To initiate this sequence, the vehicle fuel and oxidizer prevalves are opened.

On the fuel side, hydrogen flows through the pumps, thrust chamber coolant jacket, turbine bypass valve (#3), GO_2 heat exchanger and into the injector in a gaseous state. On the oxidizer side, oxygen will flow through the pumps, GO_2 heat exchanger, GO_2 start bypass valve (#7) and into the injector in a gaseous state. The igniter valves (#8 and #9) are opened, and the spark igniters are activated to initiate thrust chamber combustion.

No major problems are expected during this mode of operation. Transient analyses should be performed to determine the required time for engine conditioning.

(2) Pumped-Idle Mode

The pumped-idle mode is initiated by the following sequence:

(a) Open the LH_2 and LO_2 shutoff valves (#1 and #2).

(b) Close the turbine bypass valve (#3) to direct all hydrogen flow through the pump turbines. As soon as pump breakaway torque is overcome and both pumps are rotating, the turbine bypass valve is modulated to control the transient from tank-head idle to pumped idle.

Two concerns are evident during this phase of operation. One concern is that one pump may break away before the other, causing an abnormal mixture ratio. The other is that the pump acceleration rates need to be controlled so that the pumps do not cavitate during the transient. Modulation of the turbine flow control valve (#4) may minimize the off-mixture ratio condition. However, because the injector and thrust chamber pressures are low during this stage of operation, sensing of pump turbine speeds may be required to control modulation of the turbine bypass and turbine flow control valves.

(c) As engine system pressures are ramped up to the pumped-idle, steady-state level, the GO_2 start bypass valve closes and the fuel and oxidizer tank pressurization valve (#5 and #6) open to provide autogenous pressurization of the propellant tanks.

(d) The turbine bypass valve is modulated to control the pumped-idle, steady-state thrust level, and the turbine flow control valve is modulated to control mixture ratio.

(3) Full Thrust

The transient from pumped idle to full thrust is controlled by modulating the turbine bypass valve to control thrust and limit thrust overshoot. The turbine flow control valve is modulated to

control mixture ratio. Transient analyses are necessary to assure optimum engine control during the ramp from pumped idle to full thrust.

(4) Shutdown

The engine can be shut down from the full-thrust, pumped-idle or tank-head idle thrust levels. Shutdown is accomplished by closing the LO_2 and LH_2 shutoff valves, the igniter valves, and turbine bypass valve. As the propellant pressures decay, the GO_2 start valve remains latched in the closed position, and the fuel and oxidizer tank pressurization valves close. If a restart is not planned within a specified length of time, the vehicle prevalves are closed, and the turbine bypass and GO_2 start bypass valves are opened. Valve sequence timing should be determined by transient analysis in the future design analysis effort.

b. Passive System

(1) Tank-Head Idle Mode

This mode of operation is the same as described for the active system except that, on the fuel side, hydrogen will flow through the pumps, thrust chamber coolant jacket, fuel vent valve, GO_2 heat exchanger and into the injector in a gaseous state.

(2) Pumped-Idle Mode

The pumped-idle mode is initiated by the following sequence.

III, C, Controls Analysis (cont.)

(a) Open the LH_2 shutoff valve (#1).

(b) Close the fuel vent valve (#4) to direct all hydrogen flow through the pump turbines.

(c) As pump discharge pressures rise, the fuel discharge pressure opens the turbine bypass valve (#3) to the pumped-idle position, and the oxidizer pump discharge pressure closes the GO_2 start bypass valve and opens the LO_2 shutoff valve to the pumped-idle position.

The same concerns (i.e., mixture ratio variation due to uneven pump breakaway torque and pump cavitation due to rapid pump acceleration) that were listed for the active system are also applicable to the passive system. In fact, they are of greater concern because of the absence of feedback control. Some degree of control over pump cavitation may be realized by sensing a limit function, such as, for example, maximum pump speed vs time or minimum pump inlet pressure. An on-off signal can then be generated to monemtarily open the fuel vent valve to reduce turbine inlet pressure and pump acceleration. Mixture ratio is more difficult to control because the fuel and oxidizer pump turbines are not directly connected. It may help to orifice the LO_2 shutoff valve actuator to slow the rate of valve opening and reduce the possibility of the mixture being oxidizer-rich during the transient. These concerns need to be evaluated in transient analysis design studies.

(d) When pump discharge pressures reach the pumped-idle, steady-state level, the fuel and oxidizer tank pressurization valves (#5 and #6) are fully open to provide autogenous pressurization of the propellant tanks.

(e) At the pumped-idle, steady-state thrust level, the preset turbine bypass valve determines the thrust level, and the preset LO_2 shutoff valve determines the mixture ratio.

(3) Full Thrust

The turbine bypass valve and the LO_2 shutoff valves are step-actuated to the full-thrust positions.

The concerns are the same during the transition from pumped idle to full thrust as they were from tank-heak idle to pumped idle. Here again, the fuel vent valve may be used to trim pump acceleration, and the LO_2 shutoff valve actuator can be orificed to afford some control over mixture ratio during the transient. Thrust overshoot may be controlled by orificing the turbine bypass valve actuator so that the valve closing rate descreases as it is closed to the full-thrust position.

At the full-thrust, steady-state level, the preset settings of the turbine bypass valve and LO_2 shutoff valve will determine the thrust level and mixture ratio, respectively.

(4) Shutdown

Shutdown of the passive system is similar to that described for the active system. The LO_2 and LH_2 shutoff valves, igniter valves, and turbine bypass valve are closed. As propellant pressures decay, the fuel and oxidizer tank pressurization valves close, and the GO_2 start valve remains latched in the closed position. If a restart is not immediately planned, the vehicle prevalves are closed, and the fuel vent valve and GO_2 start bypass valve are opened. Valve sequencing and

timing need to be established by transient analyses.

3. Timing Gears For Mixture Ratio Control

Although the use of timing gears (passive control) between the high-pressure fuel and oxidizer turbopumps to aid in engine mixture ratio control was considered, their selection cannot be made with confidence at this time. The use of inter-turbopump gearing nas been used in the RL-10 engine, but for much shorter service life and cycle time requirements. Gear life would have to be demonstrated with a representative set of gearing before making a definite commitment to the feasibility of this concept. Some of the pros and cons concerning the use of gears are discussed in the paragraphs which follow.

Chemically bonded, dry-film, friction-reducing compounds have been applied to gear sets of the RL-10 engine's timing gears. Cooling is provided by vaporized liquid hydrogen. No other liquids are employed. The RL-10 A-3-3 used molybdenum disulfide and graphite carried in varnish (Ref. 10). Pratt and Whitney more recently reported that they would use molybdenum disulfide and antimony oxide in a silicone binder and xylene carrier with gaseous, hydrogen-cooled gears (Ref. 11). The resultant gear life was reported to be doubled. However, experience was obtained only on a laboratory scale, and absolute life numbers were not reported. Without technology testing to define the load-life expectancy and start-shutdown cycles, it would be premature to apply dry-film lubrication to flight hardware.

A dry-film lubricated timing gear set can provide positive speed ratio control between main propellant pumps. Although a fixed speed ratio does provide a large degree of mixture ratio control, it does not

eliminate the need for a MR control valve to accommodate wide propellant temperature and hardware variations unless the MR tolerance requirement is sufficiently broad.

The use of geared speed control is only practical because of the relatively small power that is to be transmitted between shafts. Due to the uncertainty of this power level during transient operation and as a result of component-to-component variations, having to design to the maximum expected power differential for the full 10 hours and 300 cycles could probably be anticipated.

Some other negative features of the timing gear design are weight and polar moment of inertia penalties. Gears are relatively massive structures for the forces they transmit. Relative to the pump impellers, they have very large diameters and can be larger than the turbine rotor itself. In addition to the weight penalty, a turbopump with timing gears will take longer to reach full-thrust level operation.

D. ENGINE CYCLE SENSITIVITY ANALYSIS

The objective of this subtask was to evaluate the baseline engine cycle's power balance sensitivity to changes in pump and turbine efficiencies, component pressure drops, turbine inlet temperature, and turbine bypass flow. Statistical deviations in these parameters were either established from historical data, where available, or were assumed to establish their effect upon the engine operating chamber pressure.

Data on Titan Second Stage production engines in support of the Titan III B/C/D vehicles show a one sigma variation of ± 1.06%, 1.69%, and 1.64% for the oxidizer pump, fuel pump, and turbine efficiencies,

respectively. These data covered 54 engines over three production contracts and is assumed to be representative for the OTV. The worst case has been assumed for the pumps (i.e., 1.69% instead of 1.06%). Three sigma variations in the pump and turbine efficiencies result in the following:

3 Sigma Pump Efficiency Variation: ± 5.07%
3 Sigma Turbine Efficiency Variation: ± 4.92%

Because these numbers are so close, deviations of ± 5% were used in the study for all turbomachinery components.

Component resistance variations were also obtained from the Titan III data. Typical values are as follows:

	%	
	One Sigma	Three Sigma
Coolant Jacket Resistance	± 6	± 18
Fuel Injector Resistance	± 4	± 12
Oxidizer Injector Resistance	± 3	± 9

Resistance is proportional to the pressure drop (ΔP) times the fluid density (ρ) divided by the flowrate ($\dot{\omega}$) squared (i.e., $R = \frac{\Delta P}{\dot{\omega}^2} \times \rho$). Assuming constant flow and densities, the above variations were used to approximate the deviations in component pressure drops. Two pressure drop deviations were evaluated in the fuel system to establish the effect of pressure drops unstream and downstream of the turbines.

Turbine inlet temperature and bypass flowrate variations were also evaluated. Because no historical statistical variations were readily

available, the turbine inlet temperature was varied ± 5% to establish its effect, and the turbine bypass flowrate was assumed to be ± 3% from the nominal 6% value.

The engine cycle analyzed in this task is the series turbine expander cycle. Again, the baseline chamber pressures used in the analyses were selected in the initial Phase "A" OTV study efforts. The nominal component parameters at each thrust level and the component deviations considered are shown in Table XXIV.

The results of this study subtask are shown on Figures 36, 37, 38, and 39. Figure 36 shows that a ± 5% deviation in the fuel pump or turbine efficiency results in approximately a ± 2.7% variation in chamber pressure over the entire thrust range. The effect of the oxidizer pump and turbine efficiency is less because this is the low horsepower system. A ± 5% deviation in the oxidizer pump or turbine efficiency only causes approximately a ± 0.6% variation in the engine thrust chamber pressure, as shown by Figure 36.

Figure 37 shows the effect of turbine inlet temperature and turbine bypass flowrate upon the cycle power balance. A ± 5% deviation in the fuel turbine inlet temperature creates approximately a ± 3.5% variation in chamber pressure. A reduction in turbine bypass flowrate from 6% of the total fuel flowrate to 3% increases the engine thrust chamber pressure by 2%, while an increase in bypass flow to 9% causes a 2% reduction in chamber pressure. Therefore, the 6% bypass flowrate can make up for component deviations that would otherwise cause a total chamber pressure change of 4%.

TABLE XXIV

NOMINAL COMPONENT DATA FOR CYCLE SENSITIVITY ANALYSIS
SERIES TURBINE

Thrust klb	Chamber Pressure, psia	Fuel Pump Efficiency, %	Oxidizer Pump Efficiency, %	Fuel Pump Turbine Efficiency, %	Oxidizer Pump Turbine Efficiency, %	Chamber Coolant Jacket Pressure Drop, psi	Injector Fuel Pressure Drop, psi	Injector Oxidizer Pressure Drop, psi	Fuel Turbine Inlet Temp, °R	Turbine Bypass Flow, % of Fuel
10	1300	62	62	73	76	131	118	233	653	6
15	1200	65.5	63.6	75	76.5	92	109	215	535	6
20	1100	67.5	65.0	77	77	76	100	197	463	6
Deviation		± 5%	± 5%	± 5%	± 5%	± 18%	± 12%	± 9%	± 5%	389

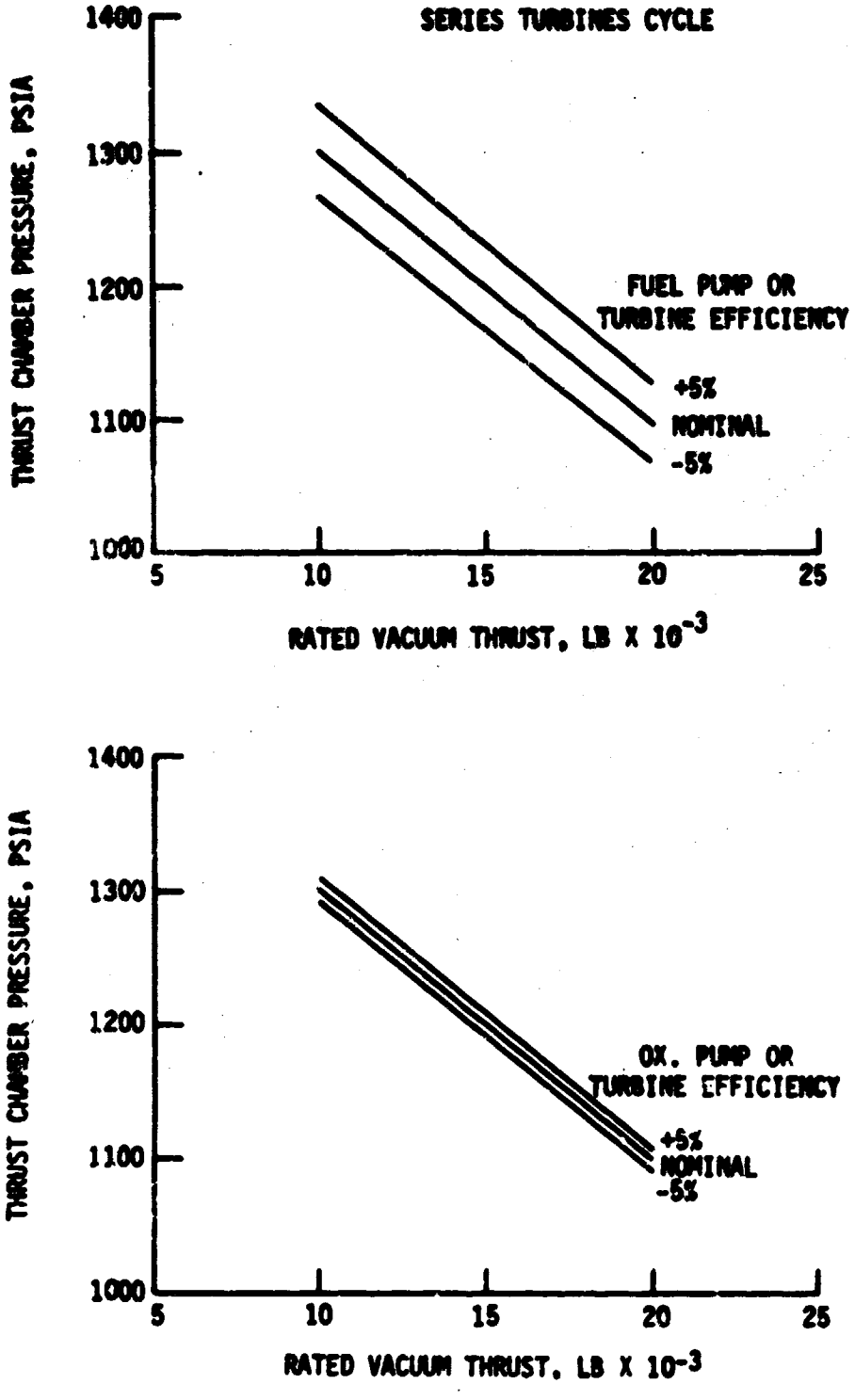

Figure 36. Expander Cycle Sensitivity to Turbomachinery Performance Variations

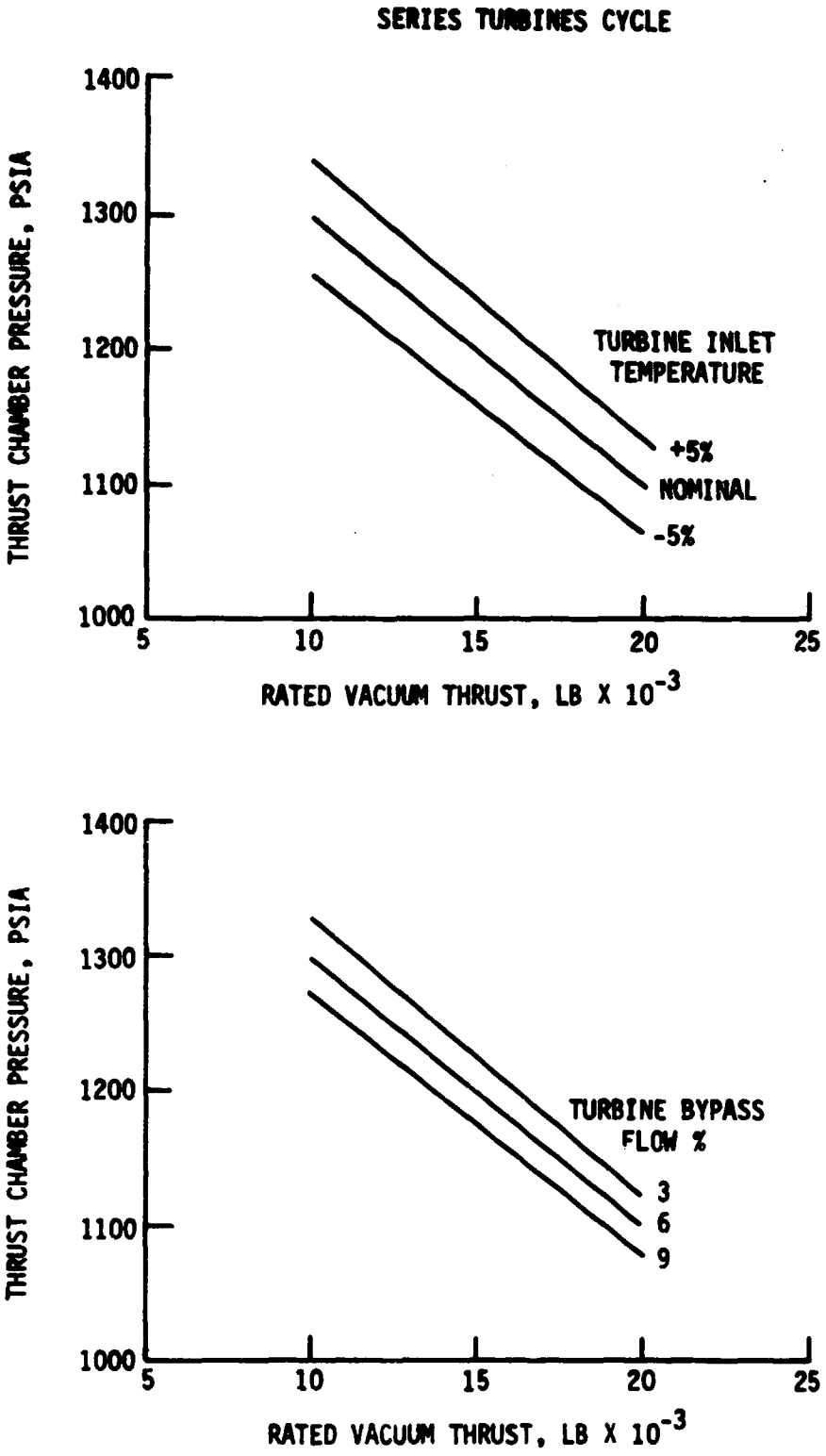

Figure 37. Expander Cycle Sensitivity to Turbine Inlet Temperature and Bypass Flow Variations

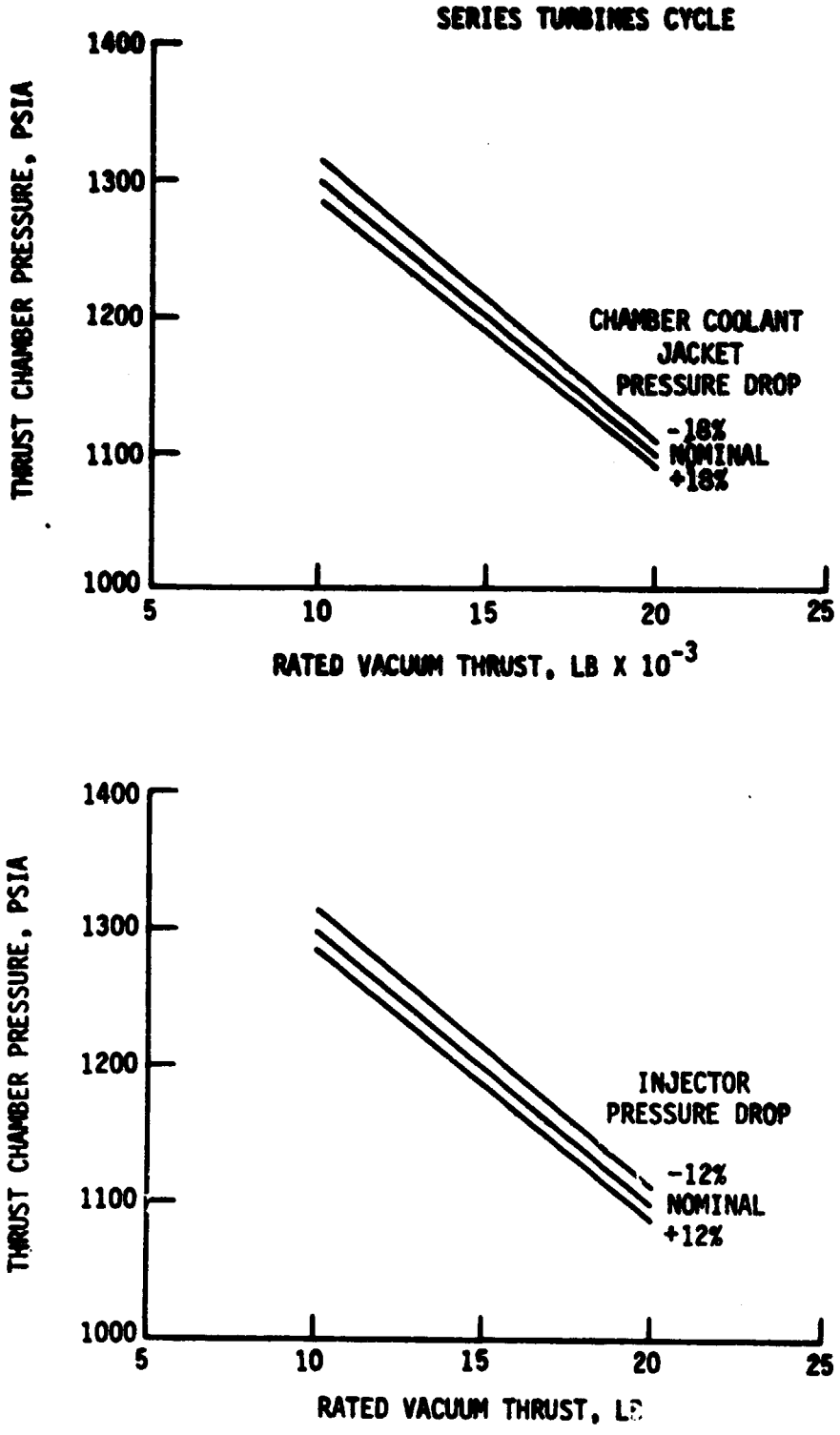

Figure 38. Expander Cycle Sensitivity to Fuel System Component Pressure Drop Variations

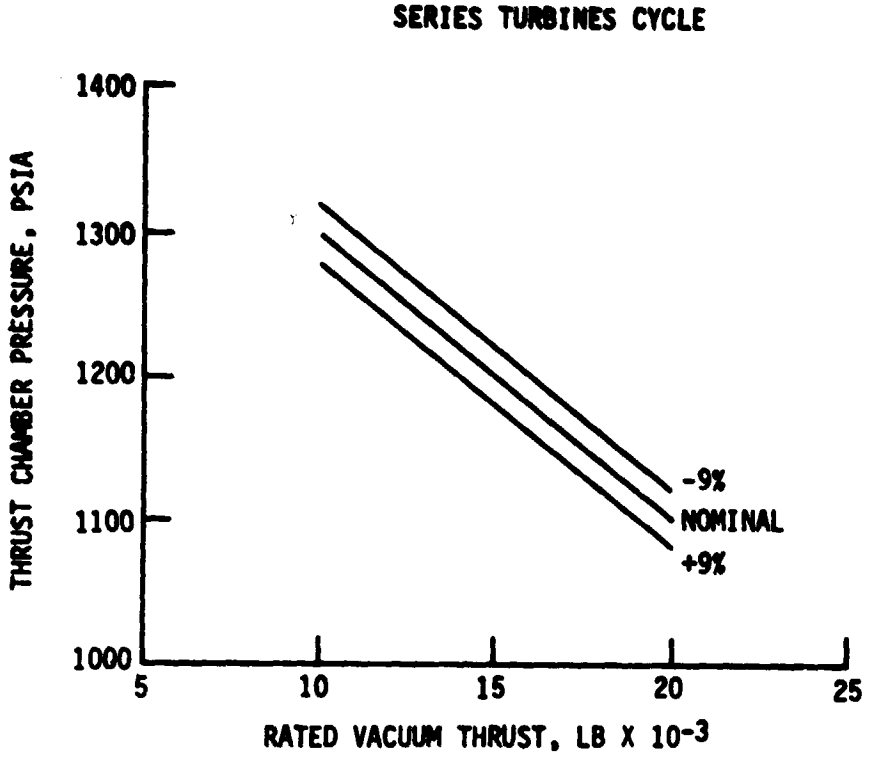

Figure 39. Expander Cycle Sensitivity to Oxidizer System Component Pressure Drop Variations

III, D, Engine Cycle Sensitivity Analysis (cont.)

Figure 38 shows the expander cycle engine's sensitivity to fuel system pressure drops upstream and downstream of the turbines. A ± 18% deviation in the combustion chamber coolant jacket pressure drop causes a ± 1% change in chamber pressure. The ± 12% variation in the fuel system injector pressure drop also results in about a ± 1% change in chamber pressure.

Figure 39 shows the effect of a ± 9% deviation in the oxidizer system injector pressure drop. This results in approximately a ± 1.6% change in chamber pressure over the entire thrust range.

All variations discussed in the previous paragraphs assume only single component deviations. The performance of a component was varied while the others were held at their nominal values. A worse case was also analyzed. The worse case consisted of reducing the fuel pump, fuel pump turbine, oxidizer pump, and oxidizer pump turbine efficiencies by 5%, reducing the turbine inlet temperature by 5%, increasing the coolant jacket pressure drop by 18%, and increasing the fuel system injector pressure drop by 12%. The turbine bypass flow was fixed at 6%. This resulted in a 13.4% decrease in thrust chamber pressure at a thrust level of 15K lb. Thus, the chamber pressure variations are almost additive as shown below:

	Deviation %	Chamber Pressure Variation %
Fuel Pump Efficiency	-5	2.7
Oxidizer Pump Efficiency	-5	0.6
Fuel Turbine Efficiency	-5	2.7
Oxidizer Turbine Efficiency	-5	0.6

III, D, Engine Cycle Sensitivity Analysis (cont.)

	Deviation %	Chamber Pressure Variation %
Turbine Inlet Temperature	-5	3.5
ΔP Coolant Jacket	-18	1.0
ΔP Fuel Injector	-12	1.0
	Total	12.1

This is a worse case deviation, and it should be noted that not all predictions would be expected to be at their worse case, 3 sigma values. The drivers are obviously the fuel turbomachinery efficiencies and turbine inlet temperature.

If component performance is not as predicted, thus necessitating a change in operating chamber pressure level at a given thrust, the engine performance (I_s) and weight will only be slightly affected. Figure 40, extracted from the initial Phase A efforts, shows the variation of engine weight with the operating pressure level for a fixed engine envelope. The figure shows that the weight variations are not significant. The variation of engine performance about the nominal chamber pressure levels is shown on Figure 41. The figure shows that a 10% variation in the operating thrust chamber pressure level results in less than a 1 (one) sec change in delivered specific impulse. The nominal performance values at each thrust level are as follows:

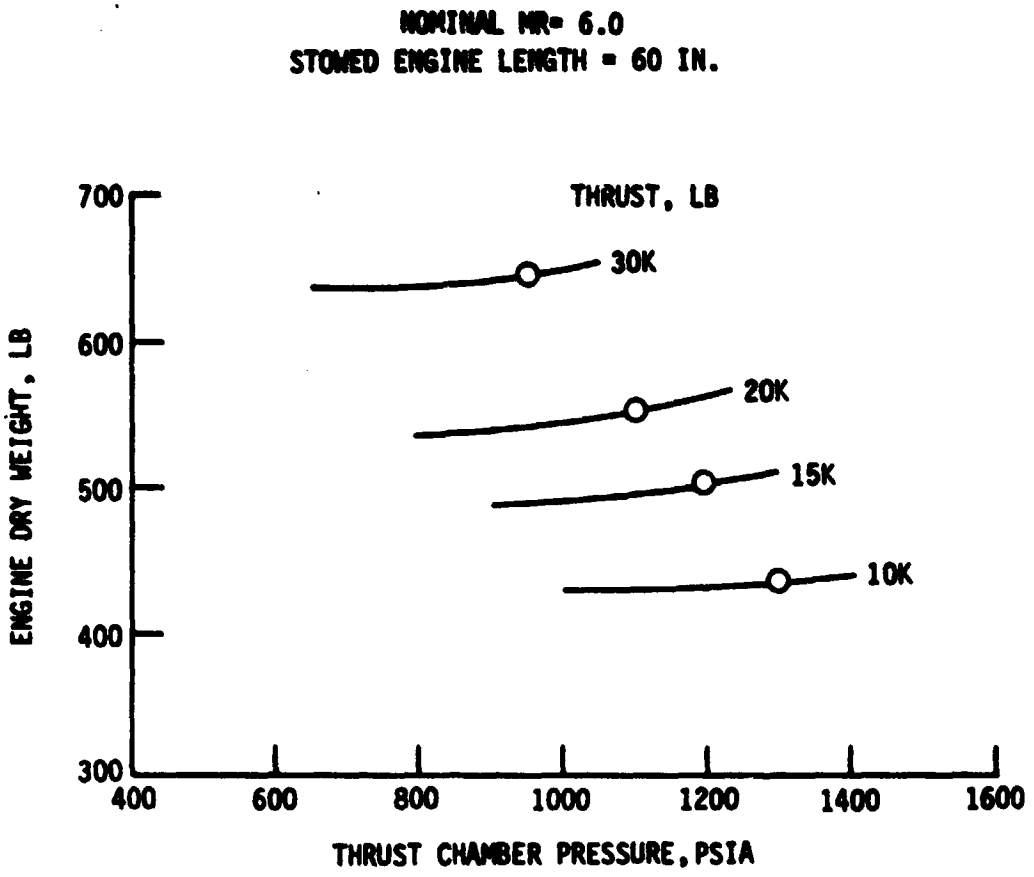

Figure 40. Advanced Expander Cycle Engine Weight vs Chamber Pressure

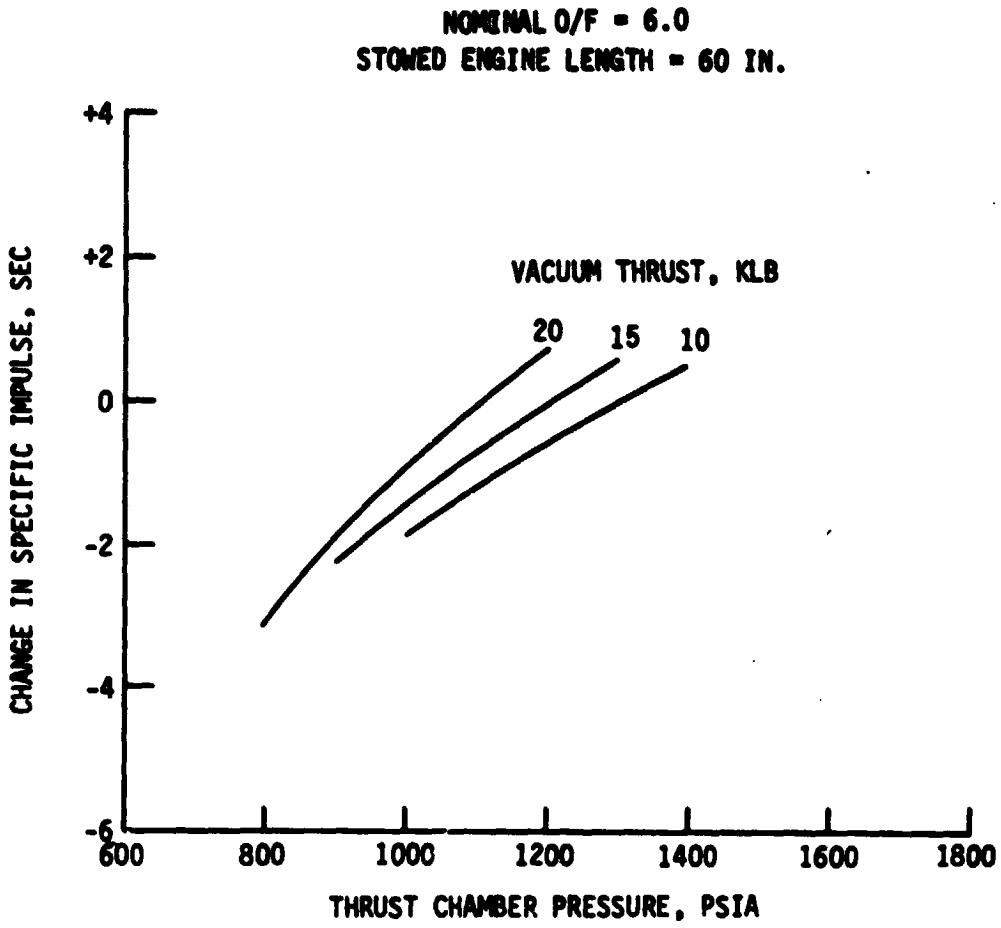

Figure 41. Effect of Thrust Chamber Pressure Upon Delivered Engine Specific Impulse

III, D, Engine Cycle Sensitivity Analysis (cont.)

Vac. Thrust, klb	Thrust Chamber Pressure, psia	Engine Delivered Specific Impulse, sec	Nozzle Area Ratio
10	1300	480.2	792
15	1200	477.2	473
20	1100	474.2	322

E. CHILLDOWN/START PROPELLANT CONSUMPTIONS

Engine chilldown/start propellant consumption estimates were made assuming a tank-head idle mode condition. Tank-head idle mode is a pressure-fed mode of operation with saturated propellants in the tanks. Its purpose is to thermally condition the engine without non-propulsive dumping of the propellants.

Chilldown propellant estimates were made by reviewing and scaling the results of past studies. Those analyses utilized are reported in References 7, 8, 12, and 13. Reference 8 (OOS Sutdies) presents scaling relationships and results that require empirical data for correlation, while Reference 7 (RL-10 Derivative Study) analyzes specific design points and has the benefit of empirical data to adjust analytical models. Therefore, the predictions of Reference 7 were used to adjust the OOS models. The adjusted data from Reference 8 are presented in Figure 42, and the results are summarized in Table XXV.

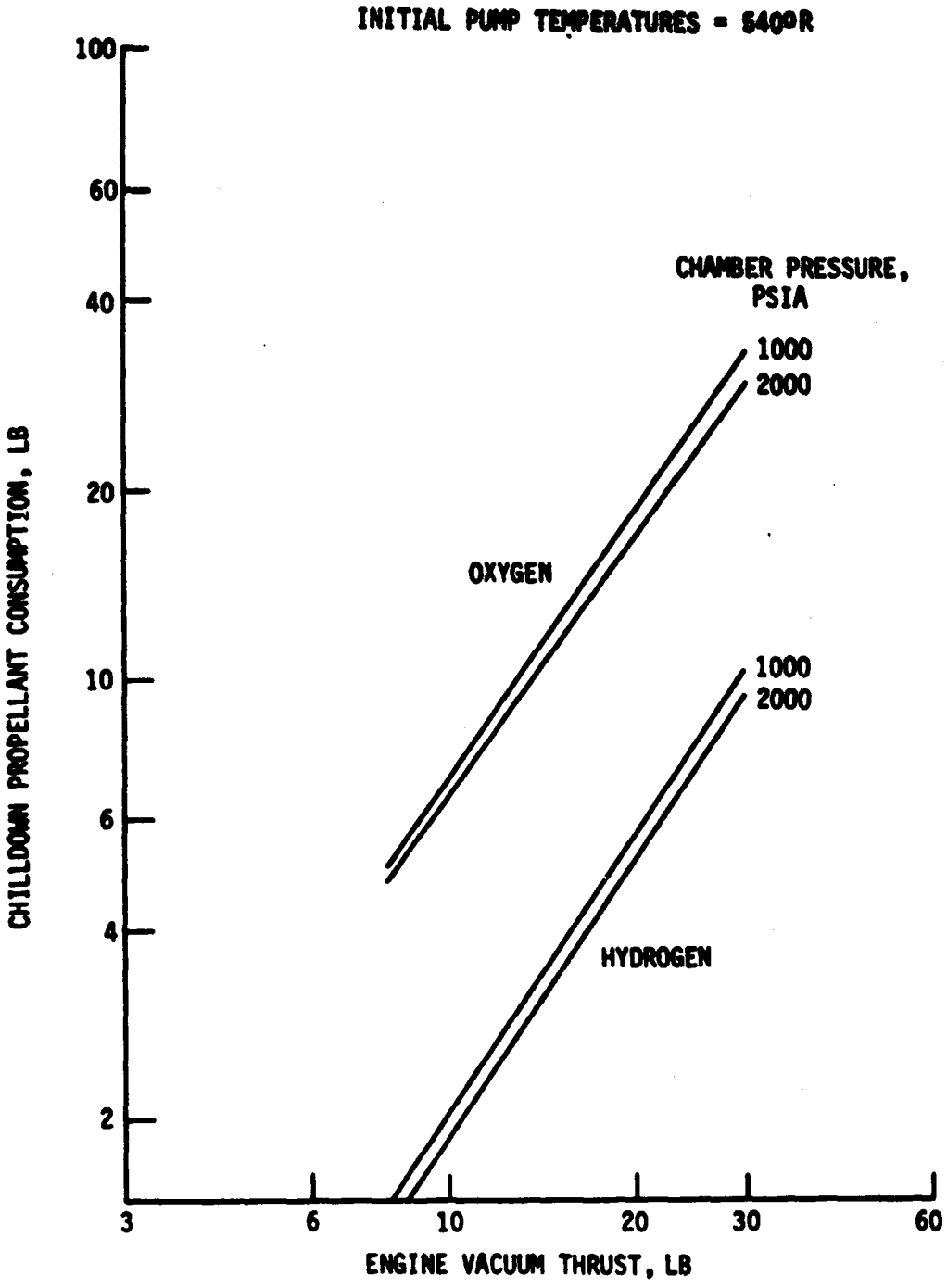

Figure 42. Chilldown Propellant Consumption Parametric Data

TABLE XXV

CHILLDOWN PROPELLANT CONSUMPTION ESTIMATES
INITIAL PUMP TEMPERATURES = 540°R

Thrust, klb	Chamber Pressure, psia	Total Propellant Consumption, lb
10	1300	9.0
15	1200	16.0
20	1100	24.0

IV. TASK II: ALTERNATE LOW-THRUST CAPABILITY

A. OBJECTIVES AND GUIDELINES

The objectives of this task were to assess the feasibility and design impacts of a requirement that the advanced expander cycle engine be adaptable to extended low-thrust operation at approximately 1K to 2K lbF. The rated full-thrust level used in this evaluation was 15K lbF which was selected to be consistent with Contract NAS 8-33574 Orbit Transfer Vehicle Advanced Expander Cycle Engine Point Design Study efforts (Ref. 4).

The primary guideline used in this study was to establish a low-thrust operating point that would not compromise the engine at rated thrust operation. However, this did not preclude the use of "kits" to obtain the low-thrust goal. Kits could take the form of turbine flow area modification, a new replacement low-thrust injector, or even new pumps. The engine low-thrust operating point is a dedicated condition, and the engine is not required to operate at both thrust levels (15K lbF and low-thrust) on the same mission.

B. SUMMARY OF LOW-THRUST ANALYSES RESULTS

The analyses showed that operation of the engine at 10% of rated thrust is feasible, provided that the following "kits" are added to the engine.

- Replace the oxidizer injection elements with smaller size ones to avoid chugging instability.
- Install an orifice downstream of the coolant jacket to keep the coolant jacket exit pressure above the critical pressure of hydrogen.

IV, B, Summary of Low-Thrust Analyses Results (cont.)

- Increase the oxidizer pump flow by adding a recirculation line and valve between the boost pump and main pump to avoid pump instability.

Other pertinent study results are summarized in the following paragraphs.

Service life/reliability is not predicted to be less than that of the basic engine. Engine modifications required to provide the low-thrust capability are minor. Cooling the chamber and tube bundle nozzle was an area of concern, but thermal analyses showed that both the chamber and tube bundle nozzle can be designed to meet the service life requirements at both thrust levels without compromising the basic engine.

The estimated delivered specific impulse at low thrust is shown on Figure 43 at a mixture ratio of 6.0. This performance estimate was made by using simplified JANNAF performance procedures. Test data is required to verify the results. For this analysis, it was assumed that the injector can be modified to provide the necessary stability margin and produce the same enregy release efficiency (ERE) as the basic engine design.

The maximum recommended engine mixture ratio for an operating point at 10% of rated thrust is 10.0 This estimate is based upon running the fuel pump at a minimum flowrate for stable operation and increasing the oxygen pump flowrate to achieve the proper thrust level. This results in a significant specific impulse loss, indicating that operation in a mixture ratio range of 6.0 to 7 is better.

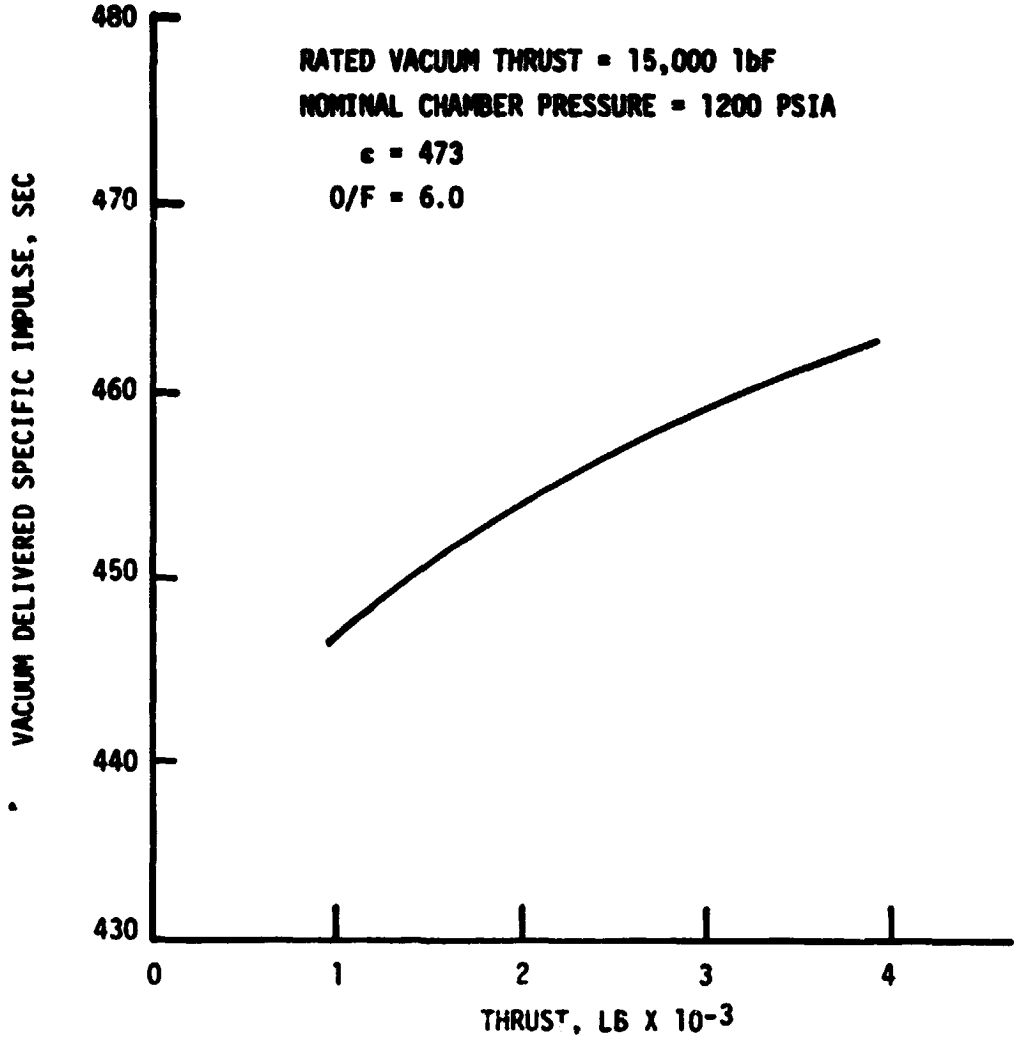

Figure 43. Alternate Low-Thrust Capability Performance Estimate

IV, B, Summary of Low-Thrust Analyses Results (cont.)

The estimated change in the engine DDT&E cost to provide the low-thrust operating condition is $15M. This additional cost is incurred to design, develop, and test the low-thrust injector, demonstrate injector/chamber compatibility, and flight-certify the low-thrust engine. This program is assumed to be conducted in parallel with the rated thrust engine development.

The impact of kitting upon the basic engine weight is negligible.

C. INJECTOR MODIFICATION ANALYSIS

1. Analysis

Table XXVI shows some significant injection/combustion parameters which were estimated or calculated at various throttle operating points between thrust levels of 15K to 1K at a mixture ratio of 6.0. Fuel injection velocity either remains constant or increases slightly due to increased coolant bulk temperature rise. Thus, the compressible gH_2 $\Delta P_f/P_c$ ratio remains adequate throughout the entire throttle range and does not adversely affect feed system stability. On the other hand, the incompressible LO_2 injection velocity is directly proporational to thrust. Therefore the oxidizer injection ΔP_{ox} is proportional to P_c^2, and the $\Delta P_{ox}/P_c$ ratio decreases linearly with thrust, aggravating LO_2-inducer chug instability.

The oxidizer combustion time lag almost varies inversely with P_c or thrust, as shown on Table XXVI. A preliminary chug stability analysis utilized these oxidizer combustion time lags to estimate the necessary $\Delta P_{ox}/P_c$ ratio. The simplified chug analysis solutions are conservative for two reasons: (1) they are based upon assumed liquid/liquid injectors having nearly equal fuel and oxidizer combustion time lags where both are rate limiting and (2) it neglects to account for any momentum exchange efficiency

TABLE XXVI

THROTTLING EFFECT UPON COMBUSTION PARAMETERS

Parameters	Units						
Percent Thrust		100	50	25	25	13.3	6.7
Thrust	(lbf)	15,000	7500	3750	3750	2000	1000
Chamber Pressure	(psia)	1200	600	300	[illegible]	160	80
Mixture Ratio, O/F		6.0	6.0	6.0	6.0	6.0	6.0
Inj. Vel. Ratio, V_f/V_o		8.2	17.9	38.4	[illegible]	19.2	42.5
Inj. Mom. Ratio, W_oV_o/W_fV_f		.726	.335	.156	.625	.313	.141
Result Cone Angle	(deg)	12.6	7.4	3.9	11.5	7.0	3.6
Fuel Pump Disch. Temp.	(°R)	90	70	55	55	47	40
Fuel Turbine Inlet Temp.	(°R)	535	581	642	642	713	805
Fuel Inj. Man. Temp.	(°R)	473	514	568	568	630	712
Oxid. Elem. Dia.	(in)	.100	.100	.100	.050	.050	.050
Propellant Circuit		Oxid Fuel	Oxid Fuel	Oxid Fuel	Oxid Fuel	Oxid Fuel	Oxid Fuel
Flowrate	(lbm/sec)	26.94 4.49	13.50 2.25	6.75 1.125	6.75 1.125	3.60 0.60	1.80 0.30
Injector ΔP	(psid)	215 109	54 59	13 32	215 32	61 19	16 11
Injection Velocity	(fps)	168 1385	84 1505	42 1613	168 1613	90 1727	45 1913
$(\Delta P/P_c)_{inj}$		.179 .091	.090 .098	.044 .107	.717 .107	.381 .119	.200 .138
$(\Delta P_{ox}/P_c)$ Req'd Chug Stab		.07	.15	.27	.04	.09	.19
Oxidizer Atom./Vap.							
Mass Median Drop Radius	(in)	.00165	.00216	.00292	.00091	.00128	.00165
Atom. Wave Length	(in)	.849	1.002	1.215	.411	.526	.713
ΔX-20% Oxid. Vap.	(in)	.109	.148	.216	.113	.161	.222
L_{gen} (LO_2, throat)	(in)	124.0	91.2	62.3	119.4	83.6	60.7
% Oxid. Vap.	%	100.0	100.0	99.9	100.0	100.0	99.8
Atom. Time Lag	(msec)	.421	.994	2.411	.204	.487	1.320
20% Vap. Time Lag	(msec)	.054	.147	.429	.056	.149	.411
Total Oxid. Time Lag	(msec)	.475	1.141	2.840	.260	.636	1.731

IV, C, Injector Modification Analysis (cont.)

of the axial H_2 injection velocity upon the LO_2 swirl coaxial spray which was assumed in the analysis. Table XXVI presents an estimate of the necessary $\Delta P_{ox}/P_c$ as a function of the thrust and associated combustion time lags for 84 swirl coaxial elements having oxidizer orifice diameters of ∿.100 in. for the point design and ∿.050 in. diameter for the low thrust injector modification. These preliminary results indicate that chug stable combustion capability between a range from full, down to approximately half thrust can be maintained without modification. At progressively lower thrust levels, the required oxidizer ΔP requirements increase dramatically due to reduced oxidizer injection velocities and longer time lags. By 1/4 thrust, the LO_2 injection velocity has decreased to 40 fps. At this point the LO_2 swirl cone is expected to collapse due to increased surface tension effects and chugging instability becomes highly probable. Consequently, the LO_2 element should be modified to assure at least 40 fps minimum injection velocity regardless of thrust, which results in approximately 20% minimum $\Delta P_{ox}/P_c$ at 1K thrust. This also results in about a .050 in. LO_2 diameter at 1K thrust and is the only component design modification deemed necessary for satisfactory thrust chamber combustion operation.

Given the freedom to modify the LO_2 element resistance, the injector can be modified to avoid feed system coupled combustion instabilities. Within the range of chug stable operation, the oxidizer combustion time lags can also be adjusted to avoid chamber longitudinal mode resonance frequencies. Therefore, the selection of a low-thrust operation point is not dictated by thrust chamber combustion capabilities.

Atomization/vaporization analyses of the point design injector and the low-thrust modification indicate that the LO_2 vaporization will be adequate at all thrust levels in the 18-in. long chamber. Combustion

efficiency, then, is not expected to vary significantly with thrust, nor will the axial combustion distribution be altered enough to have noticeable effects upon combustion chamber thermal compatibility. The chamber pressure reduction at low thrust, will however cause a decrease in Kinetic (ODK) performance, Similarly, at low thrust, the mass flowrate reduction in fixed hardware will increase the boundary layer performance loss. This will result in slightly lower performance than from an engine designed for low-thrust operation only.

2. Discussion of Results

The OTV point design engine can be reduced in thrust with minor modification from 15K to 1K without significantly affecting combustion performance efficiency or injector face/chamber wall thermal compatibility. Likewise, high frequency transverse mode combustion instability is not expected to be detrimentally affected. Primarily, the operational limitations consist of feed system chugging instabilities and potential coupling of the injector response with the chamber longitudinal mode resonances under certain operating conditions which should be determined in future efforts.

It has been analytically estimated that while the point design engine can be conservatively throttled down to at least 50% of rated thrust, even by the most optimistic assumptions it cannot be throttled below 25% (3750 lbF) of thrust before encountering chug instabilities. However, the only limitation is due to inadequate oxidizer injection element ΔP which can be readily corrected by allowing for two alternate dash no. swirl coaxial elements which differ only in their oxidizer port injection diameters (e.g., .100 in. dia for 15K point design and .050-in. dia for a 1K low-thrust engine). The injector manifolding, combustion chamber and nozzle geometry, coaxial element length and OD, and fuel orifice areas can

all be kept identical. Because an injection element substitution (kit) is required for any thrust level below 4K, it makes no difference from a combustion standpoint whether the low-thrust value of 2K, 1K, or any other value is selected.

In order to achieve an adequate H_2 bulk temperature rise to drive the expander cycle turbines, a relatively long (L' = 18 in.) chamber length was selected. This causes the chamber longitudinal mode acoustic resonance frequencies to fall into a frequency regime susceptible to injection element responses. The longitudinal mode chamber impedance remains essentially fixed at its acoustic mode sensitive frequencies, independent of engine throttling, but the injector response varies widely with the injection flowrates (velocity). Thus, even though the point design engine will be nominally optimized to be free of longitudinal mode instabilities at full thrust, it should be anticipated that the engine can fall in and out of sensitive resonance modes within various throttle ranges which have not been established and were beyond the scope of this initial assessment.

3. Recommendations

a. Replace the oxidizer coaxial injection elements so that the point design engine can provide acceptable combustion characteristics down to 1K thrust.

b. Conduct more detailed chug stability margin analysis and longitudinal mode combustion stability analyses at the selected low-thrust operating point(s).

IV, C, Injector Modification Analysis (cont.)

c. Determine optimum element design modifications which are required to stabilize combustion at the selected low-thrust operating condition.

D. LOW-THRUST THERMAL ANALYSIS

This subtask addressed the thermal design feasibility of low-thrust operation with an engine designed for normal operation at 15K lbF with a chamber pressure of 1200 psia. The desired reduction in thrust to 1K to 2K lbF presents a problem from a thrust chamber cooling standpoint because the coolant pressure is only slightly supercritical at 2K lbF and is below the critical pressure at 1K lbF. In these regions, heat transfer characteristics are very poorly defined; moreover, previous experience has indicated the possibility of flow instability in this regime. These analyses considered low-thrust operation at supercritical coolant pressures, assuming the hydrogen heat transfer correleation (Ref. 14) applicable for high supercritical pressures to be valid in the near critical region. Since two-phase analyses at subcritical coolant pressures would require extensive computer program development, they were beyond the scope of the present effort. Estimated coolant inlet conditions as a function of thrust are shown in Figure 44. At 2K lbF, the coolant jacket inlet pressure is 235 psia, and the critical pressure of hydrogen is 188 psia. For thrusts less than 2K lbF, an orifice must be placed downstream of the coolant jacket to maintain the hydrogen pressure through the coolant jacket above critical.

Low-thrust analyses were conducted for both the chamber and nozzle cooling systems. In the baseline design, these components are cooled in parallel, with 85% of the hydrogen flowing though the chamber. The interface area ratio is 8:1. A preliminary flow stability analysis is included for the chamber, based on a modification derived from Ref. 15 to

account for axial variations in channel design and heat flux.

1. Chamber Analyses

The baseline chamber (ε_c = 3.66, L' = 18 in.) was designed during previous Phase A study efforts. This chamber employs rectangular channels in a zirconium-copper liner. Low-thrust results compared with full-thrust operation are summarized in Table XXVII. Wall temperatures in most of the chamber are reduced at low thrust due to higher coolant bulk temperatures. Heat trasnfer coefficients for hydrogen improve with heating and can more than offset the increased sink temperature seen be the wall. This is shown in Table XXVII by the reduction in wall temperature at the outlet compared with the increased coolant inlet bulk temperature rise. During low-thrust operation, with the attendant reduced hydrogen tempeature, the wall temperature adjacent to the cooling inlet (area ratio 8:1) increases significantly because of the lower heat transfer coefficient of very cold hydrogen. Because the inlet region wall temperatures are very low at full thrust, this increase is not of concern. Of greater importance is the temperature differential between the gas-side surface and the electroformed nickel closure because it controls thermal strain and, thus, cycle life. Table XXVII indicates that this differential is significantly lower at reduced thrust at all chamber locations due to the lower heat fluxes and excellent thermal conductance through the lands to the nickel outer wall. The allowable differentials for 300 cycles are included in Table XXVII; note that the inlet region is overcooled at full thrust.

The stability number is shown in the last column of Table XXVII. Theoretically, if this number is greater than zero, stability is predicted. However, comparison of the predictions of Ref. 15 with test data indicate a model bias, such that the inception of instability was generally observed

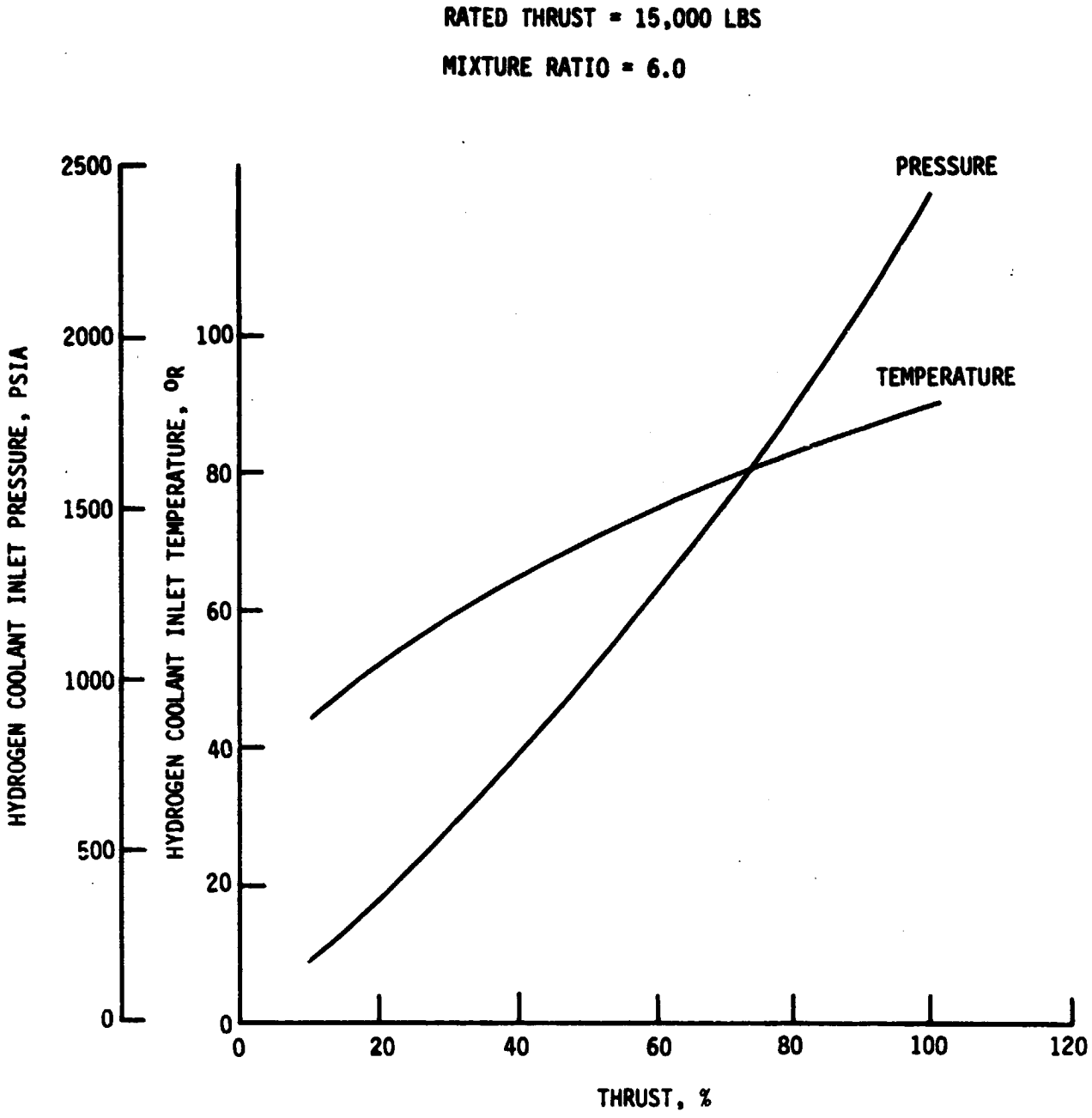

Figure 44. Estimated Coolant Jacket Propellant Inlet Conditions During Throttling

TABLE XXVII

CHAMBER LOW-THRUST THERMAL ANALYSES

Thrust Klb	Coolant T_{in}, °R	Coolant ΔT_b, °F	Coolant ΔP, psi	Wall Temperature, °F Inlet	Wall Temperature, °F Outlet	$T_{wg}-T_{NI}$, °F Inlet	$T_{wg}-T_{NI}$, °F Outlet	300 Cycle $T_{wg}-T_{Ni}$, °F Inlet	300 Cycle $T_{wg}-T_{Ni}$, °F Outlet	Stability Number
15	90	407	93	17	842	283	659	860	665	85
4	57	544	33	237	671	116	291	690	580	-7
3	52	581	26	330	663	92	238	640	560	-10
2	47	631	19	425	660	66	178	590	518	-11

- WALL TEMPERATURE AT OUTLET IS REDUCED.
- INLET IS OVERCOOLED (WALL TEMP. INCREASE ACCEPTABLE).
- ACTUAL Twg - T_{Ni} IS LESS THAN MAXIMUM REQUIRED TO MEET SERVICE LIFE.
- INCEPTION OF FLOW INSTABILITY PREDICTED AT -15.

at numbers less than -15. Based on this bias, the low-thrust cases of Table XXVII are seen to be stable by a small margin.

With regard to the near critical or subcritical pressure operation, the chamber pressures for 1K and 2K lbF are about 80 and 160 psia, respectively. Figure 44 shows the LH_2 coolant jacket inlet temperature to be between 40 and 47°R. The critical pressure of LH_2 is 188 psia, and its critical temperature is 59°R. Therefore, if the H_2 critical conditions occur within a high heat flux section of the chamber, it will be extremely difficult to reliably cool it for long life capability due to the wide variations in coolant heat capacity (C_p), density (ρ), thermal conductivity (k), and viscosity (μ) near the critical point. Some design flexibility exists, such as installing an orifice in the fuel line between the cooled chamber and fuel injector manifold to keep the H_2 pressure above the critical pressure in the coolant passages. This places the burden upon the fuel pump, but the engine can be power-balanced (see Section IV,G) because of the higher turbine inlet temperatures at low thrust (shown in Figure 45). The orifice would constitute part of the low-thrust "kit" design modification and would make cooling to 1K lbF possible.

2. Nozzle Analyses

A nozzle tube bundle was also designed in previous Phase A study efforts. In this design, 15% of the cold hydrogen is used in a two-pass A-286 tube bundle. The number of tubes (326) was selected to provide a cycle life of 300 cycles. At all thrust levels considered in this analysis, the coolant inlet exhibits the highest thermal strain as well as the maximum wall temperature.

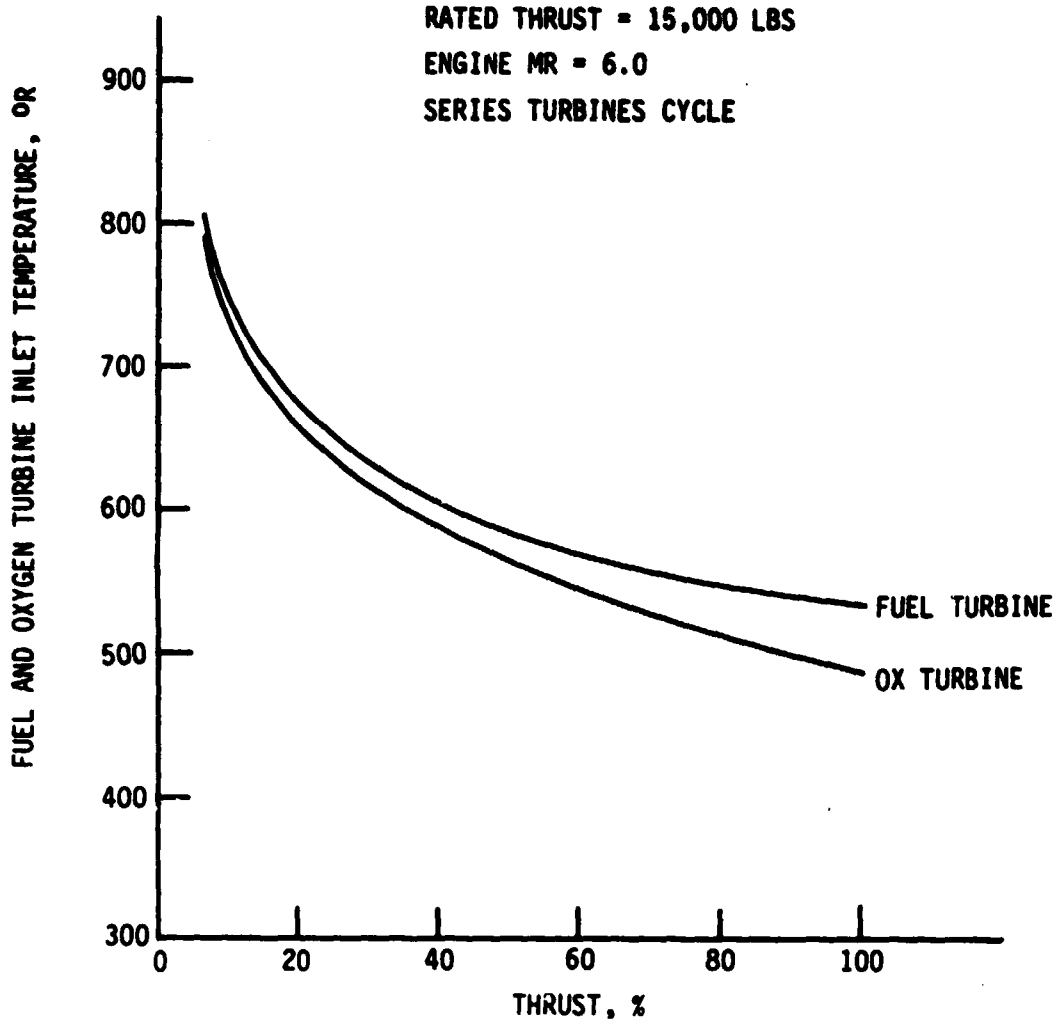

Figure 45. Fuel and Oxidizer Turbine Inlet Temperature vs % Thrust

IV. D. Low-Thrust Thermal Analysis (cont.)

Comparative results for low-thrust and full-thrust operation are given in Table XXVIII. As thrust is reduced, there is an increase in both the maximum wall temperature and maximum wall temperature differential (Twg - Tb) which control thermal strain. The attendant reduction in cycle life results from the lower estimated coolant inlet temperatures (Figure 44) associated with reduced thrust and the corresponding degradation in coolant heat transfer coefficient noted previously. To illustrate this result, alternate low-thrust analyses were conducted with a fixed inlet temperature equal to that at full thrust (90°R); in this case, the wall temperatures at the inlet for reduced thrust were well below that for full thrust.

It should be noted that the nozzle design can be modified to accommodate low-thrust operation without penalizing full-thrust operation. The nozzle is cooled in parallel with the chamber and must be orificed because it has a much lower pressure drop than the chamber. By overcooling at full thrust, the desired cycle life can be obtained at low thrust. The increased pressure drop required merely reduces the orifice pressure drop.

3. Thermal Analysis Conclusions

Operation of the baseline 15K C7V chamber liner and nozzle tube bundle at thrust levels as low as 1K to 2K was determined to be feasible. For both components, the wall temperature at the coolant inlet was found to increase at low thrust because of poor coolant heat transfer at the reduced coolant inlet temperatures. This results in a degradation of cycle life for the nozzle, but not the chamber. However, the nozzle can be redesigned to provide the desired cycle life without penalizing the full-thrust design. A preliminary flow stability analysis of the chamber indicates that it is marginally stable at 2K lbF and would also be marginally stable at 1K lbF.

TABLE XXVIII

NOZZLE LOW-THRUST THERMAL ANALYSES

Thrust Klb	Coolant ΔT_b, °F	Wall Temperature, °F			$T_{wg}-T_b$, °F		
		Inlet	Turn	Outlet	Inlet	Turn	Outlet
15	661	1011	722	826	1381	777	535
4	812	1244	689	831	1647	708	422
3	-	1285	-	-	1693	-	-
2	866	1319	668	838	1732	668	386

CONCLUSIONS:

- MAX. WALL TEMP. AND TEMP. DIFFERENTIAL INCREASE, REDUCING CYCLE LIFE
- OVERCOOL THE NOZZLE AT INLET (DOES NOT PENALIZE ENGINE AT RATED THRUST)

IV, Task II: Alternate Low-Thrust Capability

E. TURBOPUMP ANALYSES

Analyses were also undertaken to predict the performance of the OTV turbopumps operating at low engine thrust levels. The purpose of this subtask was to examine the low-thrust off-design performance of the pumps and turbines and identify operating regions where actual and potential instabilities can exist. Low-thrust off-design performance was based on pump and turbine designs which conform to the performance requirements of the OTV engine operating at 100% thrust and design mixture ratio. Tables XXIX and XXX contain the operating specifications for the turbopumps and engine at both the nominal MR of 6.0 and the off-design mixture ratio operating point of 7.0.

1. Flow Schematic

Figure 46 is the flow schematic showing the significant groupings of the turbomachinery components which were analyzed. On the fuel side, liquid hydrogen (LH_2) flows from the tankage through the boost pump to the main stage. Subsequently, the fuel flows through the thrust chamber and absorbs heat, changing phase from liquid to gaseous. A diverter valve allows a portion of the flow to bypass both the fuel and oxidizer turbines; this controls engine thrust level. The second valve in the system permits flow to bypass the fuel turbine; this allows for adjustments in fuel turbine power and engine mixture ratio.

Exhaust gas from the turbines is subsequently combined with the flow from the turbine bypass valve and delivered to the engine combustion chamber. Liquid oxygen flows from the tankage through the boost and main stage pumps and subsequently to the engine thrust chamber.

TABLE XXIX

MAIN PUMP DESIGN PARAMETERS

Rated Thrust 15 klb

	ENGINE MIXTURE RATIO 6.0		ENGINE MIXTURE RATIO 7.0	
	LOX	LH_2	LOX	LH_2
INLET TEMPERATURE, °R	162.7	37.8	162.7	37.8
INLET PRESSURE, psia	46.6	51.0	46.6	51.0
VAPOR PRESSURE, psia	15.0	18.0	15.0	18.0
NET POSITIVE SUCTION HEAD, ft	64.1	1075	64.1	1075
VOLUMETRIC FLOWRATE, GPM	170.3	456.0	174.9	401.1
SUCTION SPECIFIC SPEED, $(RPM)(GPM)^{1/2}/(ft)^{3/4}$	20000	10240	20000	9226
SPEED, RPM	34720	90000	34260	86490
DISCHARGE PRESSURE, psia	1487	2473	1463	2290
HEAD RISE, ft	2921	78910	2872	72945
NUMBER OF STAGES	1	3	1	3
SPECIFIC SPEED, $(RPM)(GPM)^{1/2}/(ft)^{3/4}$	1140	931	1155	890

TABLE XXX

MAIN TURBINE DESIGN PARAMETERS

Rated Thrust = 15 klb

	ENGINE MIXTURE RATIO			
	6.0		7.0	
	LOX	LH_2	LOX	LH_2
INLET PRESSURE, psia	1471	2286	1430	2138
INLET TEMPERATURE, °R	488.5	535	513.3	557
FLOWRATE, lb/sec	4.22	4.22	3.71	3.71
GAS PROPERTIES				
Cp, SPECIFIC HEAT AT CONSTANT PRESSURE, BTU/LB-°R	3.652	3.652	3.652	3.652
γ, RATIO OF SPECIFIC HEATS	1.395	1.395	1.395	1.395
SHAFT HORSEPOWER	235.6(1)	1013(2)	239(1)	837(2)
PRESSURE RATIO (TOTAL TO STATIC)	1.109	1.544	1.122	1.485
TURBINE BYPASS FLOWRATE, lb/sec	0.27(3)		0.24 (3)	

(1) Includes 5% horsepower penalty for boost pump drive flow.

(2) Includes 3% horsepower penalty for boost pump drive flow.

(3) 6% of total available hydrogen flow.

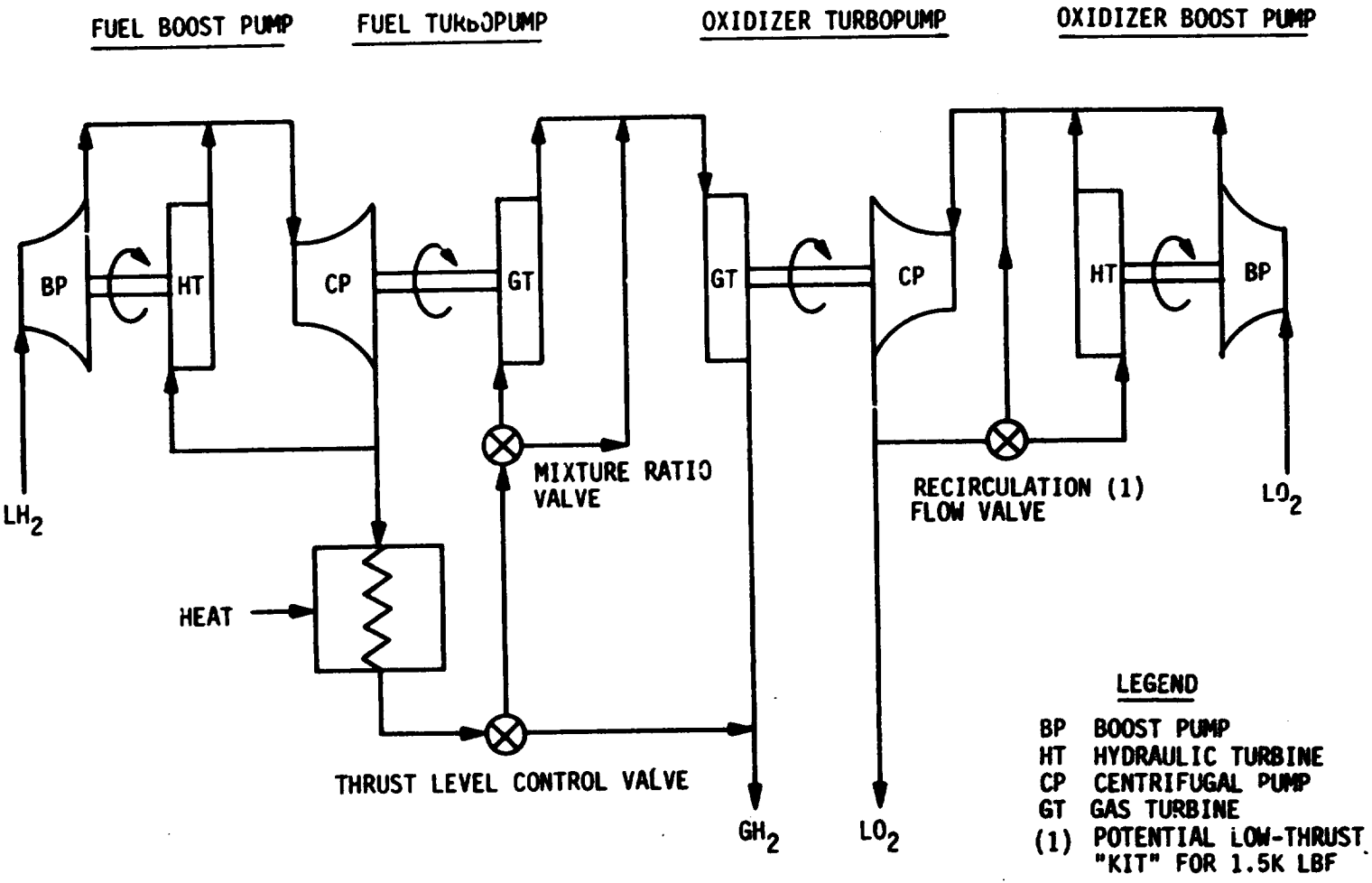

Figure 46. Flow Schematic Showing Turbomachinery Grouping

IV, E, Turbopump Analyses (cont.)

Each boost pump is driven by a hydraulic turbine. Flow for each of these turbines comes from the discharge of the respective main stage pumps and is returned to the main staged through recombination with the boost pump discharge.

2. Oxidizer Turbopump Preliminary Design Analysis

The performance of the oxidizer pump is predicted from the design point definition and a preliminary impeller design. Table XXIX shows design point parameters and corresponding values for the main OTV oxidizer pump. Table XXXI reflects the preliminary main oxidizer pump design characteristics resulting from the design point operating specification and the criteria of Reference 16.

Based on the information of Table XXIX and the calculated design values, the prediction of pump characteristics in terms of head rise, flow, and shaft speed were completed. In addition, overall pump efficiency was also predicted at off-design flow conditions, as shown in Section IV.G.

Figure 47 shows the oxidizer discharge head with respect to flow and shaft speed. Also shown in this figure is the required engine operating characteristic at a mixture ratio of 6.0 and at the stability limit. The engine operating characteristic is always in the region of negative slope for all of the shaft speed curves shown. Accordingly, the oxidizer pump has stable operating characteristics in a speed range from 10,000 to 34,720 RPM, which corresponds to an engine thrust level from 13.3 to 100% of design thrust.

TABLE XXXI

OTV OXIDIZER PUMP PRELIMINARY DESIGN CHARACTERISTICS

Shaft Speed	34720 RPM
Impeller Inlet Diameter	1.47 in.
Impeller Discharge Diameter	2.94 in.
Inlet Meridional Velocity	47.9 ft/sec
Discharge Meridional Velocity	67.3 ft/sec
Number of Blades	4 partial, 4 full
Blade Discharge Angle	28.5°
Overall Efficiency	63.6%
Hydraulic Efficiency	77.3%
Head Coefficient	.472
Number of Stages	1

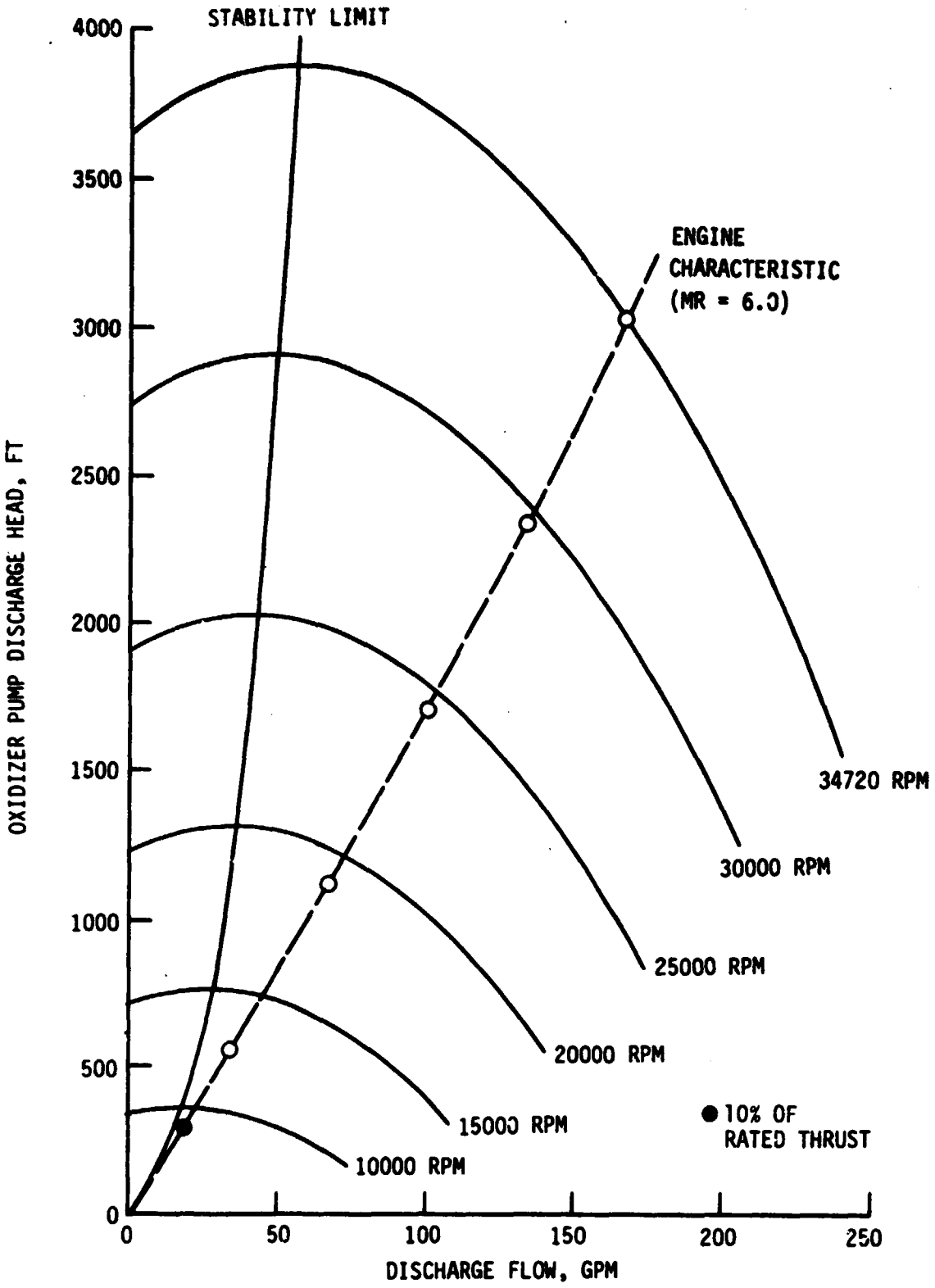

Figure 47. Oxidizer Pump Characteristics

IV, E, Turbopump Analyses (cont.)

Figure 48 illustrates the required shaft power of the oxidizer turbine in terms of pump mass flowrate. It was assumed that the boost pump recirculating turbine drive flow would absorb 5% of the power required by the main stage pump. As shown in the figure, the oxidizer turbine power varies between 236 HP at 34,720 RPM and 5 HP at 10,000 RPM. These two points correspond to engine thrust levels at 100% and 13.3% respectively.

Based on the power requirements of the turbine and the predicted inlet temperatures, pressures, and mass flow, a preliminary turbine design was formed. This single-stage turbine has a mean diameter of 5.545 inches. Figure 49 is a sketch of the flow passage and identifies the pertinent design point parameters and values.

Generalized performance of the oxidizer turbine is reflected in Figure 50. The top curve shows the estimated efficiency with respect to the blade speed ratio. At the bottom, the variation of normalized weight flow is shown for corresponding turbine pressure ratios.

3. Fuel Turbopump Preliminary Design Analysis

As with the oxidizer turbopump, the fuel turbopump preliminary design is based on the design point parameters shown in Tables XXIX and XXX and the criteria of References 16 and 17. Table XXXII shows the results of the preliminary design calculations.

Figure 51 shows the fuel pump discharge head-capacity relationship for shaft speeds varying between 90,000 and 20,000 RPM. Figure 52 shows the required power of the fuel turbine with respect to the fuel pump flowrate for various shaft speeds. As illustrated on Figure 51, the engine characteristic is located in the negatively sloped region of the discharge head-

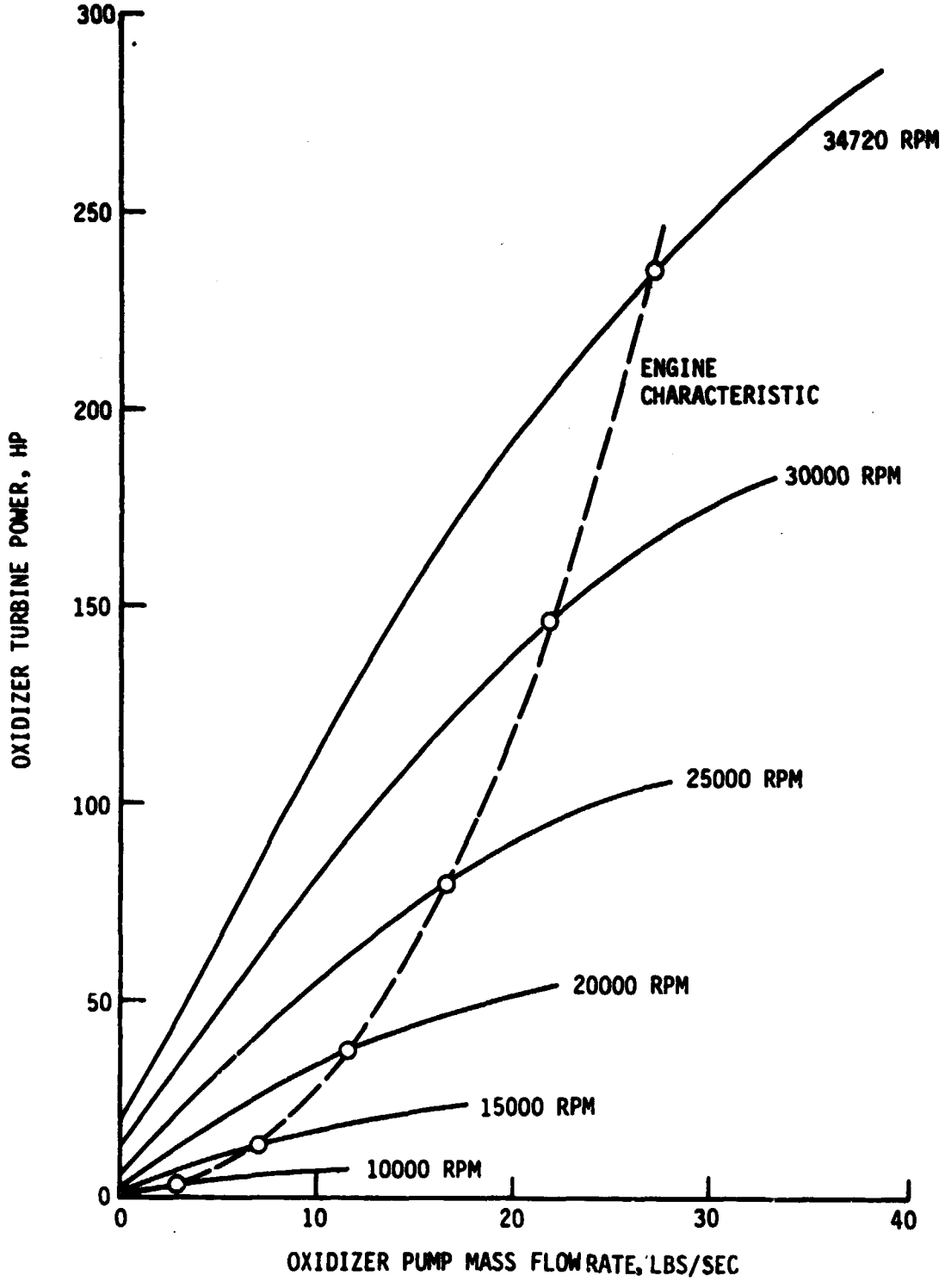

Figure 48. Oxidizer Turbine Power With Respect to Oxidizer Pump Flowrate

DESIGN POINT

P_o = 1471 PSIA
T_o = 488.5 °R
P_e = 1326 PSIA
$\dot{W}$ = 4.22 LB/SEC
N = 34,720 RPM
FLUID: GH_2

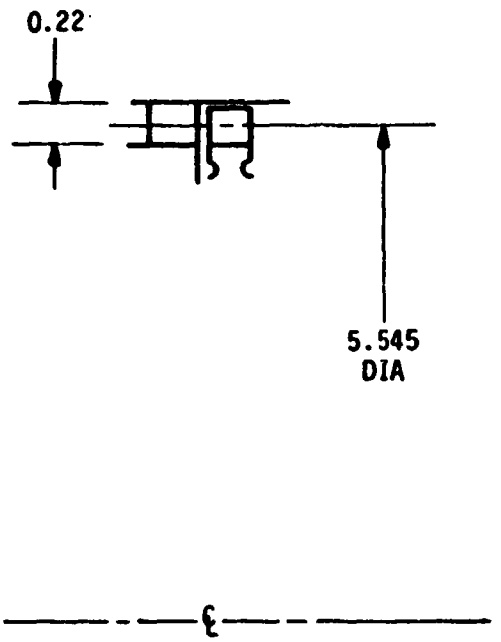

Figure 49. Oxygen Pump Turbine Design Characteristics

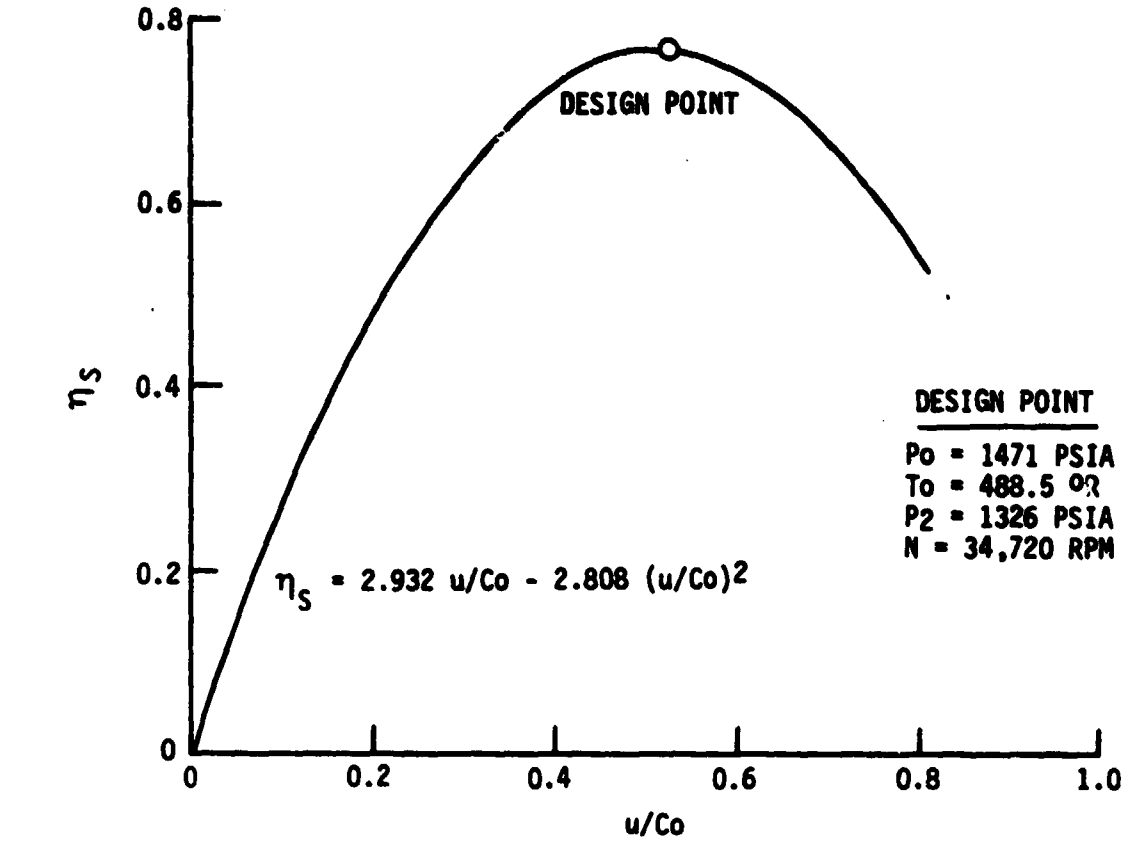

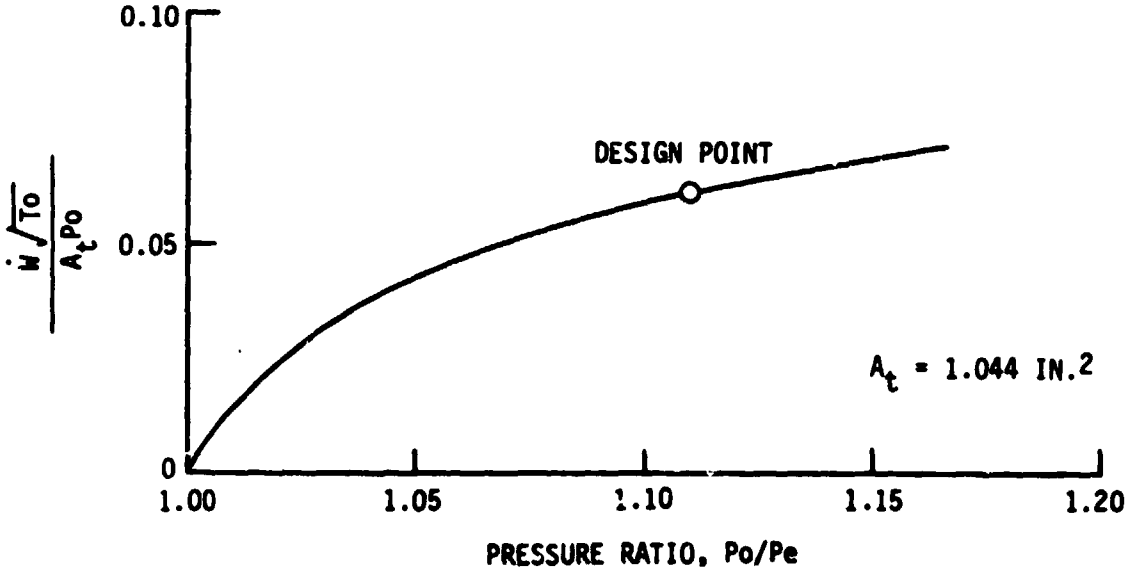

Figure 50. LOX Turbine Performance

TABLE XXXII

OTV FUEL PUMP PRELIMINARY DESIGN

Shaft Speed	90000 RPM
Impeller Inlet Diameter	1.68 in.
Impeller Discharge Diameter	3.36 in.
Inlet Meridional Velocity	263.1 ft/sec
Discharge Meridional Velocity	285.4 ft/sec
Number of Blades	6 full, 6 partial
Blade Discharge Angle	40.3°
Overall Efficiency	65.5%
Hydraulic Efficiency	78.7%
Stage Head Coefficient	0.486
Number of Stages	3

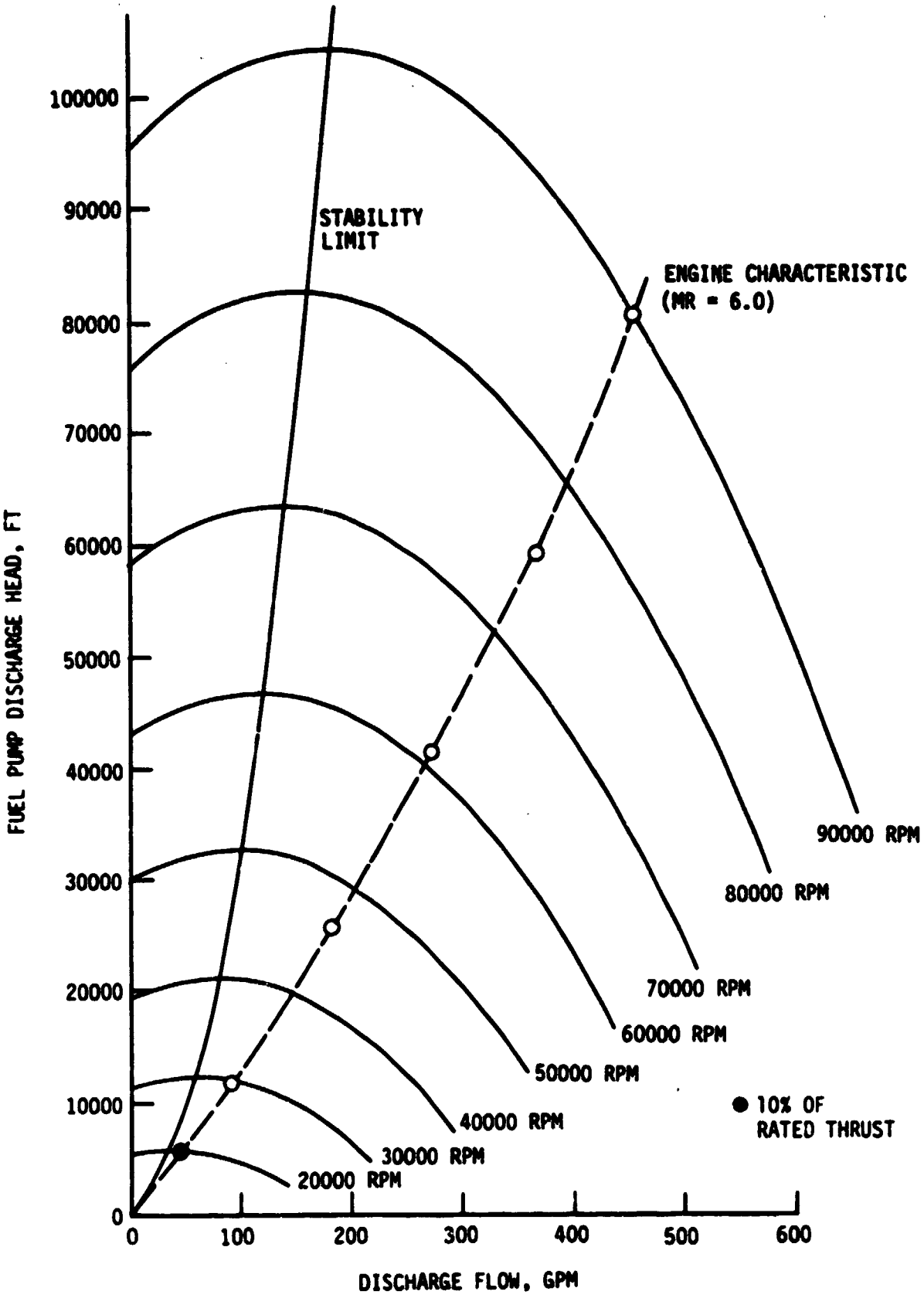

Figure 51. OTV Fuel Pump Characteristics

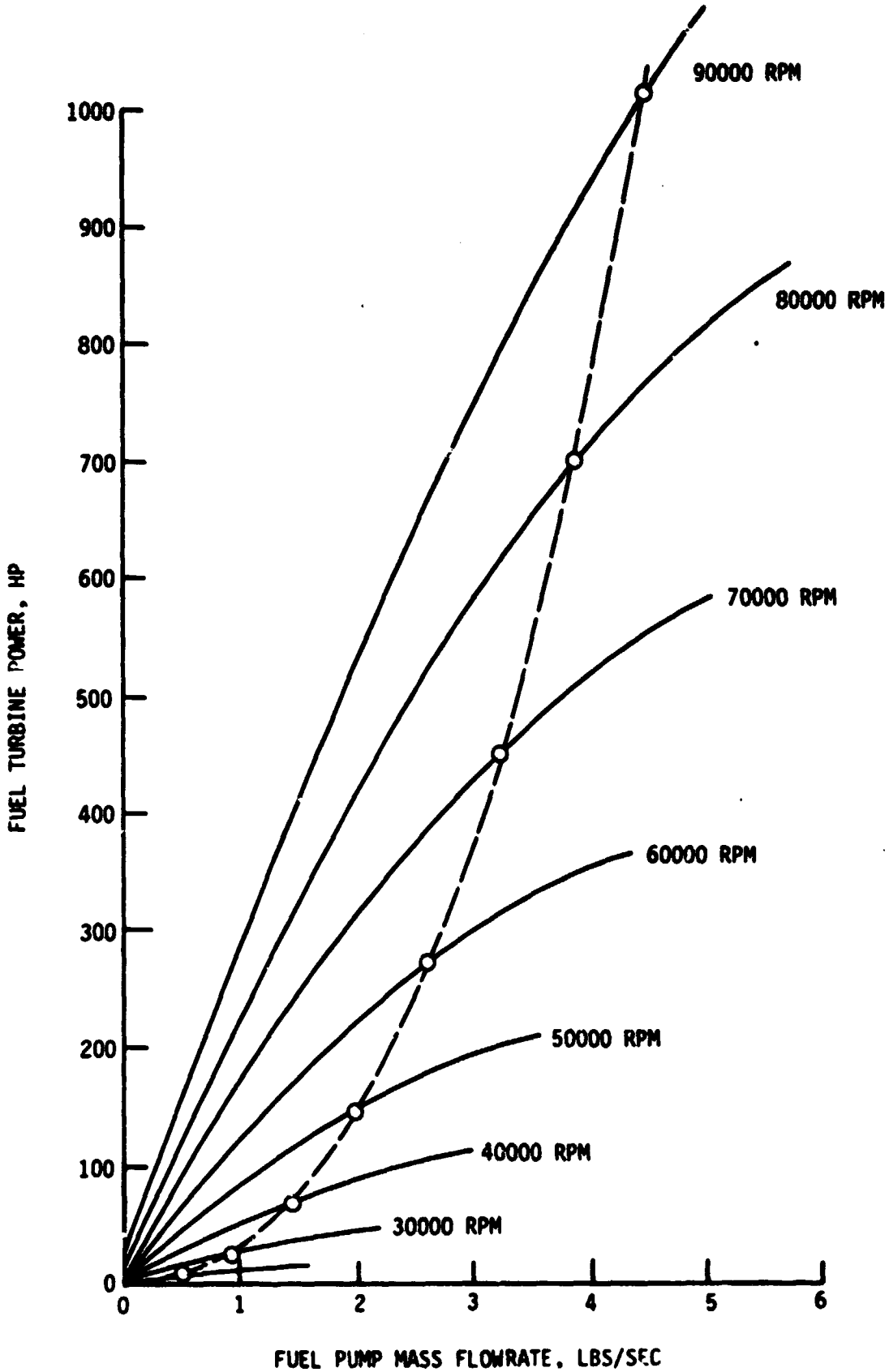

Figure 52. Fuel Turbine Power With Respect to Fuel Pump Flowrate

capacity curves for the various shaft speeds, indicating that the pump should operate between 10 and 100% of full thrust without any instabilities.

A two-stage turbine was selected to drive the fuel pump. Figure 53 illustrates the basic flow passage configuration associated with this turbine, and Figure 54 shows its performance in terms of efficiency, blade speed ratio, normalized weight flow, and pressure ratio.

4. Overall Turbopump Performance

Turbopump efficiency is defined as the product of pump and turbine efficiencies. Figure 55 illustrates this composite efficiency for both the fuel and oxidizer turbopumps. Also shown is the minimum required efficiency which was calculated on the basis of the assumption that all of the fuel flow, including that bypassing the turbines through the thrust level control valve, would be available for energy conversion. The figure shows that there is sufficient margin between the preliminary design estimate and the minimum requirement so that system power balancing at the low-thrust levels should not present a problem. This was verified by the cycle analysis results presented in Section IV,G.

5. Turbopump Analysis Conclusions

The study results indicate that no modifications are required for the oxidizer and fuel turbopump to operate without instabilities to rated thrust levels of 13.3 (2K) and 10% (1.5K), respectively. The operating range for the pumps is shown in Table XXXIII.

DESIGN POINT

P_o = 2286 PSIA

T_o = 535°R

P_e = 1481 PSIA

$\dot{W}$ = 4.22 LB/SEC

N = 90,000 RPM

FLUID - GH_2

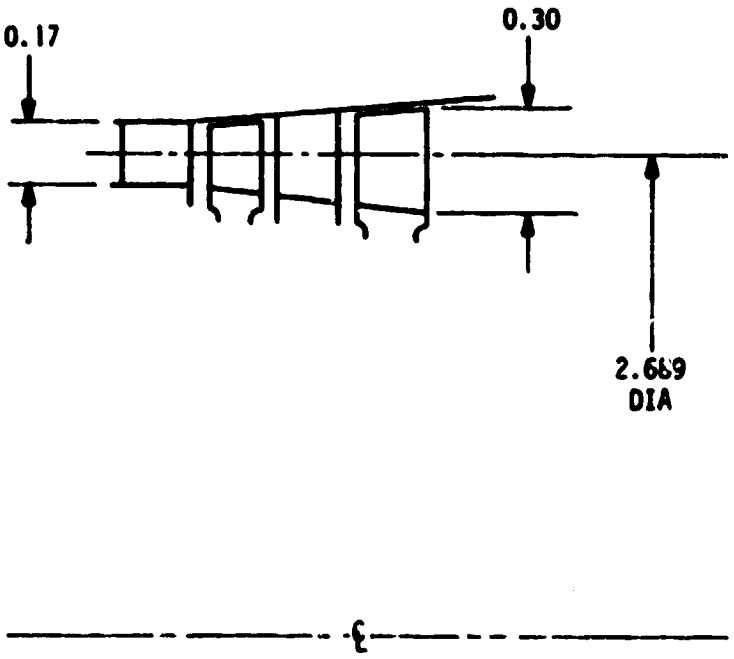

Figure 53. Hydrogen Pump Turbine Design Characteristics

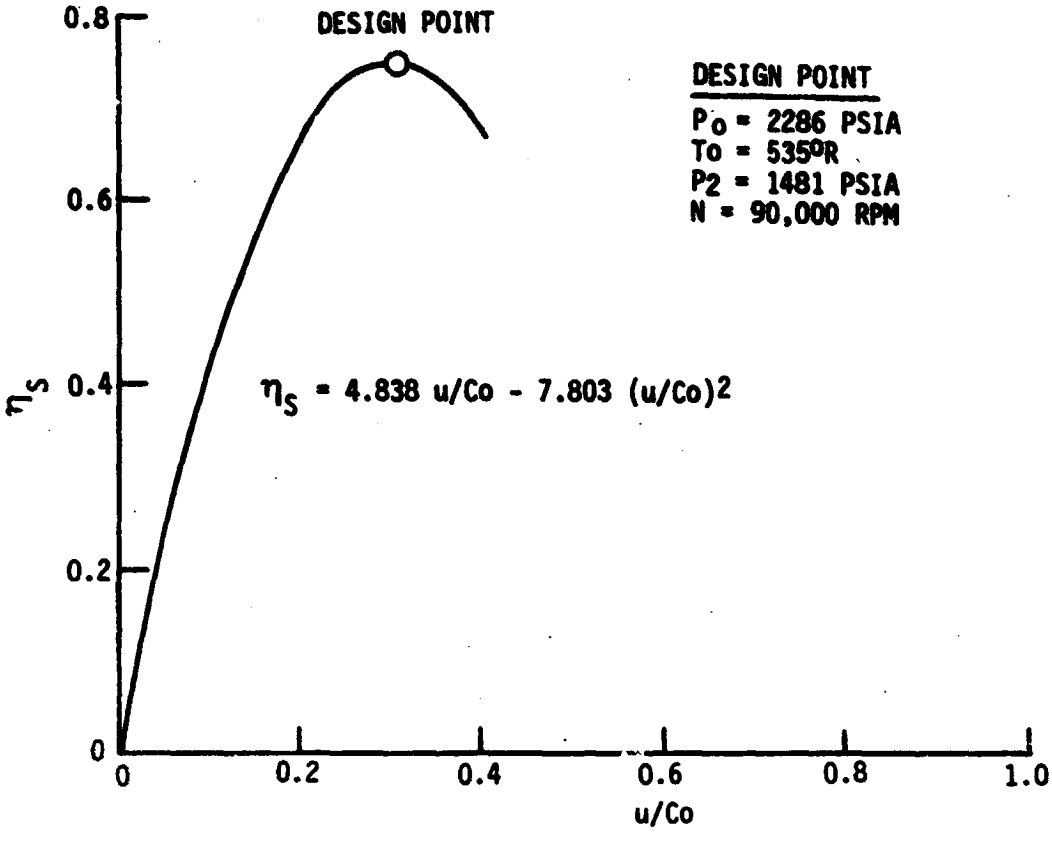

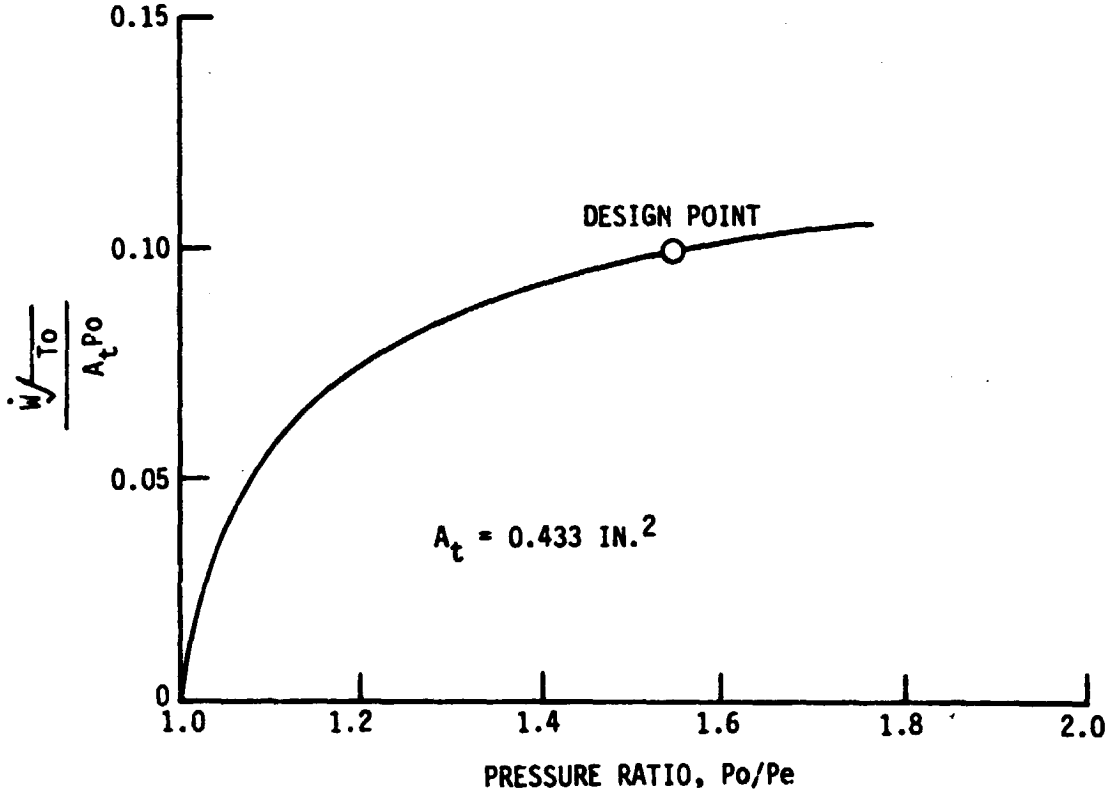

Figure 54. LH_2 Turbine Performance

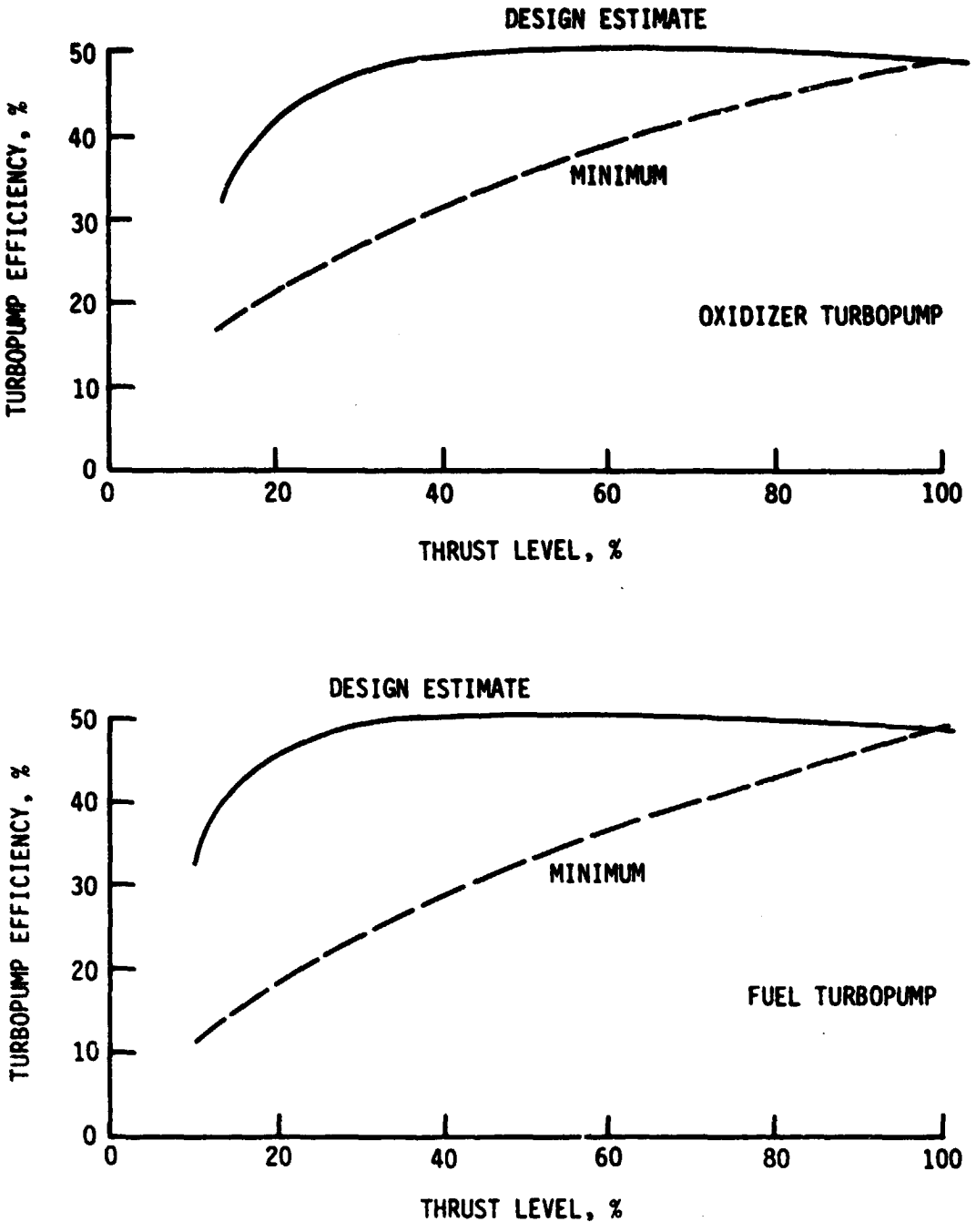

Figure 55. Comparison of Estimated and Minimum Required Turbopump Efficiencies

TABLE XXXIII

RANGE OF TURBOPUMP VARIABLES

	OXIDIZER PUMP		FUEL PUMP	
	MINIMUM*	MAXIMUM	MINIMUM*	MAXIMUM
Thrust Level (%)	13.3	100.0	10.0	100.0
Flowrate (GPM)	23	170	47	456
Shaft Speed (RPM)	10000	34720	20000	90000
Discharge Heat (ft)	352	3015	5794	80572

*NO MODIFICATIONS

IV, E, Turbopump Analyses (cont.)

The study results also show that there is sufficient cycle power balance margin at low thrust so that low-thrust pump flows can be increased to avoid instability at even lower thrust levels. This can be accomplished by adding a recirculation line and valve between the main pump and boost pump as shown on Figure 46 for the oxidizer pumping system. This oxidizer recirculation "kit" would get the thrust level to a value at least as low as the fuel-side, and "kitting" the fuel-side might allow for even lower thrust operation. The concern here is that the recirculation flow may get too hot to be dumped back into the main pump inlet. More detailed analyses and/or experimental data are required to firmly fix the minimum thrust level.

F. LOW-THRUST CONTROLS ANALYSIS

An active control system was selected during the Task I, Advanced Expander Cycle Engine Optimization (Section III.C) which was conducted for this study. The cycle schematic, showing the location of the controls, is presented in Figure 56. These controls were also analyzed for low-thrust operation. It has been concluded that new valves or a valve "kit" are not required. The rationale for this conclusion is discussed in the following paragraphs.

Because the engine is required to operate in the pumped-idle mode, the turbine bypass valve used for the full-thrust mode (Valve #3, Figure 56) can also be modulated to control the required steady-state, low-thrust level. Equal percentage flow characteristics can be designed into the valve so that a given percent change in opening at the pumped-idle thrust level would have the same percentage effect on flow as it would have at the full-thrust level. This same design philosophy can be applied to the turbine flow control valve (Valve #4, Figure 56) which is utilized to control engine

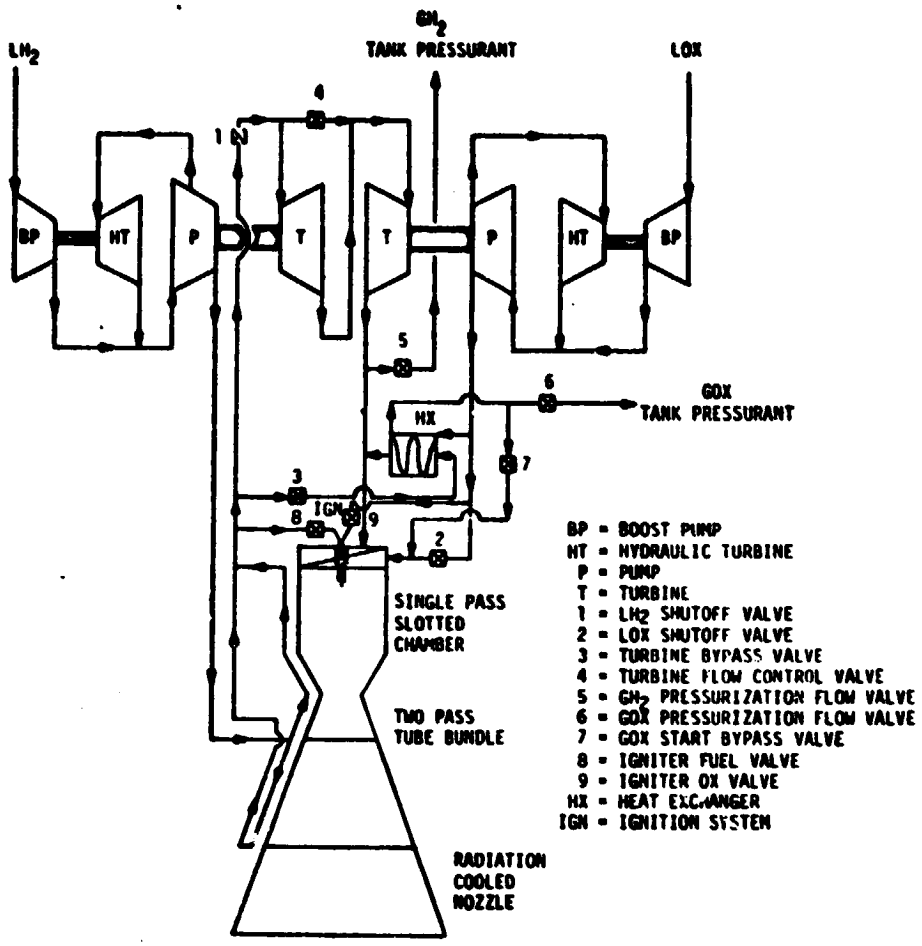

Figure 56. Phase A Advanced Expander Cycle Engine Flow Schematic

mixture ratio. These flow control valves can be designed to accommodate any selected low thrust level.

No functional problems are anticipated for the remaining valves in the engine system. If engine weight is a problem, the full-thrust engine valves could be replaced by a smaller set of valves designed to operate at a discrete low-thrust point. Although this would save about 25 lb of engine weight, it probably is not worth the additional cost.

G. LOW-THRUST ENGINE SYSTEM ANALYSIS

The objectives of this subtask were to establish engine operating conditions at low-thrust operating points and to determine engine power balance limits, if any. The thermal, turbopump, and injector design analyses results were used to evaluate the expander cycle power balance over a thrust range of 7K lbF to 1K lbF, or 50% to 6.7% of rated thrust, respectively.

Coolant jacket pressure drop data used in this analysis are shown in Figure 57. The turbine inlet temperatures were previously shown in Figure 45. Pump design and off-design efficiency data are shown on Figures 58 and 59 for the main oxygen and hydrogen pumps, respectively. The turbine performance curves were shown in Figures 50 and 54 for the oxidizer turbine and hydrogen turbine, respectively.

The injector pressure drop criteria used in the analysis are shown in Figure 60. These criteria are based upon the results of the injector modification analysis. Below 50% of rated thrust, the oxidizer elements were assumed to be sized to meet a minimum injector stiffness ($\Delta P/P_c$) requirement of 15% until the injection velocity reached 40 fps at about 8% thrust. Two typical orifice sizes in this range are shown in the figure.

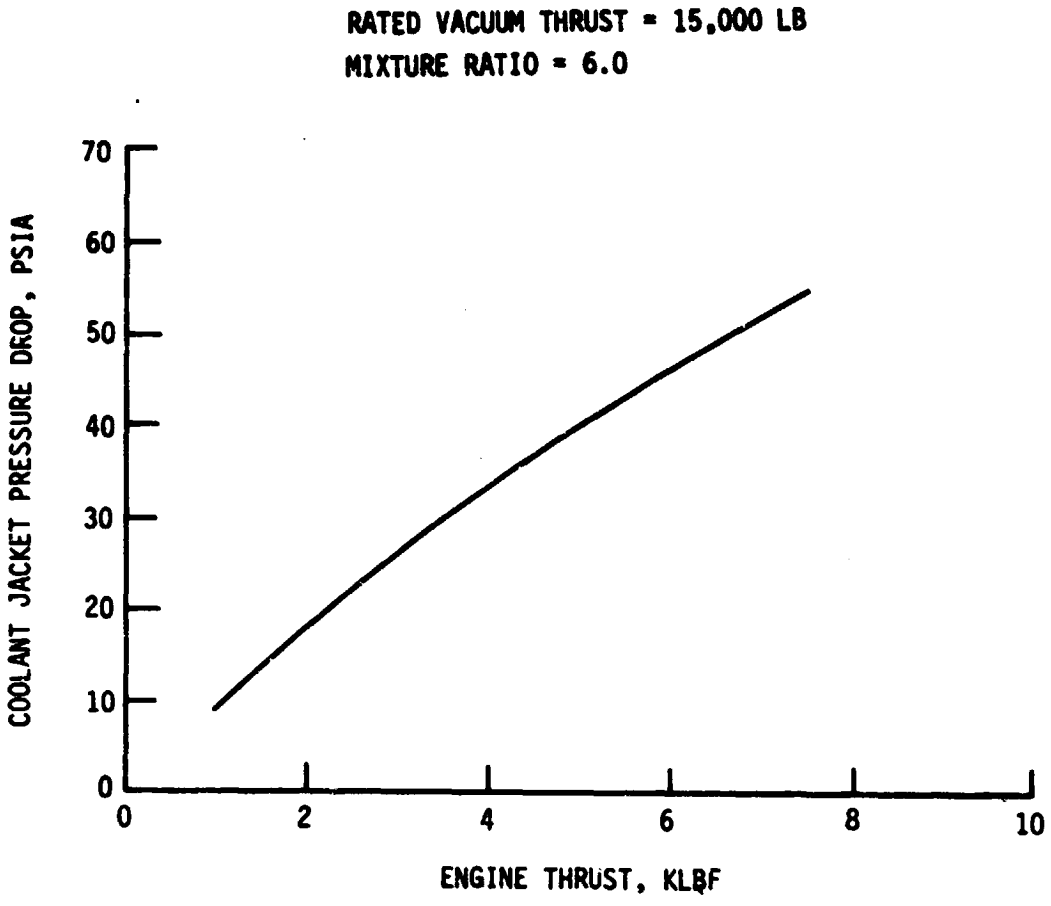

Figure 57. Coolant Jacket Pressure Drop vs Thrust

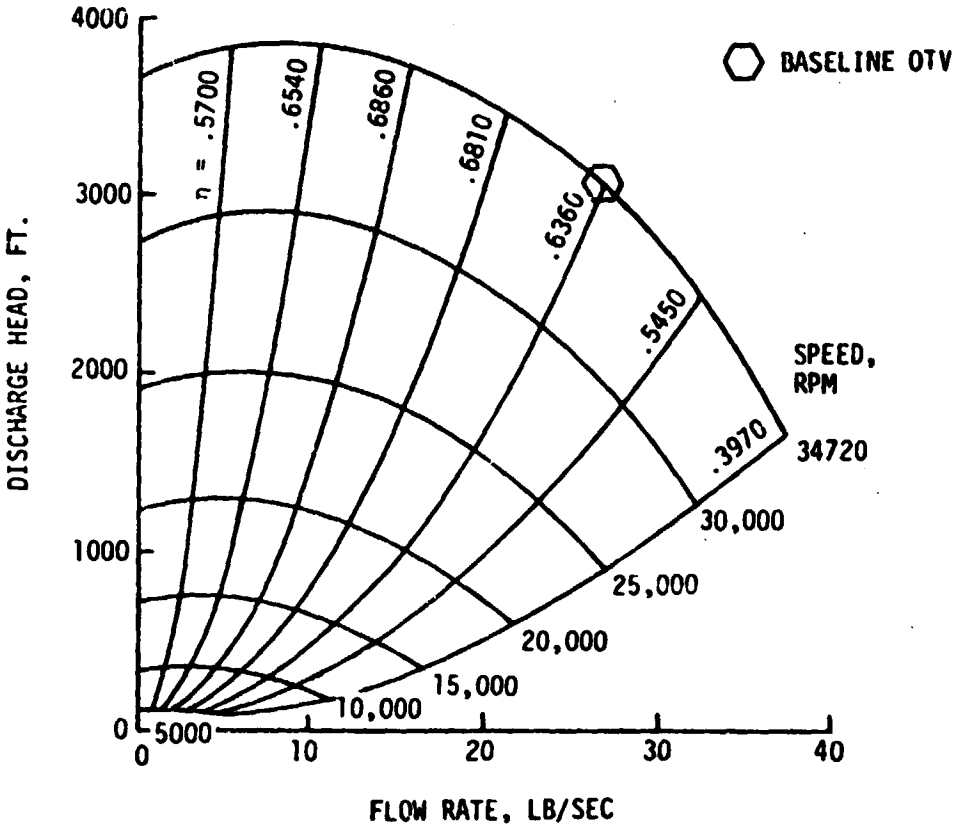

Figure 58. Main Oxygen Pump Performance Map

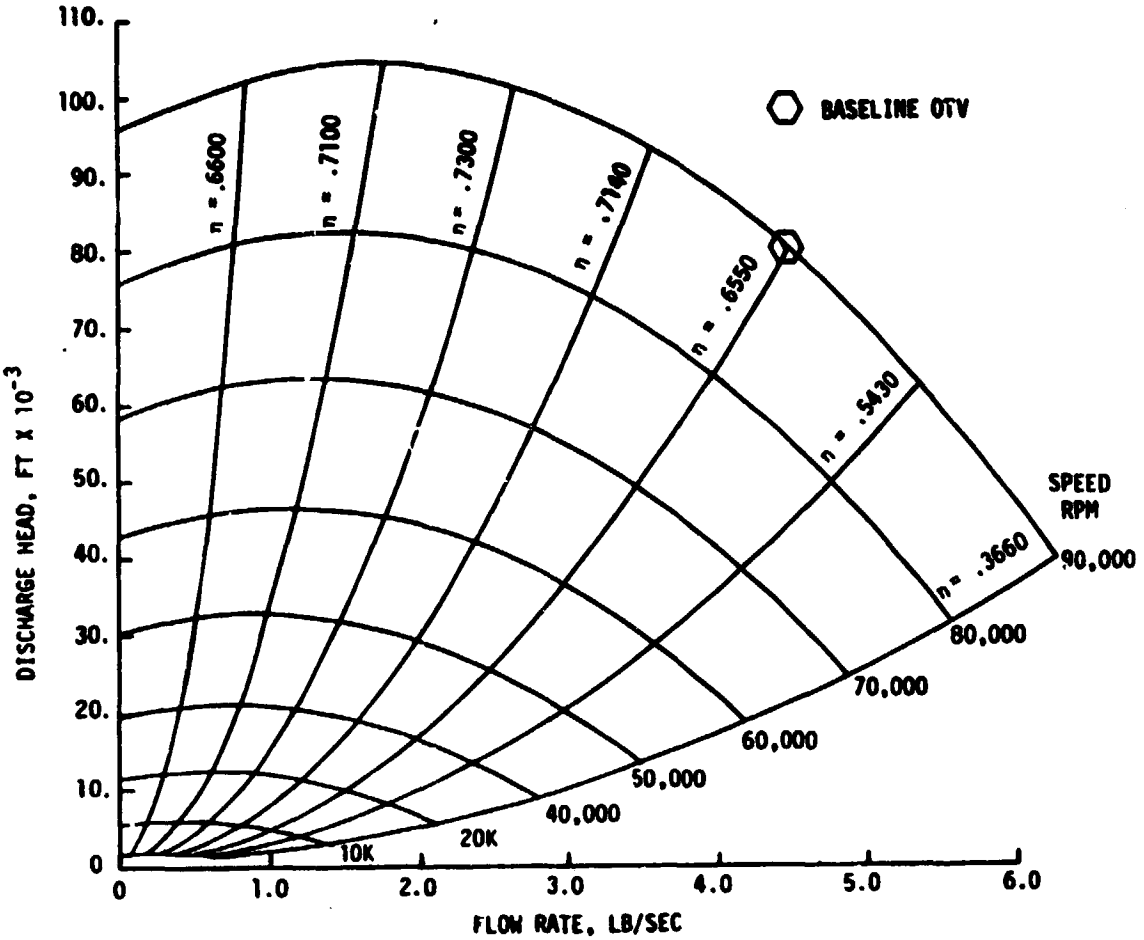

Figure 59. Main Hydrogen Pump Performance Map

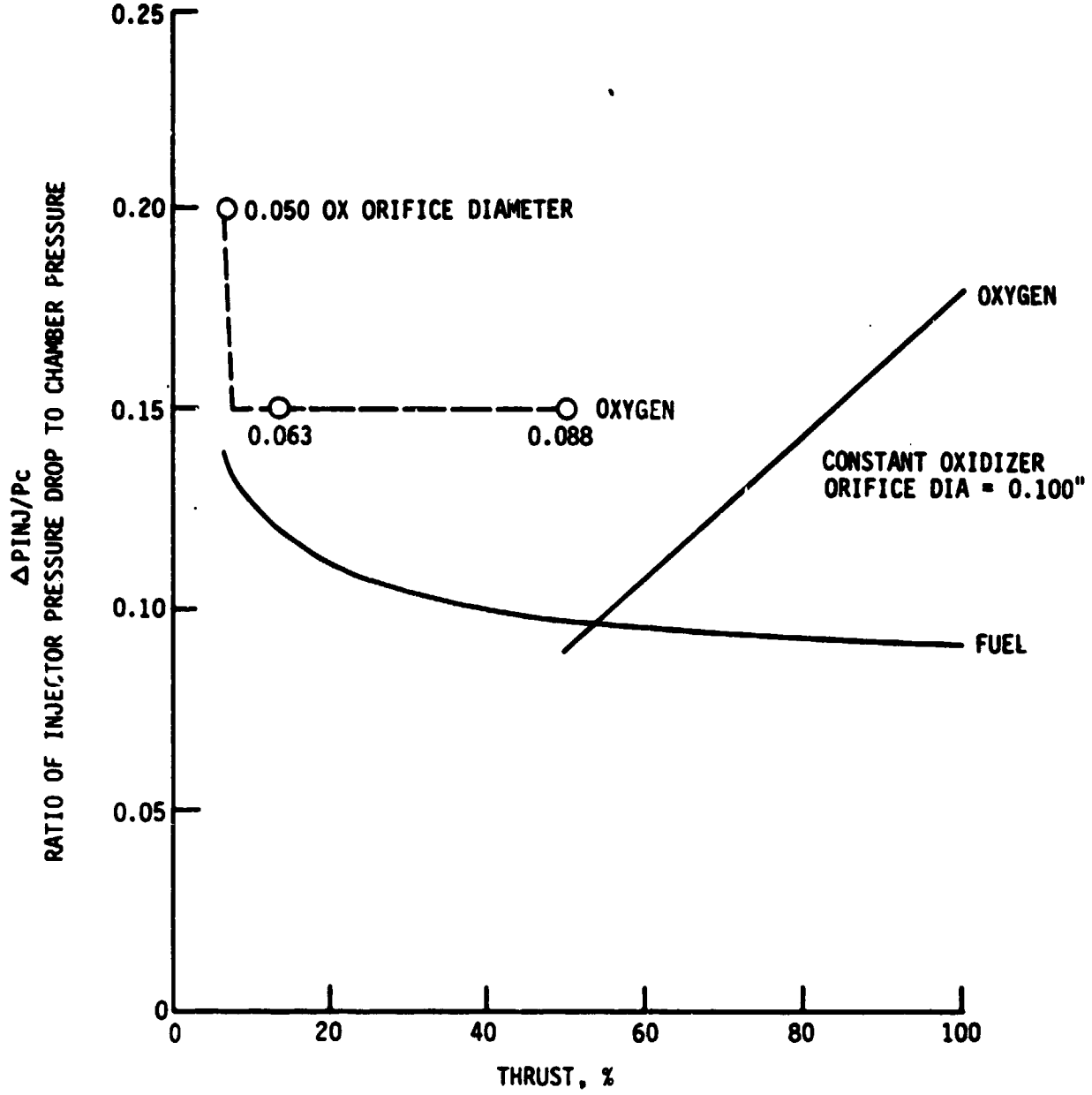

Figure 60. Injector Pressure Drop Criteria

IV, G, Engine System Analyses (cont.)

An orifice size of .050 in. was selected for the 1K lbF operation (6.7% thrust).

The results of the engine power balance analysis are shown in Figures 61 and 62. Figure 61 shows the pump discharge pressure requirements as a function of thrust. The hydrogen pump discharge pressure is purposely kept relatively high in the very low thrust region to maintain the coolant jacket exit pressure above the critical pressure of hydrogen. This avoids the problems associated with two-pahse cooling.

The turbine pressure ratio requirements as a function of thrust are shown in Figure 62. The very low pressure ratios are evidence of the ease with which the cycle is power-balanced at low thrust. The turbine bypass flow is increased at low thrust because pump horsepowers are reduced and the turbine inlet temperatures are increased. The turbine bypass flow needed to match power balance and turbine flow parameter requirements is shown in Figure 63.

H. LOW-THRUST TECHNOLOGY

The following technology programs were identified for the alternate low-thrust option.

- Conduct an experimental, hot-test program to verify the performance (C*), heat transfer, and stability of the thrust chamber assembly at the low-thrust operating point. This program should be combined with a rated thrust injector/ chamber technology program.

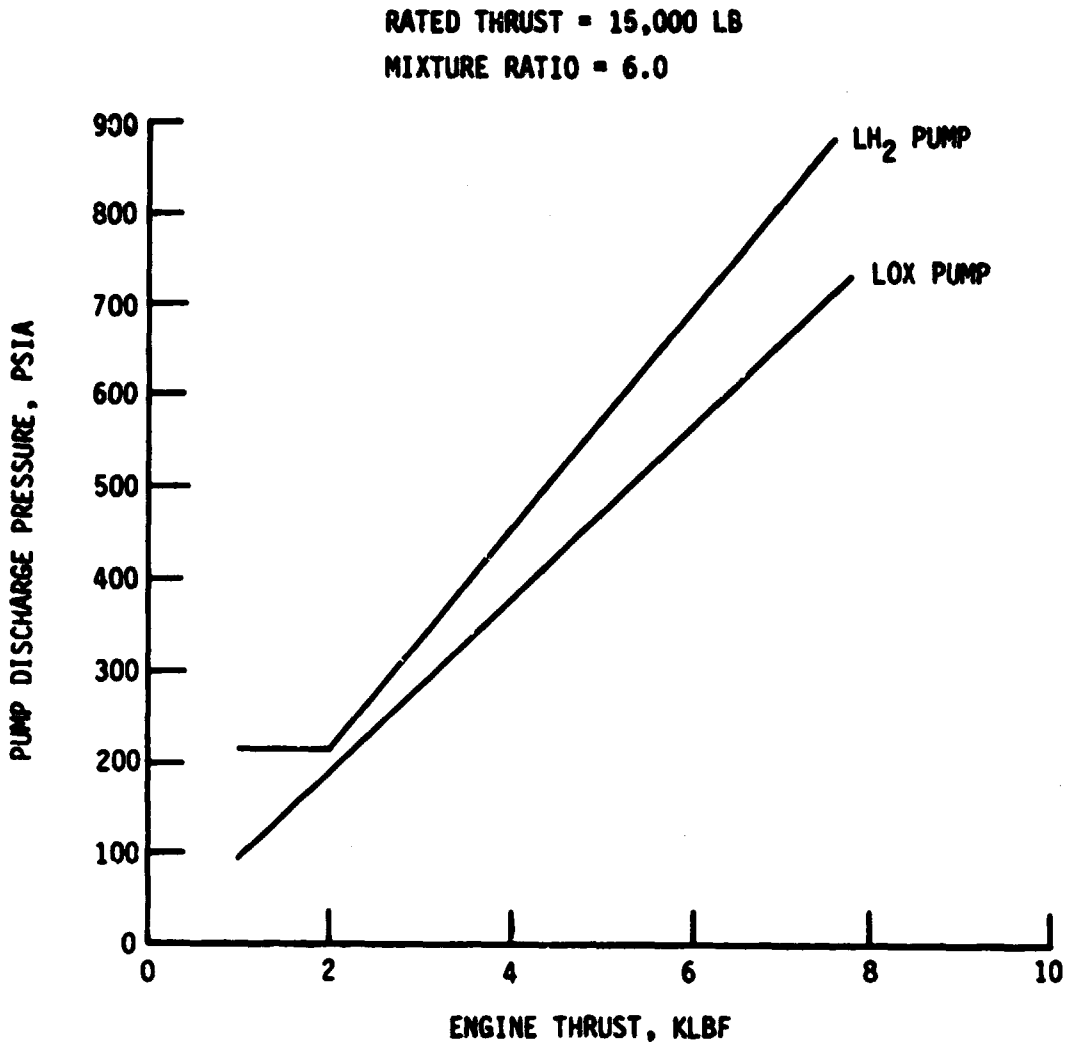

Figure 61. Pump Discharge Pressure Requirements at Low Thrust

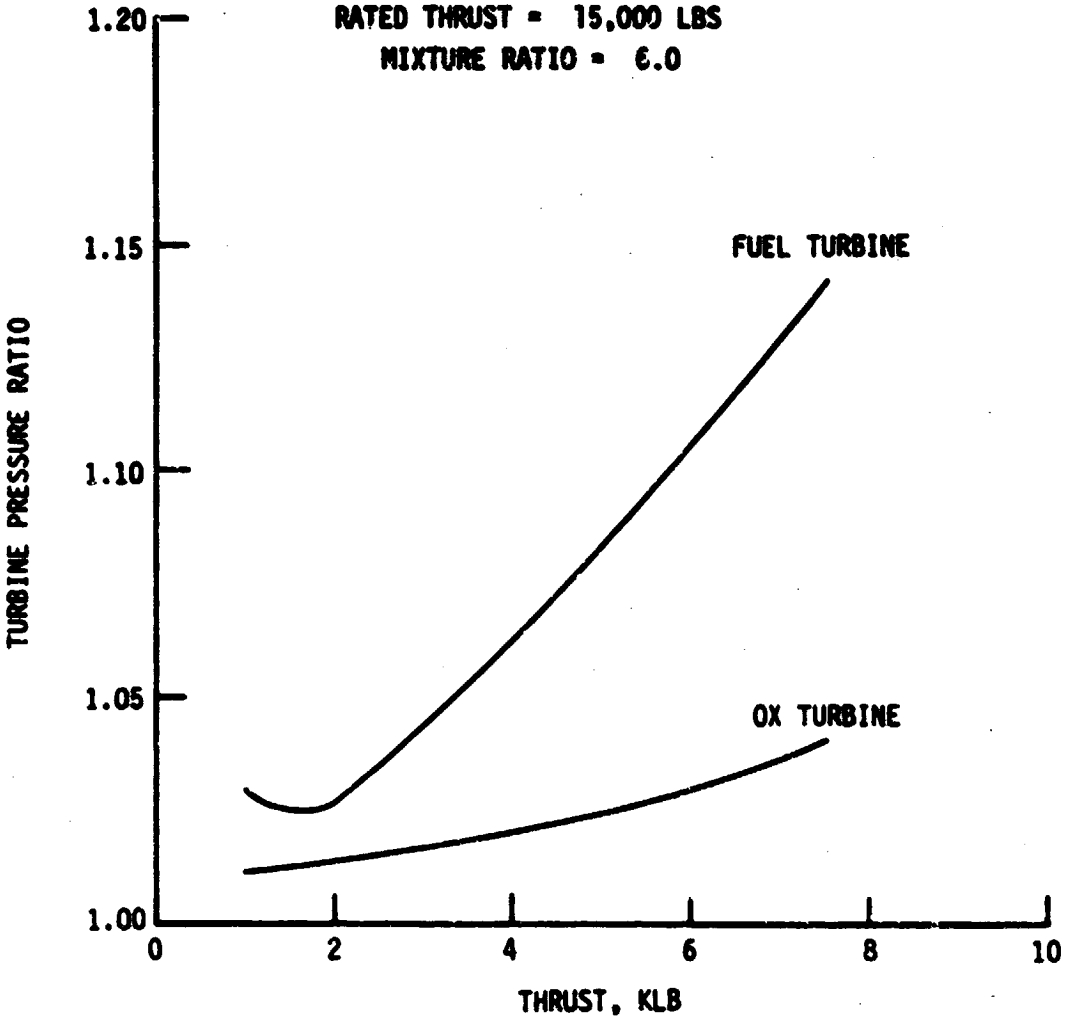

Figure 62. Turbine Pressure Ratio Requirements at Low Thrust

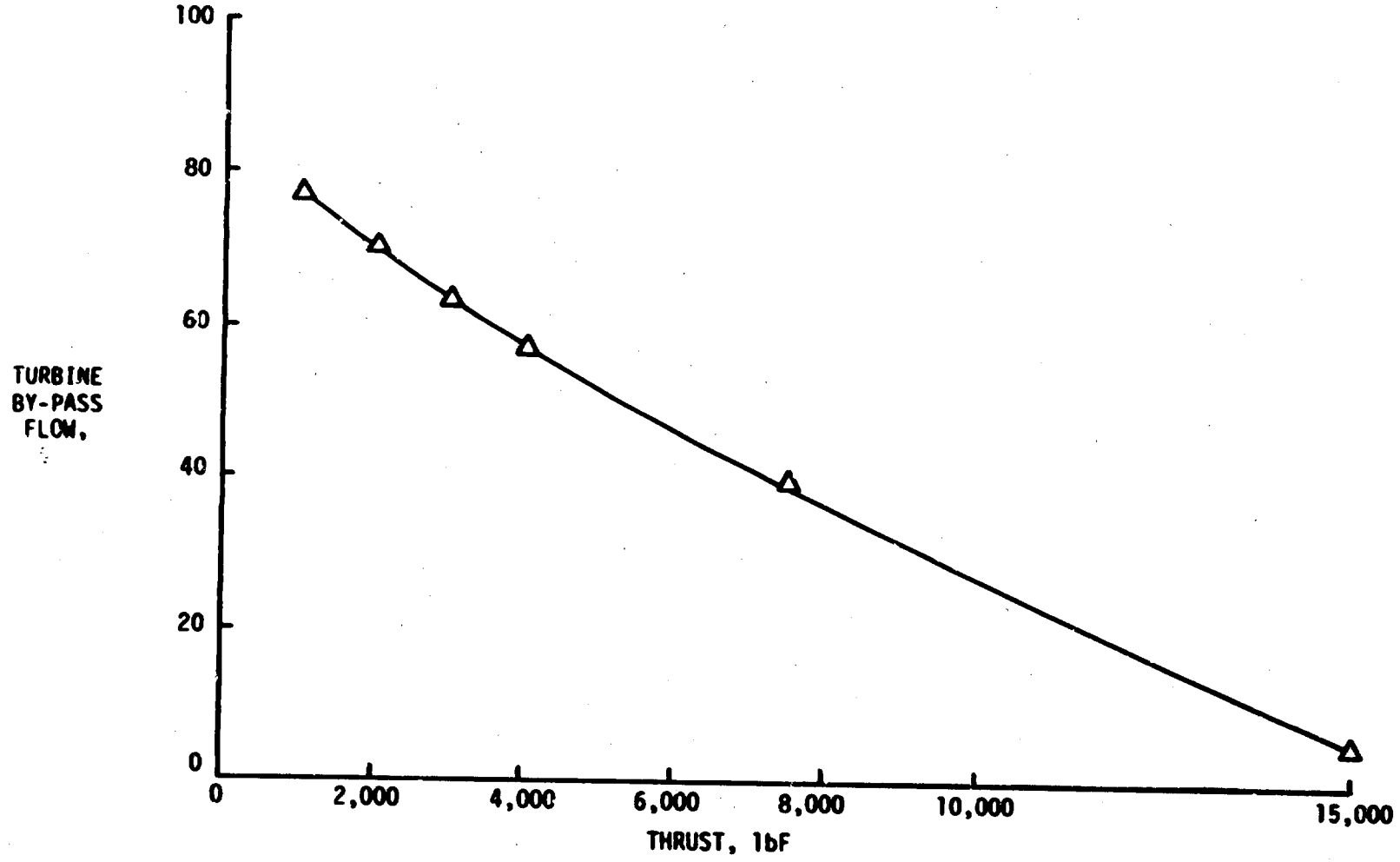

Figure 63. Turbine Bypass Flow vs Thrust

IV, H, Low-Thrust Technology (cont.)

- Design and demonstrate a throttling valve (ring gate) that is internal to the turbopump assembly and located at the impeller discharge. The advantage of this valve is that it eliminates the need for a valve and line that would be required if a portion of the discharge flow were recirculated to the pump inlet in order to maintain stable pump operation. It also eliminates the concerns associated with the dumping of a relatively hot recirculation flow into the pump inlet.

- Experimentally evaluate single channel flow stability for changing area channels with heat addition and develop a flow stability computer model that simualtes the chamber design.

- Evaluate two-phase flow and transition from two-phase to single-phase flow on heat transfer.

- Verify turbopump operation, efficiencies, and stability at low thrust. Again, this should be conducted as part of a rated thrust pump technology program.

V. TASK III: SAFETY RELIABILITY, AND DEVELOPMENT RISK COMPARISON

A. SAFETY AND RELIABILITY ANALYSES

The primary objective of this subtask was to perform an in-depth analysis to provide comparative data on crew safety and mission reliability for both advanced expander cycle and staged-combustion cycle OTV Engine candidates. A mathematical model was also developed to evaluate the advantages and disadvantages of single and multiple engine systems.

1. Mission Reliability and Crew Safety Goals

A rocket engine system, when used in conjunction with a man-rated vehicle, is considered to be "man-rated" if there is a "satisfactory" probability of mission success and the likelihood of crew "loss" due to engine system-induced effects is remote. Underlying it is a design philosophy which takes into account the influence of potential single point failures jeopardizing the safe return of the crew and/or mission success. Consequently, man-rating is quantified both in terms of engine reliability (R) and crew risk (CR).

A "satisfactory" probability of mission success, as traditionally defined by aerospace experience, is .99 minimum. Defining a crew risk goal is more difficult. Figure 64 shows one method. A loss of two lives in one hundred missions (at 10 missions per year) seems acceptable if one compares this number to mortality rates for other hazardous careers and applies the "Manned Spacecraft Criteria and Standards" and "Shuttle Payload Safety Requirements." Accordingly, the acceptable crew risk is judged to be comparable to that of an airline pilot. It is also assumed that each astronaut will undertake 10 flights per career and that half of the mission crew risk is experienced during the STS phase ($.5(2\times10^{-3})$). Of the remainder, 75% of the failures are due to the OTV vehicle (Figure 65)

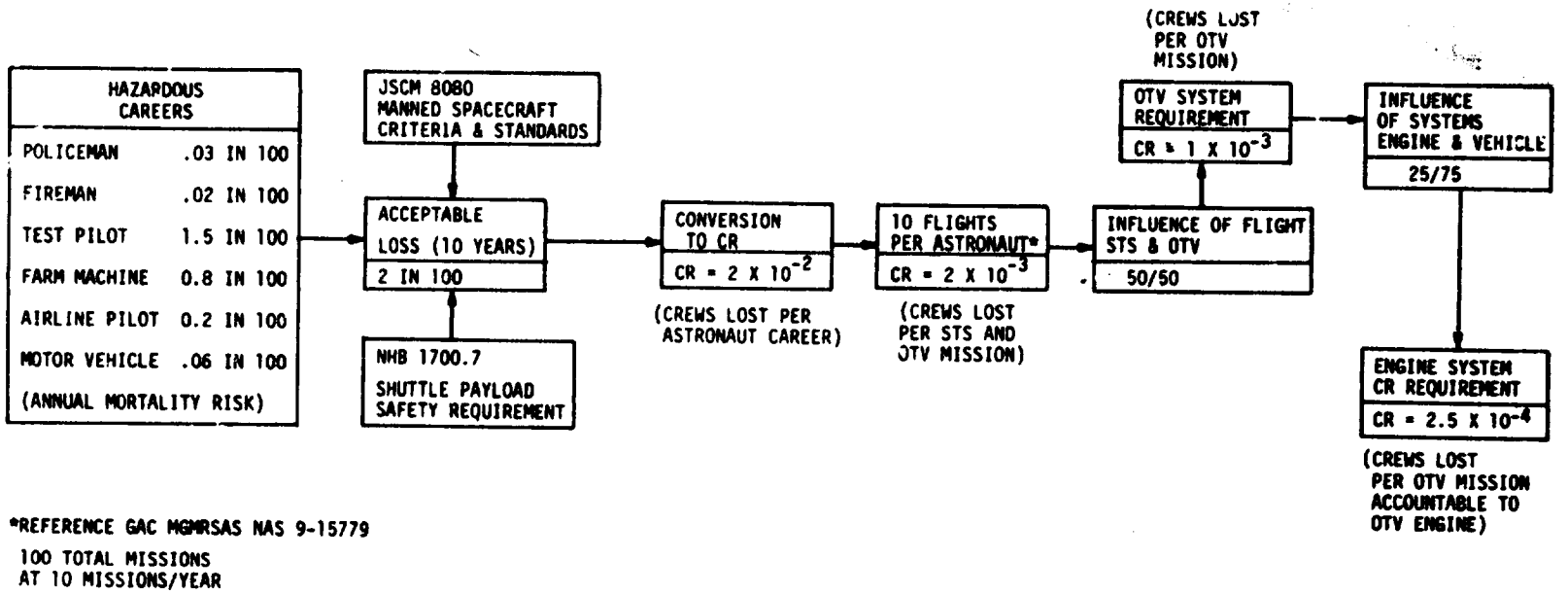

*REFERENCE GAC MGMRSAS NAS 9-15779
100 TOTAL MISSIONS
AT 10 MISSIONS/YEAR

Figure 64. Determining Acceptable Crew Risk

OTV CRITICAL SUBSYSTEM		% ALLOCATION GRUMMAN	% ALLOCATION GENERAL DYNAMICS	
MAIN PROPULSION		50	(25)	CONSERVATIVE ESTIMATE USED
VEHICLE	RCS	10	10	
	EPS	8	8	
	AVIONICS	7	17	
	ECLS	10	10	
	RADIATION PROTECTION	12	2	
	CREW TRANSFER	3	3	
	FOOD/WATER	0	0	
	OVERALL STRUCTURE	0	0	
	PROPELLANT FEED PRESSURIZATION AND VENT	-	25	

THE OTV PROPULSION SYSTEM IS VERY IMPORTANT TO BOTH MISSION SUCCESS AND CREW SAFETY

Figure 65. Preliminary Allocation of Failure Likelihood

V, A, Safety and Reliability Analyses (cont.)

and the remaining 25% becomes the acceptable crew risk value for the OTV engine system ($2.5x10^{-4}$). For this crew safety and reliability analysis, a satisfactory probability of mission success for the vehicle was assumed to be .99, and an acceptable probability of crew loss attributable to the engine is defined as $2.5x10^{-4}$.

2. Mathematical Model

A parametric study was conducted to determine how one-, two- and three-engine systems conform to these man-rating requirements. The basic assumptions used to build the model are as follows:

- Failure Rate Calculation - The total failure rate (λtotal) of an engine system is calculated on a per cycle basis and is divided into three parts. The three basic failure categories are classified as follows:

  Catastrophic (λCAT) - Failure damages the entire engine system, with resultant loss of crew and mission.

  or

  Fail Safe (λFS) = Failure shuts down the engine involved, which could result in stranding the crew and possible mission loss.

  or

  Fail Operational (λFO) - Minor failure. The engine is still operational. Results in low performance but does not endanger crew life. Possible mission loss.

A preliminary Failure Modes and Effects Analysis for pump-fed rocket engines was conducted to determine the most common failures.

V, A, Safety and Reliability Analyses (cont.)

These results were combined with the OTV mission model to obtain the criticality of each type of failure through each mission phase. For the entire mission, a % allocation of each type of failure rate was made as follows:

5% Catastrophic
60% Fail Safe
35% Fail Operational

Mathematically,

$$\lambda\text{total} = \underbrace{.05\ \lambda\text{total}}_{\lambda CAT} + \underbrace{.6\ \lambda\text{total}}_{\lambda FS} + \underbrace{.35\ \lambda\text{total}}_{\lambda FO}$$

(Note that further research of hard data is required to firm up this apportionment, but a 5% allocation for catastrophic failures is considered to be a conservative assumption).

Those failures that affect the crew either by loss of life or stranding are used to calculate the crew risk. Therefore, for a single-engine system, the crew risk is as follows:

$$CR = \lambda CAT + \lambda FS = .65\ \lambda\text{total}$$

The mission model used for the analysis assumes five (5) engine burns per mission are typical: two from Low-Earth Orbit (LEO) to Geosynchronous Earth Orbit (GEO) and three back to LEO (per NASA TMX-73394, Ref. 2). Four engine systems were evaluated: a single 20K lbF engine; a twin 10K lbF engine system; a three 10K lbF engine system; and

V, A, Safety and Reliability Analyses (cont.)

a three 7K lbF engine system. The twin and three 10K lbF engine systems require that two engines must fire on the first burn and that one must fire on all subsequent burns. The three 7K lbF engine system requires that all three engines must fire on the first burn and that two must fire on the remaining burns to successfully complete the mission.

It is assumed that a number of engines in the system is not restricted by volumes that may cause gimbaling problems (i.e., inadequately maintained vehicle stability). Likewise, weight and engine length constraints are not addressed in this model.

a. Model Results

As the engine-out capability of an engine system increases, the total system failure rate decreases and the system reliability increases. Figure 66 compares systems with single-engine reliabilities of .99. The inconsistency of the three 7K lbF engine system is due to the disadvantage of there being a three times greater chance that catastrophic failures will override the partial engine-out capabilities. Notice the λFS and λFO decrease to negligible amounts with complete engine-out capability. Figure 67 shows that the relative results do not change for various single-engine reliabilities.

A single-engine reliability of 0.99 was assumed in the example of Figure 66, but the crew risk requirement is not addressed although it is obvious that multiple engines would reduce crew risk. Figure 68 shows the single-engine reliabilities needed to meet both requirements for each engine system researched. Reliability differences are small but relate to many engine tests.

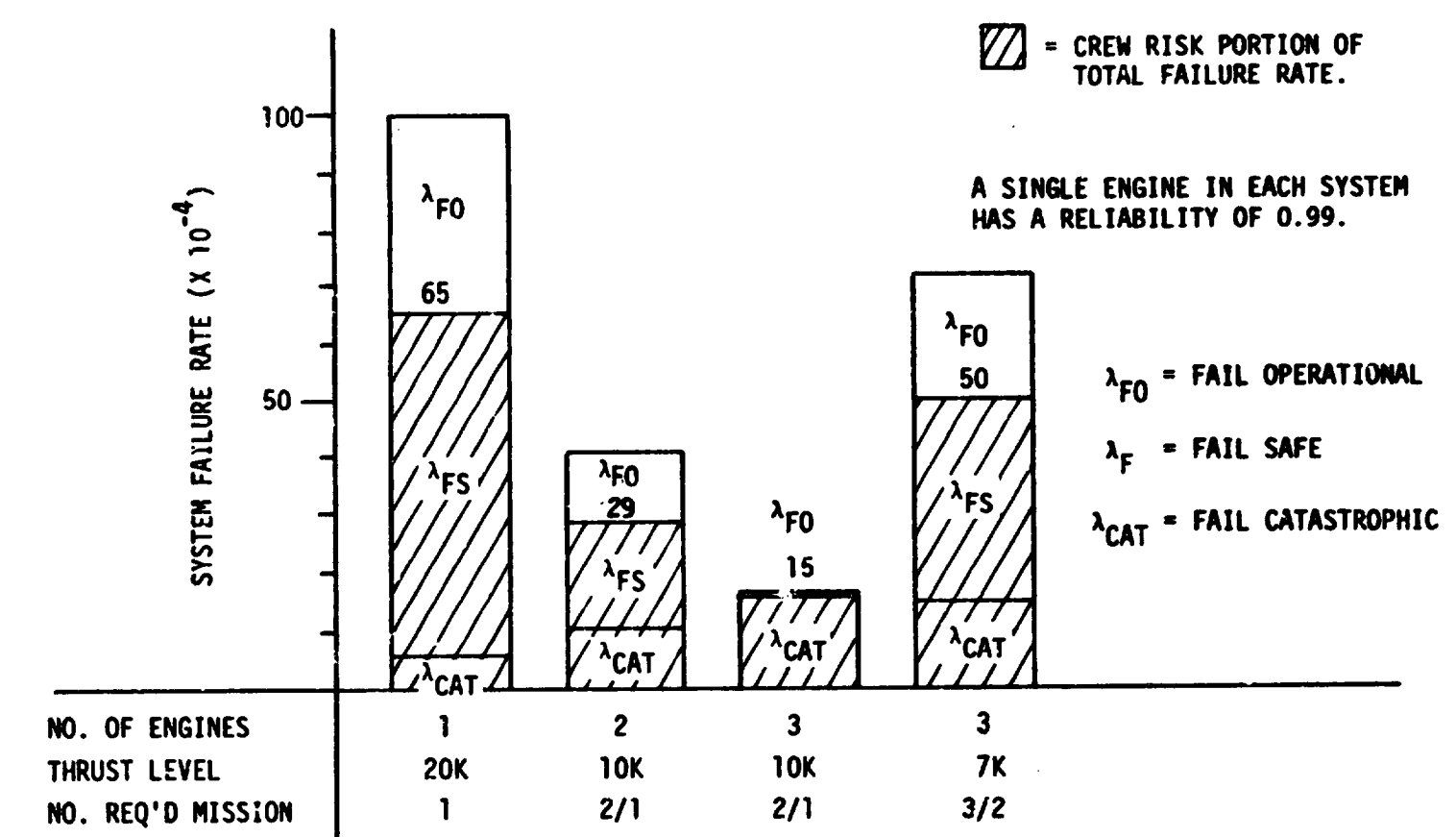

Figure 66. Failure Rate Comparison of Multi- Engine Systems

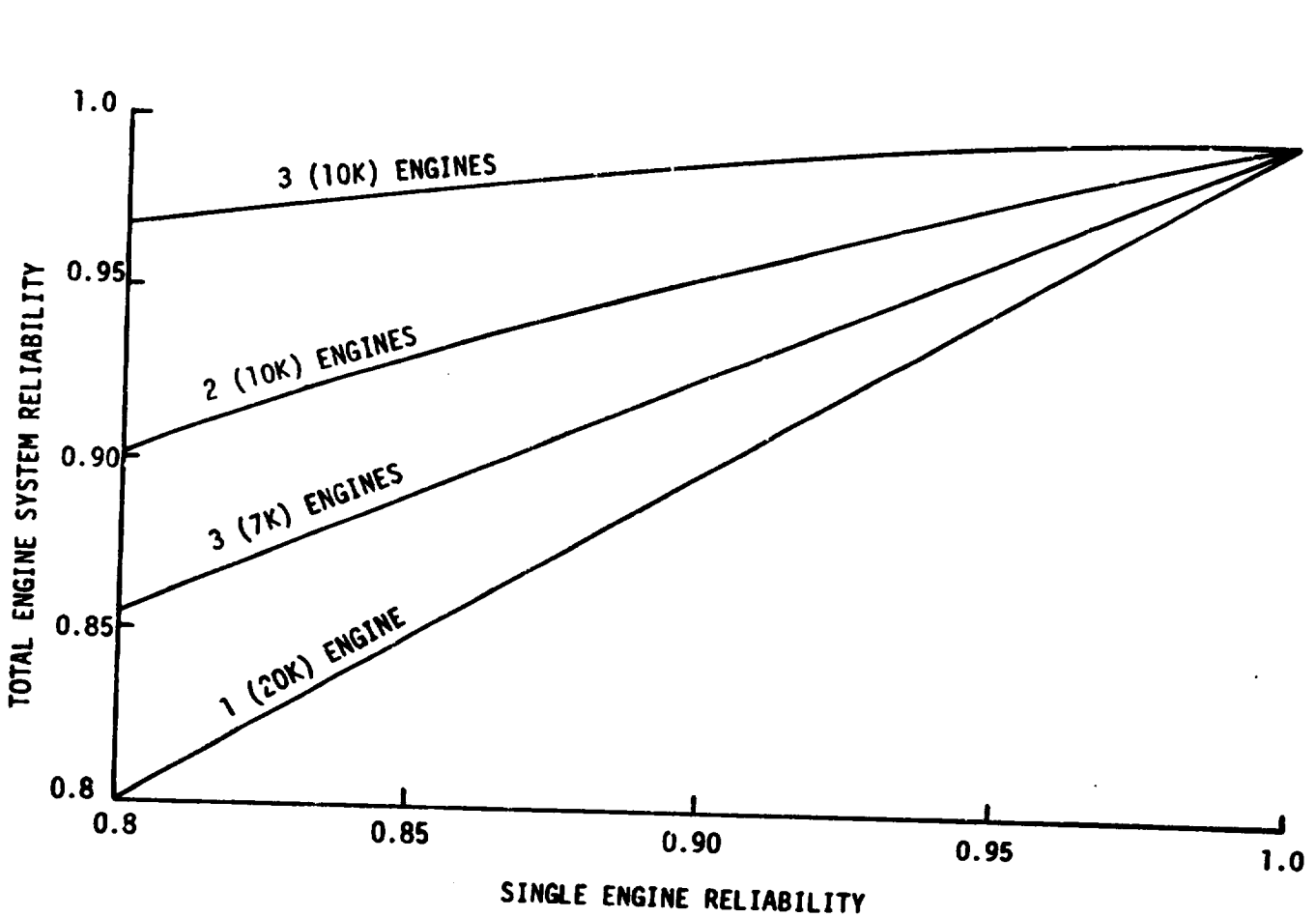

Figure 67. Engine System Reliability for Various Single Engine Reliabilities

# ENGINES IN SYSTEM	# ENGINES REQUIRED DURING MISSION	CREW RISK = CREW RISK GOAL	SINGLE ENGINE RELIABILITY NEEDED	ENGINE SYSTEM RELIABILITY OBTAINED
1 (20K)	1 ALL BURNS	2.5×10^{-4}	0.9996	0.9996
2 (10K)	2 FIRST BURN 1 SUBSEQUENT	2.5×10^{-4}	0.9993	0.9997
3 (10K)	2 FIRST BURN 1 SUBSEQUENT	2.5×10^{-4}	0.9983	0.99975
3 (7K)	3 FIRST BURN 2 SUBSEQUENT	2.5×10^{-4}	0.9995	0.99965

ASSUMPTIONS: 5 BURNS PER MISSION

5% OF THE SINGLE ENGINE λ DUE TO CATASTROPHIC FAILURE

60% OF THE SINGLE ENGINE λ WILL STRAND CREW

35% OF THE SINGLE ENGINE λ WILL NOT ENDANGER CREW LIFE

Figure 68. Meeting Crew Risk Requirements

V, A, Safety and Reliability Analyses (cont.)

b. Observations

- Multiple-engine installations are required to meet crew safety goals. The three 10K lbF engine system with complete engine-out capabilities meets both crew risk and system reliability requirements with the lowest single-engine reliability requirement. However, it is only slightly better than the twin-engine installation.

- The catastrophic portion of the failure rate is the big driver.

- The initial Phase A study results showed that the twin-engine installation was superior to the three engine system on a payload basis (~400 lb). In addition, engine maintenance and production costs were also shown to increase, with a slight decrease in DDT&E cost. Therefore, the twin engine installation appears to be the best compromise when all factors are considered.

- To further validate the results presented herein, the apportionment of the total failure rate used in the analyses should be verified with "hard" data.

- The engine should carry instrumentation that could detect impending failures and shut down the engine before catastrophic failures can occur.

V, A, Safety and Reliability Analyses (cont.)

3. Expander vs Staged-Combustion Cycle Engine

Using the previously discussed model, a comparison between expander cycle and staged-combustion cycle engines was made. ALRC's "Phase A OTV Engine Study Engine Requirements and Concept Selection Review" dated 24 October 1978 and presented at NASA/MSFC (see summary in Ref. 1), included a failure rate comparison at the component level. The analysis was simplified by omitting common and/or poorly characterized components which would not influence system selection. Specifically, a myraid of electrical/electronic purge/bleed/service lines and valves were omitted. Although these parts contribute greatly to maintenance cost, they usually represent less than 10% of the flight failure rate. In addition, the components would be similar for either cycle and thus had no bearing on this comparison.

Because the expander cycle is simpler, has less severe operating conditions, and fewer active component single point failures, the predicted failure rate for the expander cycle for both internally redundant and nonredundant configurations is lower than that for the staged-combustion cycle engine. In comparing both cycles, it was concluded that the expander cycle has a 33% lower failure rate than the staged-combustion engine. Adding redundant igniters, propellant valves, and electrical controls decreases the failure rate by 33% for each engine design.

Using these percentage differences and the reliability model, Figures 69 and 70 present a summary of the requirements for multi-engine system failure rates and associated crew risks. From these figures the following is apparent:

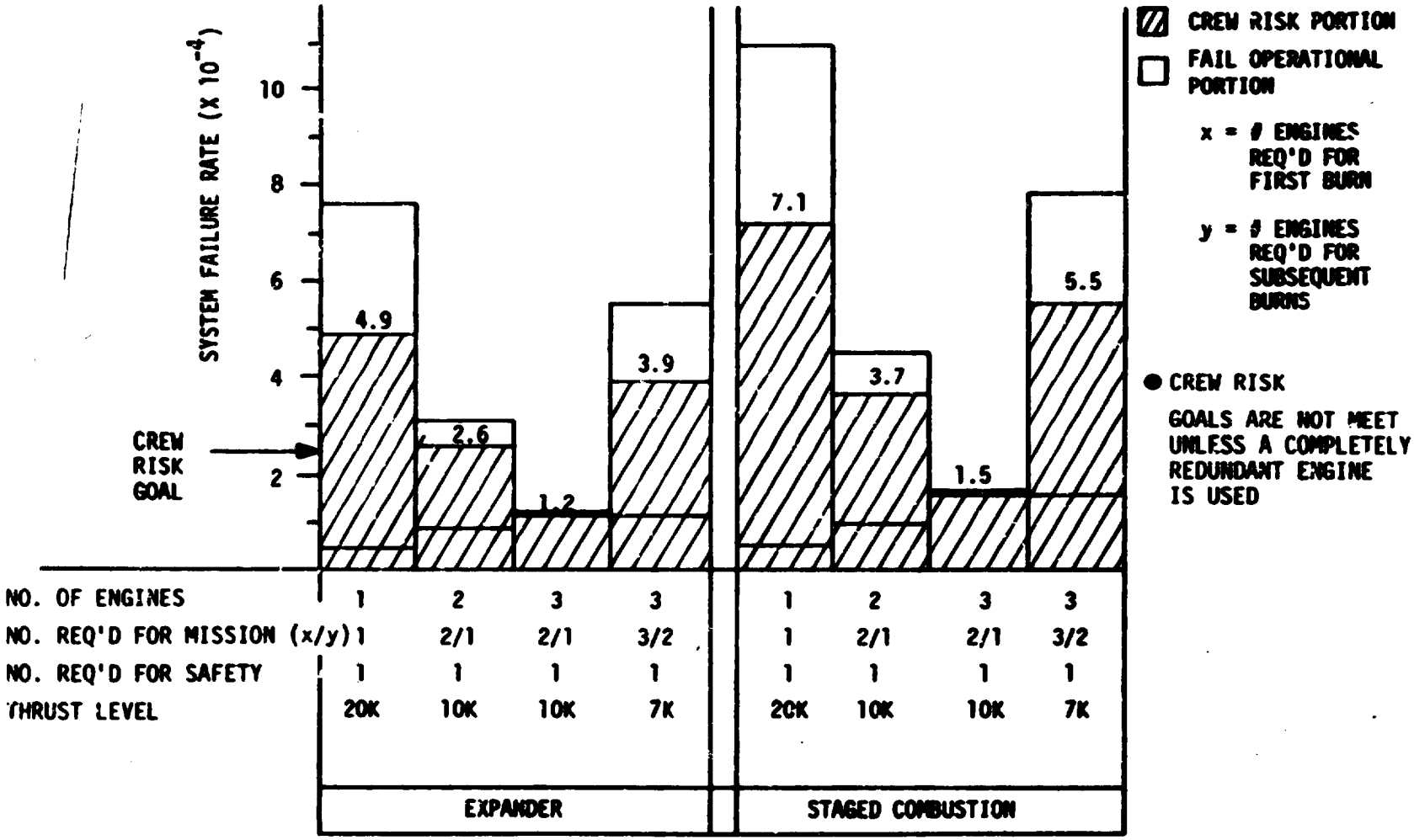

Figure 69. Engine Design Comparison With No Redundant Engine Components

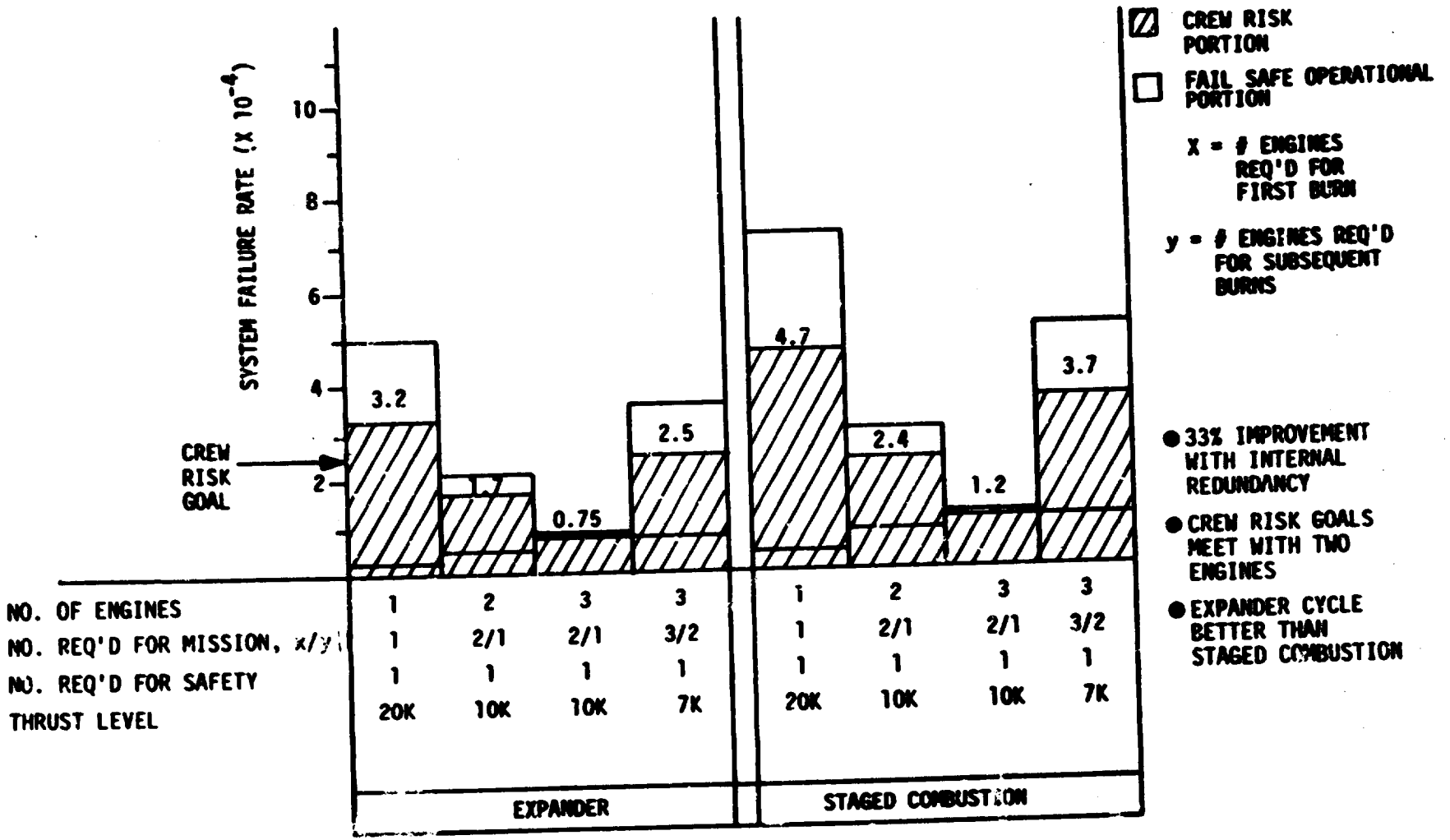

Figure 70. Engine Design Comparison Using Redundant Engine Components

V, A, Safety and Reliability Analyses (cont.)

a. A two 10K lbF engine system meets the crew safety requirement with internally redundant components. (The payload penalty for internally redundant components is much less than that imposed by a fully redundant engine.)

b. The three 10K lbF engine system, in which one engine is totally redundant, meets the 2.5×10^{-4} goal in every case. (However, there is a relatively large payload penalty for having a fully redundant engine.)

c. The three 7K lbF engine system is not as good as the twin 10K lbF engine installation.

d. In all cases, the expander cycle design has a lower failure rate and crew risk than the staged-combustion cycle.

4. Improving Engine System Reliability and Reducing Crew Risk

Throughout this discussion, engine system reliabilities of .99 or higher are shown to be required. These are state-of-the-art numbers. Historically, ALRC has achieved these numbers by utilizing the following techniques:

- Optimizing internal redundancy to eliminate single point failures as defined by the Failure Modes and Effects Analysis.

- Keeping the engine design simple. Engine complexity leads to more possible failures.

C-3

V. A. Safety and Reliability Analyses (cont.)

- Externally semi-redundant engines (multi-engine systems) provide engine-out capability in the event that one engine should fail. This lowers the change of stranding the crew and reduces the probability of a mission loss.

- Use of an integrated hazard control system that predicts when a catastrophic failure is about to occur and shuts down the problem engine before the vehicle, mission, and crew are lost. It must be noted that this type of so-called "smart" engine system is more practical in a multi-engine context because the remaining engine(s) can be used to return the crew to LEO or complete the mission. Shutting down a single engine would strand the crew in all cases, except when in the vicinity of the Orbiter.

- A crew override would correct a failure in the hazard control system. If a good engine is shut down, the crew should have the final decision on whether or not it should be restarted.

Combining all these factors -- internal and external redundancy, simplicity, hazard control system, and crew overirde, -- the high reliability and crew risk goals can be met.

Using these concepts along with effective testing during DDT&E, mistakes can be designed out inexpensively on paper rather than during production. An example of reaching higher reliabilities faster is shown in Figure 71. The ALRC philosophy on the OME-E program concentrated on "making the engine right the first time." A single-engine reliability

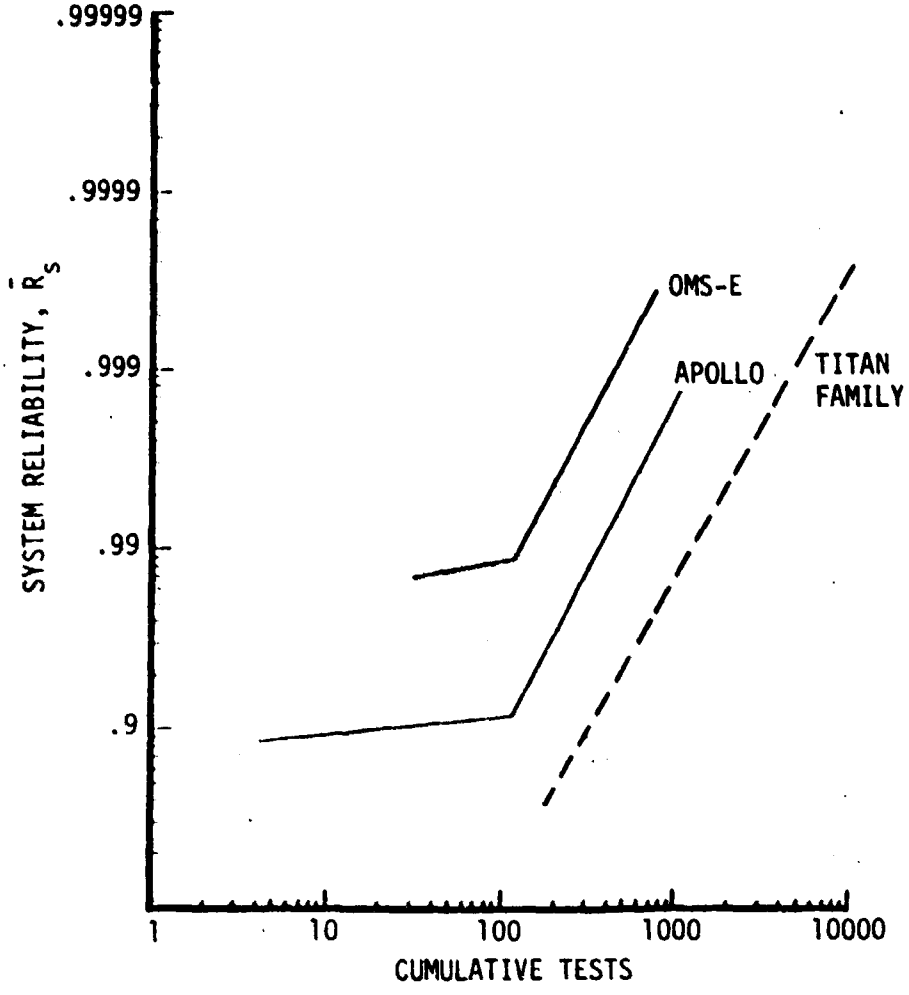

Figure 71. ALRC Engines Reliability History

of .9992 was reached after only 476 tests. In comparison with the Apollo program, OMS-E achieved an order of magnitude advancement in the reliability with the same amount of testing. It is believed that we can do at least this well with the expander cycle OTV engine.

5. Safety and Reliability Analyses Conclusions

As a result of this analysis, following conclusions have been reached:

- Quantifying crew risk and determining its acceptability is a value judgement. However, though a comparison of other career risks, 2.5×10^{-4} is a realistic goal to set for the OTV engine.

- The twin 10K lbF engine system seems to be a good compromise between all decision-making factors, e.g., weight, volume, crew risk, reliability, payload and cost.

- The three 7K lbF engine system has no advantages in terms of mission reliability, crew risk, payload, or life cycle cost.

- The complete engine-out feature of the three 10K lbF engine system makes it an attractive configuration when only minimum mission failure rate and crew risk are considered. However, payload and life cycle cost considerations do not favor this system.

V, A, Safety and Reliability Analyses (cont.)

- The single 20K lbF engine is impractical to meet crew risk requirements.
- The expander cycle engine is the best candidate considering crew risk, mission reliability, payload, and life cycle cost.
- To reach optimum engine design more efficiencly, the reliability and crew risk considerations must be introduced into the engine design during its inception.

B. DEVELOPMENT RISK COMPARISON

The objective of this subtask was to develop a comparison between the engine concepts detailed in the initial efforts on Contracts NAS 8-32996 (Ref. 5) and NAS 8-32999 (Ref. 1) for engine development risk. The development risk comparison is expressed in terms of the probability of achieving the schedules shown in the referenced studies and of attaining slipped and advanced versions of these schedules. In addition, schedule cost impacts are also addressed by utilizing NASA/MSFC normalized cost data. The approach to the study was to evaluate potential problems that might occur during the engine development program and to assess the impact of the occurrence of these problems upon both the DDT&E schedule and cost.

The engine concepts recommended were the staged-combustion and expander cycles (Contracts NAS 8-32996 and NAS 8-32999, respectively). The DDT&E schedule, presented in Ref. 5 for the staged-combustion cycle, is shown in Figure 72. The detailed DDT&E schedule, which was developed to the lowest work breakdown structure (WBS) element for the expander cycle

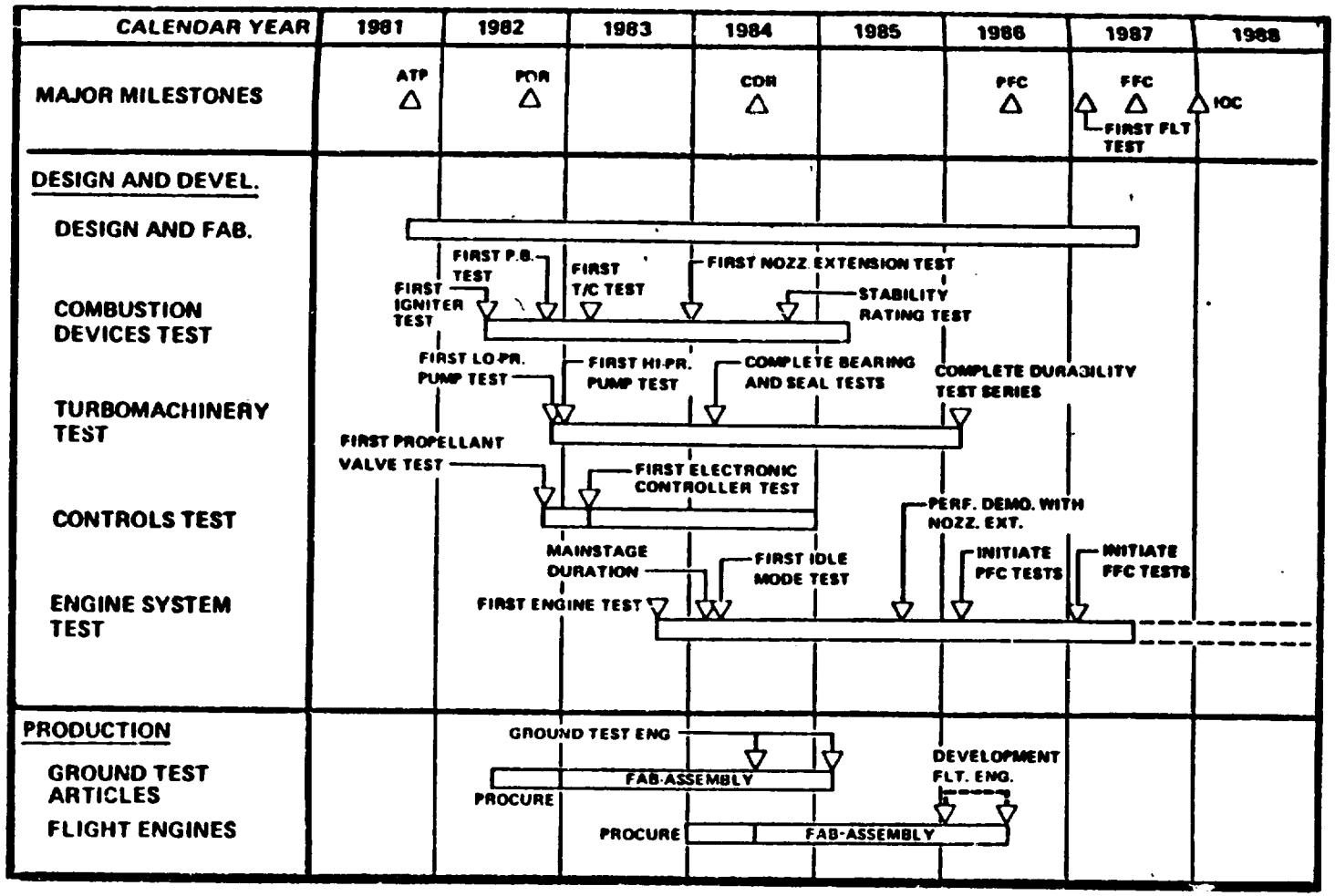

Ref: Orbit Transfer Vehicle Engine Study, Phase A, Final Report, Contract NAS 8-32996, Rocketdyne Division, Rockwell International, 9 July 1979.

Figure 72. Baseline OTV DDT&E Schedule, Staged-Combustion Cycle

engine in Ref. 1, is shown on Figure 73. The expander cycle engine schedule is 100% success-oriented, while ALRC programmatic analysis results indicated that the 5-3/4-year staged-combustion cycle engine program shown in Figure 72 is representative of a nominal schedule.

Because the expander cycle engine schedule was 100% success-oriented, nominal and stretched schedules were developed for this engine. Shorter and longer DDT&E schedules were established for the staged-combustion cycle engine. Schedule and cost variations were established by examining historical development problem areas and estimating their impact upon both schedule and cost on the basis of historical precedent. Short schedules are set up, assuming that no major problems will occur during the engine development program. Nominal schedules are set up, assuming that they can absorb an average number of problems, and can solve them in an average amount of time. Long schedules are set up on the assumption that all potential development problems will occur and provide for a sufficiencly large time frame to solve them satisfactorily.

The historical development problems considered, along with the schedule and cost impacts, are shown in Table XXXIV. This table was established by considering both program uncertainties and engine complexity. Engine complexity was assumed to be proportional to the square root of the component operating pressure levels. The schedule slips shown are those that might occur during component development if steps were not taken to anticipate key problems and preplanned courses of action taken to solve potential problem areas. Of course, the schedule slips are not additive because many problems would occur during parallel component development; for example, pacing elements, like a preburner in a staged-combustion cycle, can delay development of other components such as the thrust chamber and turbopump.

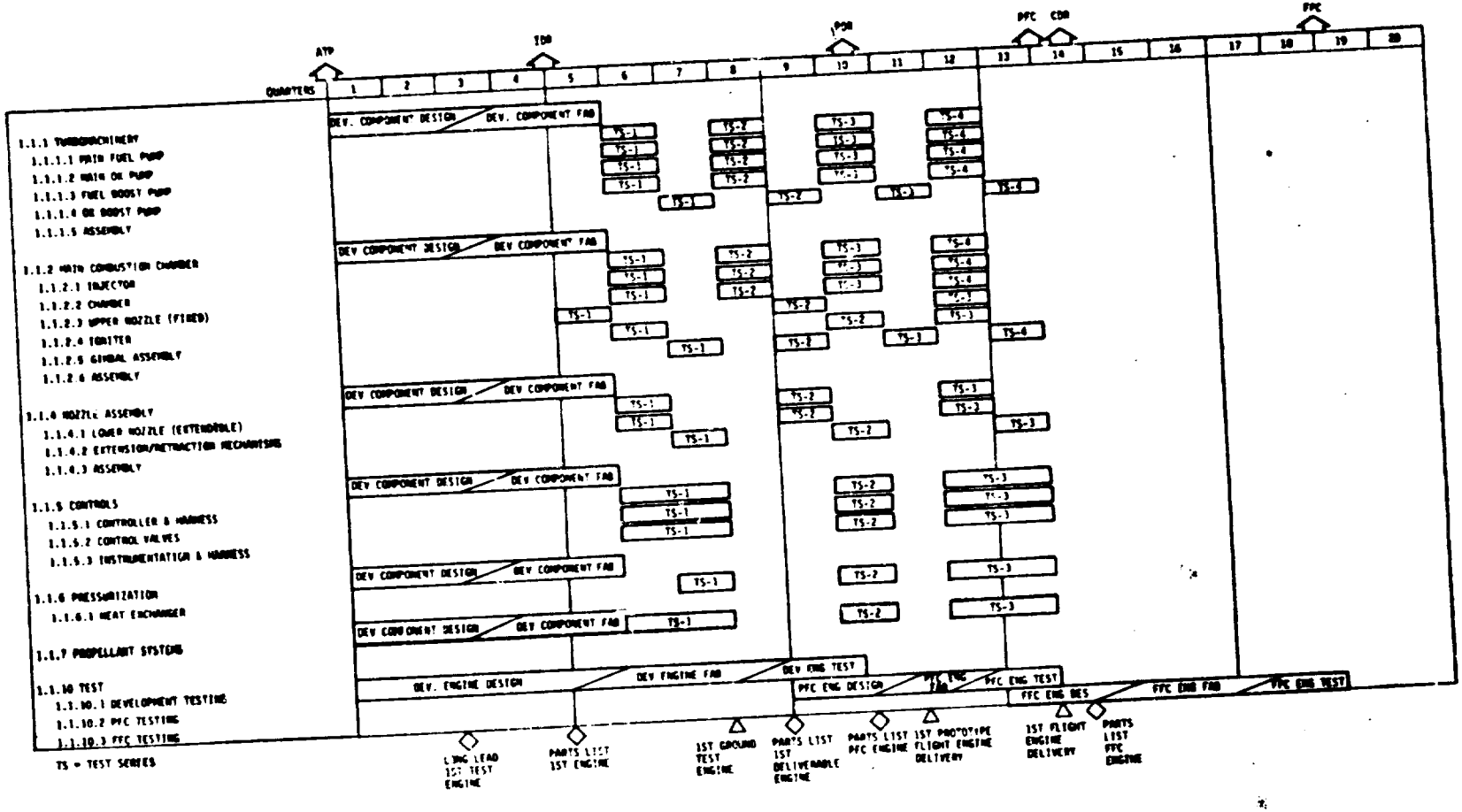

Ref: Orbit Transfer Vehicle (OTV) Engine Phase "A" Study, Final Report. Contract NAS 8-32999, ALRC, 29 June 1979.

Figure 73. Baseline OTV DDT&E Schedule, Advanced Expander Cycle

TABLE XXXIV

PROBLEM RECOVERY - DDT&E COST AND SCHEDULE IMPACT

PROBLEM	CYCLE	SCHEDULE SLIP MONTHS	COST INCREASE MILLION $	ASSUMED SOLUTION
PREBURNER STABILITY	STAGED COMBUSTION	8	34	RESONATOR RETUNE
	EXPANDER	0	0	
MAIN BURNER STABILITY	S.C.	8	20	RESONATOR RETUNE
	EXPANDER	8	12	
PREBURNER GAS UNIFORMITY	S.C.	10	42	INJECTOR REDESIGN
	EXPANDER	0	0	
MAIN BURNER LOW PERFORMANCE	S.C.	7	17	INJECTOR ELEMENT MODIFICATION
	EXPANDER	7	10	
LOW TURBINE POWER	S.C.	0	0	LONGER CHAMBER
	EXPANDER	9	14	
LOW TURBOPUMP EFFICIENCY	S.C.	10	19	REDESIGN IMPELLER
	EXPANDER	10	13	
CYCLE BALANCE LOW POWER	S.C.	17	44	REDESIGN PUMP
	EXPANDER	14	16	
TURBINE CYCLE LIFE	S.C.	17	44	REDESIGN TURBINE
	EXPANDER	0	0	
CHAMBER CYCLE LIFE	S.C.	21	43	NEW CHAMBER
	EXPANDER	21	24	
VALVE LEAKAGE	S.C.	7	11	REDESIGN SEALS
	EXPANDER	7	4	
ONE FAILURE:OTHER COMPONENTS	S.C.	17	21	APPROPRIATE SOLUTION
	EXPANDER	17	14	

V. B. Development Risk Comparison (cont.)

The schedule analysis resulted in the following program durations:

Schedule	DDT&E Program Duration, Years: Expander Cycle	Staged-Combustion Cycle
Short (Success-Oriented)	4.5	4.75
Nominal (Probable)	5.5	5.75
Long (Maximum)	7.0	8.25

Short, nominal, and long schedules are shown in Figure 74, 75, and 76 for the expander cycle engine and in Figures 77, 78, and 79 for the staged-combustion cycle engine. The format of figures obtained from the referenced studies has been modified slightly to provide a consistent comparison. An initial design review (IDR) is scheduled about the time major component development testing is to start. The preliminary design review (PDR) is assumed to be held upon the completion of the engine development tests. A critical design review (CDR) is assumed to be held immediately after the completion of the preflight certification (PFC) tests and before committing all final flight certification (FFC) hardware.

The cost risk associated with each schedule was calculated in the following manner. For the short schedules, the probable cost increase was computed as the square root of the sum of the individual cost uncertainties squared. The maximum cost increase was calculated as the sum of the individual cost uncertainties. The potential cost overrun estimates are shown in Table XXXV. The cost risk for the nominal schedules is the difference between the probable and maximum cost increases. The cost risk associated with the long schedule is assumed to be negligible.

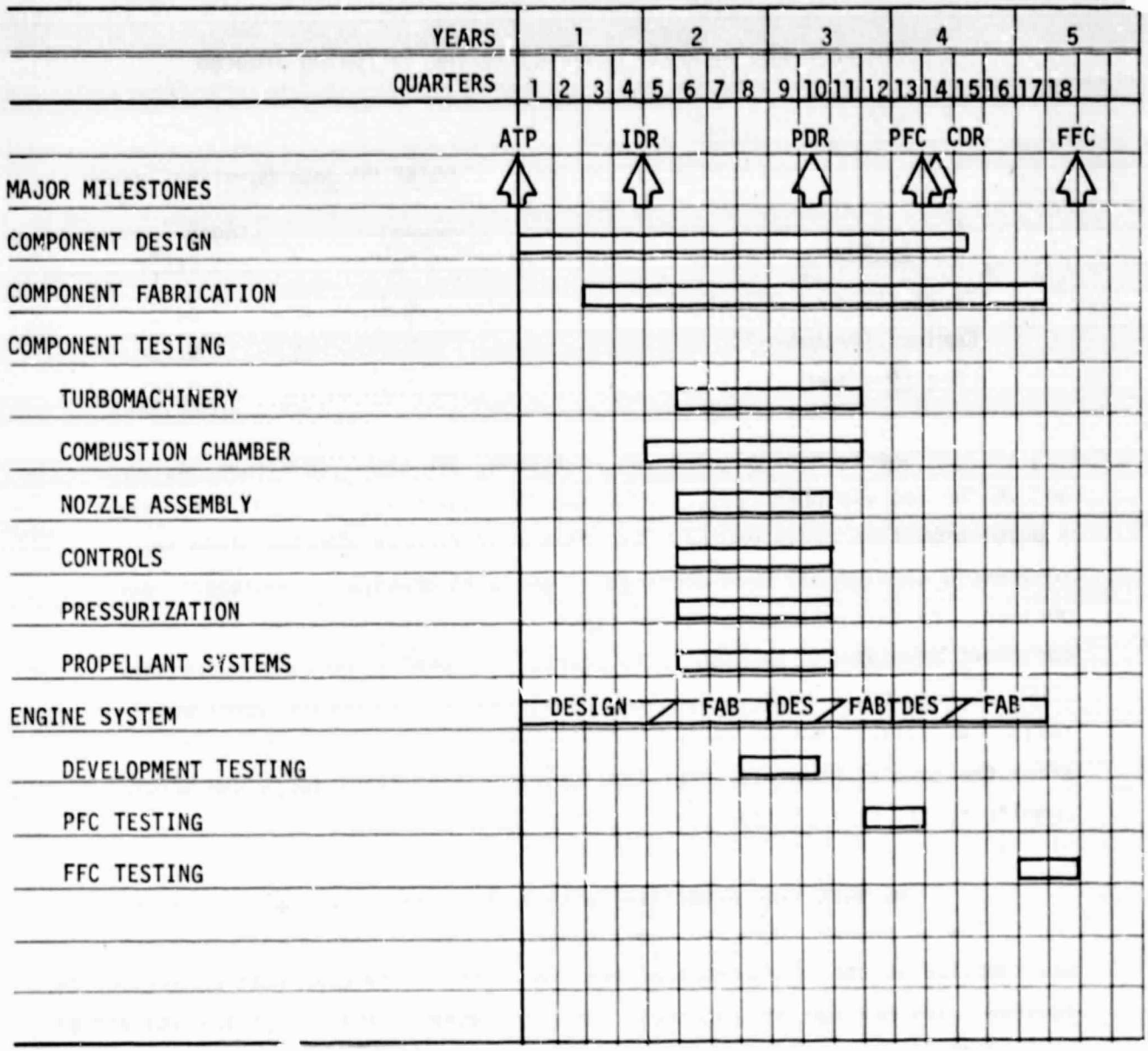

Figure 74. Advanced Expander Cycle Engine Short DDT&E Schedule (4.5 years)

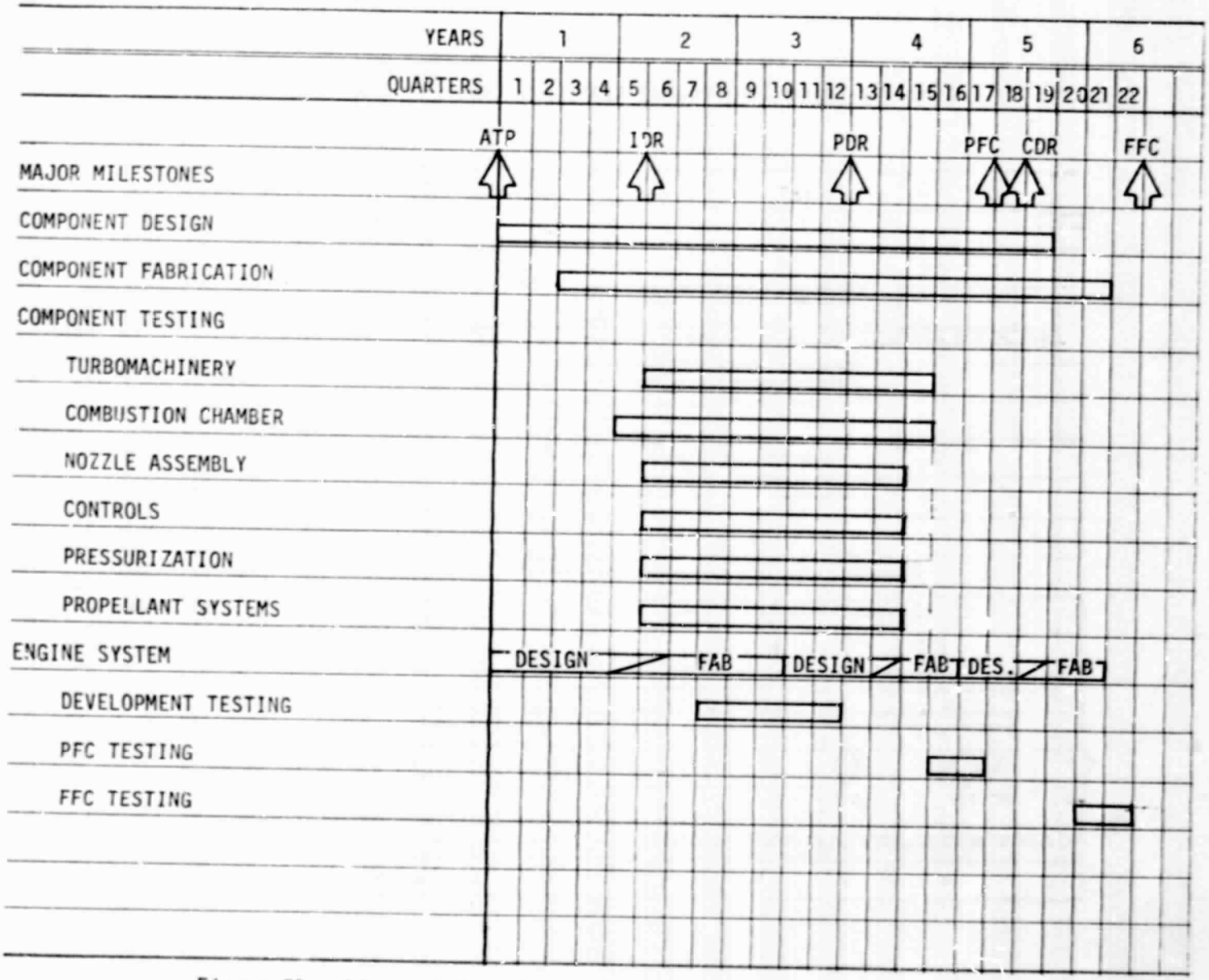

Figure 75. Advanced Expander Cycle Engine Nominal DDT&E Schedule (5.5 years)

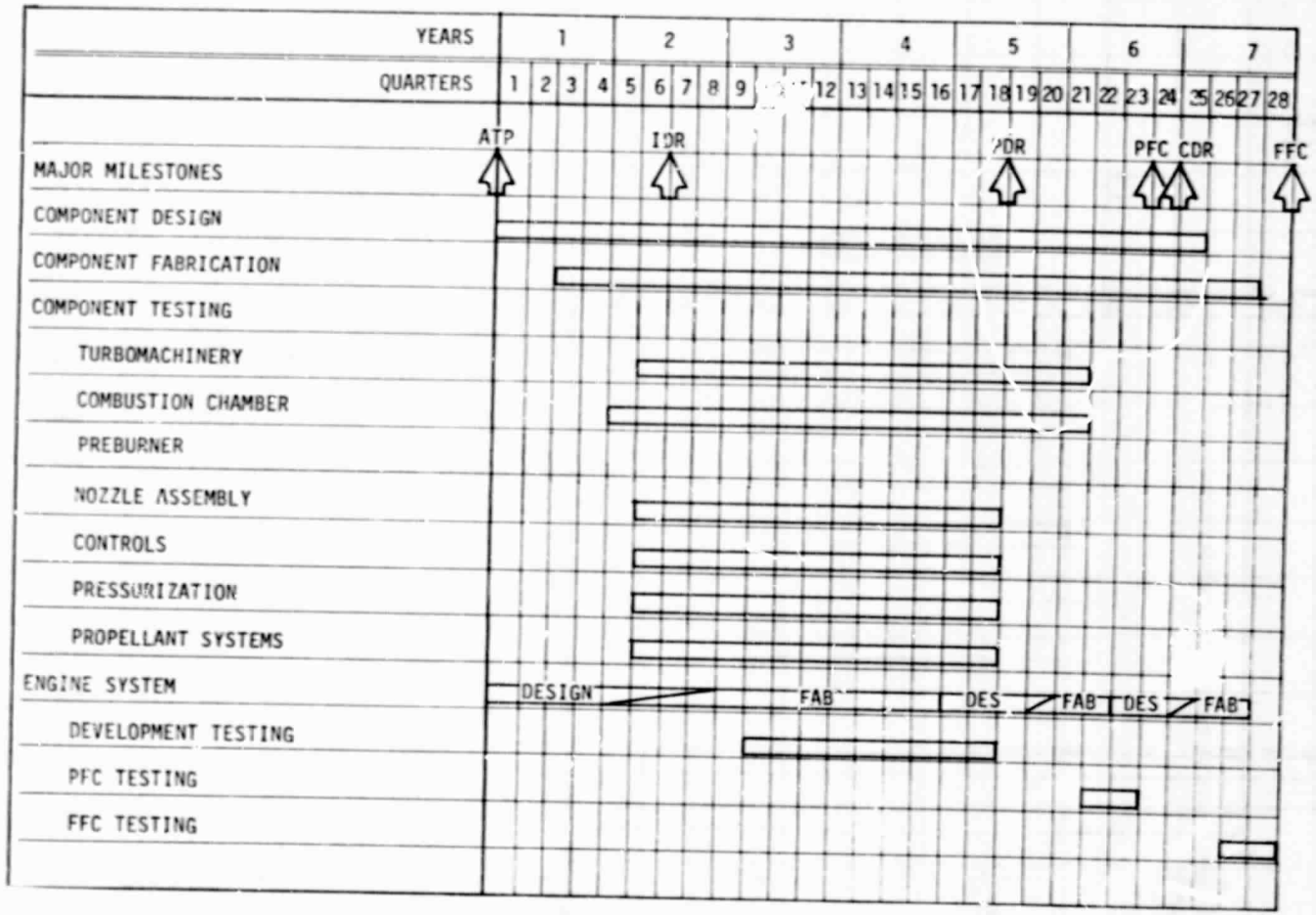

Figure 76. Advanced Expander Cycle Engine Long DDT&E Schedule (7.0 years)

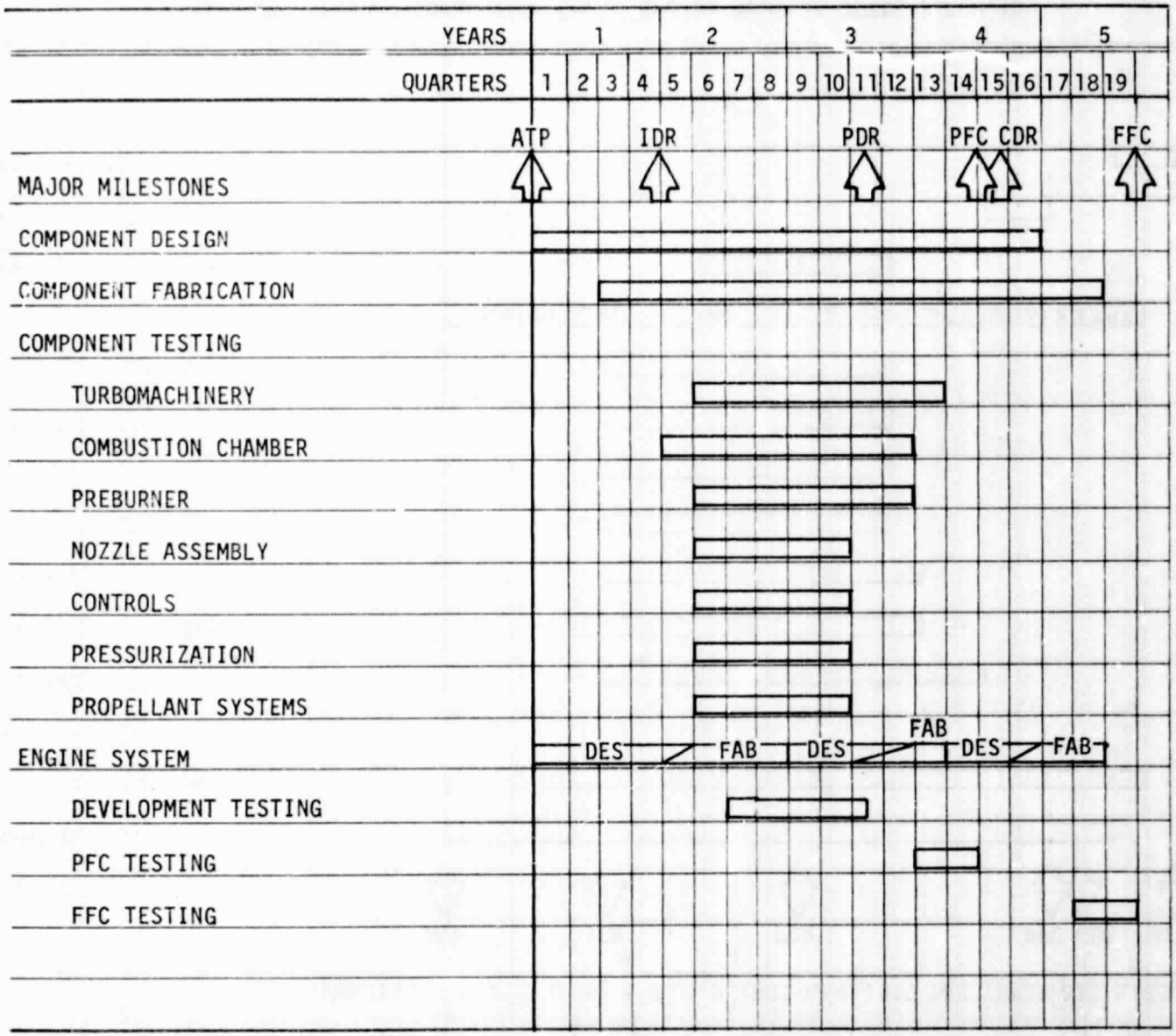

Figure 77. Staged-Combustion Cycle Engine Short DDT&E Schedule (4.75 years)

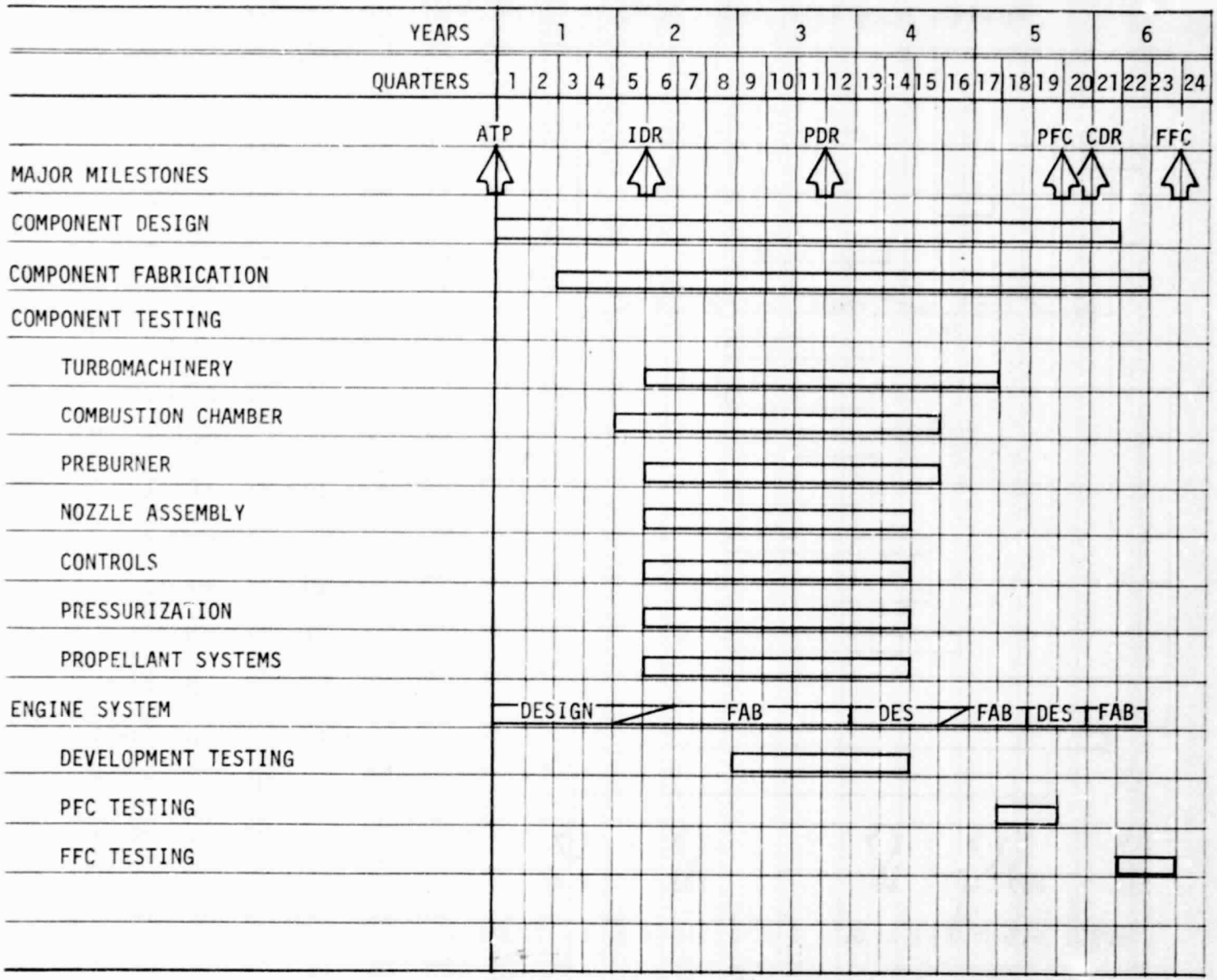

Figure 78. Staged-Combustion Cycle Engine Nominal DDT&E Schedule (5.75 years)

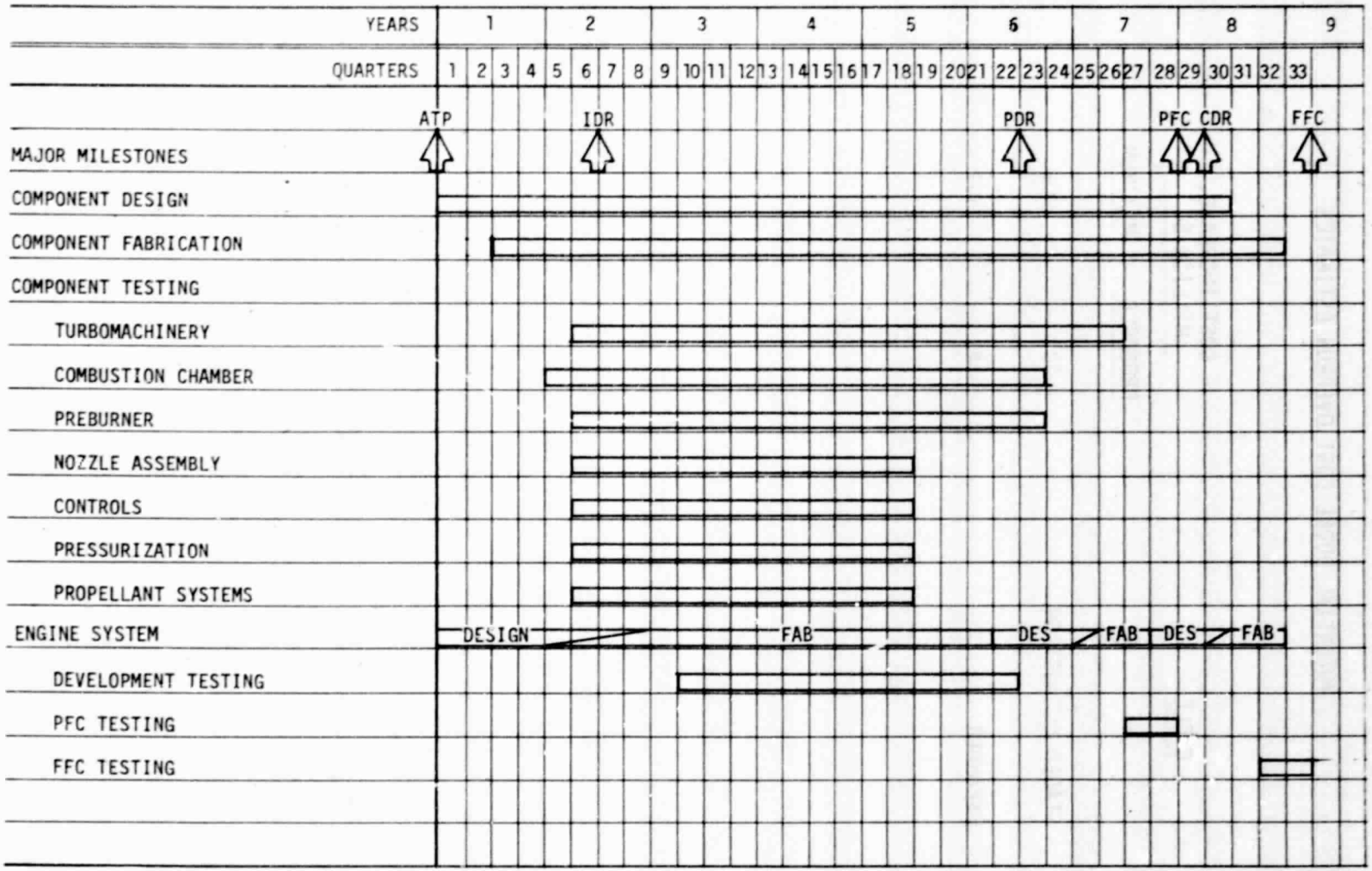

Figure 79. Staged-Combustion Cycle Engine Long DDT&E Schedule (8.25 years)

TABLE XXXV

POTENTIAL DDT&E COST OVERRUN ESTIMATES

CYCLE	COST INCREASE, MILLION $	
	PROBABLE	MAXIMUM
STAGED COMBUSTION	101	295
EXPANDER	41	107

V, B, Development Risk Comparison (cont.)

The development schedule and cost risk assessment for the 10K lbF engine is summarized in Table XXXVI. The planned DDT&E cost shown on the table for the short, success-oriented programs were obtained from NASA/MSFC-supplied normalized parametric engine cost data for Contracts NAS 8-32996, - 32999, and - 33444. The costs for the nominal and long schedules were determined by maintaining the short schedule manloading over the extended program durations. Compared to the short program, this results in increased costs, but reduced cost risk. For example, the nominal expander cycle engine program cost is estimated to be $269M compared to a probable cost of $289M for the short program. That is, the unplanned surprise schedule increases will cost more.

The data on Table XXXVI also show that both schedule and cost risk are greater with a staged-combustion cycle engine. This is primarily due to the additional combustion device (preburner) and increased system interactions. Using a nominal program as a baseline, the schedule risk with a staged-combustion cycle engine is one year greater and the cost risk is almost 3 times greater than with an expander cycle engine. The probable DDT&E cost of a staged-combustion cycle engine is approximately 75% more than for the expander cycle engine.

TABLE XXXVI

DEVELOPMENT RISK ASSESSMENT

ENGINE THRUST = 10K lb

ENGINE CYCLE	PLANNED SCHEDULE	PLANNED DDT&E DURATION, YEARS	SCHEDULE RISK, YEARS	POTENTIAL DDT&E DURATION, YEARS	MINIMUM PLANNED DDT&E COST, (4) M $	DDT&E COST RISK, M $	POTENTIAL DDT&E COST, M $
EXPANDER	SHORT (1)	4.5	1.0 to 2.5	5.5 to 7.0	248	41.0 to 107.0	289 to 355
	NOMINAL (2)	5.5	1.5	7.0	269	66.0	335
	LONG (3)	7.0	---	7.0	314	---	---
STAGED COMBUSTION	SHORT (1)	4.75	1.0 to 3.5	5.75 to 8.25	342	101.0 to 295.0	443 to 637
	NOMINAL (2)	5.75	2.50	8.25	394	194.0	588
	LONG (3)	8.25	---	8.25	524	---	---

(1)Assumes 100% success-oriented program.
(2)Program planned to handle an average number of development problems.
(3)Program planned to handle all potential development problems.
(4)NASA/MSFC supplied normalized cost data.

VI. TASK IV: COST AND PLANNING COMPARISON

The objectives of this task were to provide cost and planning information and data on a 20K lbF staged-combustion cycle engine for comparison with the data provided for an advanced expander cycle engine during the initial Phase A OTV study efforts (Refs. 1 and 6). The following subtasks were conducted:

- Establish a Work Breakdown Structure (WBS)
- Programmatic Analysis and Planning
- Cost Estimates (see Ref. 3)

The WBS established for use in making the cost estimates was structured in concert with NASA/MSFC during the initial Phase A efforts. The major program elements are summarized in Figure 80. The WBS first level is the OTV main engine. The second WBS levels are DDT&E (Design, Development, Test and Evaluation), Production, and Operations.

The WBS for the staged-combustion cycle engine is shown in Table XXXVII. Cost estimates were made to the fourth WBS level, summarized to the third level and spread over the program duration to the second level. The same WBS structure was used for the advanced expander engine cycle candidate, except for DDT&E item 1.1.3 (preburner) which does not apply for this type engine. This WBS provides a consistent set of guidelines for cost estimation on each engine concept. The staged-combustion cycle and expander cycle engine cost estimates are presented in References 3 and 6, respectively.

The engine DDT&E schedules and the development risk assessments were shown and discussed previously in Section V,B.

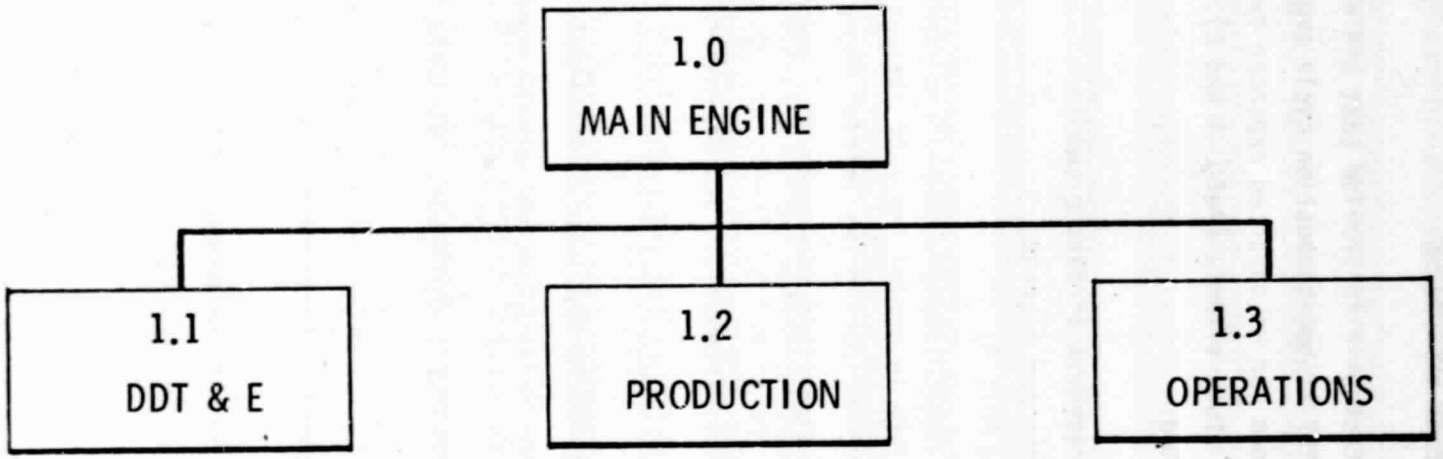

Figure 80. Work Breakdown Structure (WBS) Summary

TABLE XXXVII

WORK BREAKDOWN STRUCTURE (WBS)

1.0	Main Engine
1.1	DDT&E
1.1.1	Turbomachinery
1.1.1.1	Main Fuel Pump
1.1.1.2	Main Oxidizer Pump
1.1.1.3	Fuel Boost Pump
1.1.1.4	Oxidizer Boost Pump
1.1.1.5	Assembly and Checkout
1.1.2	Main Combustion Chamber
1.1.2.1	Injector
1.1.2.2	Chamber
1.1.2.3	Upper Nozzle (fixed)
1.1.2.4	Igniter
1.1.2.5	Gimbal Assembly
1.1.2.6	Assembly and Checkout
1.1.3	Preburner
1.1.3.1	Injector
1.1.3.2	Combustor
1.1.3.3	Igniter
1.1.3.4	Assembly and Checkout
1.1.4	Nozzle Assembly
1.1.4.1	Lower Nozzle (Extendible)
1.1.4.2	Extension/Retraction Mechanisms
1.1.4.3	Assembly and Checkout
1.1.5	Controls
1.1.5.1	Engine Controller and Electrical Harness
1.1.5.2	Control Valves
1.1.5.3	Instrumentation and Electrical Harness
1.1.5.4	Assembly and Checkout
1.1.6	Pressurization
1.1.6.1	Heat Exchangers
1.1.6.2	Assembly and Checkout
1.1.7	Propellant Systems
1.1.7.1	Feed, Fill, Vent, Abort Dump, and Drain
1.1.7.2	Assembly and Checkout

TABLE XXXVII (cont.)

1.1.8	Initial Tooling
1.1.9	Ground Support Equipment
1.1.9.1	Handling and Protective Equipment
1.1.9.2	Checkout and Maintenance Equipment
1.1.9.3	Assembly and Checkout
1.1.10	Test
1.1.10.1	Development Testing
1.1.10.2	PFC Testing
1.1.10.3	FFC Testing
1.1.11	System Engineering and Integration
1.1.11.1	Integration of DDT&E Activities
1.1.11.2	Engine Assembly and Checkout
1.1.11.3	Engine/Vehicle Interface
1.1.12	Project Management
1.1.13	Facilities
1.1.14	Consumables
1.2	Production
1.2.1	Main Engines
1.2.1.1	Turbomachinery
1.2.1.2	Combustion Devices
1.2.1.3	Controls
1.2.1.4	Pressurization
1.2.1.5	Propellant Systems
1.2.1.6	Engine Assembly
1.2.2	Initial Spares
1.2.3	Facility Maintenance
1.2.3.1	Manufacturing and Test Facilities
1.2.3.2	Sustaining Tooling
1.2.3.3	GSE
1.2.4	Sustaining Engineering
1.2.5	Project Management
1.2.6	Consumables

TABLE XXXVII (cont.)

1.3	Operations
1.3.1	Inplant Support
1.3.2	Field Support
1.3.2.1	Launch Support
1.3.2.2	Flight Support
1.3.2.3	Refurbishment and Maintenance
1.3.2.4	Checkout
1.3.3	Major Engine Overhaul
1.3.4	Facility Maintenance
1.3.5	Follow-on Spares
1.3.6	Project Management
1.3.7	Consumables

VI, Task IV: Cost and Planning Comparison (cont.)

The staged-combustion cycle engine DDT&E test program was set up to obtain an engine reliability in excess of .999 (see Section V,A). The estimated engine and component test requirements are shown in Table XXXVIII. The hardware required to support the DDT&E program was also estimated and is shown on Table XXXIX. Compared to an expander cycle engine, additional testing and hardware are required for the preburner, preburner/combustion chamber, and preburner/turbopump tests and evaluations. For ease of comparison, the test plan and hardware requirements have been set up to be consistent with the format presented in Reference 1 on the expander cycle engine.

The preliminary cost estimate for activation and modification of existing ALRC facilties to test the OTV engine and components is 5M calendar year 1979 dollars.

Engine production schedules were set up to support both the AMOTV and APOTV mission models shown in NASA TMX-73394 (Ref. 2). The production run is based upon a two-engine vehicle as recommended by the safety and reliability analyses. A total quantity of 44 engines (22 sets) was established for the AMOTV mission model. This includes the delivery of 2 prototype engines (1 set), 2 preflight certification engines (1 set), 4 flight qualification engines (2 sets), and 36 engines (18 sets) to support the operations phase. The APOTV mission model requires more engine deliveries. 12 additional engines (6 sets) are required to support the operations phase for a total quantity of 56 engines (26 sets). The production schedule is shown in Reference 3.

The deliverable item summary for the staged-combustion cycle engine is summarized in Table XL. Numbers are cross-referenced to the WBS. This

TABLE XXXVIII

STAGED-COMBUSTION CYCLE ENGINE
DDT&E TEST PLAN

		No. of Tests	Total
1.1.1	Turbomachinery		500
1.1.1.1	Main Fuel Pump	100	
1.1.1.2	Main Ox. Pump	100	
1.1.1.3	Fuel Boost Pump	50	
1.1.1.4	Oxidizer Boost Pump	50	
1.1.1.5	Assembly	200	
1.1.2	Main Combustion Chamber		750
1.1.2.1	Injector	250	
1.1.2.2	Chamber	150	
1.1.2.3	Upper Nozzle (Fixed)	50	
1.1.2.4	Igniter	150	
1.1.2.5	Gimbal Assembly	50	
1.1.2.6	Assembly	100	
1.1.3	Preburner		500
1.1.3.1	Injector	200	
1.1.3.2	Combustor	100	
1.1.3.3	Igniter	100	
1.1.3.4	Assembly	100	
1.1.4	Nozzle Assembly		150
1.1.4.1	Lower Nozzle (Extendible)	50	
1.1.4.2	Extension/Retraction Mechanisms	50	
1.1.4.3	Assembly	50	
1.1.5	Controls		500
1.1.5.1	Controller and Harness	200	
1.1.5.2	Control Valves	200	
1.1.5.3	Instrumentation and Harness	100	
1.1.6	Pressurization		100
1.1.6.1	Heat Exchangers	100	
1.1.7	Propellant Systems	50	50
1.1.10	Engine Assembly		600
1.1.10.1	Development	450	
1.1.10.2	PFC	50	
1.1.10.3	FFC	100	

TABLE XXXIX

STAGED-COMBUSTION CYCLE ENGINE DDT&E HARDWARE REQUIREMENTS

Components	Number
Main Fuel Pumps	12
Main Oxidizer Pumps	12
Fuel Boost Pumps	10
Oxidizer Boost Pumps	10
Injectors	26
Combustion Chambers	14
Upper Nozzles (Fixed)	10
Igniters	14
Gimbal Assemblies	8
Preburners	14
Lower Nozzles	10
Extension/Retraction Mechanisms	10
Controllers and Harness	8
Control Valves (sets)	10
Instrumentation and Harness	8
Heat Exchangers	8
Propellant Systems	10
Engines	
Development Engines	9(1)
PFC Engines	4
FFC Engines	4

(1) Assumes 50 starts per engine.

TABLE XL

DELIVERABLE ITEM SUMMARY

Rocket Engine Assembly

- 1.1.1 Turbomachinery
- 1.1.2 Main Combustion Chamber
- 1.1.3 Preburner
- 1.1.5.2 Control Valves
- 1.1.6.1 Heat Exchangers
- 1.1.7 Propellant Systems

Nozzle Assembly

- 1.1.4.1 Lower Nozzle (Extendible)
- 1.1.4.2 Extension/Retraction Mechanisms

Engine Controller and Electrical Harness (1.1.5.1)

Instrumentation and Electrical Harness (1.1.5.3)

Handling and Protective Equipment

Checkout and Maintenance Equipment

Technical Manuals (OTV Engine Procedures)

deliverable item summary is patterned after the Titan III. The engine hardware on this list would be assigned a configuration item identification (CII) number, a configuration item specification number, a part number, and a group of serial numbers for all items delivered during production. This identification is outlined on Table XLI. A strawman of a specification "tree" for the deliverable items and major subcomponents is shown in Figure 81.

For purposes of the cost estimate, the operations phase of the program was assumed to be 10 years long. A postflight maintenance and refurbishment philosophy was presented in Reference 1 for the engine and is summarized in Reference 3. The philosophy and time frames were originally structured for an advanced expander cycle engine, but are the same for the staged-combustion cycle.

TABLE XLI

CONFIGURATION ITEM IDENTIFICATION(1)

OTV Engine AJ23-XXX

Contract NAS 8-XXXXX

Description	CII No.	CII Spec.	Part Number	Serial Numbers
Rocket Engine Assembly	TBD	TBD	XXXX TBD	0000001 through 00000XX
Nozzle Assembly	TBD	TBD	XXXX TBD	0000001 through 00000XX
Engine Controller and Electrical Harness	TBD	TBD	XXXX TBD	0000001 through 00000XX
Instrumentation and Electrical Harness	TBD	TBD	XXXX TBD	0000001 through 00000XX

(1) Deliverable Hardware

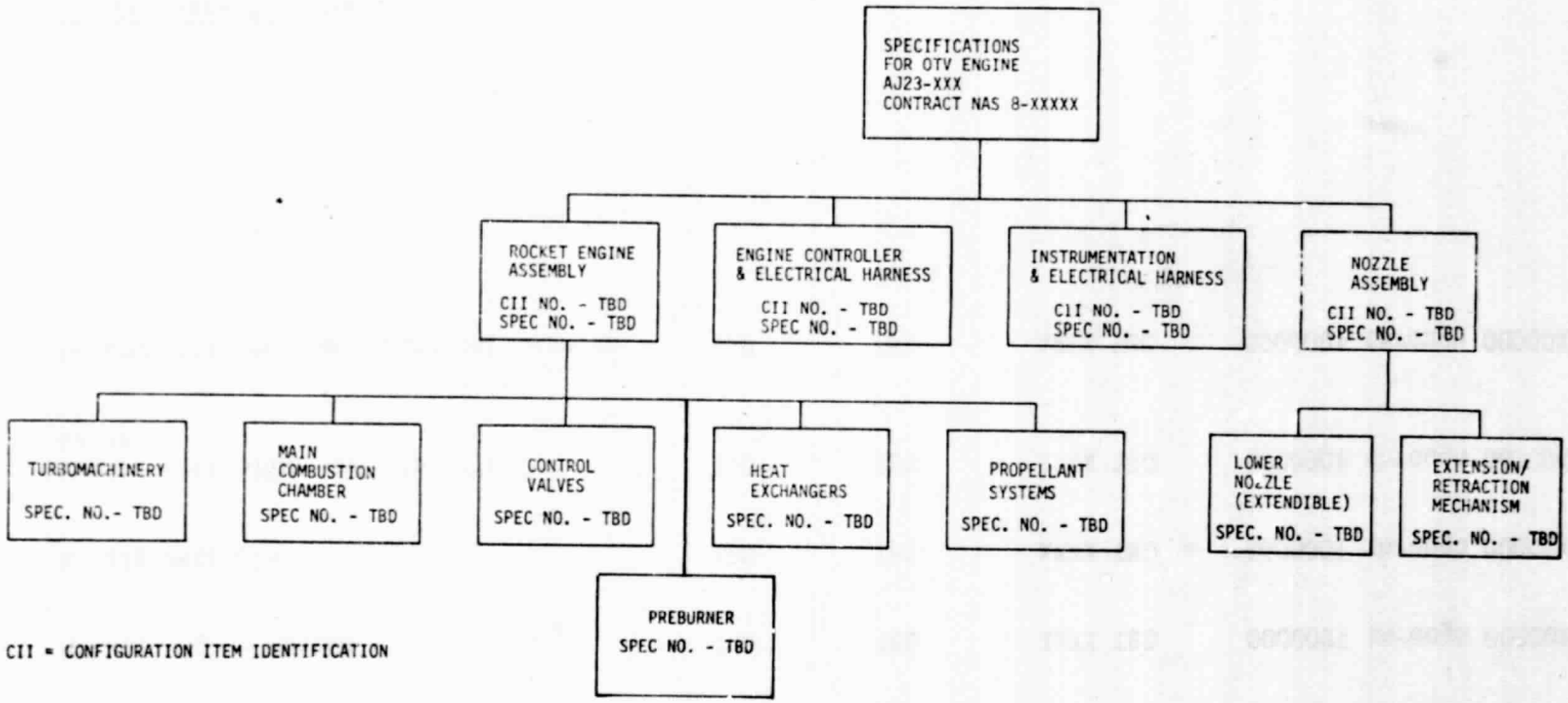

Figure 81. Preliminary Specification "Tree"

VII. TASK V: VEHICLE SYSTEMS STUDIES SUPPORT

The objective of this task was to provide support to the Orbit Transfer Vehicle System Studies contractors, Boeing and General Dynamics/ Convair, in interpreting and applying the Phase A engine study data.

A. UPDATED PARAMETERIC DATA

The engine parametric data pesented in Reference 1 was discussed at an engine/vehicle coordination meeting held at NASA/MSFC on 3 October 1979. At this meeting, it was agreed that all engine contractors should adjust the delivered specific impulse data to match the ASE experimental data reported in Reference 18. Consequently, the boundary layer loss prediction of the simplified JANNAF performance procedures was modified to match a delivered performance of 478 sec at a thrust level of 20K lb, 2000 psia chamber pressure, 400:1 area ratio, and a thrust chamber mixture ratio of 6.34:1. Figures 82 through 85 were transmitted to NASA/MSFC and the vehicle contractors to replace Figures 71, 75, 85, and 86 of Reference 1. The modified performance values are approximately 5 secs higher than those originally reported, Obviously, more high area ratio nozzle experimental performance data are required to verify prediction models.

B. ENGINE/VEHICLE CONTRACTOR MEETINGS AND DISCUSSIONS

During the course of this engine study, ALRC supported various system study reviews and coordination meetings held at NASA/MSFC. These meetings are summarized in Table XLII. As noted by the table, a special man-rating briefing was prepared and presented at the January 1980 review. This briefing covered our engine safety and reliability philosophy. (See Section V,A).

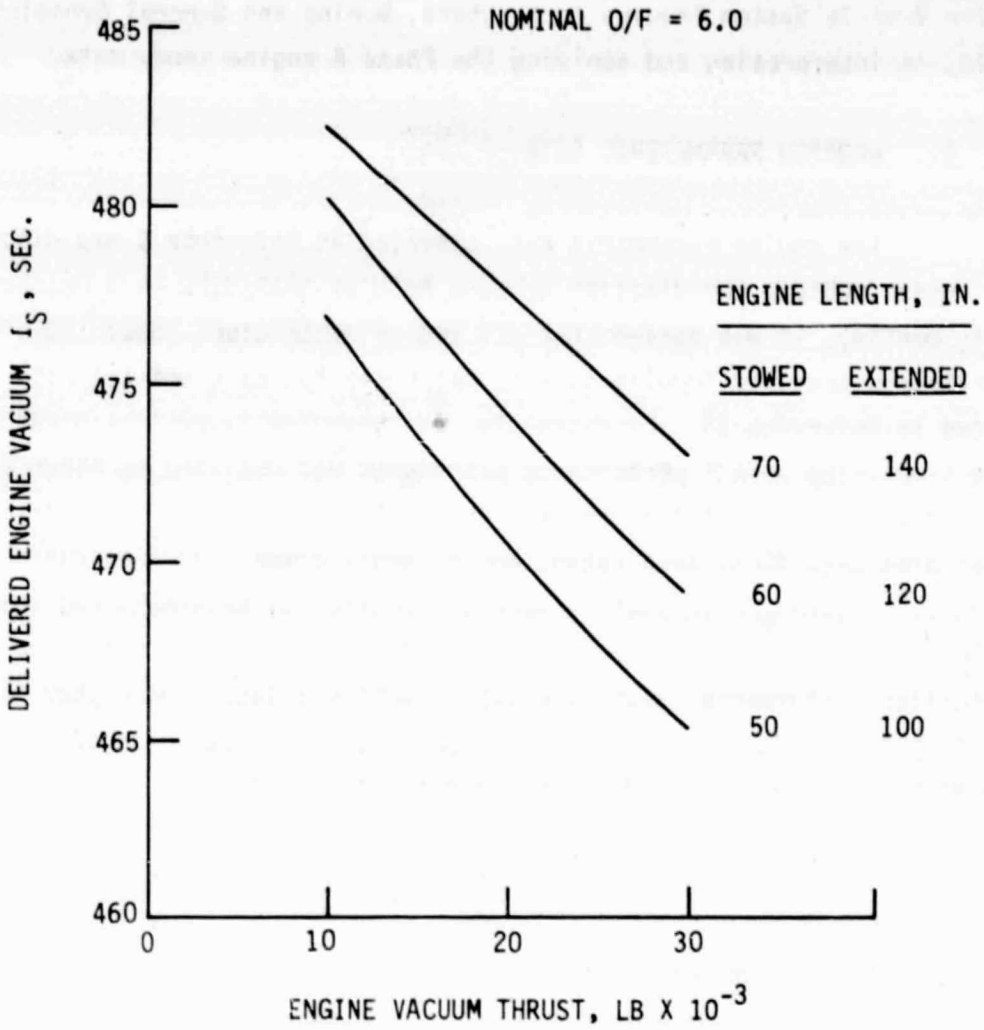

Figure 82. Advanced Expander Cycle Engine Performance Variations With Rated Thrust

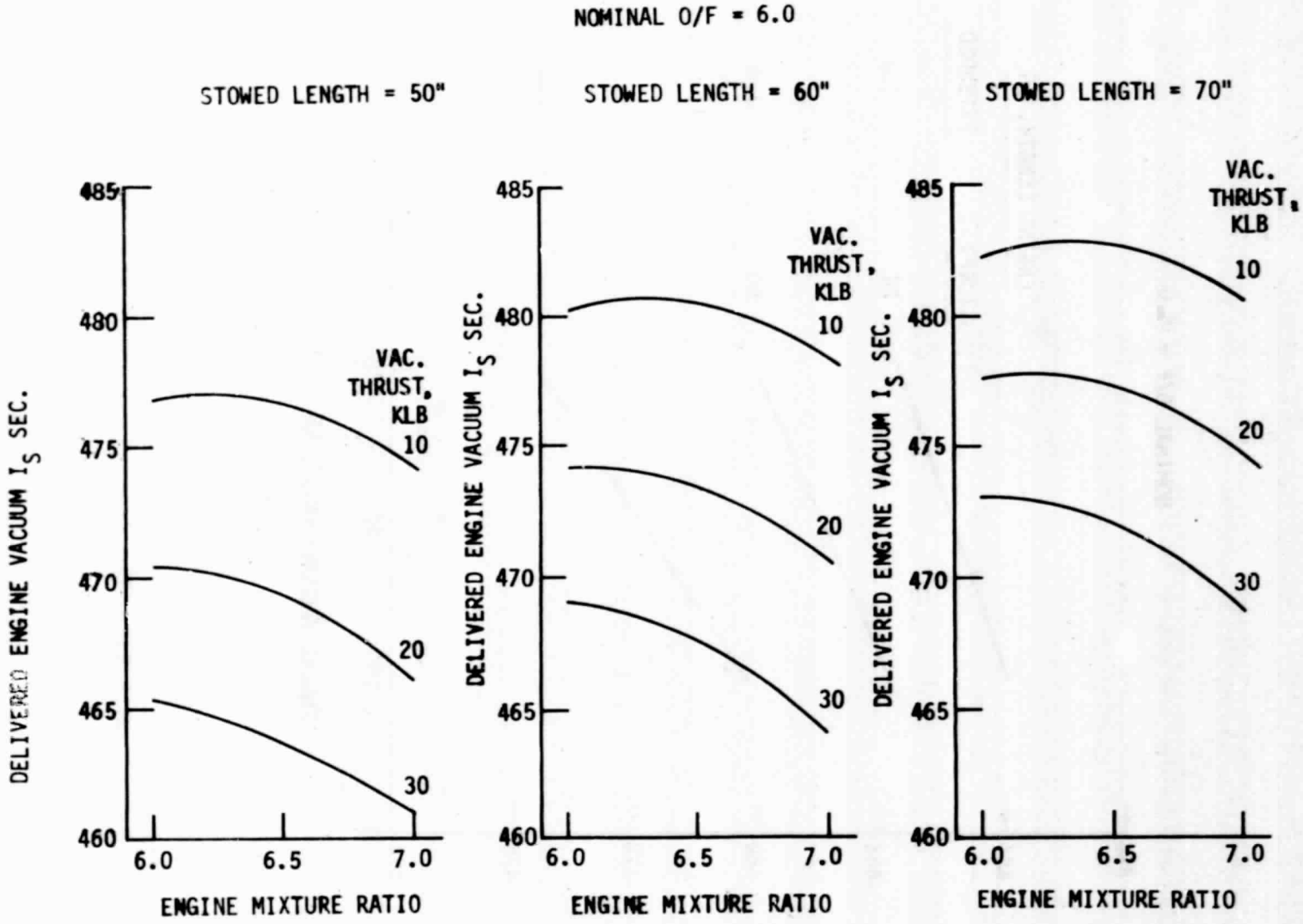

Figure 83. Advanced Expander Cycle Engine Performance at Design and Off-Design O/F

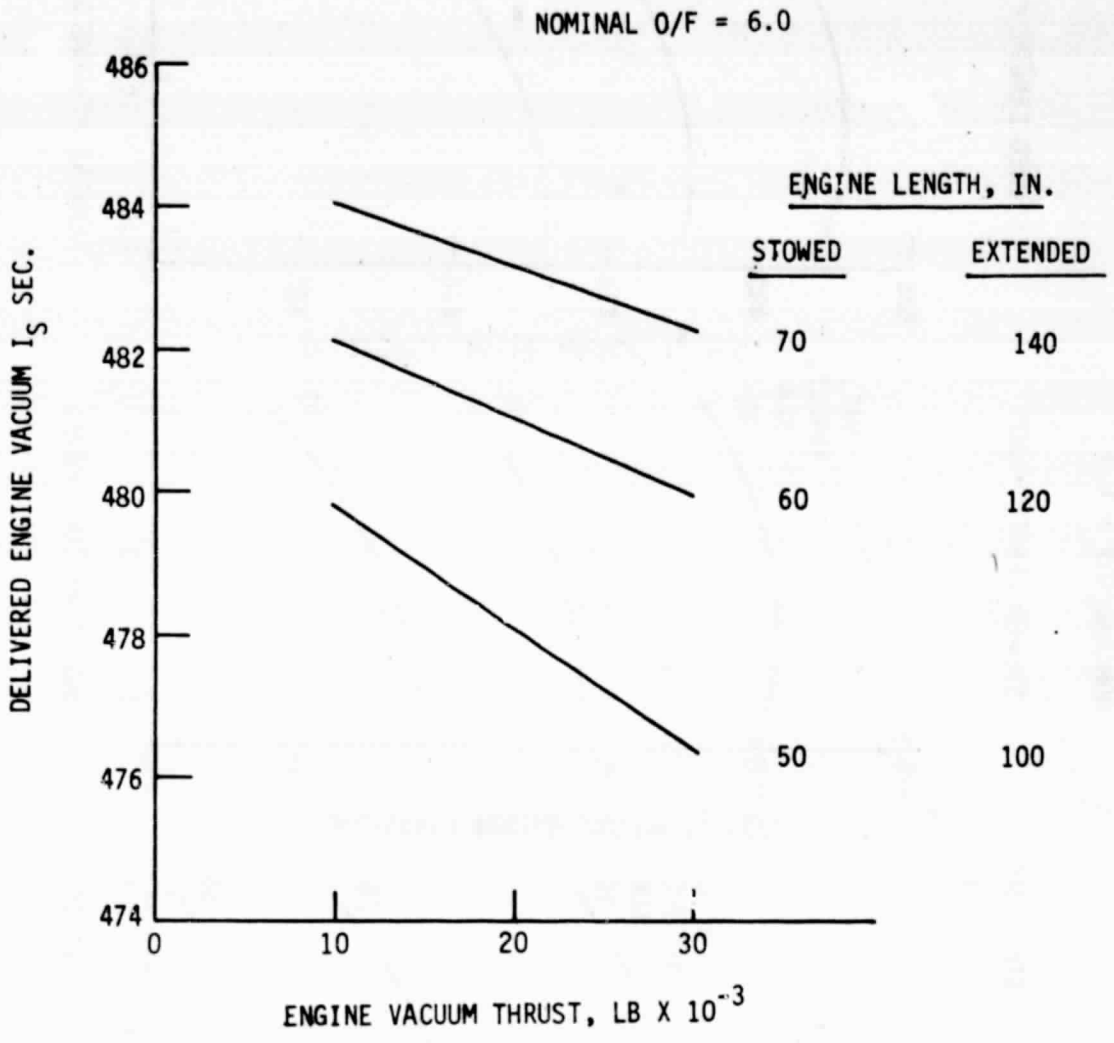

Figure 84. Staged-Combustion Cycle Engine Performance Variations With Rated Thrust

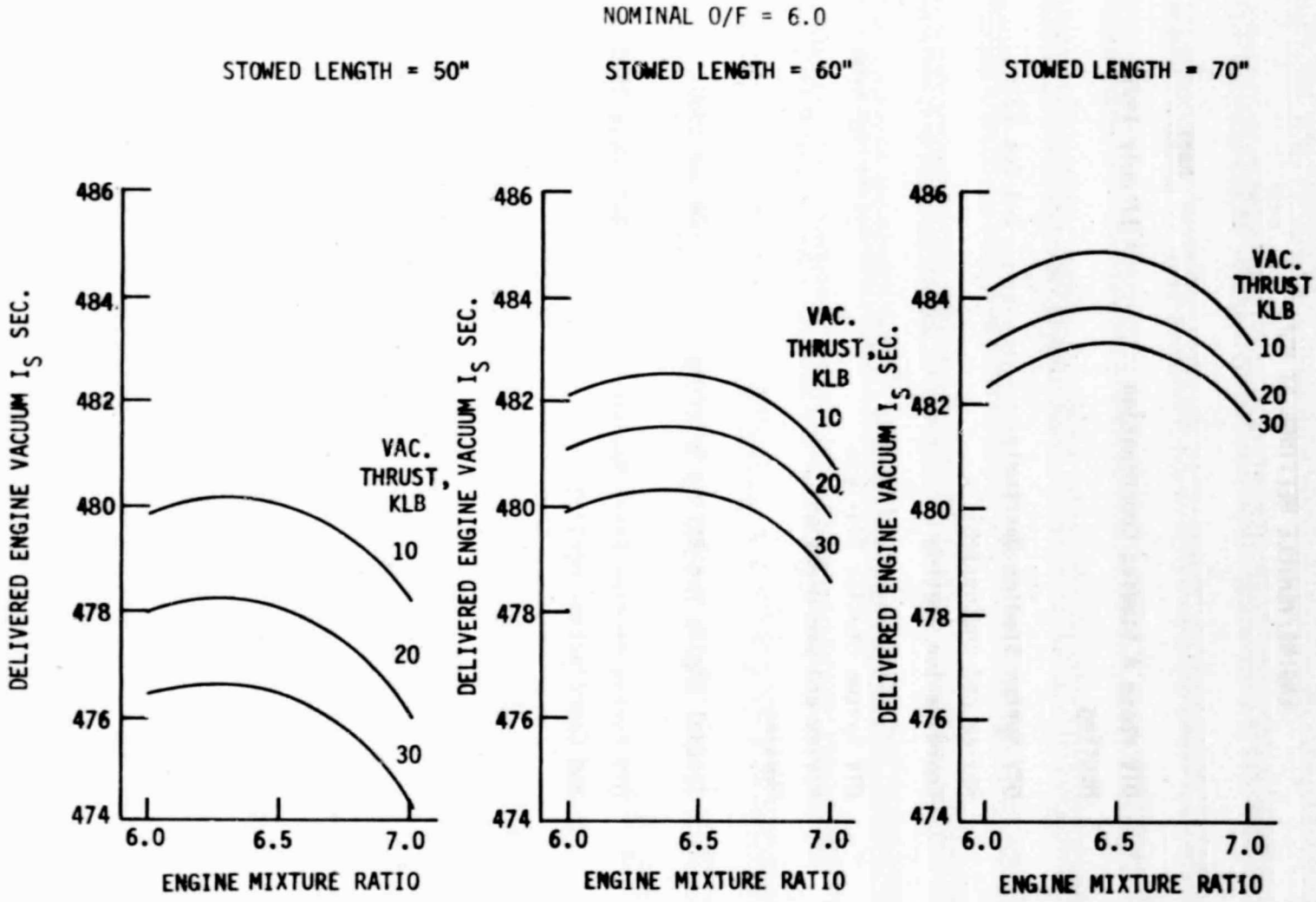

Figure 85. Staged-Combustion Cycle Engine Performance at Design and Off-Design O/F

TABLE XLII

ENGINE/VEHICLE MEETINGS AT MSFC

	DATE
° OTV Phase A Studies Coordination Meeting	17 July 1979
° OTV System Studies Quarterly Review and Engine/Vehicle Coordination Meeting	2-3 Oct 1979
° OTV System Studies Mid-Term Review and Coordination Meeting	22-23 Jan 1980
° Special Engine Man-Rating Briefing	24 Jan 1980
° OTV System Studies Final Review and Coordination Meeting	8-9 July 1980

VII, B, Engine/Vehicle Contractor Meetings and Discussions (cont.)

In addition to the formal meetings and reviews, the ALRC program manager made several informal contacts with personnel from both vehicle contractors. These contacts were made for the purpose of data dissemination and clarification. These contacts are summarized in Table XLIII.

TABLE XLIII

ENGINE/VEHICLE CONTRACTOR DISCUSSIONS

- 3 TRIPS TO CONVAIR / GENERAL DYNAMICS DURING PHASE A
- 3 TRIPS TO BOEING DURING PHASE A
- NUMEROUS TELCONS WITH:

  V. CALUORI, BOEING PROGRAM MGR.

  H. WHIPPO, BOEING PROPULSION ENGINEER

  D. HEALD, GENERAL DYNAMICS PROGRAM MGR.

  W. KETCHUM, GENERAL DYNAMICS PROPULSION ENGINEER

VIII. CONCLUSIONS AND RECOMMENDATIONS

A. CONCLUSIONS

The conclusions obtained from the results of this study extension are discussed herein and are summarized in Table XLIV. They were derived from the results of all study extension tasks undertaken. These results have clearly displayed the benefits of an advanced expander cycle engine for use on the OTV.

No engine system in existence today can fully meet the man-rating, life and high performance requirements of the OTV engine. This study has shown that of the new reusable, high-performance engine candidates considered for the OTV application, the advanced expander cycle engine is the best choice for arriving at such an engine system. The numerous benefits of this engine cycle make it the lowest risk and lowest cost option and establish it as a prime candidate for future optimization of the OTV engine.

A series turbine drive cycle, a combustion chamber length of 18 in., and a chamber contraction ratio of 3.66 were shown to be optimum for an advanced expander cycle engine. This optimization was performed for a maximum engine length with the extendible nozzle in the stowed position of 60 inches. These results could change if shorter stowed engine lengths were required.

The addition of a regenerator to the engine cycle to increase the turbine inlet temperature did not pay off substantially. However, a regenerator is a good backup in case chamber heat transfer and/or turbomachinery efficiencies are not as good as analytically predicted.

TABLE XLIV

CONCLUSIONS

- A NEW ENGINE IS REQUIRED TO MEET THE PERFORMANCE, MAN-RATING, AND LIFE REQUIREMENTS
- BASELINE THE SERIES TURBINE ADVANCED EXPANDER CYCLE FOR FUTURE EFFORTS
- REGENERATOR PROVIDES GOOD BACKUP CAPABILITY
- OPERATION OF 15K ENGINE DOWN TO 10% OF RATED THRUST APPEARS FEASIBLE
- EXPERIMENTAL VERIFICATION OF LOW-THRUST OPERATION IS REQUIRED
- EXPANDER CYCLE ENGINES OFFER LOWER CREW RISK THAN STAGED-COMBUSTION CYCLE
- A MINIMUM OF TWO ENGINES IS REQUIRED TO MEET CREW RISK GOALS
- TWIN ENGINES PROVIDE ACCEPTABLE MISSION RELIABILITY
- EXPANDER CYCLE ENGINE DEVELOPMENT RISK IS LESS THAN THAT FOR STAGED COMBUSTION CYCLE
- EXPANDER CYCLE ENGINE COSTS ARE LESS THAN THOSE FOR STAGED COMBUSTION CYCLE
- THE ADVANCED EXPANDER CYCLE ENGINE IS A HIGH-PERFORMANCE, LOW-RISK, LOW-COST OPTION

VIII, A, Conclusions (cont.)

The operation of an engine with a rated vacuum thrust level of 15K lb at 1.5K lbF appear to be feasible, provided that the following "kits" are added to the engine:

- Smaller oxidizer injection elements.
- Main oxygen pump recirculation line and valve.
- Combustion chamber coolant jacket outlet orifice.

These "kits" provide a dedicated low-thrust capability rather than the capability of operating at both high and low thrust on the same mission. Experimental verification of the low thrust operation and performance is required.

The reliability and safety analyses established a need for a twin-engine installation because a single engine cannot provide a tolerable man-safety profile. These analyses also showed that expander cycle engines are better than staged-combustion cycles because they reduce the crew risk and increase the mission reliability. The failure rate of an expander cycle engine was predicted to be approximately 33% lower than that of a staged-combustion cycle. Selective redundancy of critical engine components such as igniters, main propellant valves, and electrical controls will also decrease the engine failure rate of an engine candidate by about 33% and enhance the crew safety.

The development risk assessments of the expander and staged-combustion cycles showed that both DDT&E schedule and cost risks are greater with the staged-combustion cycle. This is primarily due to the additional combustion device (preburner) and increased system interactions in the staged-combustion cycle. Turbines in a staged-combustion cycle must

operate at steady state at high temperature and are subject to severe temperature extremes from cryogenic to 1800°R or greater during startup, steady-state, and shutdown. In contrast, the turbines of an expander cycle operate in a very benign temperature environment ranging from cryogenic to room temperature and do not experience the thermal shocks of staged-combustion cycle turbines. This all relates to the staged-combustion cycle engine having a schedule risk one year greater and a cost risk almost three (3) times greater than that of the expander cycle engine.

The DDT&E, production, and operations cost analysis results reported in Volume III (Ref. 3) show that the estimated costs for an expander cycle engine are less than those of a staged-combustion cycle in every program phase. These costs are approximately 50% greater in DDT&E, 28% greater in production, and 10% more in operations than the expander cycle costs. The expander cycle costs are lower because (1) the elimination of a preburner lowers DDT&E costs and (2) fewer components result in lower production costs and follow-on spares costs in operations.

B. RECOMMENDATIONS

This study extension and its predecessor (Ref. 1) have shown that a new advanced expander cycle engine is the best choice for the manned OTV. Therefore, technology programs should be pursued to bring this engine into being and place it in the space propulsion inventory. The recommendations are summarized in Table XLV.

Critical component technologies on the expander cycle engine should be conducted prior to entering into a breadboard engine experimental program. This will establish the technology base at a level at which

TABLE XLV

RECOMMENDATIONS

- Expander Cycle Engine Component Critical Technology Programs Should Be Initiated To:
  - Reduce Risk
  - Verify Power Balance
  - Verify Performance
- Component Technology Should Address High & Low Thrust Operation
- Continue Point Design Studies to Optimize The Advanced Expander Cycle Engine
- Conduct Detailed Design Analysis of a Breadboard Advanced Expander Cycle Engine
- Fabricate and Test a Breadboard Expander Cycle Engine and its Components

VIII, B, Recommendations (cont.)

problems can be solved in a timely manner and result in a more cost-effective engine development program. The expander cycle technologies should address the three major engine design drivers identified by the Phase A, the Point Design, and ALRC in-house efforts. These design drivers are as follows:

- Engine Turbopump Drive Power
- Development and Operational Risk Reduction
- Engine Performance

Power technology activities should be aimed at assuring or increasing the power available to the turbopump. The results of these programs are used to verify that the engine will operate at the selected design point chamber pressure, has the capability of operating at a higher pressure and performance level, or can accept greater component performance margins or tolerances. As a result, overall program economies are achieved by guaranteeing that the engine operating design point can be reached or exceeded (i.e., growth is accomplished). This saves development dollars because large variations in costs result from parallel resolution of small instant problems. Critical areas which should be addressed are the chamber heat transfer and the efficiency of the small, high head-rise, high-speed turbomachinery.

If risk reduction technologies are undertaken, it will permit the solution of design deficiencies at the technology level prior to making a commitment to a design specification and entering the engine development program. Making decisions at this point allows design iterations and decisions to be made at the low expenditure level of the overall program. Risk reduction solutions provide for higher confidence in the engine operation, which is consistent with a man-rating design philosophy. These

technologies include programs to provide data and insight in pumps axial thrust balancing, bearing life, seal life, high-speed pump dynamic balancing, oxygen pump bipropellant sealing, altitude ignition and restart, engine control, materials advancements, and manufacturing processes.

Performance technology programs are required to guarantee the performance level of the engine prior to a commitment to a specification. These programs provide a high confidence in the performance position so that payloads can be firmed up at reasonable levels prior to DDT&E. The level of performance growth is also determined by addressing items such as high area ratio nozzles, extendible nozzles, and carbon-carbon nozzle extensions.

To be cost-effective, all technologies should be conducted at both high and low thrust. In particular, the emphasis should be placed upon alleviating concerns with performance, pump stability, coolant flow stability, and two-phase coolant heat transfer at the low-thrust operating point.

The engine point design studies recently concluded (Ref. 4) should be continued to investigate the study areas recommended by the initial efforts and to further optimize the advanced expander cycle engine.

When the expander cycle data base has been updated and extended, and the best engine has been evolved, the design and demonstration of a breadboard expander cycle engine should be accomplished. This demonstration is required to verify the engine operating point and capability and eliminate major costly design iterations in the engine development program.

REFERENCES

1. Mellish, J.A., Orbit Transfer Vehicle (OTV) Engine Phase A Study, Final Report, Contract NAS 8-32999, Report 32999F, ALRC, 29 June 1979.

2. Orbit Transfer Systems with Emphasis on Shuttle Applications - 1968 - 1991, NASA Technical Memorandum TMX 73394, NASA/MSFC, April 1977.

3. Christensen, K.L., Orbit Transfer Vehicle (OTV) Engine Phase A Study, Extension 1, Final Report, Contract NAS 8-32999, Vol. III: Study Cost Estimates, ALRC, 20 August 1980.

4. Mellish, J.A., Orbit Transfer Vehicle (OTV) Advanced Expander Cycle Engine Point Design Study, Final Report, Contract NAS 8-33574, Report No. 33574-F, ALRC, 10 December 1980.

5. Orbit Transfer Vehicle Engine Study, Phase A, Final Report, Contract NAS 8-32996, Rocketdyne Division, Rockwell International, 9 July 1979.

6. Mahon, J.C., Orbit Transfer Vehicle (OTV) Engine Phase "A" Study, Final Report, Contract NAS 8-32999, Vol. III: Study Cost Estimates, ALRC, 29 June 1979.

7. Design Study of RL-10 Derivatives, Final Report, Vol. I-IV, Contract NAS 8-28989, Pratt & Whitney Aircraft, 15 December 1973

8. Luscher, W.P., Orbit-to-Orbit Shuttle Engine Design Study, Final Report, Books 1-4, Contract F04611-71-C-0040, AFRPL TR-72-45, ALRC, May 1972.

9. Dennies, P.C., Marker, H.E., and Yost, M.C., Advanced Thrust Chamber Technology, Final Report, Contract NAS 3-17825. NASA CR-135221, Rocketdyne, 5 July 1977.

10. Liquid Rocket Engine Turbopump Gears, NASA SP-8100, March 1974, p. 25.

11. Design of RL-10 Derivatives, Final Report, Vol. II, Contract NAS 8-28989, Pratt & Whitney Aircraft, FR-6011, 15 December 1973, pp. 87 & 343.

12. Zachary, A.T., Advanced Space Engine Preliminary Design, Final Report, Contract NAS 3-16751, NASA CR-121236, Rocketdyne, October 1973.

REFERENCES (cont.)

13. Bradie, R.E., and Cuffe, J.P.B., Advanced Space Engine Preliminary Design, Final Report, Contract NAS 3-16750, NASA CR-121237, Pratt & Whitney, December 1973.

14. Hess, H.L. and Kunz, H.R., A Study of Forced Convection Heat Transfer to Supercritical Hydrogen, ASME Paper No. 63-WA-205, November 1963.

15. Friedly, J.C. et. al., Stability Investigation of Thermally Induced Flow Oscillations in Cryogenic Heat Exchangers, General Electric R&D Report S-68-1023, Final Report, Contract NAS 8-21045, October 1967.

16. NASA SP-8019, Liquid Rocket Engine Centrifugal Flow Turbopumps, December 1973.

17. NASA SP-8107, Turbopump Systems for Liquid Rocket Engines, August 1974.

18. Preburner of Staged-Combustion Rocket Engine, Final Report, Contract NAS 3-19713, NASA CR-135356, Rocketdyne, February 1978.